DOT/FAA/RD-81/63

Project Report
ATC-109

Results of L Band Multipath Measurements at Operational United States (U.S.) Airports in Support of the Microwave Landing System (MLS) Precision Distance Measuring Equipment (DME/P)

J. E. Evans
P. H. Swett

23 July 1981

Lincoln Laboratory
MASSACHUSETTS INSTITUTE OF TECHNOLOGY
LEXINGTON, MASSACHUSETTS

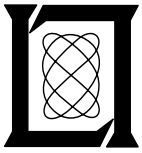

Prepared for the Federal Aviation Administration,
Washington, D.C. 20591

Technical Report Documentation Page

1. Report No.	2. Government Accession No.	3. Recipient's Catalog No.
DOT/FAA/RD-81/63		

4. Title and Subtitle	5. Report Date
Results of L Band Multipath Measurements at Operational United States (U.S.) Airports in Support of the Microwave Landing System (MLS) Precision Distance Measuring Equipment (DME/P)	23 July 1981
	6. Performing Organization Code

7. Author(s)	8. Performing Organization Report No.
James E. Evans and Paul H. Swett	ATC-109

9. Performing Organization Name and Address	10. Work Unit No. (TRAIS)
Massachusetts Institute of Technology Lincoln Laboratory P.O. Box 73 Lexington, MA 02173	11. Contract or Grant No. DOT-FA74-WAI-461
	13. Type of Report and Period Covered
12. Sponsoring Agency Name and Address	
Department of Transportation Federal Aviation Administration System Research and Development Service Washington, DC 20591	Project Report
	14. Sponsoring Agency Code ARD-310

15. Supplementary Notes

The work reported in this document was performed at Lincoln Laboratory, a center for research operated by Massachusetts Institute of Technology under Air Force Contract F19628-80-C-0002.

16. Abstract

This report presents the results of a short duration L band multipath measurement program at five major U.S. airports (St. Louis, Tulsa, Wright Patterson Air Force Base, Philadelphia and Washington National) and one smaller airport (Quonset, RI) to better quantify the expected multipath environment for the Microwave Landing System (MLS) Precision Distance Measuring Equipment (DME/P). Specific objectives included:

(1) Measurements of the principal multipath parameters (amplitude and time delay) with realistic aircraft/ground site locations at runways which had the major DME/P multipath sources (large buildings) identified in previous analytical (simulation) studies.

(2) Determination of whether significant DME/P multipath sources exist which had not been considered to date.

and

(3) Comparison of the measured results with computer simulation results obtained with simplified airport models (such as have been used for DME/P system design to date).

Particular emphasis was placed on the final approach region including the flare and rollout regions since these areas correspond to the most stringent DME/P accuracy requirements and, have not been utilized operationally with the current L band DME.

All of the above objectives were achieved although in some cases the experimental data in the flare/rollout region was of poor quality due to low signal to noise ratio. The spatial region and time delay of specular multipath generally correlated well with expectations based on simple ray tracing. With the exception of Washington National, no significant [multipath to direct signal ratio (M/D) > -10 dB] multipath was encountered in operationally relevant areas which was not predicted. The quantitative predictions of the simple airport models agreed with the experimental data, although in some cases, (especially, near threshold) the measured M/D values were considerably higher than predictions.

17. Key Words	18. Distribution Statement
Microwave Landing System (MLS) Distance Measuring Equipment (DME) DME Based Landing System (DLS) Multipath	Document is available to the public through the National Technical Information Service, Springfield, VA 22161

19. Security Classif. (of this report)	20. Security Classif. (of this page)	21. No. of Pages	22. Price
Unclassified	Unclassified	194	

ABSTRACT

This report presents the results of a short duration L band multipath measurement program at five major U.S. airports (St. Louis, Tulsa, Wright Patterson Air Force Base, Philadelphia and Washington National) and one smaller airport (Quonset, RI) to better quantify the expected multipath environment for the Microwave Landing System (MLS) Precision Distance Measuring Equipment (DME/P). Specific objectives included:

1) measurements of the principal multipath parameters (amplitude and time delay) with realistic aircraft/ground site locations at runways which had the major DME/P multipath sources (large buildings) identified in previous analytical (simulation) studies.

2) determination of whether significant DME/P multipath sources exist which had not been considered to date.

and

3) comparison of the measured results with computer simulation results obtained with simplified airport models (such as have been used for DME/P system design to date).

Particular emphasis was placed on the final approach region including the flare and rollout regions since these areas correspond to the most stringent DME/P accuracy requirements and, have not been utilized operationally with the current L band DME.

All of the above objectives were achieved although in some cases the experimental data in the flare/rollout region was of poor quality due to low signal to noise ratio. The spatial region and time delay of specular multipath generally correlated well with expectations based on simple ray tracing. With the exception of Washington National, no significant [multipath to direct signal ratio (M/D) > -10 dB] multipath was encountered in operationally relevant areas which was not predicted. The quantitative predictions of the simple airport models generally agreed with the experimental data, although in some cases, (especially, near threshold) the measured M/D values were considerably higher than predictions.

ACKNOWLEDGEMENTS

A number of people made substantive contributions to the work described in this report. A. Vierstra and R. Parr designed the key elements of the airborne system and the data acquisition system, respectively. R. Close and A. Gregory assembled much of the electronics, while C. Catalano developed the real time display software as well as a waveform playback and analysis capability on the laboratory Eclipse minicomputer.

J. Yaeger-Charriere developed much of the software used for waveform analysis and data summaries as well as processing the data and running the corresponding simulation studies.

The actual measurements at the various major airports were accomplished in a total of 2 1/2 weeks through the hard work of A. Gregory, J. Kalil and the project pilots (T. Magnan, C. Magnarelli, J. Dufort, and D. Cassalia). The ready cooperation of the airport authorities at the various airports was essential to the program pace. Particular help was extended by W. Melnick at WPAFB and T. Davidson at Lambert-St. Louis.

The measurements at Quonset Point, RI, were carried out by A. Vierstra, while the data reduction and analysis was accomplished by D. Easterday.

K. Eastburn assisted in developing and running many of the simulation scenarios, while D. Young and N. Campbell ably typed the text and figures in a very short time period.

TABLE OF CONTENTS

I. INTRODUCTION

The characteristics of L band Distance Measuring Equipment (DME) multipath in the approach and landing region have assumed increased attention as a consequence of the Federal Aviation Administration (FAA)/International Civil Aviation Organization (ICAO) program to develop a precision DME (DME/P) for the Microwave Landing System (MLS). In an earlier study of multipath effects on the DME/P [1], it was concluded that experimental measurements of the pertinant multipath parameters at representative operational airports would be very useful in:

(1) verifying that the principal multipath challenges identified in the analytical/simulation studies (specular reflections from buildings coupled with specular terrain reflections) are, in fact, the major contributions of significant DME/P multipath

and

(2) acertaining to what extent the simplified building and terrain models used to date can yield good quantitative prediction of multipath at a given location.

This report summarizes the results of experimental L band measurements at five major operational US airports (Philadelphia, Washington National, Wright Patterson AFB, St. Louis, and Tulsa) as well as a preliminary test at Quonset Point, RI.

The digital multipath measurement equipment is described in Section II. A highly mobile equipment was desired which could measure the multipath parameters of greatest interest. This was accomplished by transmitting a narrow (100 nsec - 200 nsec wide) L band pulse from an aircraft and (digitally) recording the received signal envelope at a ground antenna as a function of time as shown in Figs. 1-1 and 1-2. By examination of the digitized envelope, it was then possible to determine the pertinent multipath characteristics (amplitude and time delay relative to the direct signal level) on a given signal reception. The aircraft transmitted signals at a 10 Hz rate, corresponding to approximately 18 feet of aircraft displacement between successive measurements. This relatively dense spatial sampling of the multipath environment allowed us to use correlation between adjacent measurements to reject

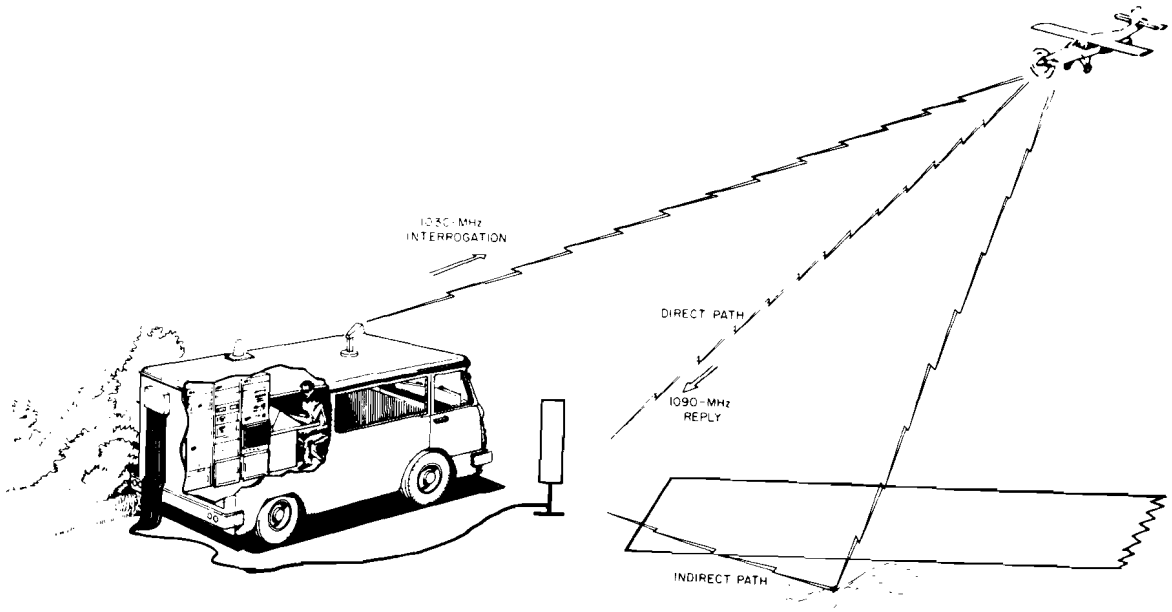

Reply pulse width ~ 100 nsec

Received amplitude digitized (8 bits) every 50 nsec

Aircraft range also recorded

Fig. 1-1. DME/P multipath measurement system.

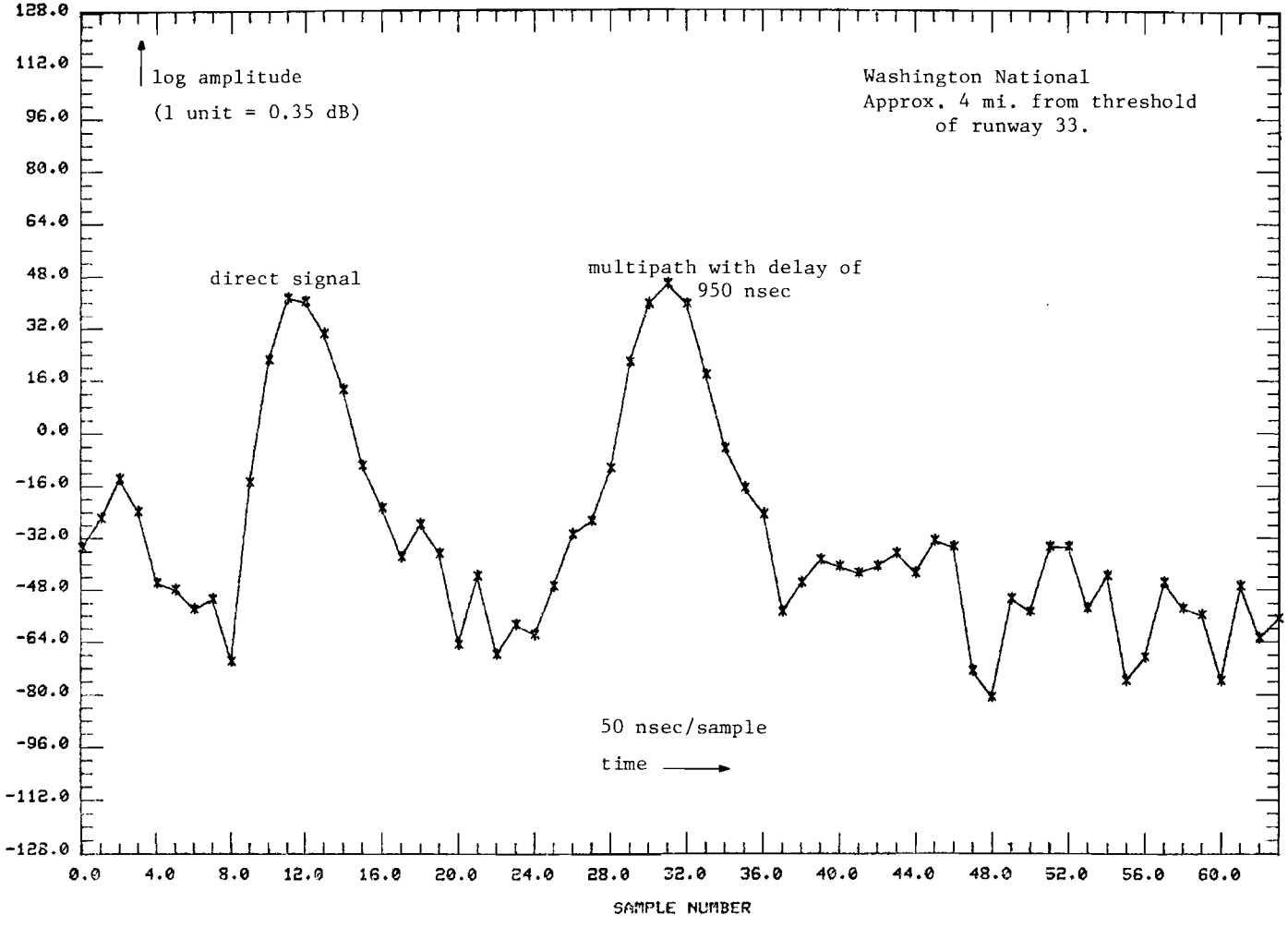

Fig. 1-2. Example of digitized waveform.

erroneous data due to cochannel interference and/or low signal to noise ratio (SNR).

Aircraft range information was obtained by having the narrow pulse transmission times controlled by a standard Air Traffic Control Radar Beacon (ATCRBS) transponder which was being interrogated by the ground measurement system. In this way, the delay time between the interrogation and received ATCRBS reply yielded the aircraft range. The flight profiles were such (e.g., centerline approaches using an ILS localizer to furnish lateral position and the ILS glideslope to furnish vertical position) that knowledge of the range generally would permit one to determine the aircraft position.

Section III describes the data reduction method. Each (digitized) received waveform was examined to locate discrete pulses according to criteria based on pulse widths and magnitude. Cochannel interference due to asynchronous replies from other ATCRBS transponders was rejected by measurement of the pulse widths. The reduced pulse parameter data are then displayed in plots of multipath level and time delay versus distance along the flight path. By considering the nature of adjacent multipath environment estimates and repeatability of the phenomena between successive (nominally) identical runs, it was possible to identify questionable data which required hand analysis of the waveforms.

Section IV to VIII describe the measurement results at Philadelphia, Washington National, Wright Patterson AFB, St. Louis (Lambert), and Tulsa International Airport. Each section begins with a description of the airport geometry, major building reflection multipath threats, and expected multipath regions. Next, the results of the received waveform analysis along the various flight paths are shown. Finally, the field data is compared with the computed multipath characteristics using a simple model of the airport environment whereby building walls are modeled by flat rectangular plates and the terrain as a flat dielectric half plane.

Section IX summarizes the preliminary results of this measurement program and makes some suggestions for further work in this area. Appendix A de-

scribes a preliminary DME/P measurement at Quonset Point, RI, where in-scope photographs were used to record the received waveform at various discrete points along the airport main runway.

II. EQUIPMENT CONFIGURATION

The need to obtain multipath data in a time schedule compatible with the ICAO program and consistent with the overall program level of effort made it imperative that the technique chosen be relatively straightforward and that the required hardware components be readily available or easily and quickly fabricated. The method that was finally adopted is shown in the block diagram of Fig. 2-1. The bulk of the hardware used was that which had previously been deployed to make terrain reflection multipath measurements [2].

A. Ground Equipment

The MLS terrain multipath measurement system has been described in detail previously [2], so our discussion here will only concern itself with those features which were unique to the DME multipath measurement program.

1. Interrogation Subsystem

A measurement is initiated by the ground transmitting an ATCRBS "B" mode interrogation at 1030 MHz through a 6-foot dish antenna. This mode is used rather than the normal A and C ATCRBS modes, since the B mode has not been used for many years and thus will not elicit replies from normal ATCRBS transponders. Thus, we avoid "synchronous garble" from other aircraft which are approximately at the same range as our test aircraft. The dish antenna was used in all cases save one site at Tulsa International Airport to

(1) provide a better SNR for our uplink

and

(2) minimize the likelihood of uplink multipath with a delay time of approximately 2 μsec from suppressing the test aircraft transponder*.

---

*The mode B interrogation consists of two 400 nsec pulses (P1 and P3) which are separated in time by 9 μsec. However, normal ATCRBS ground stations also transmit a third pulse (delayed 2 μsec after the P1 pulse) through an omni antenna to indicate situations in which the aircraft is in the sidelobes of the interrogator antenna. If an ATCRBS transponder measures a received signal level in the SLS pulse position which is comparable to the P1 pulse position level, it is not supposed to reply. Consequently, high level reflections of the P1 interrogation pulse can suppress the ATCRBS transponder if they have a multipath delay of approximately 2 μsec.

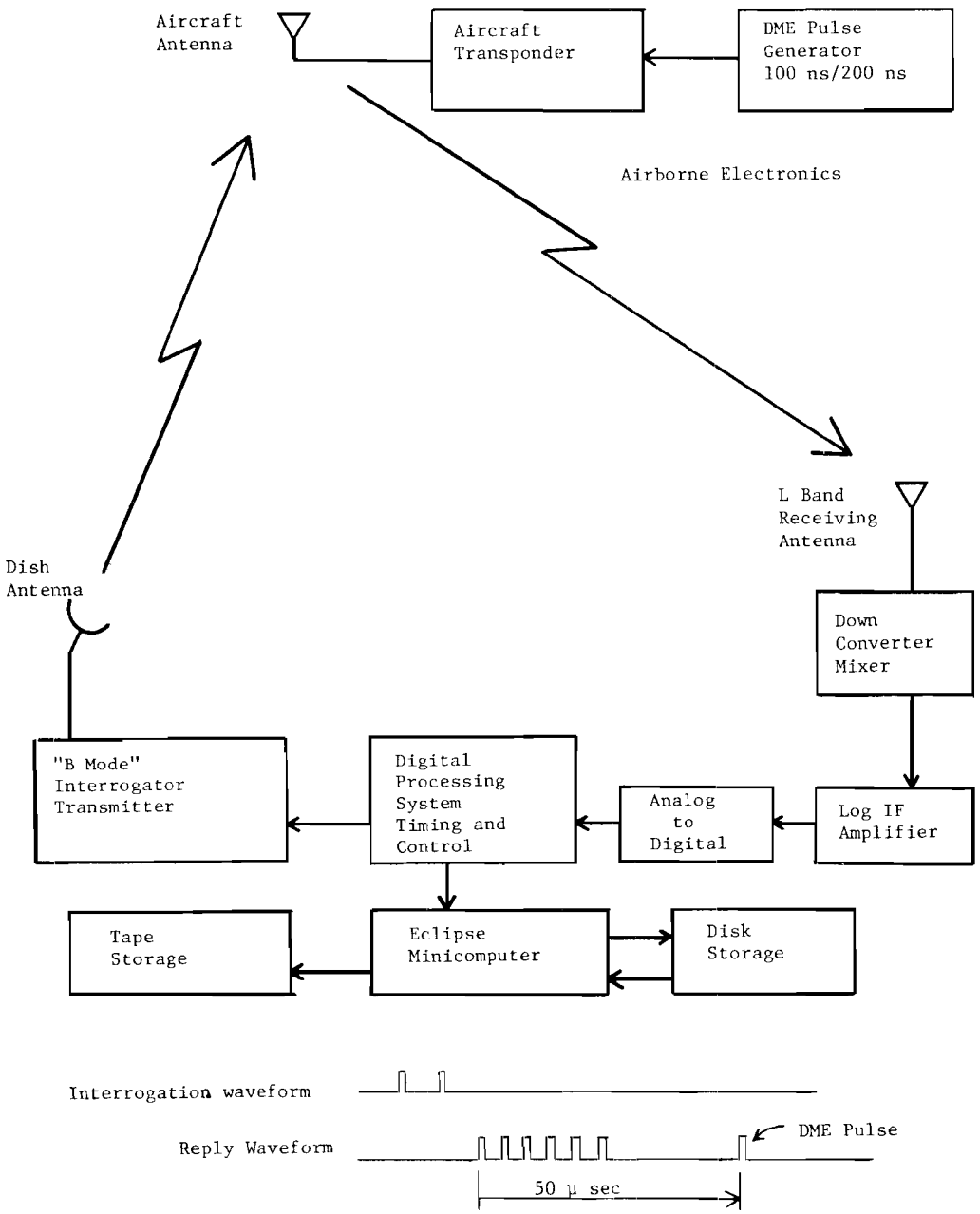

Fig. 2-1. DME hardware block diagram.

The size of this dish made it awkward to use in situations where the interrogator antenna had to be elevated to avoid shadowing by terrain and/or runway humps. At one Tulsa site, it was found necessary to use a smaller interrogation antenna which could be mounted high upon a pole attached to the roof of the van.

2. Receiving Antenna

To reduce the magnitude of the direct signal fades which can arise near threshold due to ground lobing, it has been suggested [3] that the DME/P ground antenna would

(1) have a phase center elevated some 20 - 30 feet above the local terrain at most CTOL runways

and

(2) have an elevation pattern whose gain decreases rapidly below the horizon to avoid signal lobing at high elevation angles.

Both of these features were deemed essential for the DME multipath measurement ground receiving antenna. Figure 2-2 shows the final configuration using one of the PALM system antenna elements [4] on a light weight tubular mast. The PALM antenna elements were designed to yield a rapid pattern rolloff near the horizon as shown in Fig. 2-3. The element mounting bracket was designed so that the horizon corresponded to the -6 dB point on the pattern*.

The azimuth pattern rolloff at wide angles off centerline is similar to that suggested by Kelly and LaBerge to mitigate DME/P multipath. The tubular mast had a removable center section so that the phase center could be at nominal heights of 20 feet or 30 feet. The hinged base of the array is connected to a rectangular base which was secured to the ground by driven stakes. The mast and element are then erected by a hand cranked winch. Final alignment is then achieved by adjusting three guy wires.

---

*i.e., the antenna was tilted downward 2° in elevation.

Fig. 2-2a. DME measurement equipment.

Fig. 2-2b. Measurement equipment at Washington National Airport.

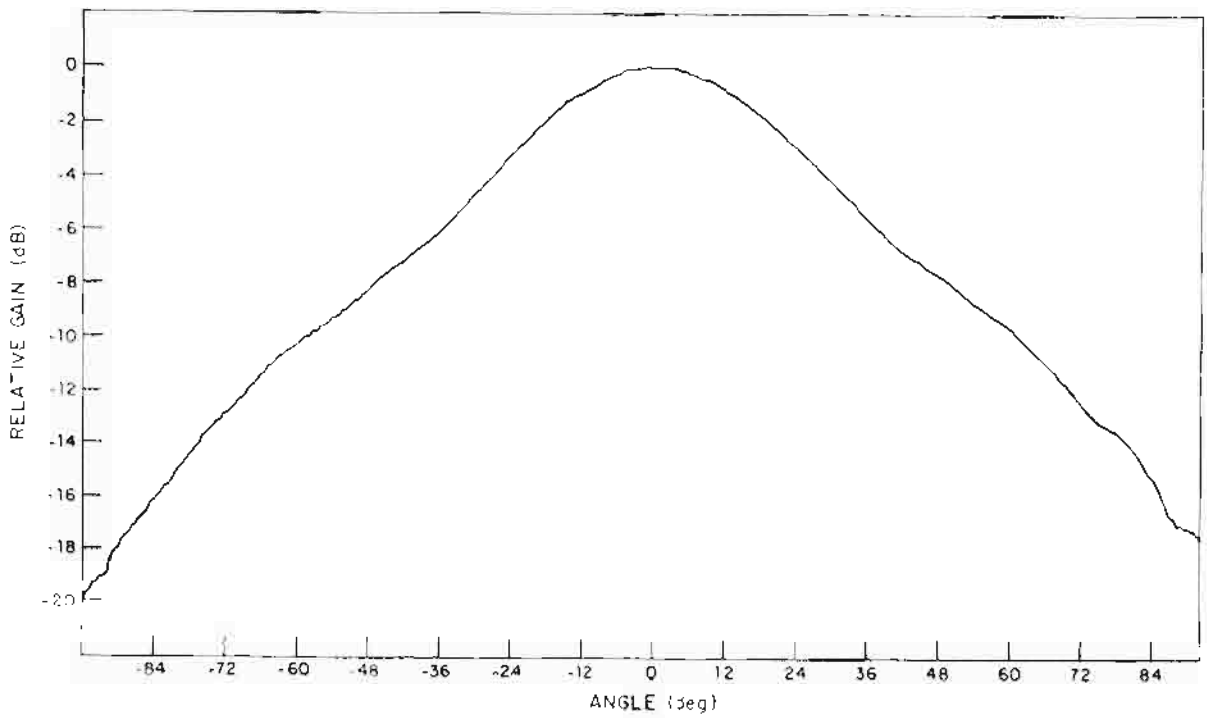

Measured azimuth pattern

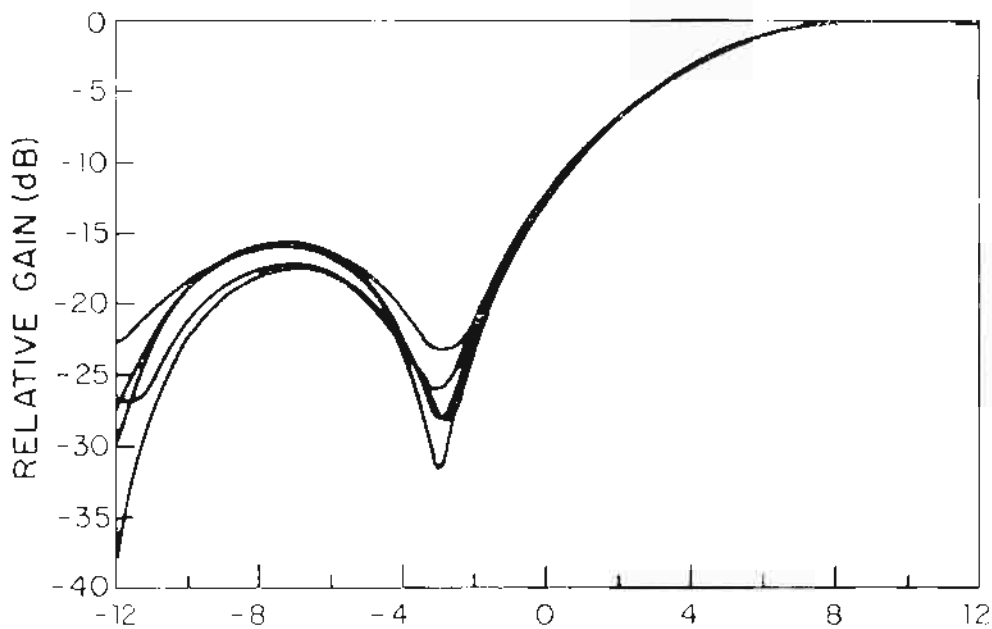

Elevation patterns for the five PALM antennas.

Fig. 2-3. Pattern cuts for receiving antenna.

3. RF/IF Electronics

A block diagram of the van electronics hardware is shown in Fig. 2-4. The basic difference between the normal MLS terrain multipath measurement receiver architecture and the DME multipath measurement architecture were hardware changes to the trigger circuit, a 10 MHz bandwidth filter in the IF and the fact that only one receiver channel was used for DME. There were also changes in the logic to create a 3.2 μs window in which the received pulse was sampled.

In DME multipath measurement operation, the 1030 MHz received signal was mixed down to a 60 MHz IF by an RHG model 1-2/10B mixer/preamp. The noise figure of the front end is 8 dB and the measured sensitivity of the front end is -78 dBm*. The dynamic range of the log IF amp is 80 dB. RF cable loss is approximately 2 dB, and IF cable loss is 1 dB. The IF filter is a CIR-Q-TEL model B2-60/10-4/50, which is a 4-pole Butterworth filter with a 10 MHz bandwidth. The burst responses of the filter are shown in Figs. 2-5a and 2-5b. The IF filter is followed by the PALM/MLS log amplifier. From there, the detected signal goes to an oscilloscope for viewing the pulses by the operator during the mission and the signal also goes to the sample/hold and the A/D converter. The response of the IF stage including the 10 MHz BW filter and the log amp is shown in Figs. 2-5c and 2-5d.

The procedure checklist at the beginning of a mission included a calibration of the receiver channel. This was to verify the operational status of the equipment. Figure 2-6 shows an amplitude calibration of the receiver. We see that the digitized amplitude is essentially logarithmically linear over a dynamic range of 70 dB.

---

*The measured sensitivity was approximately 15 dB lower than that implied by the noise figure and IF bandwidth due to losses in the mixer.

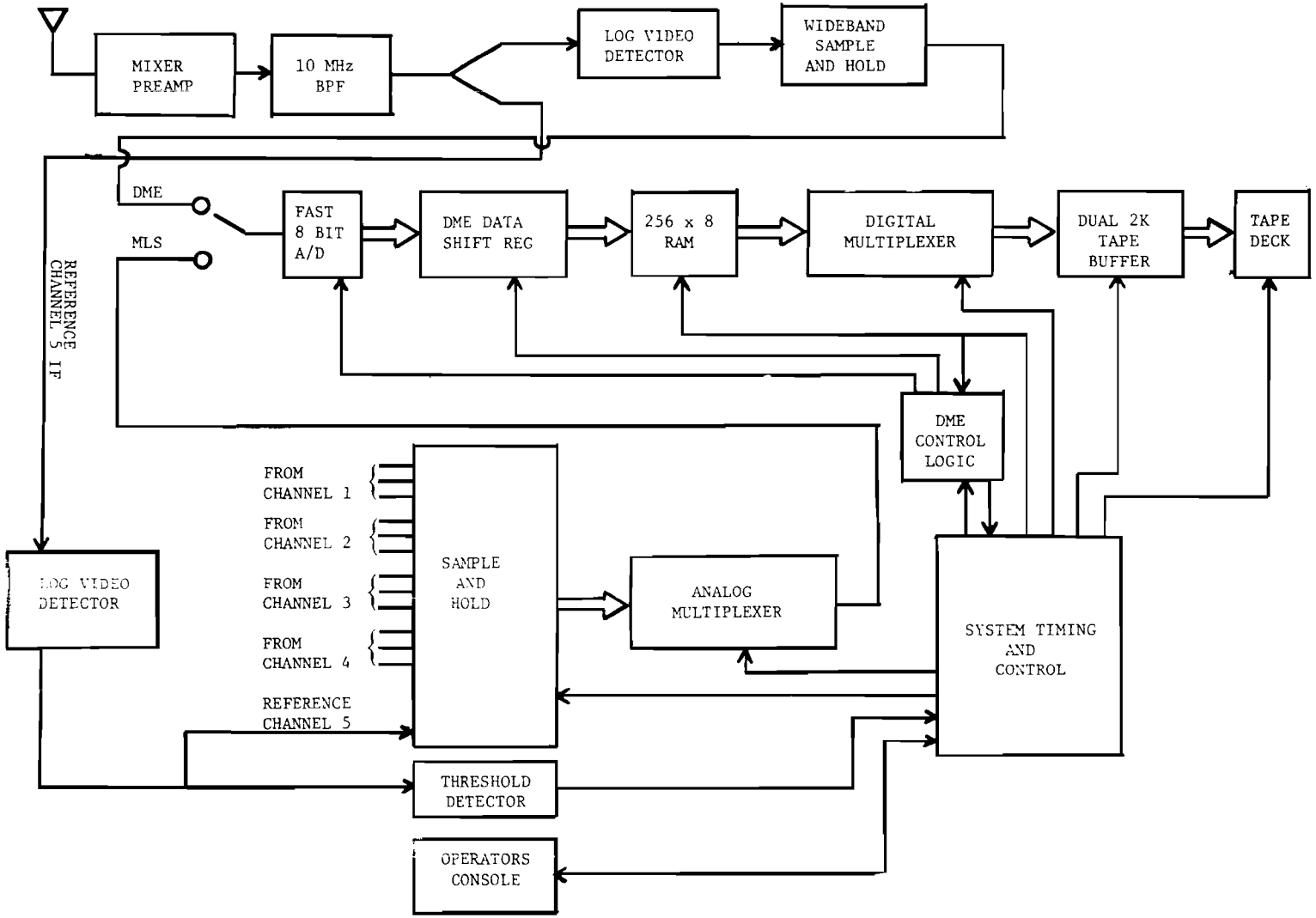

Fig. 2-4. Receiver/processor block diagram.

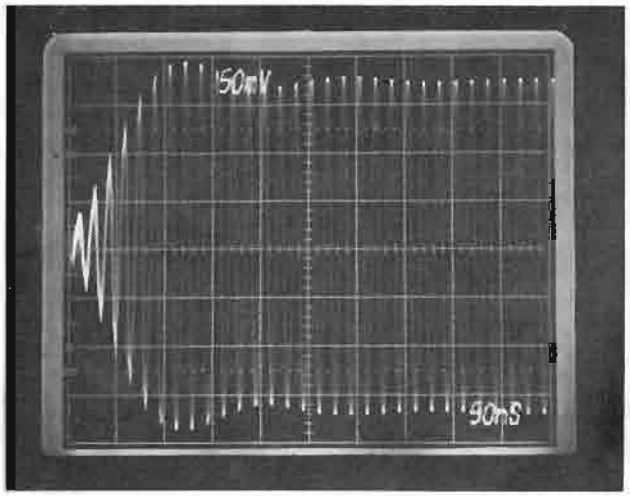

Fig. 2-5a. Gated IF response of 10 MHz BP IF filter.

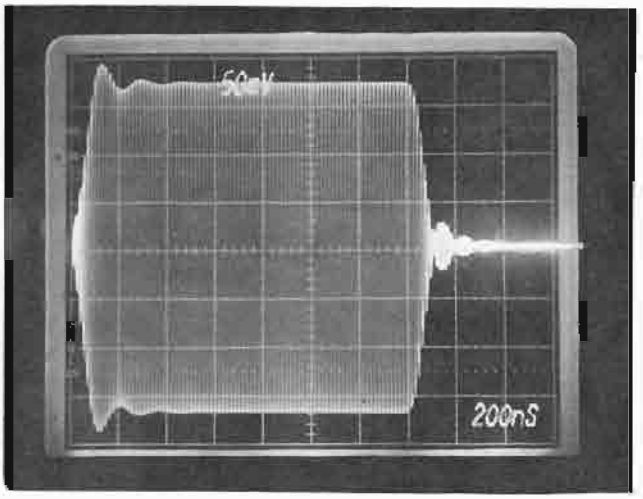

Fig. 2-5b. Gated IF burst response of 10 MHz BP IF filter.

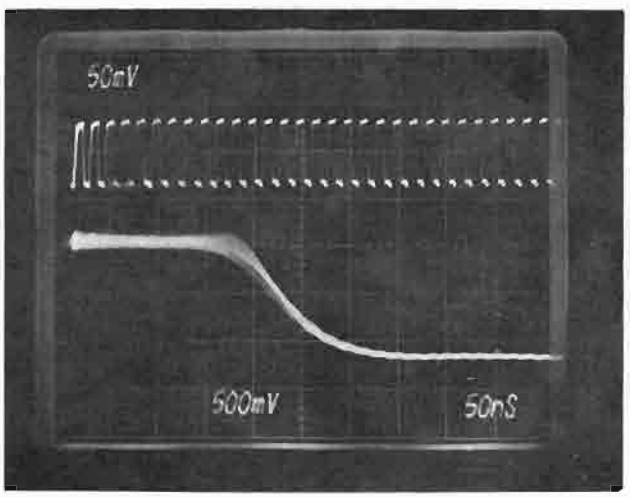

Fig. 2-5c. Gated IF response of IF filter and log AMP stage. Upper trace is stepped 60 MHz input. Lower trace is filter/ log AMP detected video output.

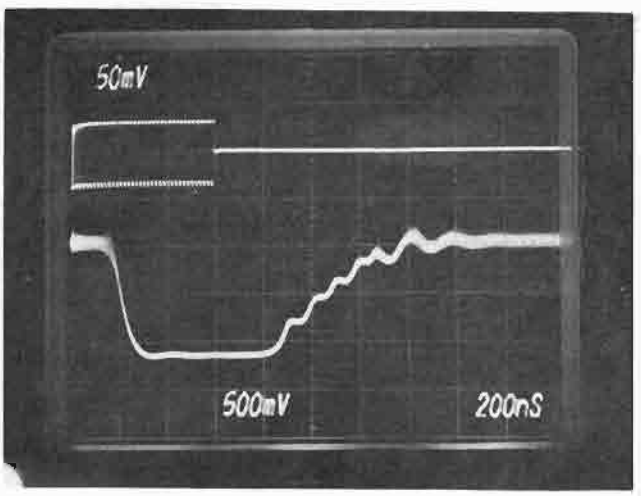

Fig. 2-5d. Gated IF burst response of IF filter and log AMP stage. Upper trace is gated 60 MHz input. Lower trace is filter/log AMP detected video output.

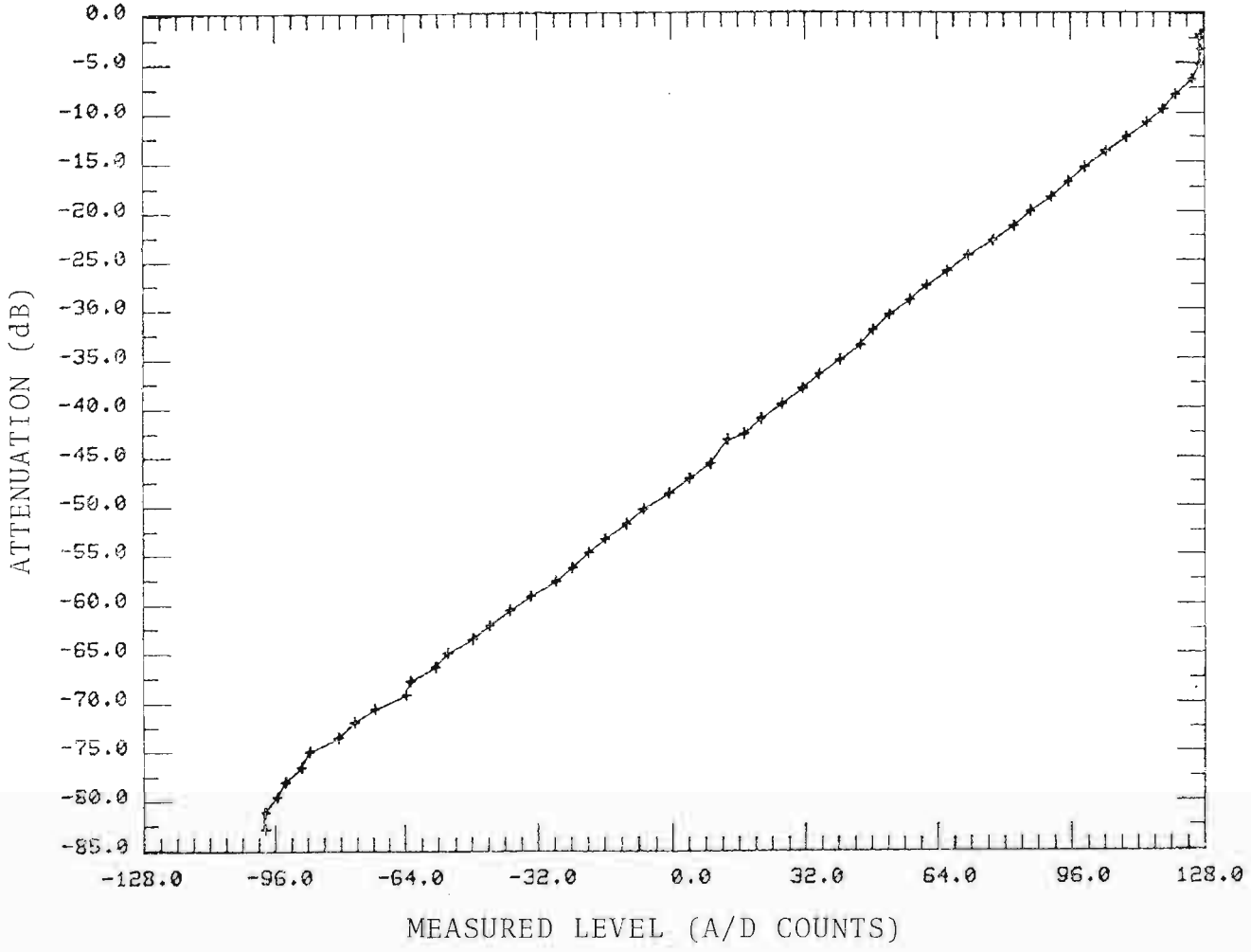

Fig. 2-6. Amplitude calibration of receiver system

4. A/D Converter

In DME mode, the fast eight bit A/D converter samples the input waveform in a burst starting about 50 μs after the opening of the range gate. Each window comprises 64 samples spaced 50 ns per sample. The TRW A/D converter was observed to follow the input waveform faithfully most of the time, but it showed an occasional tendency to glitch for a single sample for input signals with rapidly rising edges.

a. Time Tracking

Tracking of the received signal during a mission was done manually by using a joystick to adjust the relative positions of the first ATCBRS reply pulse (i.e., the F1 pulse) and an internally generated range gate signal, based on an oscilloscope display of the two signals. Maintaining the F1 pulse at the leading end of the range gate insured that the received direct DME pulse was positioned near the beginning of the 3.2 μs DME sampling interval. No further refinement or automation of the range track was used during the missions. The hardware recorded a range parameter based on the first crossing within the range gate of a fixed threshold by the input signal; however, this data was often erratic (see Section III).

5. Recording

Data recording for DME measurements was identical to the MLS terrain reflection recording described in ATC-88 Volume I [2]. Digital data is recorded on the Data General disk and then transferred to tape for a permanent record.

The graphics program, which displays the 3.2 μsec waveform sampling window, writes one frame per second, therefore 1 in 10 replies is seen on the terminal during measurements since there are 10 replies per second. The pulses can be viewed during the field mission and later they can be seen again on the van Eclipse computer or on the computers at the Laboratory.

B. Airborne System

A diagram of the airborne electronics is shown in Fig. 2-7. The DME reply pulse was generated 50 μs after the transponder F1 pulse, and the DME pulse width was selectable at either 100 ns or 200 ns. The transponder and the 200 ns selection was added to improve the signal/noise ratio when necessary. The DME pulse peak power is approximately 160 watts for the 200 ns setting.

Photographs of the transponder DME pulse are shown in Fig. 2-8a and 2-8b for the 100 ns and 200 ns widths, respectively. These photographs were made using a detector with an approximate square law characteristic.

Several L band antennas were available on the Beechcraft Bonanza which could be used to receive and transmit. For the bulk of the tests, a bottom-mounted antenna roughly abreast of the wings was utilized. However, a top-mounted antenna just aft of the cockpit was used for the taxiing tests so as to reduce the signal loss due to ground lobing and have the antenna near the DME/P minimum operational height above ground. The pattern of the specific antenna was not measured; however, it should be quite similar to that of a Piper Cherokee (both single engine small G/A aircraft). Figure 2-9 shows the L band pattern for a model Piper Cherokee in the same configuration used in the flight tests (flaps up, wheels down). The pattern is seen to be reasonably flat in the horizontal plane.

C. System Power Budgets

The power budgets for the interrogation and reply links under the "nominal" airport conditions assumed to date in DME/P power budgets [3] are shown in Tables 2-1 and 2-2. The low height of the interrogator antenna substantially increases the ground reflection lobing loss; however, this is largely compensated by the high gain of the directive dish. The minimum triggering level (MTL) shown is a typical value for ATCRBS transponders. The receiving antenna has a smaller gain than the transmitting dish; however, its greater height offsets much of the gain differences at low aircraft altitudes.

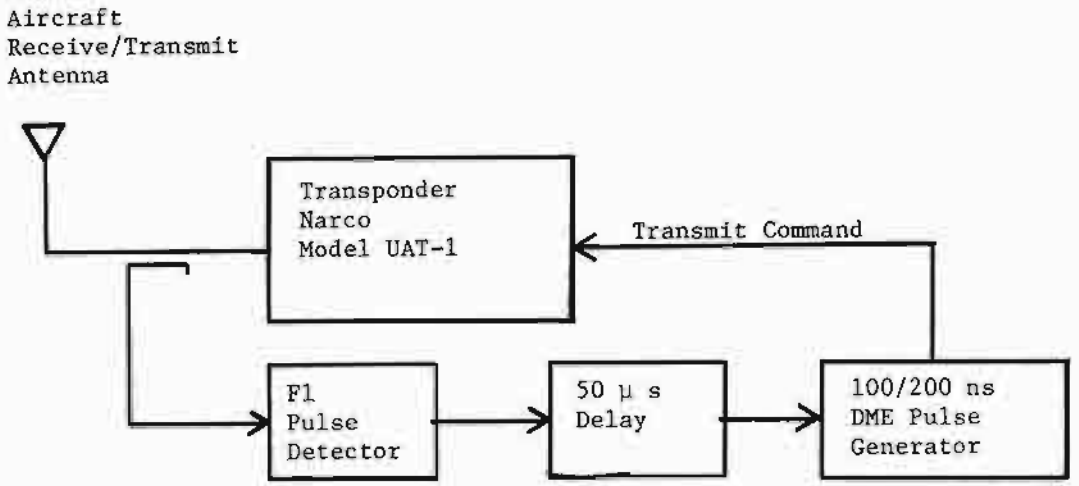

Fig. 2-7. DME Airborne Electronics

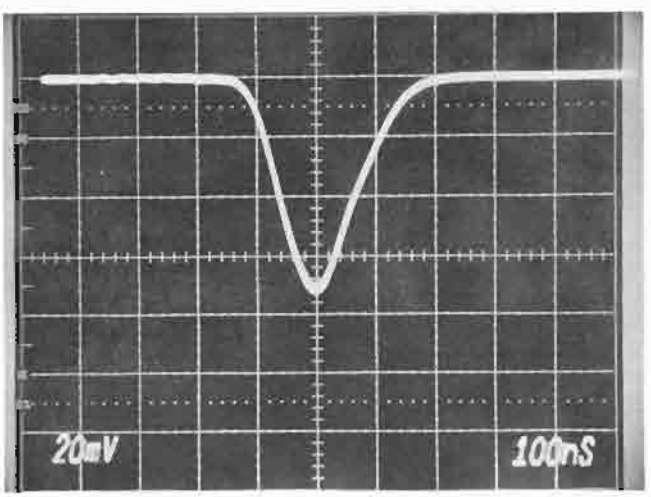

Fig. 2-8a. Detected 100 ns DME pulse at transponder output. 3 dB = 1.3 vertical divisions.

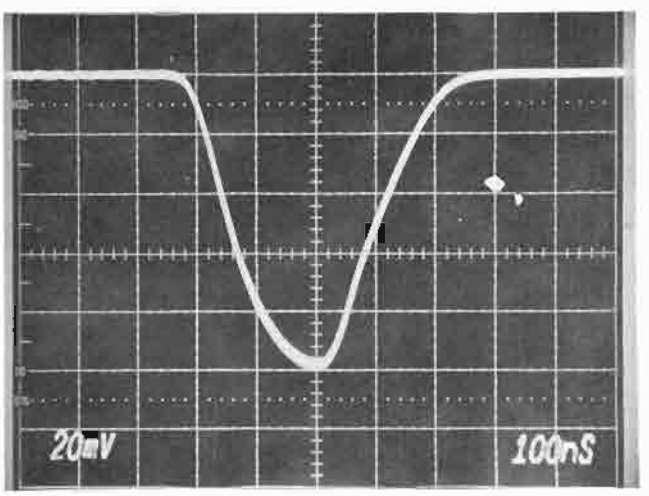

Fig. 2-8b. Detected 200 ns DME pulse at transponder output. 3 dB = 1.7 vertical divisions.

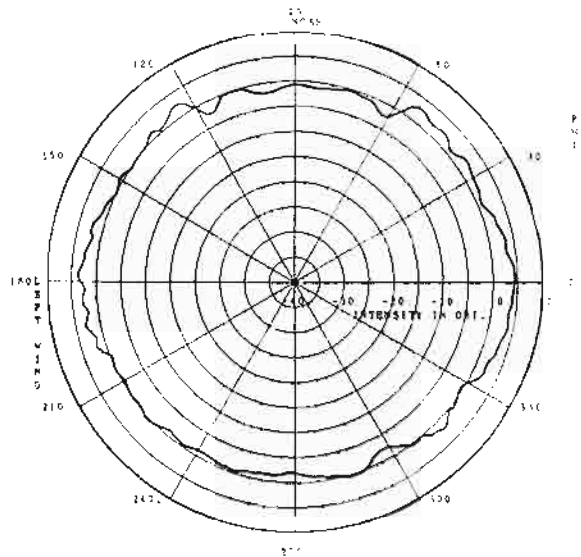

Fig. 2-9. Horizontal plane antenna pattern of Piper Cherokee model aircraft, flaps up, wheels down (from [10]).

TABLE 2-1

DME MULTIPATH MEASUREMENT SYSTEM UPLINK POWER BUDGET

	Aircraft Location		
	Cat II DH	Threshold	Rollout
Aircraft Altitude (ft.)	50	50	15
Range (ft.)	14,500	12,000	10,000
ERP	74 dBm	74 dBm	74 dBm
Path Loss	-105 dB	-104 dB	-102 dB
Ground Reflection Lobing Loss	-7 dB	-11 dB	-21 dB
Received Signal at a/c Antenna	-38 dBm	-41 dBm	-49 dBm
Aircraft Antenna Gain	0 dB	0 dB	0 dB
Coupling Loss xpdr to antenna	-4 dB	-4 dB	-4 dB
Received Power	-42 dBm	-45 dBm	-53 dBm
Margin (MTL = -70 dBm)	+28 dB	+25 dB	+17 dB

Assumptions:

Interrogator dish height 5 feet
DME site 2000 ft. behind stop end of 10,000 ft. runway
Effective Radiated Power (ERP):

transmitter output 200 watts	+53 dBm
ground coupling and cable loss	-3 dB
ground antenna gain (6 foot dish)	+24 dB
	+74 dBm

TABLE 2-2

DME MULTIPATH MEASUREMENT SYSTEM REPLY POWER BUDGET

	Aircraft Location		
	Cat II DH (100')	Threshold (50')	Rollout (15')
ERP	+46 dBm	+46 dBm	+46 dBm
Path Loss	-105 dB	-104 dB	-102 dB
Ground Multipath Loss*	0 dB	0 dB	-4 dB
Receiving Antenna Peak Gain	13 dB	13 dB	13 dB
Elevation Near Horizon Pattern Rolloff	-6 dB	-6 dB	-6 dB
Received Power	-52 dBm	-51 dBm	-53 dBm
Cable Loss** (30 feet)	-3 dB	-3 dB	-3 dB
Receiver MTL†	-78 dBm	-78 dBm	-78 dBm
SNR (video)	+23 dB	+ 24 dB	+22 dB

Assumptions:

*Receiver height = 30 feet
Receiver antenna 2000 ft. behind stop end of a 10,000 ft. runway

**Front end at bottom of array as opposed to behind receiving element.

†Measured front end sensitivity.

Effective Radiated Power (ERP)	
transmitter power (100 watts)	50 dBm
coupling and cable loss	-4 dB
aircraft antenna gain	0 dB
ERP	+46 dBm

ATTN2 = 40 dB

ATTN1 ADJUSTED UNTIL A/C XPDR STOPS RESPONDING

ATTN3 ADJUSTED UNTIL RECEIVED PULSE SNR IS TOO LOW TO IDENTIFY PULSES IN THE RECEIVED WAVEFORM

110219-N

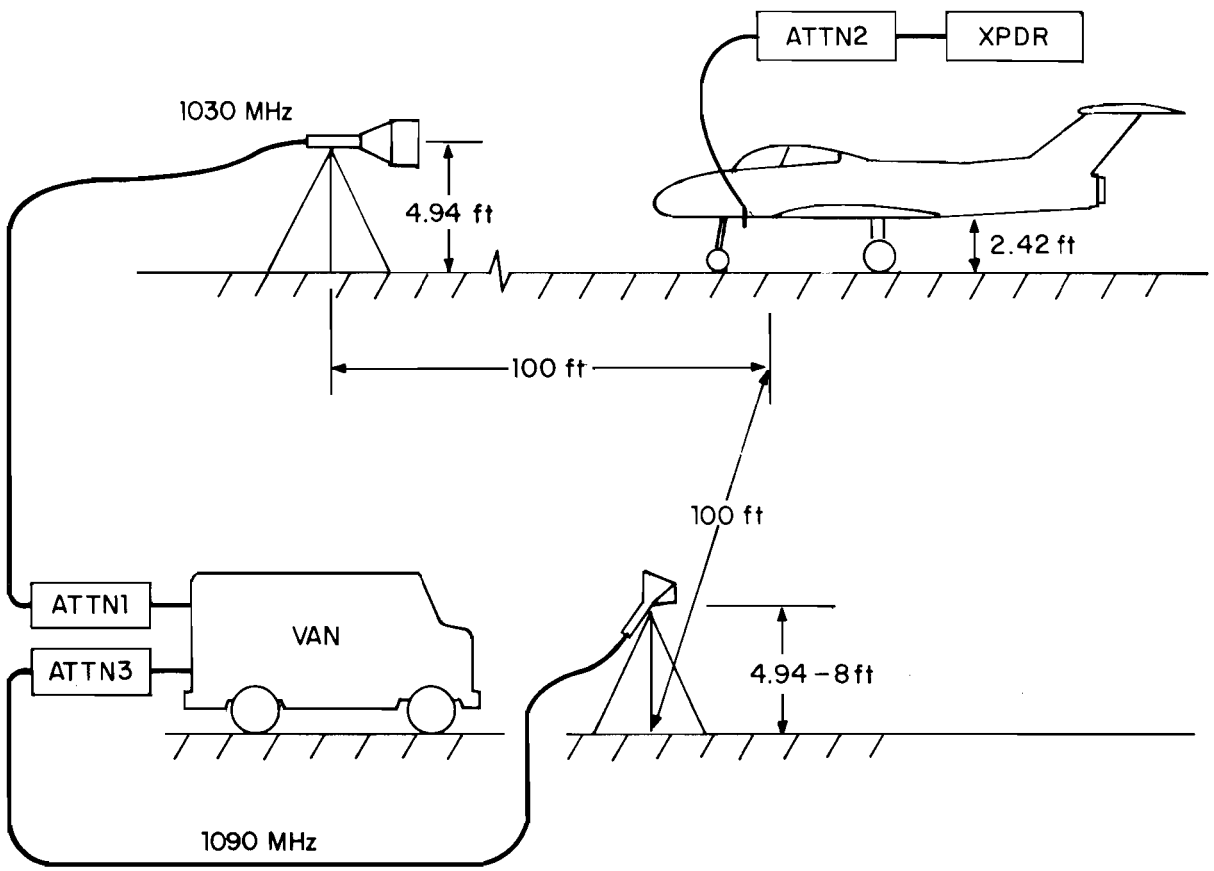

Fig. 2-10. Taxiway test of measurement equipment power budgets.

To validate the power budgets of Tables 2-1 and 2-2, tests were carried out on a taxiway adjacent to the Lincoln Laboratory Flight Facility at Hanscom AFB. For the uplink test, the transmitting antenna heights were chosen to yield a ground reflection in quadratuare with the direct signal (see Fig. 2-10). Table 2-3 shows the corresponding power budget using a simple Alford dipole element as the transmitting antenna. The observed attenuation required in this case to reach MTL was 65 dB, which is within 1 dB of the attenuation called for in Table 2-3.

When the Alford element was used as the receiving antenna for the transponder reply, the required attenuation to cause loss of signal was 73 dB, which agrees quite well with the budget indicated in Table 2-4. The PALM element used as a receiving antenna in the same location required 66 dB attenuation to cause loss of transponder reply which was initially surprising, since the PALM element peak gain is 5 dB higher than the Alford antenna peak gain.

However, the PALM element phase center height was 8 feet so that the aircraft antenna was at an elevation angle of -1.43° with respect to the element boresighted pattern. This corresponds to a point near the first null of the PALM elevation pattern in which the pattern is 20 dB down with respect to the peak gain. Consequently, we would expect the required attenuation to reach 15 dB SNR with the PALM element to be as much as 15 dB less than that with the Alford. The actual difference was 7 dB, which could be explained by assuming that the array was tilted back 2° for the test. This could easily have been the case, since the normal alignment procedure was not utilized on the taxi test.

The conclusion reached then was that the taxiway test experimental results basically confirmed many of the key features in the power budgets of Tables 2-1 and 2-2. This is an important issue, since if the experimental losses during tests are greater than predicted using a simple runway reflection model, this would need to be incorporated in the DME/P decision-making process.

TABLE 2-3

UPLINK POWER BUDGET FOR TAXIWAY TEST

Transmitter Output (200 watts)	+53 dBm
Coupling, Cable Loss	-3 dB
Alford Gain	+8.8 dB
	+58.8 dBm
Path Loss (100 feet)	-62 dB
Ground Multipath Gain Due to Lobing*	+3 dB
Received Signal Level at A/C Antenna	0 dBm
Cabling, Coupling Loss to Transponder	-4 dB
Signal at Transponder in Absence of any Attenuation	-4 dBm
Transponder MTL	-70 dBm
Required Attenuation to reach MTL	66 dB

*The geometry parameters of Fig. 2-10 are such that the ground reflection should be in quadrature with the direct signal.

TABLE 2-4

DOWNLINK POWER BUDGET FOR TAXIWAY TEST

Transponder Output (100 watts)	+50 dBm
Coupling, Cable Loss (estimated)	-4 dB
Antenna Gain	0 dB
Effective Radiated Power	+46 dBm
Path Loss (100 feet)	-62 dB
Ground Multipath Gain Due to Lobing (approx.)	+3 dB
Received Signal at Ground Antenna	-13 dBm
Receiving Antenna (Alford Dipole) Gain	+8.8 dB
Cable Loss (30 feet) (Using same cable as with experiment)	-3 dB
Signal at Front End	-7.2 dBm
Receiver Sensitivity	-78 dBm
SNR at Input w/o Attenuation	+71 dB
Attenuation to Reach Threshold	~73 dB

III. DATA ANALYSIS PROCEDURE

In this section, we describe the algorithms used in analyzing the digitized waveforms to ascertain the multipath environment.
The principal focus for the automated analysis has been specular reflections which are manifested by large pulses which are well separated from the direct signal as shown in Fig. 3-1. In these cases, fairly simple criteria are used to identify the pulses:

(1) peak amplitude corresponding to an SNR $\geq$ approximately +10 dB or the minimum M/D ratio of concern (typically -20 dB)

(2) pulse width between -6 dB points which lies in the interval (W -50 μsec, W +100 μsec) where W = expected pulse width in μsec. (W = 150μsec for the narrowest pulses used)

The first pulse encountered in the digitized time interval which meets the above criteria is assumed to be the direct signal. The peak level of the pulse is taken to be the direct signal amplitude and the point midway between the first leading and trailing edge digitized amplitudes which are at least 6 dB down from the peak level is taken to be the centroid.

If no pulses meeting the above criteria were encountered in the digitized waveform, an "M" is placed on the M/D plot at the -25 dB M/D level and no symbol is placed in the corresponding time delay (τ) plot. If only a "direct" pulse is encountered, an "X" is plotted at -20 dB on the M/D plot with no corresponding symbol on the τ plot.

Any additional pulses meeting criteria (1) and (2) are assumed to be multipath. Their peak amplitude and centroid are computed as for the direct signal. The displayed M/D ratio represents the ratio of peak amplitudes while the relative time delay is computed as the time between the respective pulse centroids.

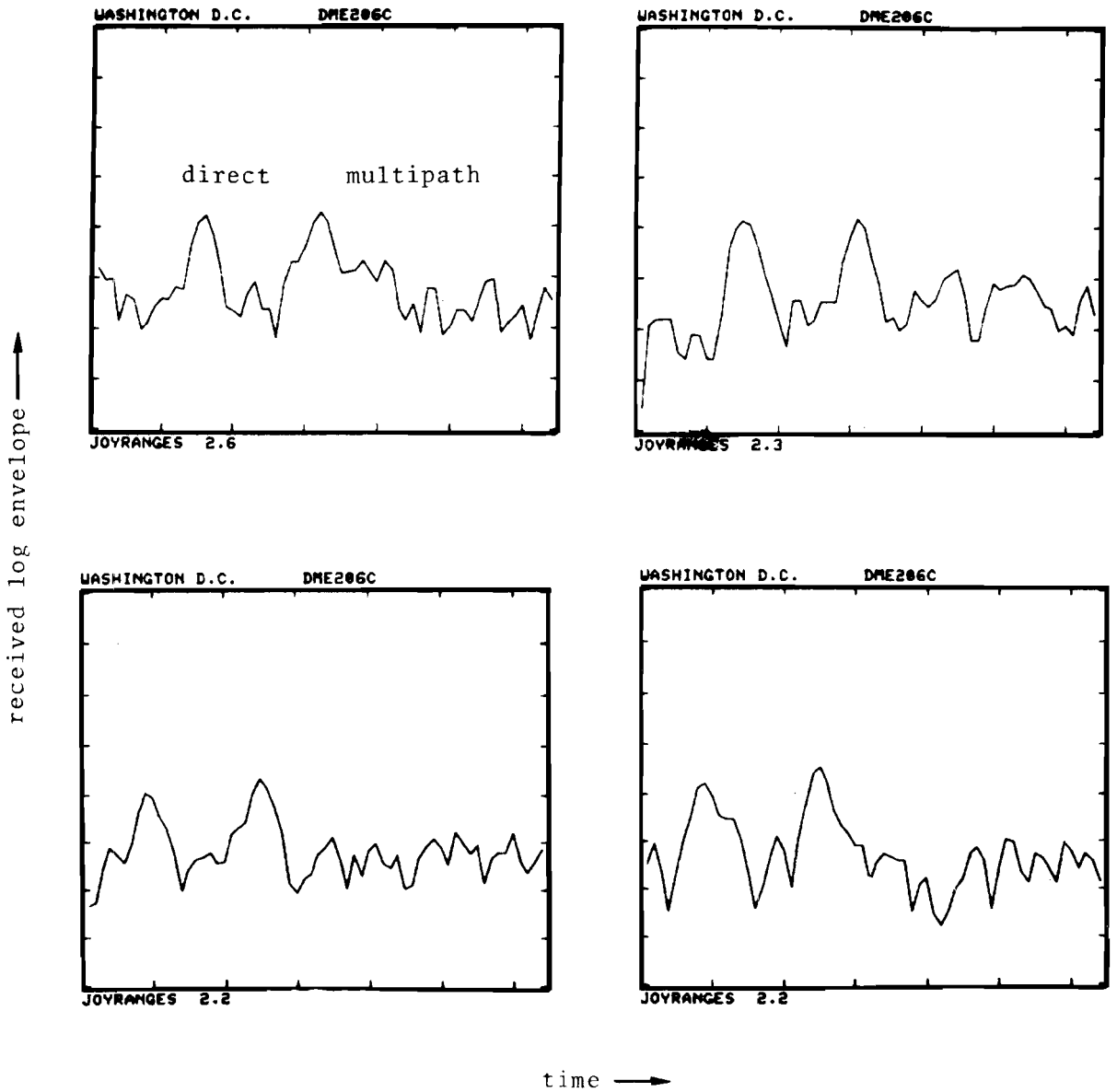

Fig. 3-1. Example of received waveforms with multipath (Washington, D.C. at 1 nm from threshold).

The first multipath signal encountered after the direct signal is denoted by an "X" in the M/D level and τ plots. Succeeding multipath signals, if any, are denoted by the letters Y, Z, A, and B, respectively, on both plots.

Several special cases deserve mention. The replies of other ATCRBS transponders to other ATCRBS interrogators may lie within the data recording interval. These "fruit" pulses are readily identified since their pulse width is approximately 450 nsec (see Fig. 3-2). Measurements with fruit present are flagged in the summary plots with an "F" at an M/D level of -30 dB as a warning that the data on that individual measurement may have been corrupted by the fruit.

If the amplitude at the beginning of the digitized interval is above the threshold, but decreasing, the data is ignored until the amplitudes begin to arise. This is done to avoid declaring the end of a "fruit" pulse as the direct signal.

Occasionally, the A/D converters would fail to properly track a rapidly rising signal for one sample on the leading edge. This gave rise to sharp "glitches" in the digitized waveform (see Fig. 3-3), which was completely inconsistent with valid pulses passing through the IF filters. Since these artifacts arose only on the leading edge of high level pulses, it was straightforward to recognize them and reduce their effects by replacing the "glitch" level by the average of the adjacent samples (equivalent to interpolation between the adjacent samples).

The manual method of setting the 3.2 μs waveform sampling aperture is, of course, vulnerable to loss of data if the sampling gate drifted too far away from the F1 pulse. To a significant degree, situations in which this arose could be identified by erratic time behavior in the tracking gate range versus time plot since the actual flight profiles along runway centerline were flown at roughly constant velocity. Time intervals where erratic behavior arose (see, e.g., Fig. 3-4) were generally excluded from analysis.

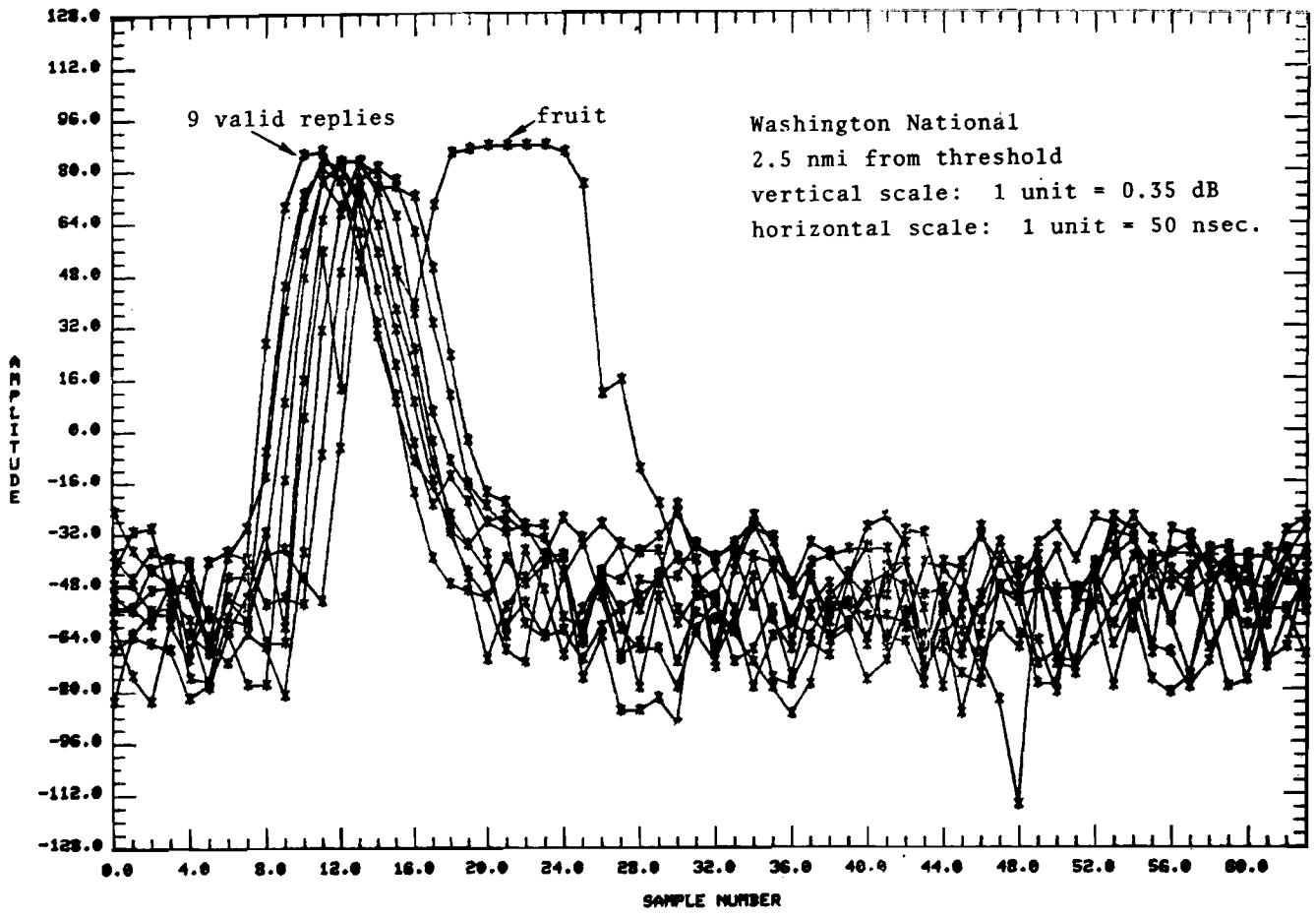

Fig. 3-2. Example of fruit interference.

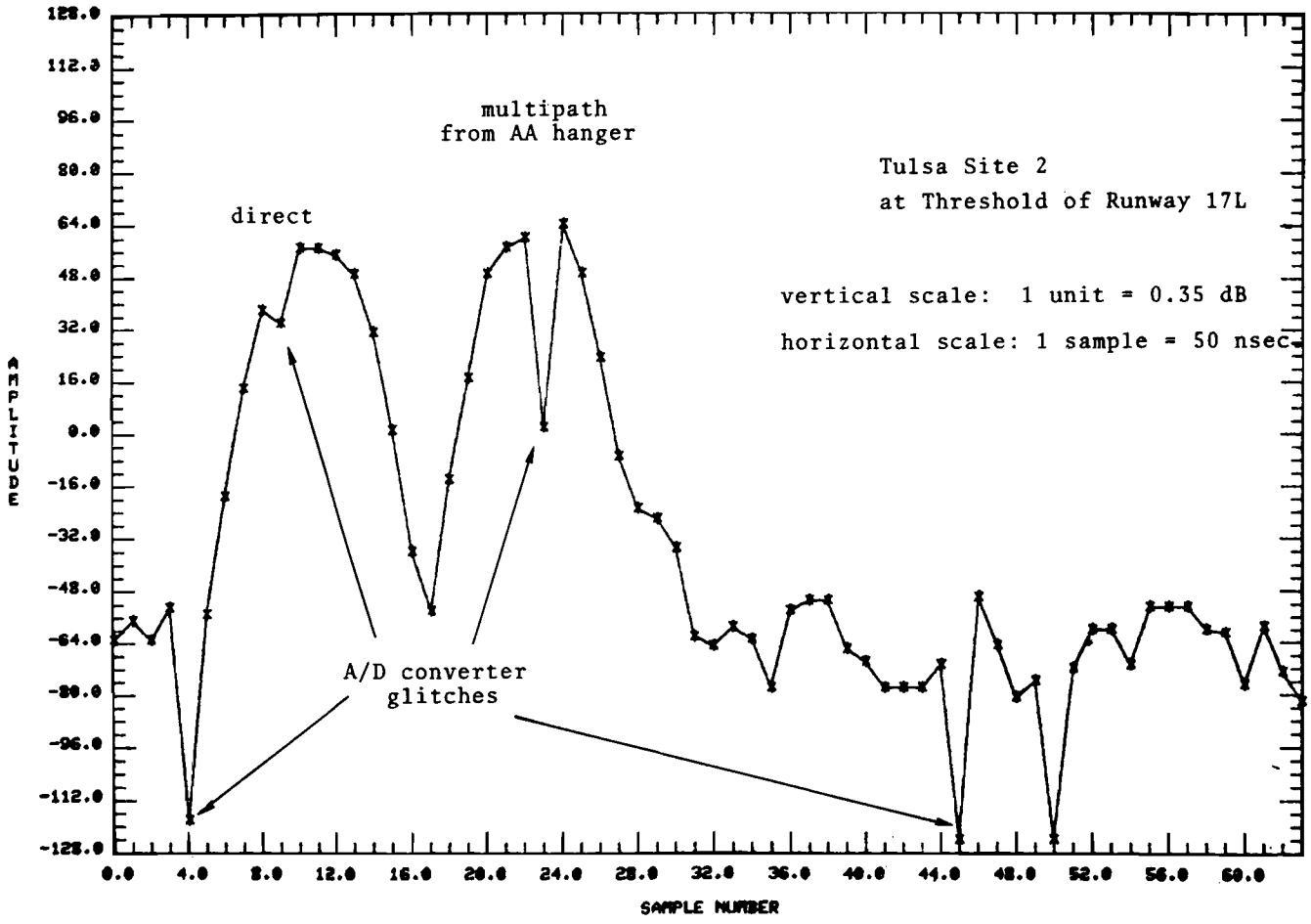

Fig. 3-3. Example of irregular A/D converter action.

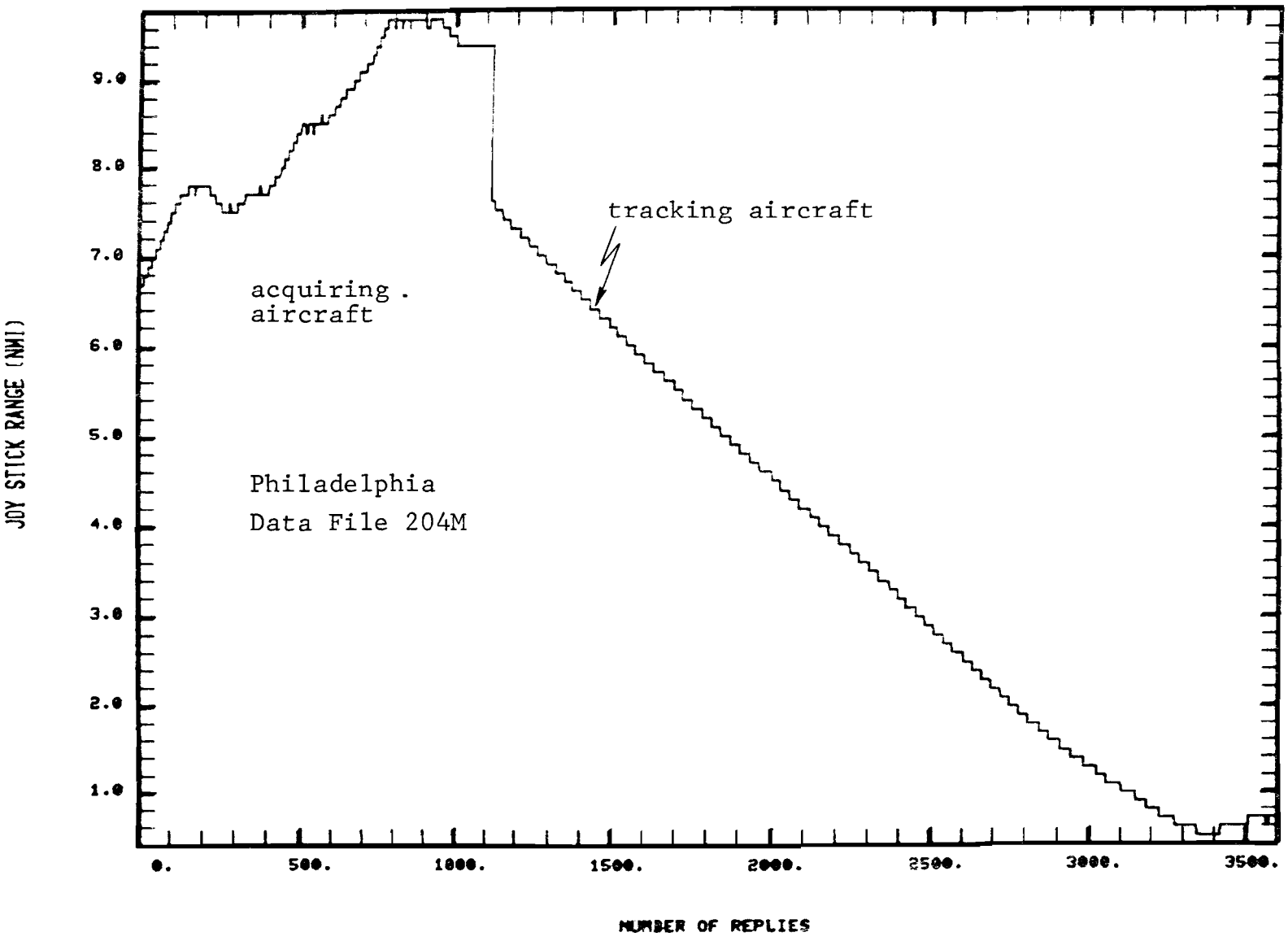

Fig. 3-4. Example of tracking gate effective range.

It had been hoped that the PALM range output [5], which determines the round trip time to the F1 pulse arrival using a simple amplitude comparison within the manual tracking gate, would also be useful in delineating loss of track. However, it gave very erratic behavior in many cases which cannot be explained in terms of tracking gate misalignment (see, e.g., Fig.3-5). Our current hypothesis is that either the severe multipath environment may have caused erratic triggering and/or the triggering circuit may have been defective.

The other function of the PALM ranging mode was to have been to furnish a distance reference for correlation of different approaches and correlation with simulation results. The raw sampling window position (i.e., "joystick" range) was not satisfactory in this respect due to its coarse quantization (0.1 nmi). However, by fitting a piecewise linear function to the measured joystick range versus time, it was possible to generate a smoothed (i.e., interpolated) range versus time plot which would yield the desired range quantization. Such a smoothed range function was created for each approach and used as the ordinate for both M/D level and τ plots*.

Diffuse reflections may be viewed as specular reflections from many small reflectors, especially irregular terrain features. Theoretical treatments of diffuse scattering from terrain [7] suggest that substantial contributions would come from the so called "glistening surface" which gives rise to a received waveform resembling a Gaussian random process. The validity/utility of such models for terrain reflections at L band has not yet been established experimentally; thus, it was not clear what criteria should be utilized in estimating the diffuse component. One possible criteria is to compare the general background level prior to and following the direct signal. However,

---

*We considered plotting all runs versus time to threshold, but this would have yielded problems in data comparison between approaches made at different ground speeds and/or in cases where the ground speed varied significantly during an approach.

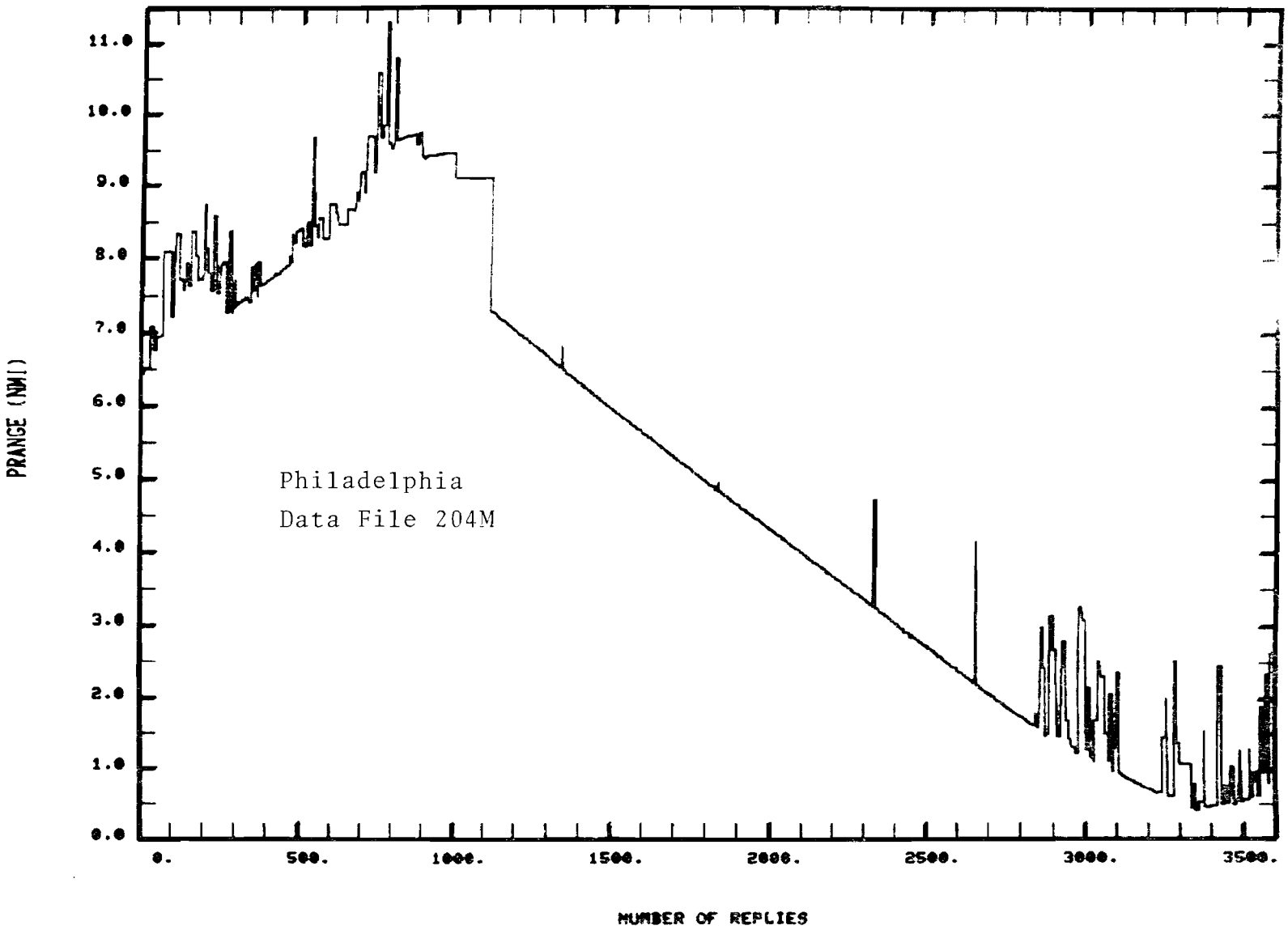

Fig. 3-5. Example of measured PALM range output

this did not yield a clear indication of the diffuse multipath level on the cases attempted due to

(1) insufficient waveform data prior to the direct signal

and

(2) corruption of the metric by specular pulses

Additionally, the diffuse multipath delays between 0 and 200 nsec are of the greatest practical interest and these would be obscured in all cases by the direct signal pulse.

IV. LAMBERT-ST. LOUIS INTERNATIONAL AIRPORT

A. Multipath Environment

Figure 4-1 is an aerial photograph of Lambert-St. Louis International Airport which shows the reflection rays corresponding to the major anticipated threats for an aircraft landing on runway 12R (currently a category I ILS runway). Fig. 4-2 shows additional airport geometry details. The major multipath threats were expected to be the large McDonnell Douglas (M-D) aircraft factory buildings shown in Figs. 4-3 to 4-4. The main factory building has predominantly masonry fronts (Gunite) punctuated by windows, while hangars 42 and 45 have several large vertical doors with windows.

The various low buildings (e.g., aircraft shelters) and a parking lot between the buildings and the threshold of runway 12R are expected to prevent some of the building reflections from reaching a receiver, especially if the receiver is at a low altitude. Similar circumstances arise for reflections from the terminal buildings shown in Fig. 4-5.

The expected multipath relative time delays for a centerline approach are as follows:

Building	τ (nsec)
McDonnell-Douglas main factory	1440
McDonnell-Douglas Hangar 42	2440
McDonnell-Douglas Hangar 45	3300
Terminal buildings	310

The runway contour (shown in Fig. 4-6) slopes downward from the localizer site toward the approach end of the runway. Thus, it was not deemed necessary to erect the receiver antenna to its full height*. The transmitter antenna was sited to the immediate left of the ILS localizer as shown in Figs. 4-1 and 4-2 with a phase center height of approximately 10 feet. Figure 4-7 shows the equipment at the measurement site. At the time the measurements were made,

*Obstruction clearance criteria also entered in this decision.

108795-R

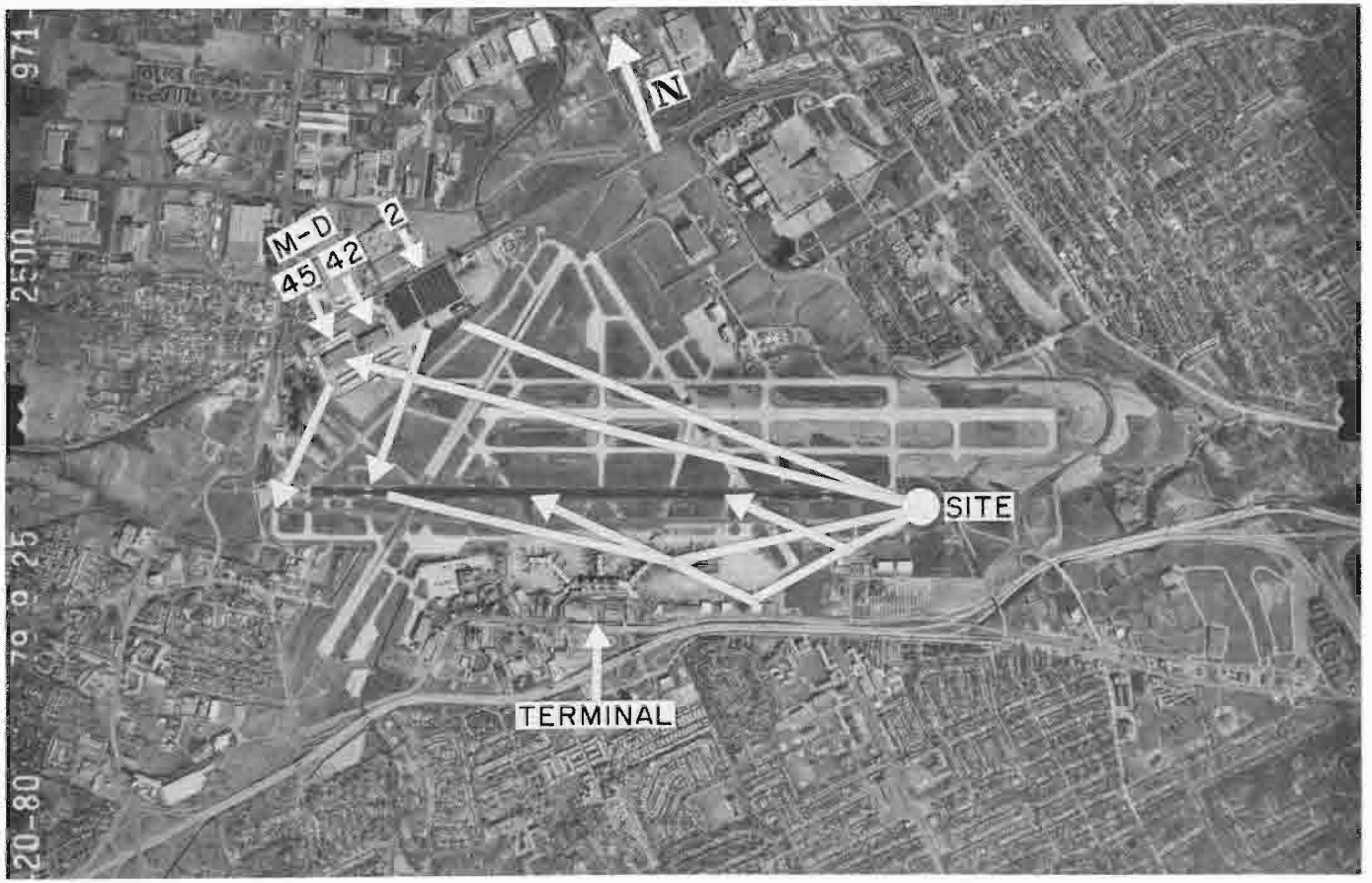

Fig. 4-1. Lambert-St. Louis International, St. Louis, Missouri, showing azimuth reflection paths.

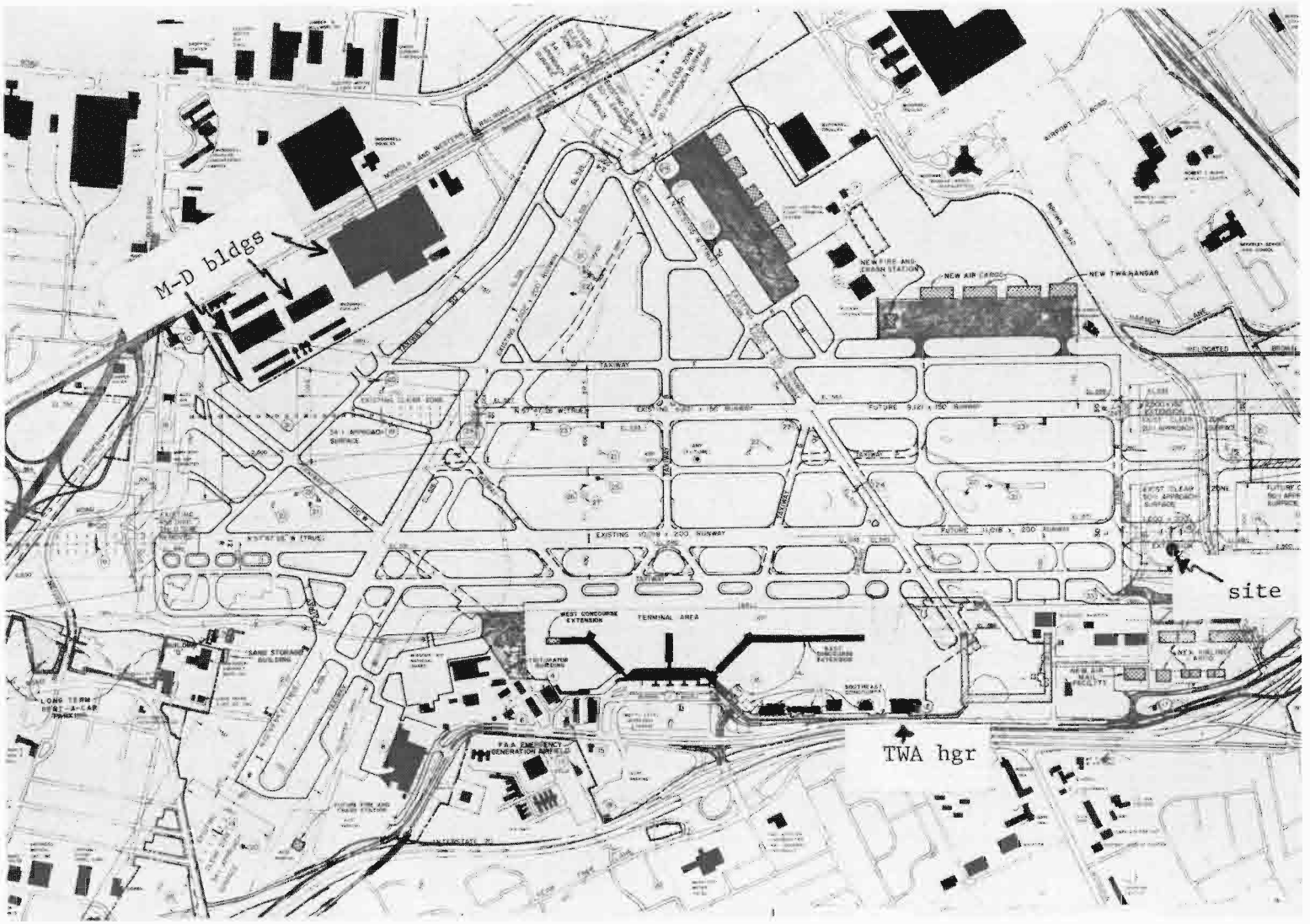

Fig. 4-2. St. Louis - Lambert Airport Layout.

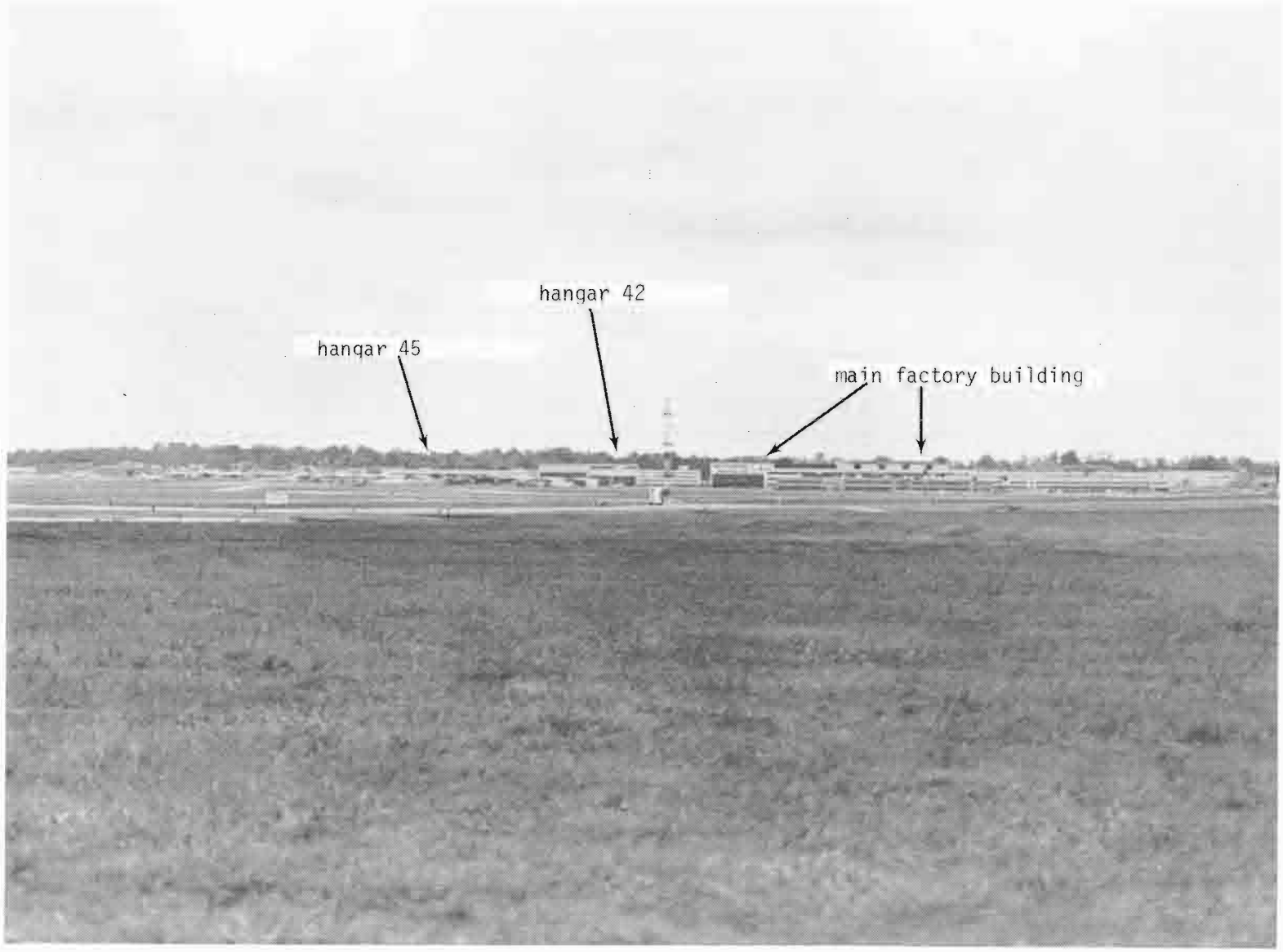

Fig. 4-3. McDonnel-Douglas buildings as seen from ILS localizer site.

Fig. 4-4. ILS localizer and McDonnell-Douglas buildings from St. Louis multipath measurement site.

Fig. 4-5. St. Louis (Lambert) terminal area buildings as seen from measurement site.

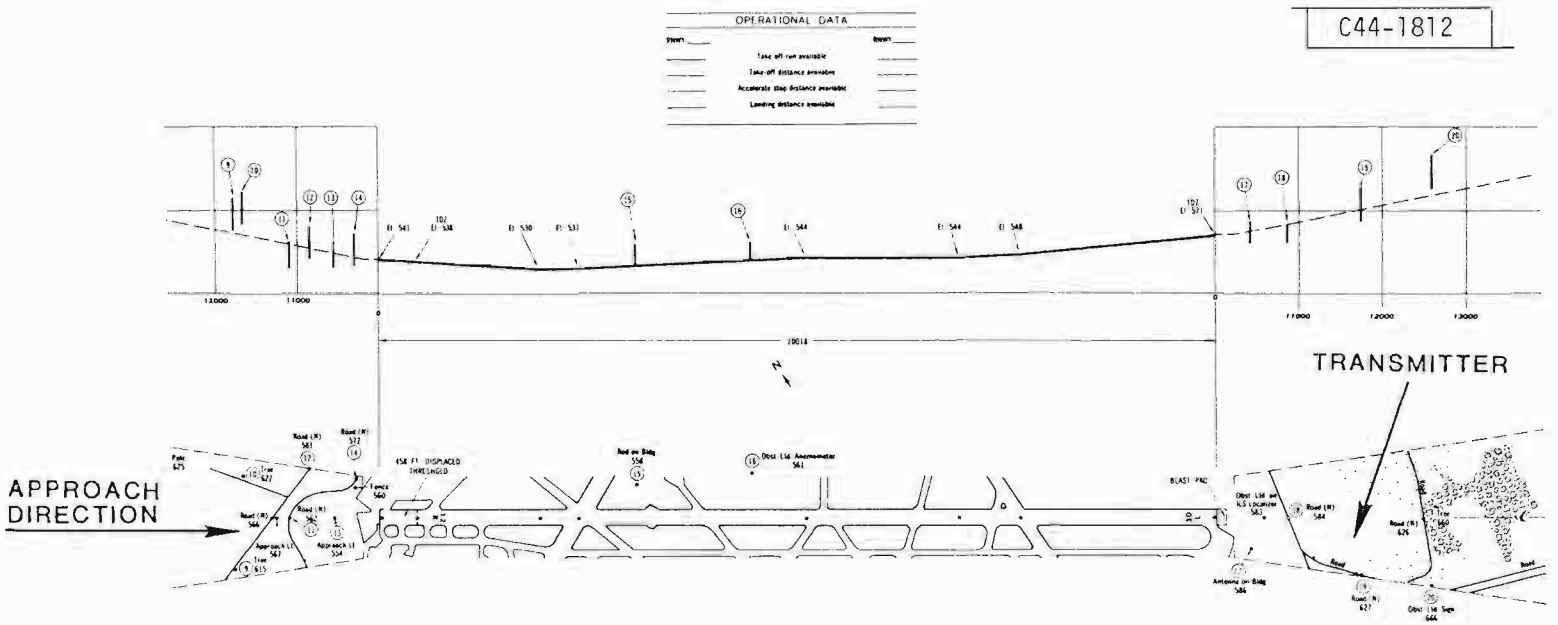

Fig. 4-6. Runway 12R-30L contour at Lambert Field - St. Louis.

Fig. 4-7. Multipath measurement equipment being erected at St. Louis (Lambert).

the ground was covered by approximately one foot of snow with two to three foot deep drifts in the grass covered areas, but the runway was clear.

B. Measurements Made

Table 4-1 summarizes the measurements made at St. Louis. A total of two taxi tests and 14 centerline approaches at approximately 110 knots were made between the hours of 12:32 a.m. and 3:30 a.m. February 13. This late hour was necessitated by the air traffic activity at the airport.

C. Waveform Analysis Results

All of the approaches accomplished at St. Louis have been analyzed and representative results will be described in this section.

The taxiway tests were inconclusive due to low SNR caused by a depression in the taxiway. By increasing the narrow pulse width to 200 nsec, the transponder output power was increased enough to permit reply tracking on the approaches.

Figure 4-8 shows the multipath levels and corresponding time delays for a centerline approach with a 50 foot threshold crossing height. Figures 4-9 and 4-10 show the corresponding results for two other tests with the same nominal flight profile. Figures 4-11 to 4-14 show representative waveforms corresponding to high M/D levels in the region near threshold and when over the runway.

None of the approach data summaries indicated any specular multipath in the region of 2.3 nmi to 0.3 nmi from the threshold*. The region near threshold where multipath is expected (recall Fig. 4-1) corresponds to 1.7 nmi in joystick range.

We see that moderate to low level multipath is indeed encountered in that

*Isolated multipath declarations which do not correlate with adjacent samples as far as M/D level τ are concerned and, do not appear on other nominally identical profiles are assumed to be due to fruit and/or low SNR.

TABLE 4-1

PDME MULTIPATH MEASUREMENTS AT LAMBERT (ST. LOUIS) INTERNATIONAL AIRPORT
February 13, 1981

Taxiway Tests:

2 runs transmitting/receiving through top antenna on aircraft (runs 213A, 213B)

Flight Tests:

1. Profile 1 (3° glideslope, 50-foot threshold crossing height, 15-foot height along runway)

   10 runs [runs 213C through 213K, 213P, 2130, one run aborted (213C)]

2. Profile 2 (3° glideslope, 25-foot threshold crossing height, 10-foot height along runway)

   4 runs (runs 213L through 2130)

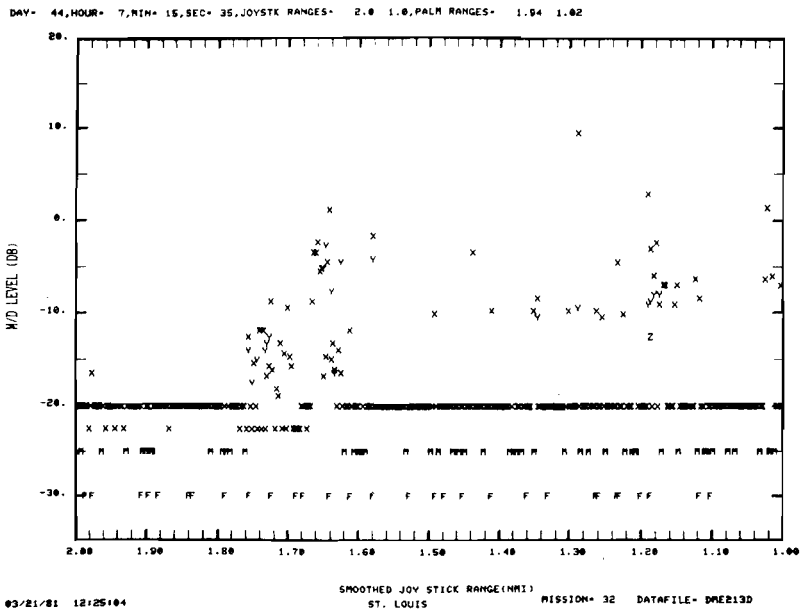

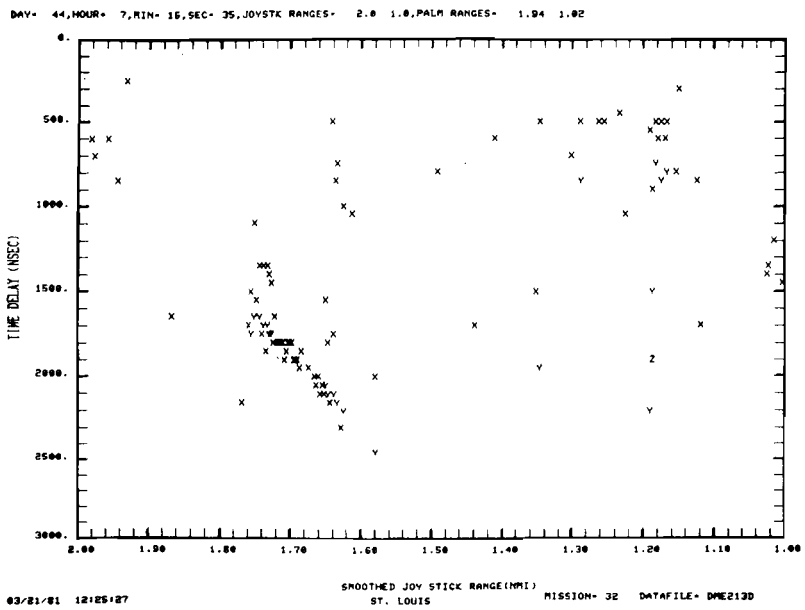

Fig. 4-8a. Data summary for St. Louis's approach with 50 ft. threshold height.

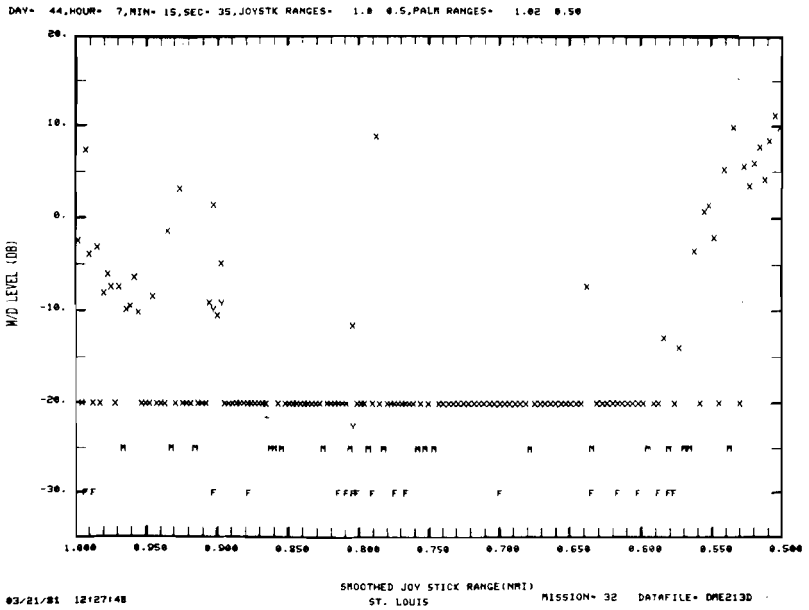

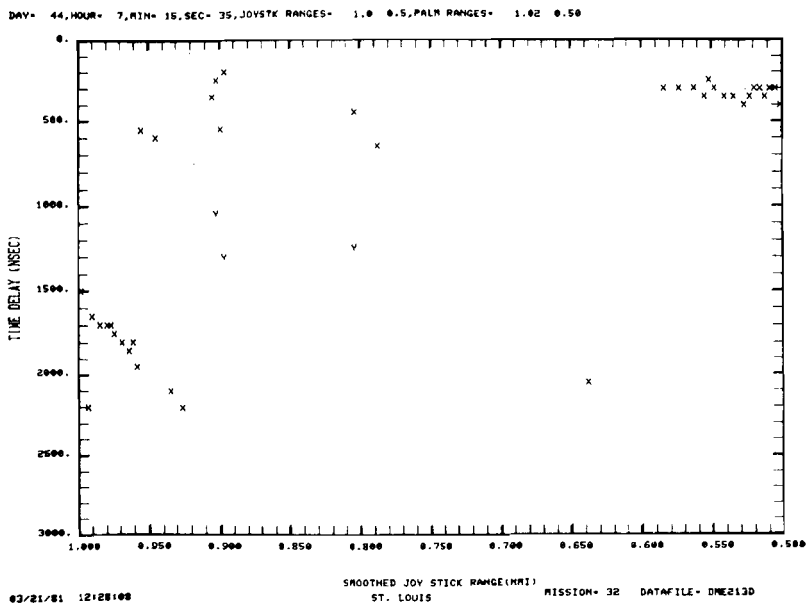

Fig. 4-8b. Data summary for St. Louis's approach with 50 ft. threshold height.

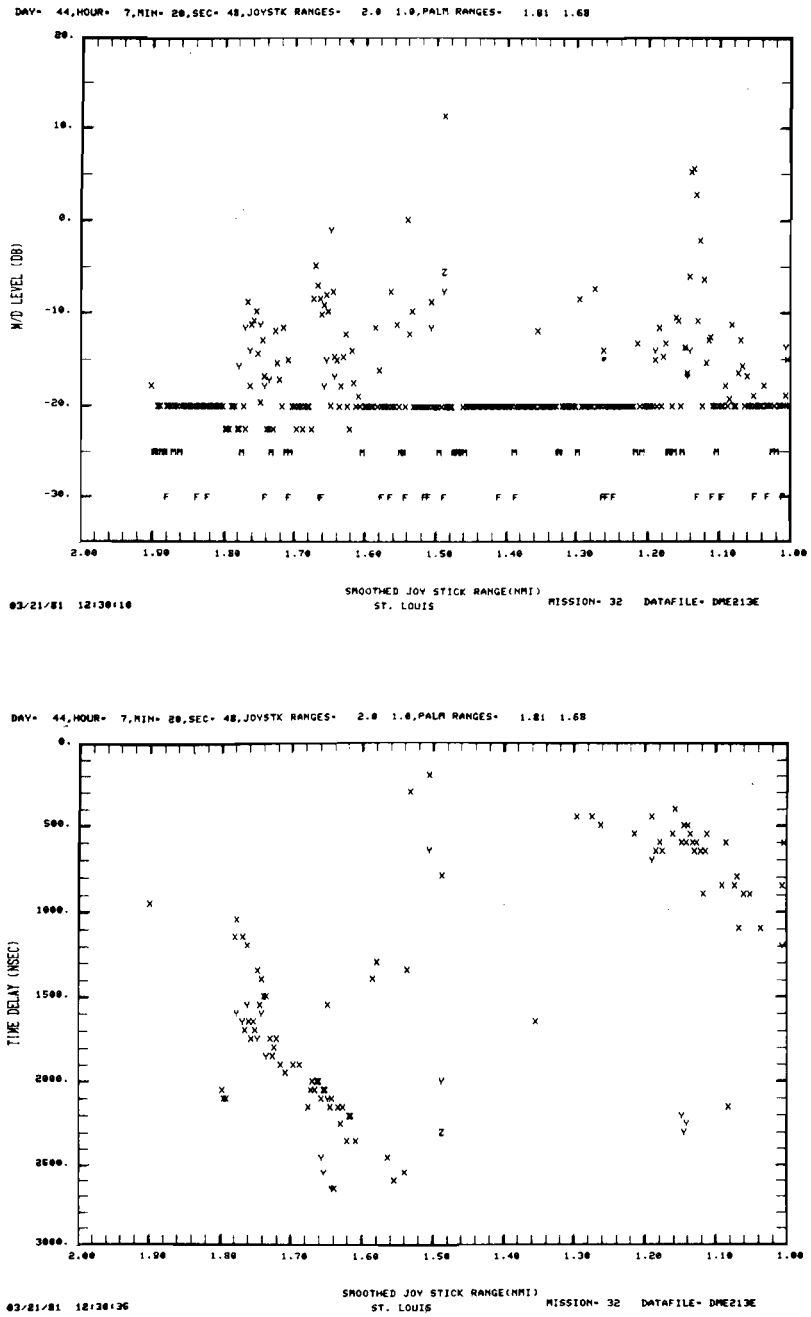

Fig. 4-9a, Data summary for St. Louis's approach with 50 ft. threshold height.

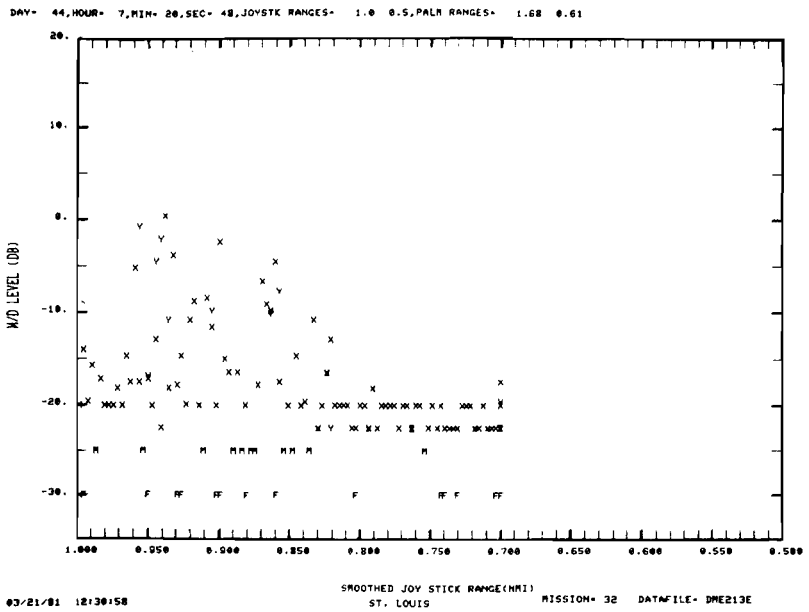

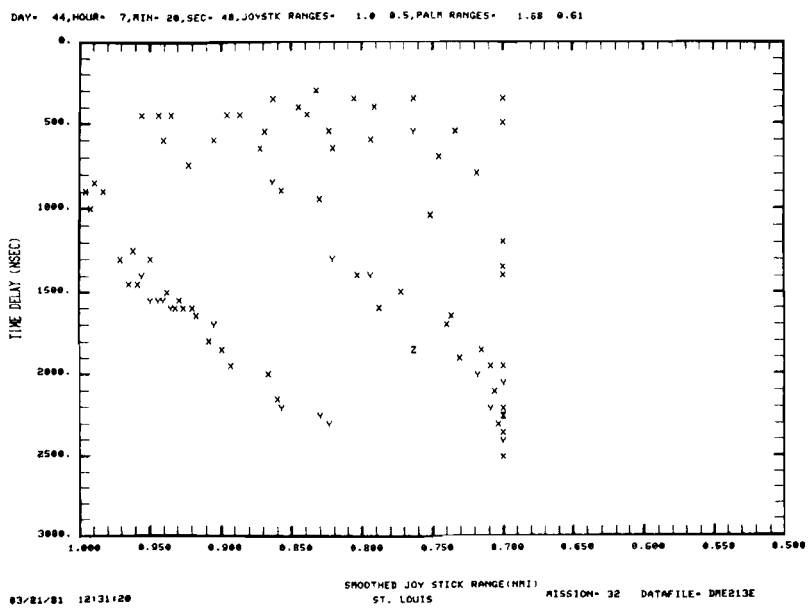

Fig. 4-9b. Data summary for St. Louis's approach with 50 ft. threshold height.

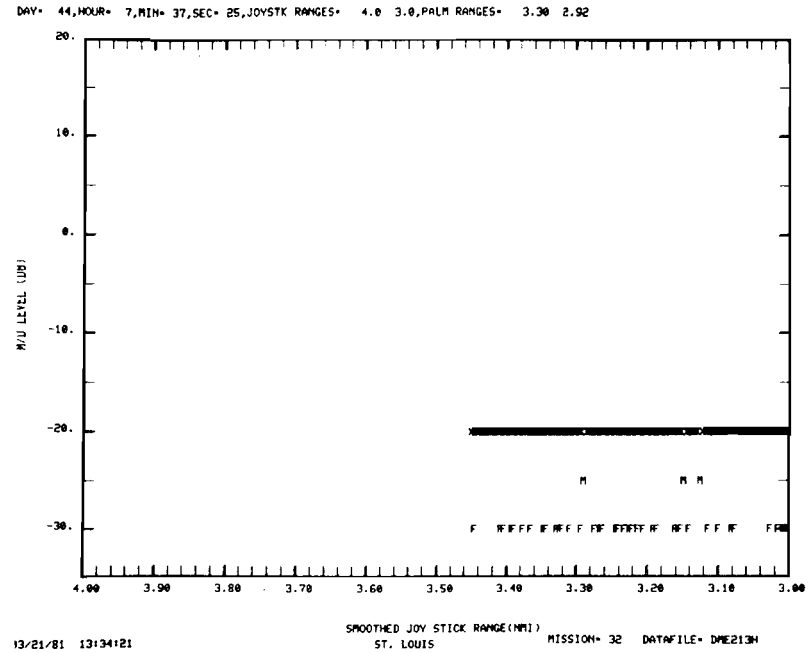

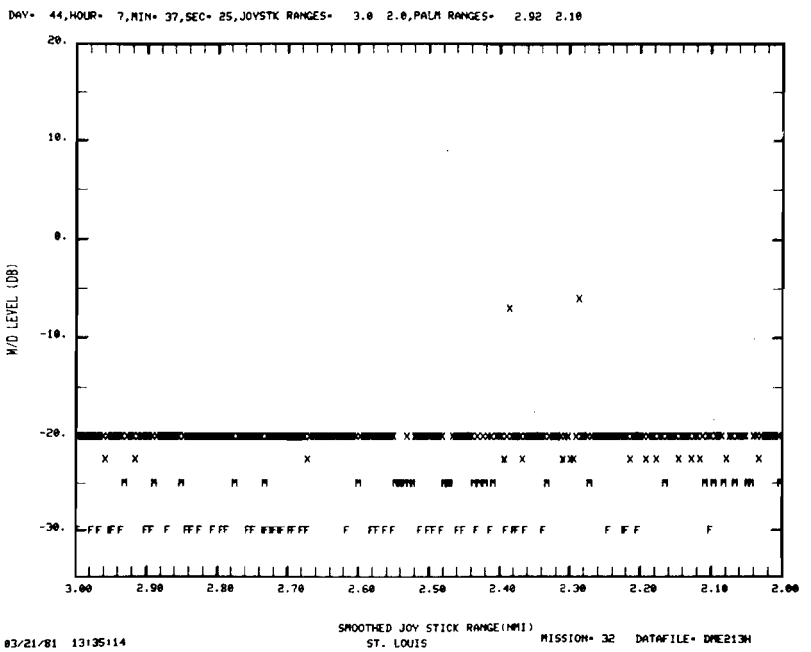

Fig. 4-10a. Data summary for St. Louis's approach with 25 ft. threshold height.

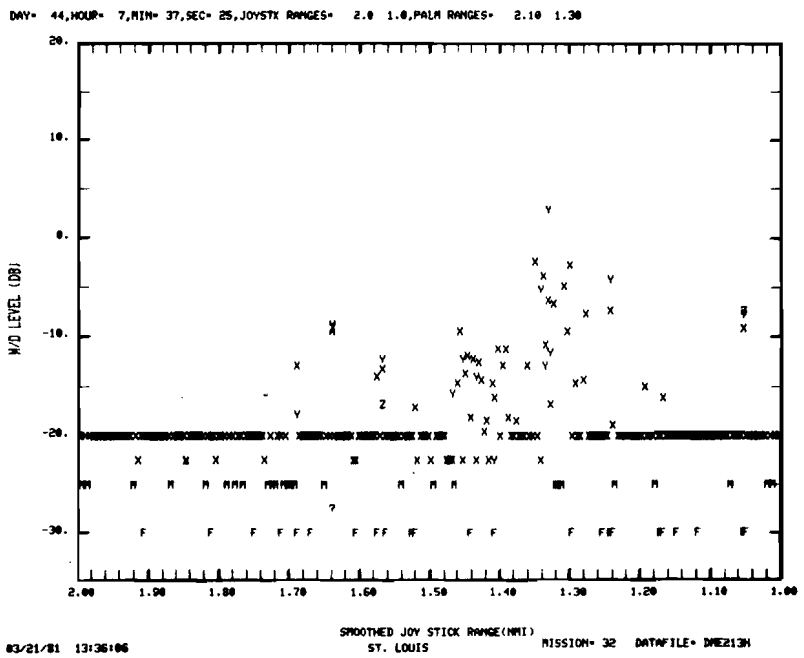

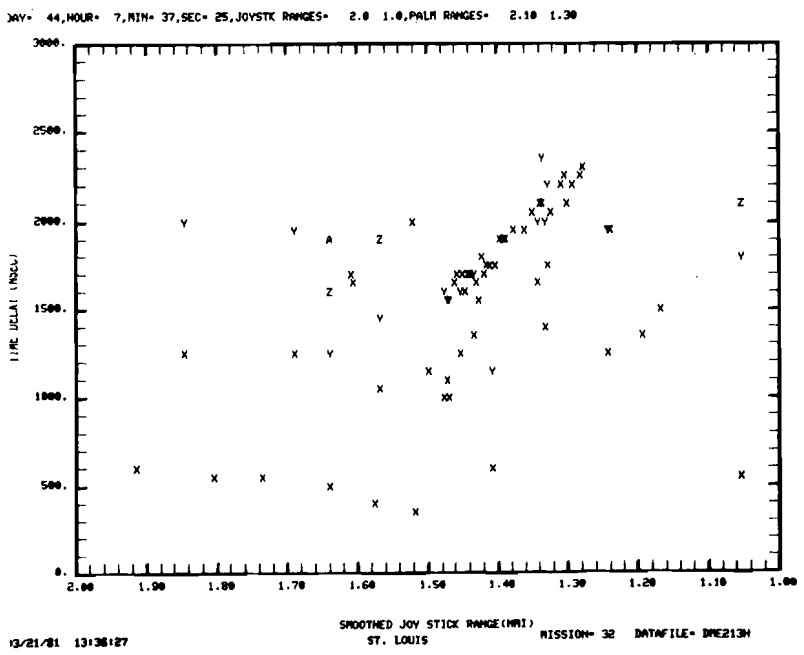

Fig. 4-10b. Data summary for St. Louis's approach with 25 ft. threshold height.

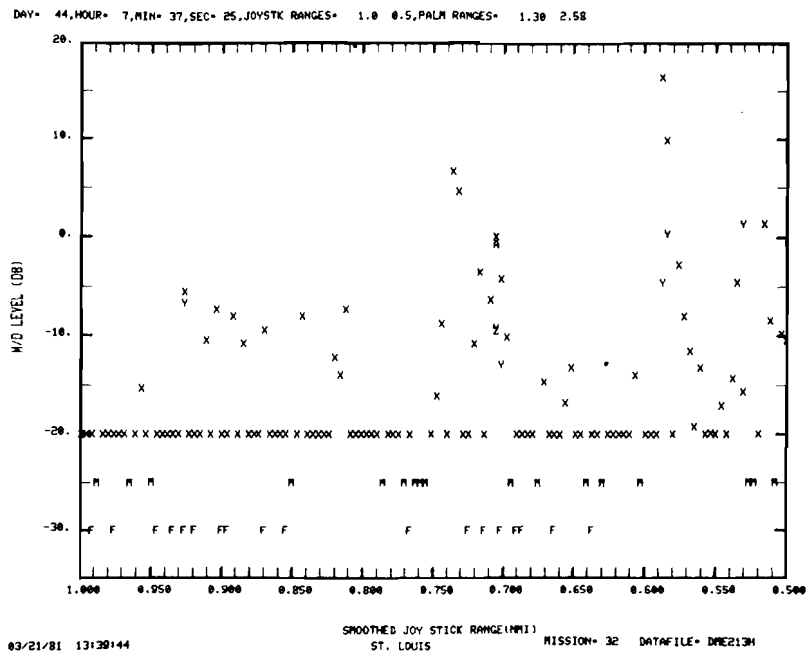

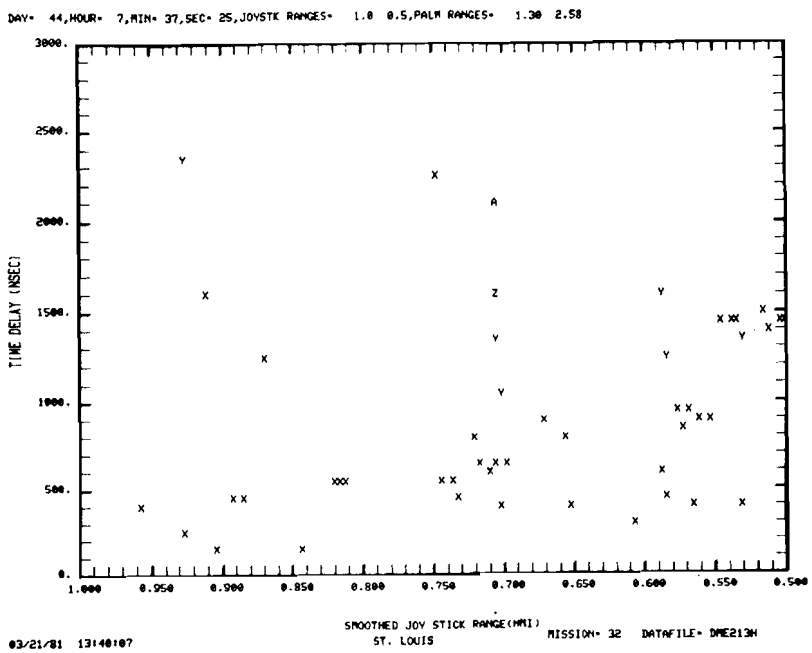

Fig. 4-10c. Data summary for St. Louis's approach with 25 ft. threshold height.

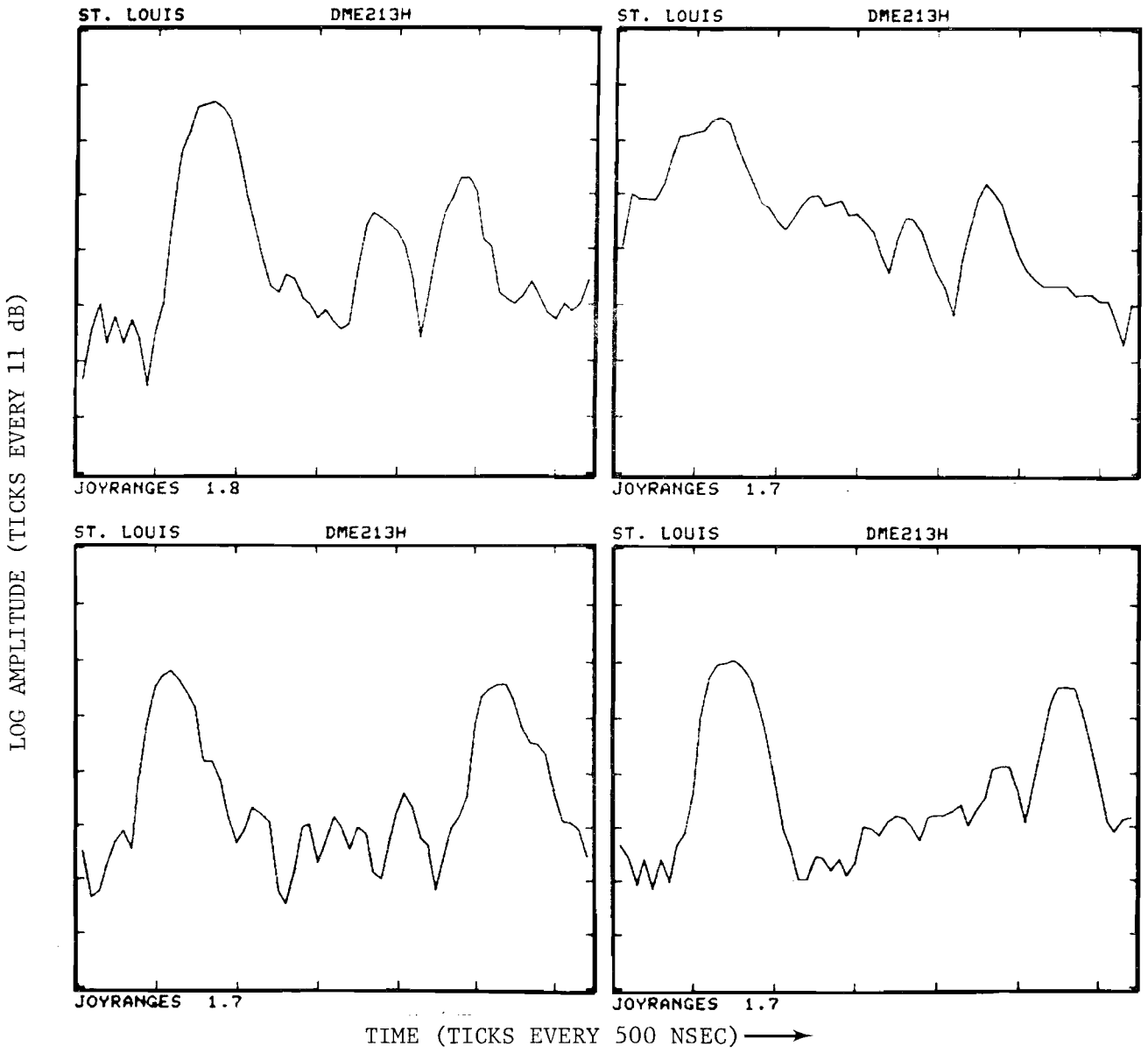

Fig. 4-11. St. Louis waveforms at threshold (50 ft. AGL).

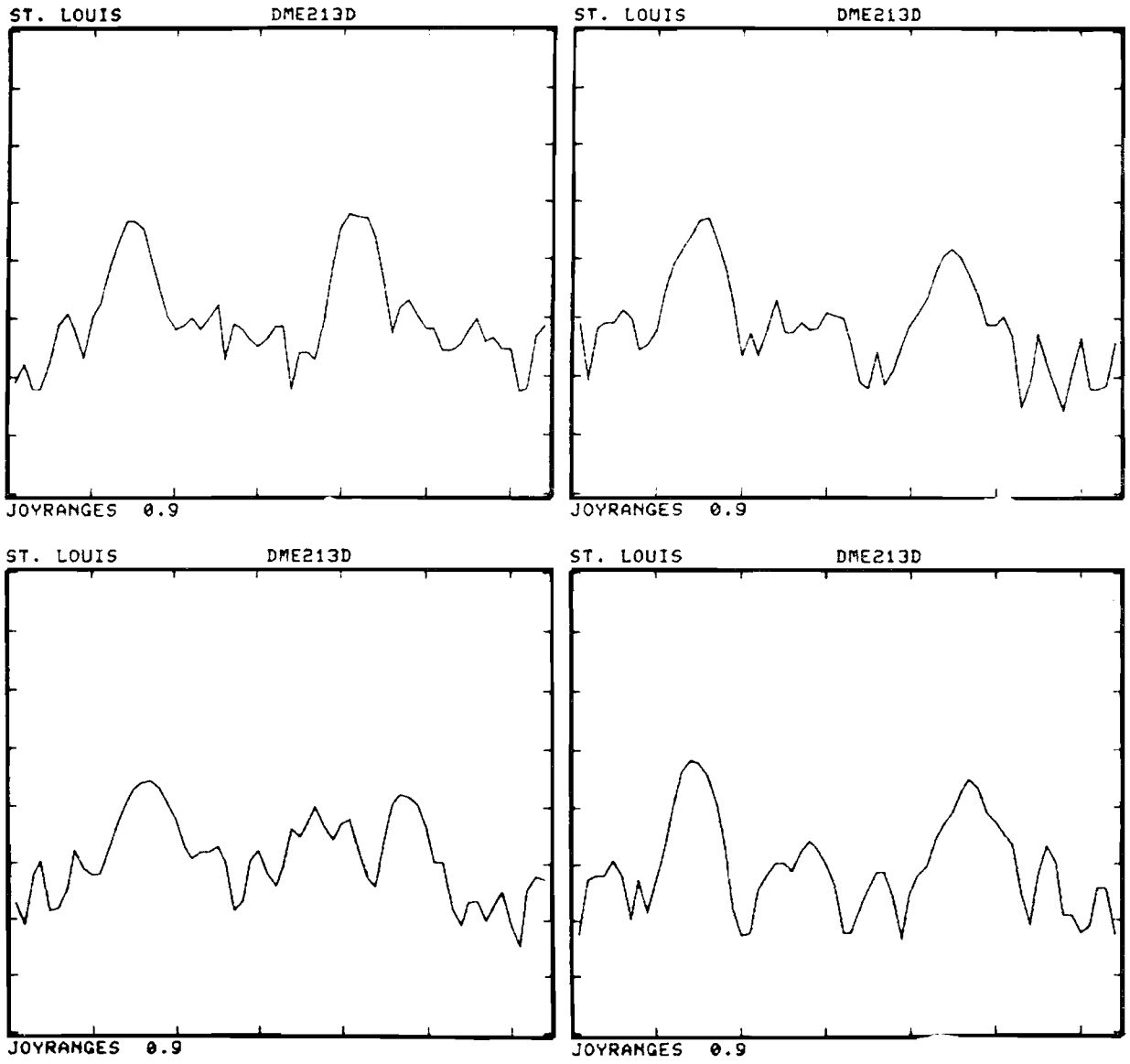

Fig. 4-12. St. Louis waveforms at 1 nmi from localizer (25 ft. AGL).

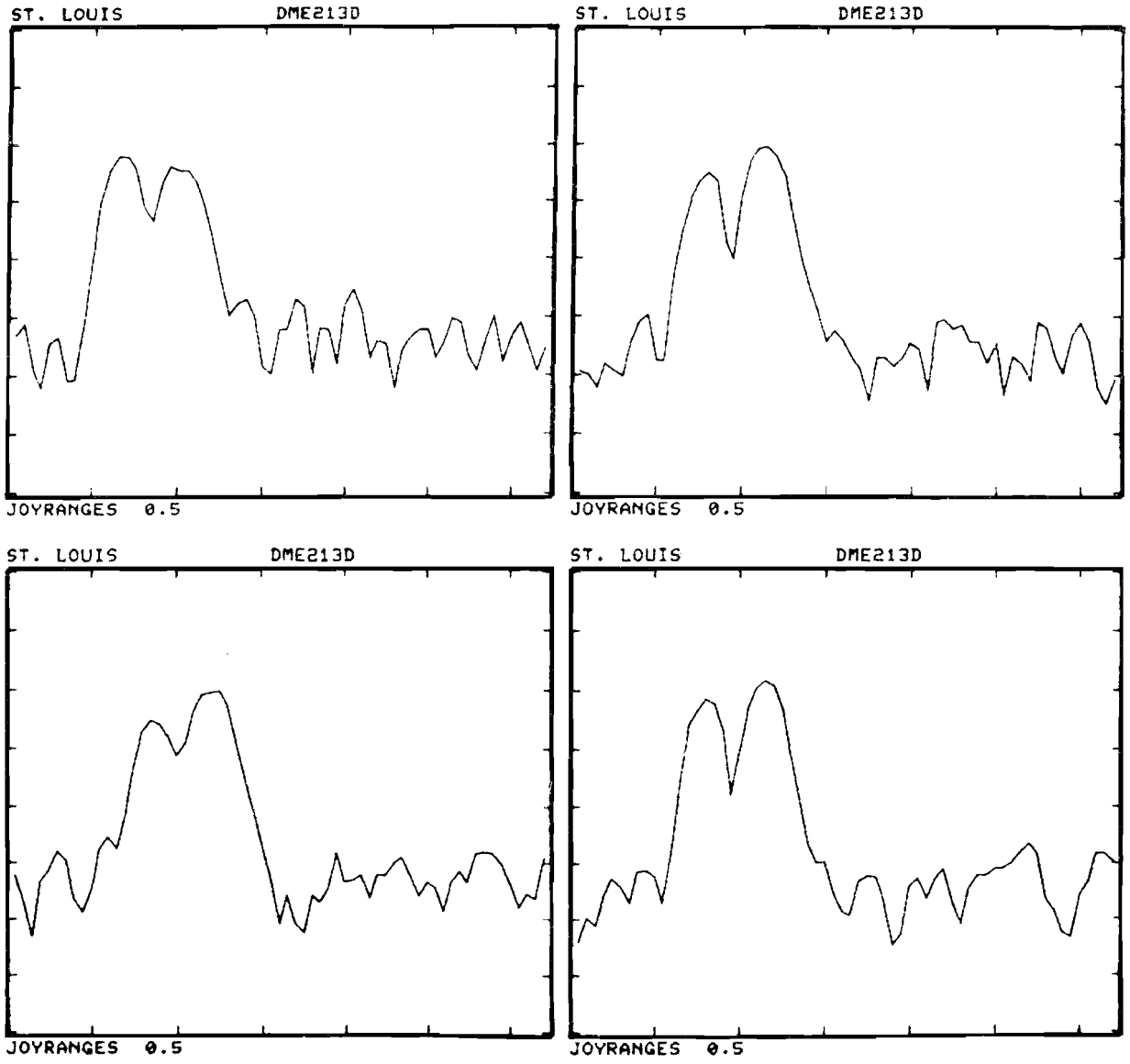

Fig. 4-13. St. Louis waveforms 0.5 nmi from localizer (25 ft. AGL).

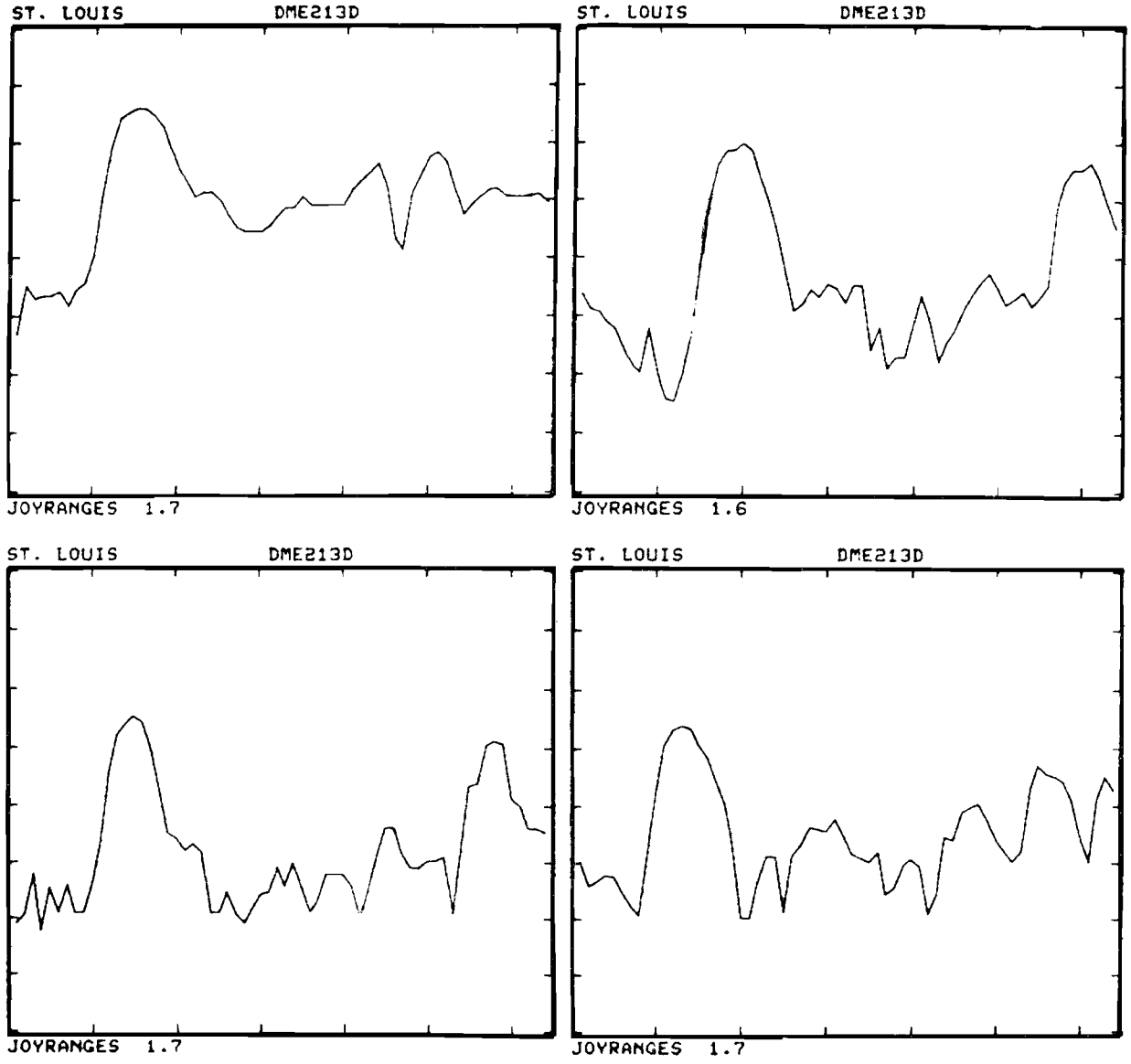

Fig. 4-14. St. Louis waveforms at threshold (25 ft. AGL)

TABLE 4-2

FLIGHT PROFILE FOR LAMBERT SIMULATION

Way Point	Distance From Threshold (nmi)	Distance Along Flight Path (feet)	Height (ft)
1	0.50	0	200
2	0.00	3000	50
3	-0.083	3500	29
4	-0.16	3804	20
5	-1.32	10854	20

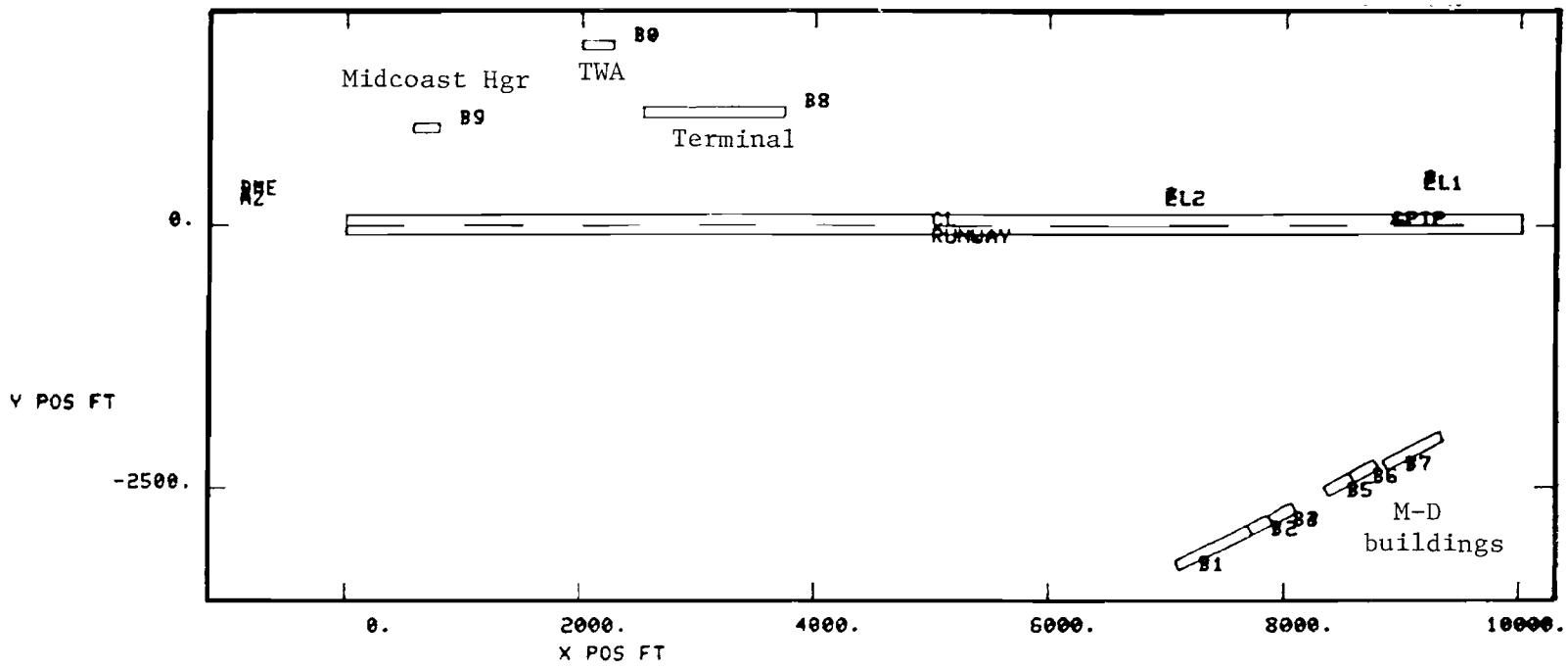

DME peak levels

OBST	RANK	AMP	DIST	RDOP
G	3	0	3820.0	-0.
B1	7	9	4600.0	-88.
B2	5	4	4380.0	-85.
B3	8	9	4200.0	-85.
B4	9	11	4200.0	-85.
B5	10	11	3640.0	-82.
B6	11	12	3420.0	-88.
B7	6	8	2880.0	-90.
B8	1	0	5340.0	-3.
B9	4	0	9840.0	-7.
B0	2	0	7280.0	-11.

Fig. 4-15. Airport map for Lambert - St. Louis simplified scenario.

region with multipath delays in the expected range of delays (1.4 μs to 2.4 μs). Further down the runway, high level (> -6 dB M/D) is encountered with delays of approximately 300 - 500 nsec as well as some multipath with long delays. We attribute the short delay multipath to reflections from the terminal area buildings while the longer delay multipath probably arises from the fences and parking lots, etc. in front of the McDonnell-Douglas hangars.

There are some noticeable differences betwen various flights in terms of precise joystick range at which the threshold multipath is encountered and the M/D levels. The joystick range differences probably reflect the track gate location relative to the P1 pulse, whereas the M/D level differences probably reflect differences in height over runway threshold (the heights shown in Table 4-1 are necessarily approximate given the time of day at which the tests were conducted).

D. Simulation Results

Figure 4-15 shows the airport map for a simulation of the DME measurement geometry. The various McDonnell-Douglas building walls were represented by flat plates whose height corresponded to the physical height except in the case of the east end of the McDonnell-Douglas main factory which was represented by two separate plates to account for the interspersing of glass windows with metal and stucco siding. The terminal building wing was represented by a single 50 foot high flat metal plate as were the TWA and Midcoast Aviation hangars. The assumed flight profile is shown in Table 4-2. No account was taken of the runway or terrain contours nor of the various intervening obstacles which partially block the building reflections [2].

Figure 4-16 shows the effective* M/D level and relative time delay for the various plates as a function of distance along the flight path. We see that multipath from the M-D building 42 with a level of approximately -8 dB is

*See reference [1] for the definition of effective M/D level.

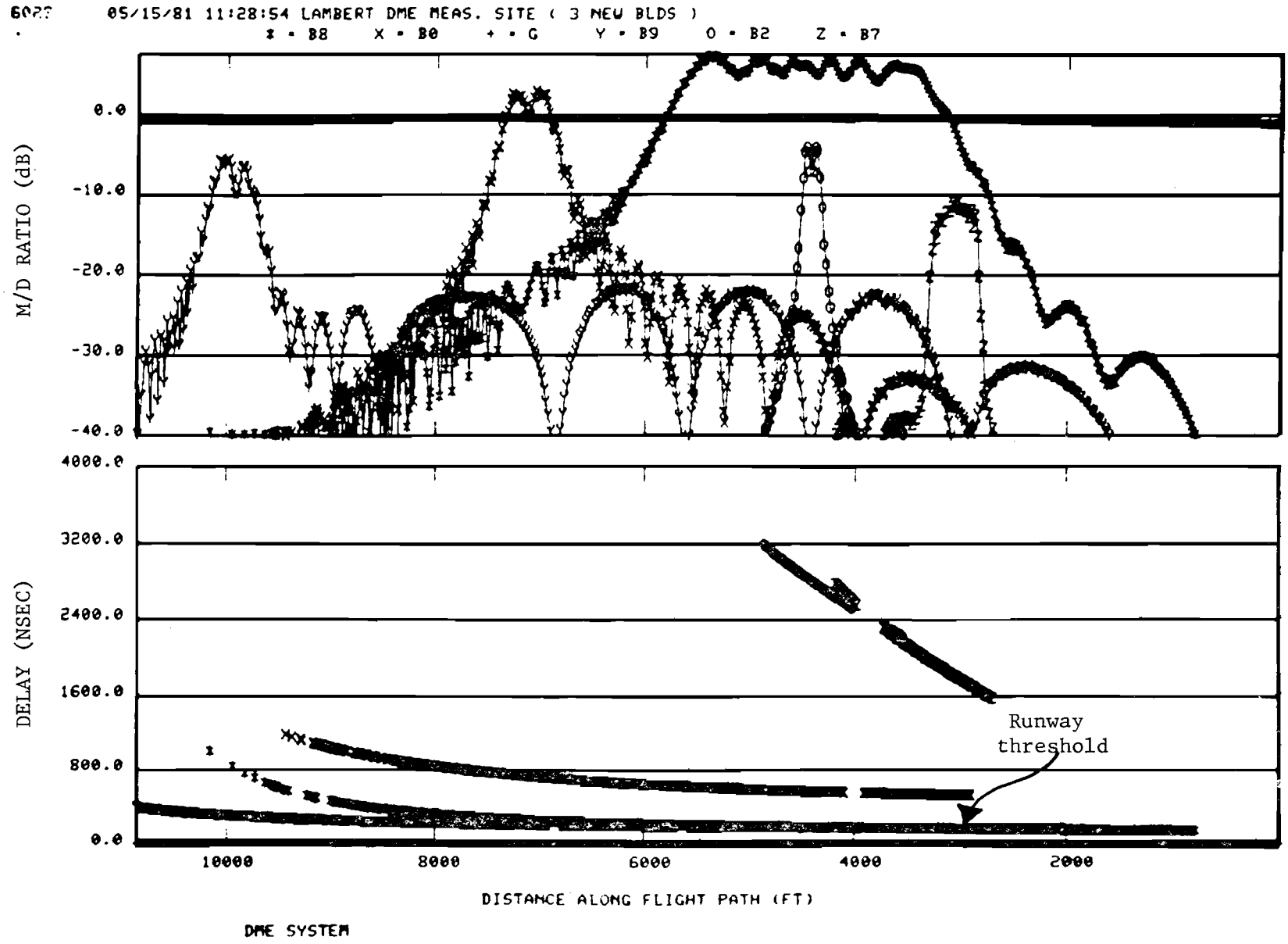

Fig. 4-16. Computed multipath characteristics for Lambert - St. Louis scenario.

expected near threshold with a time delay of approximately 1.4 μs to 2.0 μs. This level agrees reasonably well with the measured results in Figs. 4-8 to 4-10. Similar levels/time delays are predicted from the other M-D buildings in a 1200 foot region (0.2 nmi) starting 1200 feet (0.2 nmi) after threshold and, in fact, this appears to be the case although several very high level M/D experimental points occur which are not suggested by the simulation model. These undoubtedly arise from the complicated fine structure of the M-D building surfaces which was not considered in developing the simulation airport model.

The experimental data multipath after threshold has delays comparable to those predicted for the terminal building east concourse; however, the levels and spatial duration are significantly less than suggested by the simulation result. This dramatic difference arises because the loading gates and parked aircraft block most of the multipath from the building surface. The experimental short duration multipath at 1.0 nmi joystick range correlates with the region predicted for the TWA hangar multipath.

E. Summary

The multipath regions at St. Louis in the approach and flare regions correlated fairly well with the specular regions associated with the large buildings which face the runway. The M/D levels and time delays predicted using the MLS propagation model and a very simple airport model agree fairly well for the M-D buildings modeled, although some isolated measurements suggested M/D levels much higher than predicted.

The measured M/D levels for the terminal concourse wing were substantially lower than suggested by the simple airport model. The low terminal concourse levels are attributed to blockage of the reflection paths by the parked aircraft and jetways. Similar phenomena were noted in C band multipath measurements at Logan airport [13]. The general lower levels in the field data for the TWA hangar reflect blockage by the intervening buildings.

It is interesting to compare these L band M/D levels with the C band levels measured in a previous program [2] which are shown in Fig. 4-17. We see that the L-band multipath levels were considerably (e.g., 10 dB) in excess of those measured at C band in the region approximately 1000 ft. after threshold, but similar in the region near threshold.

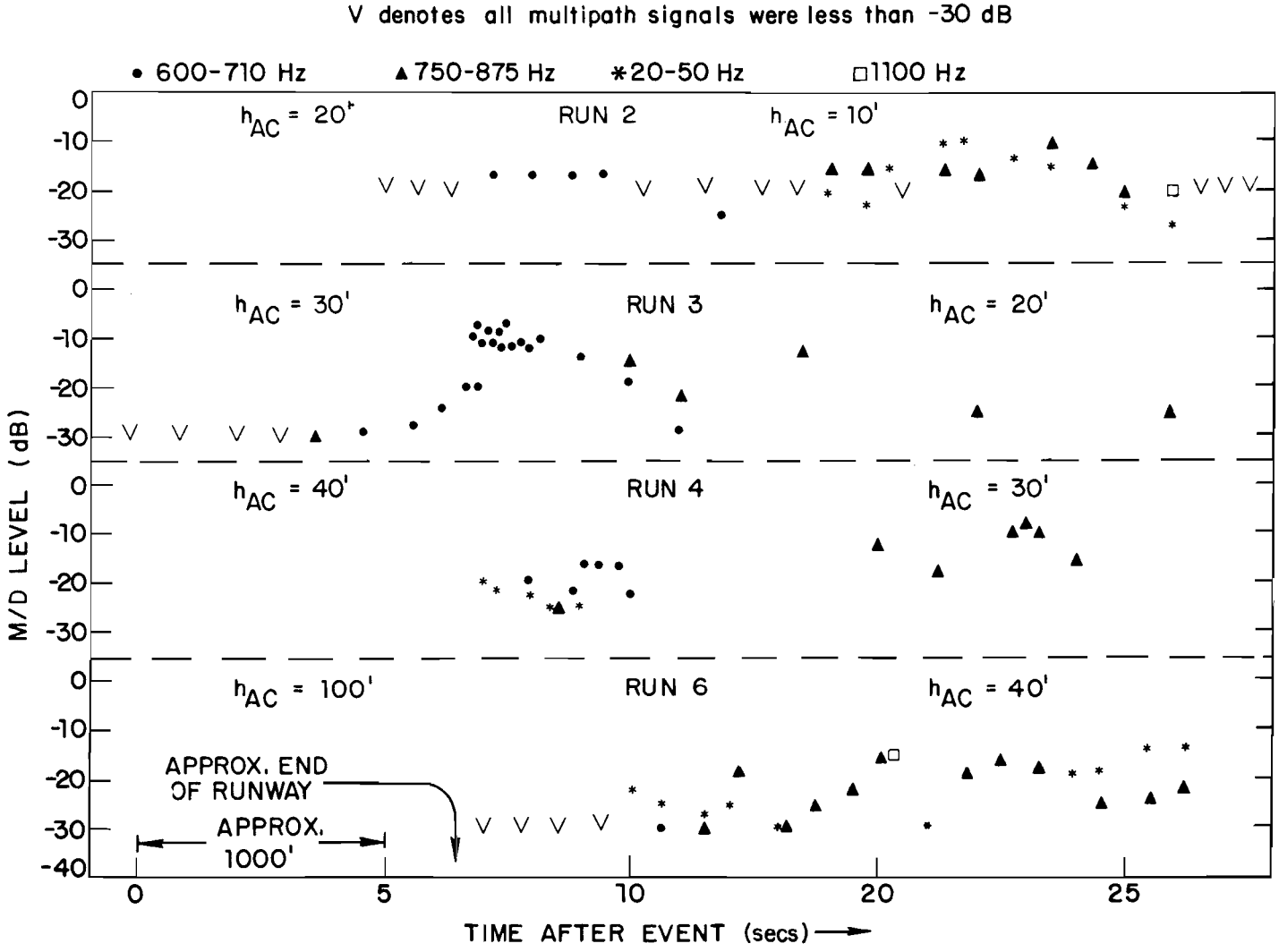

Fig. 4-17. Summary of St. Louis (Lambert) C-band multipath characteristics (from [2]).

V. TULSA INTERNATIONAL AIRPORT

A. Multipath Environment

Figure 5-1 shows a map of Tulsa International Airport together with reflection rays from the buildings most likely to cause DME multipath for aircraft landing on runway 35R (currently a category I ILS runway). These buildings are the American Airlines (AA), Rockwell International, and McDonnell-Douglas (M-D) hangars shown in Figs. 5-2 to 5-4. The large M-D building parallel to and behind the hangar can cause some multipath, but much of it is blocked by various small hangars and other buildings. In contrast, the multipath from the AA hangar is almost totally unblocked by intervening obstacles.

The expected multipath relative time delays for a centerline approach to runway 35R are as follows:

Building	τ (nsec)
M-D hangar	1500
M-D building	2000
AA hangar	700

The runway contour (Fig. 5-5) shows a large hump peaking near the intersection with runway 8-26. For this reason, at site 1, the transmitter antenna was placed on the measurement van at a location adjacent to the building housing the transmitter (Fig. 5-6) for the runway 35R ILS localizer.

Measurements were also made at a second site to discern the multipath environment for aircraft landing on runway 17L. The transmitter site and reflection rays for this site are shown in Fig. 5-7. Considerable difficulties were encountered at this site in achieving an adequate uplink SNR even though the transmitting dish was placed on top of the van. It was found that by using a small dipole antenna mounted on a pole atop the van at a height above ground level (AGL) of approximately 30 feet, that an adequate uplink margin was finally obtained.

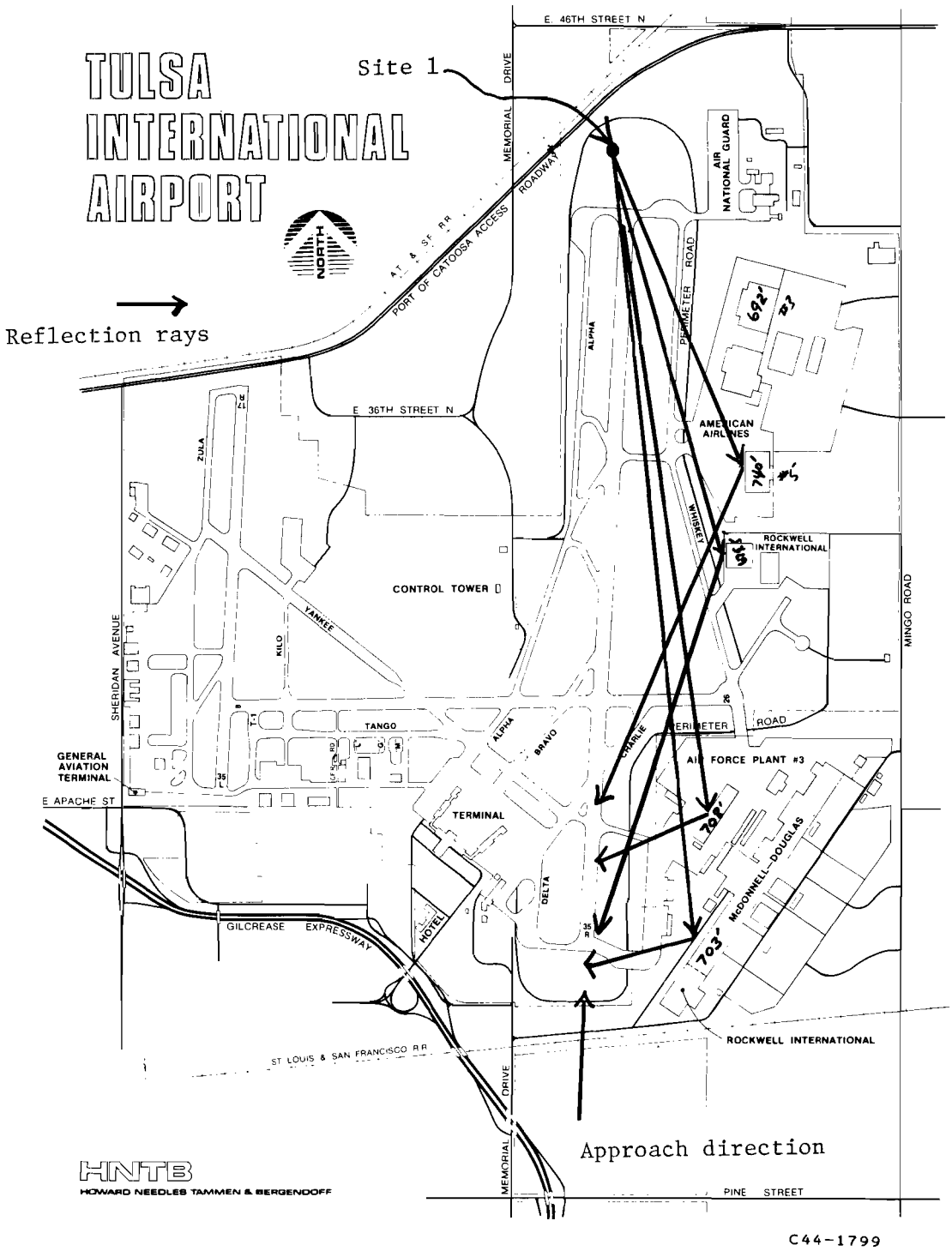

Fig. 5-1. Tulsa Site 1 measurement geometry and reflection rays.

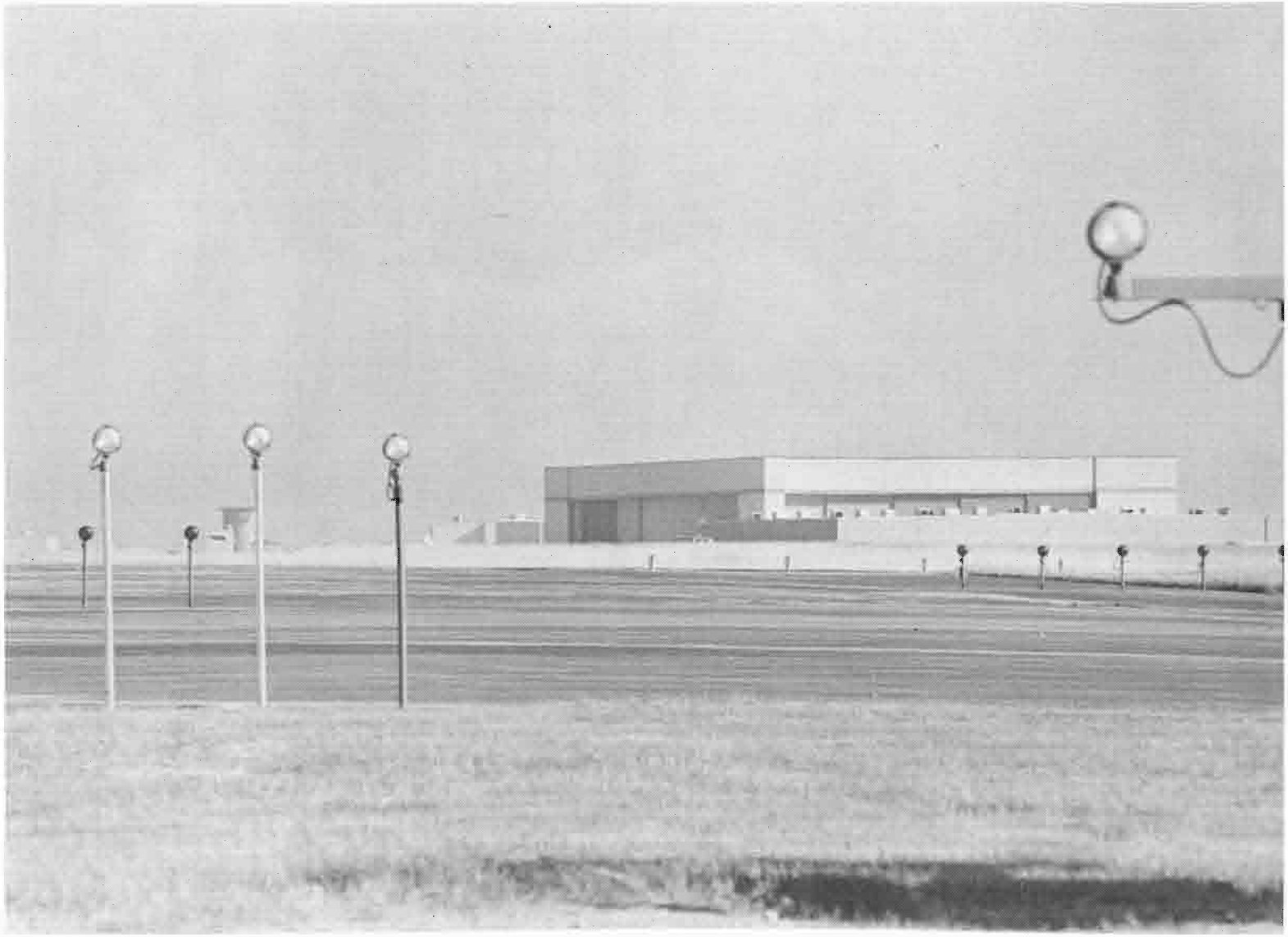

Fig. 5-2. American Airlines hangar as seen from threshold of runway 17L.

Fig. 5-3. American Airlines and McDonnell Douglas buildings as seen from measurement site 1.

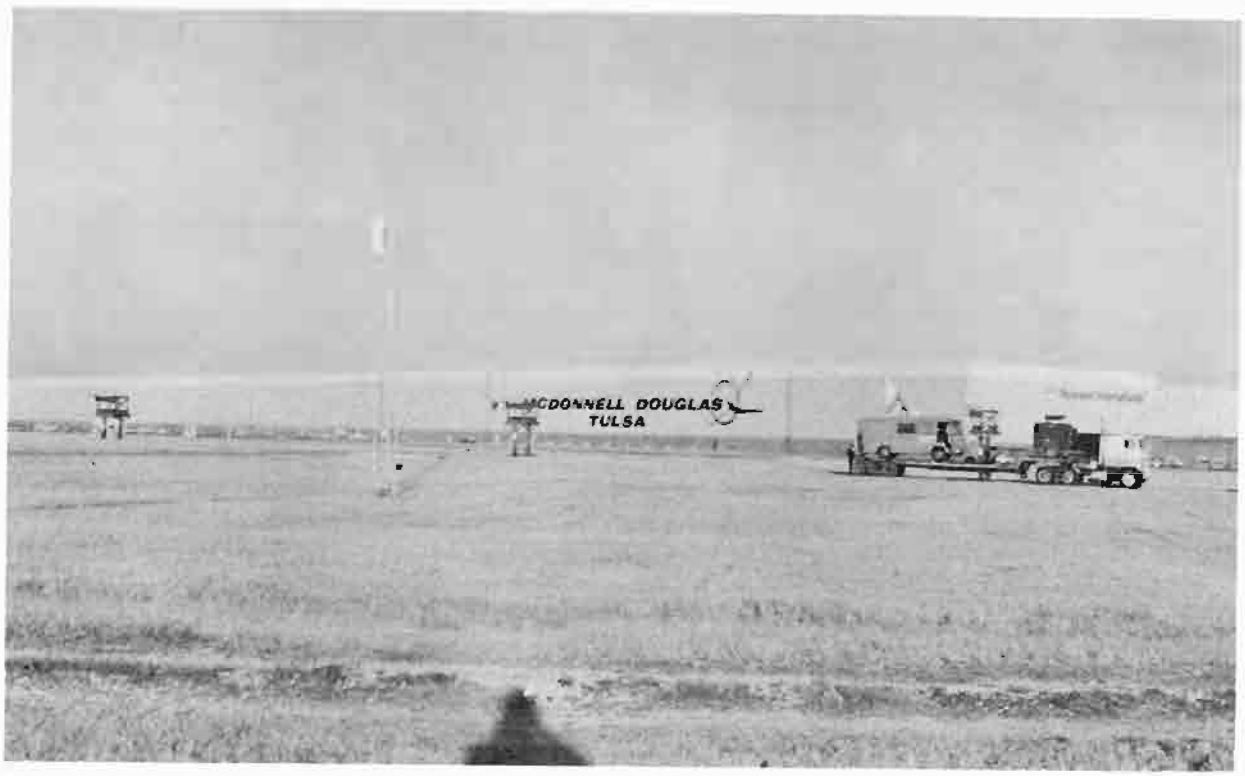

Fig. 5-4. McDonnell Douglas building and measurement equipment at Tulsa site 2.

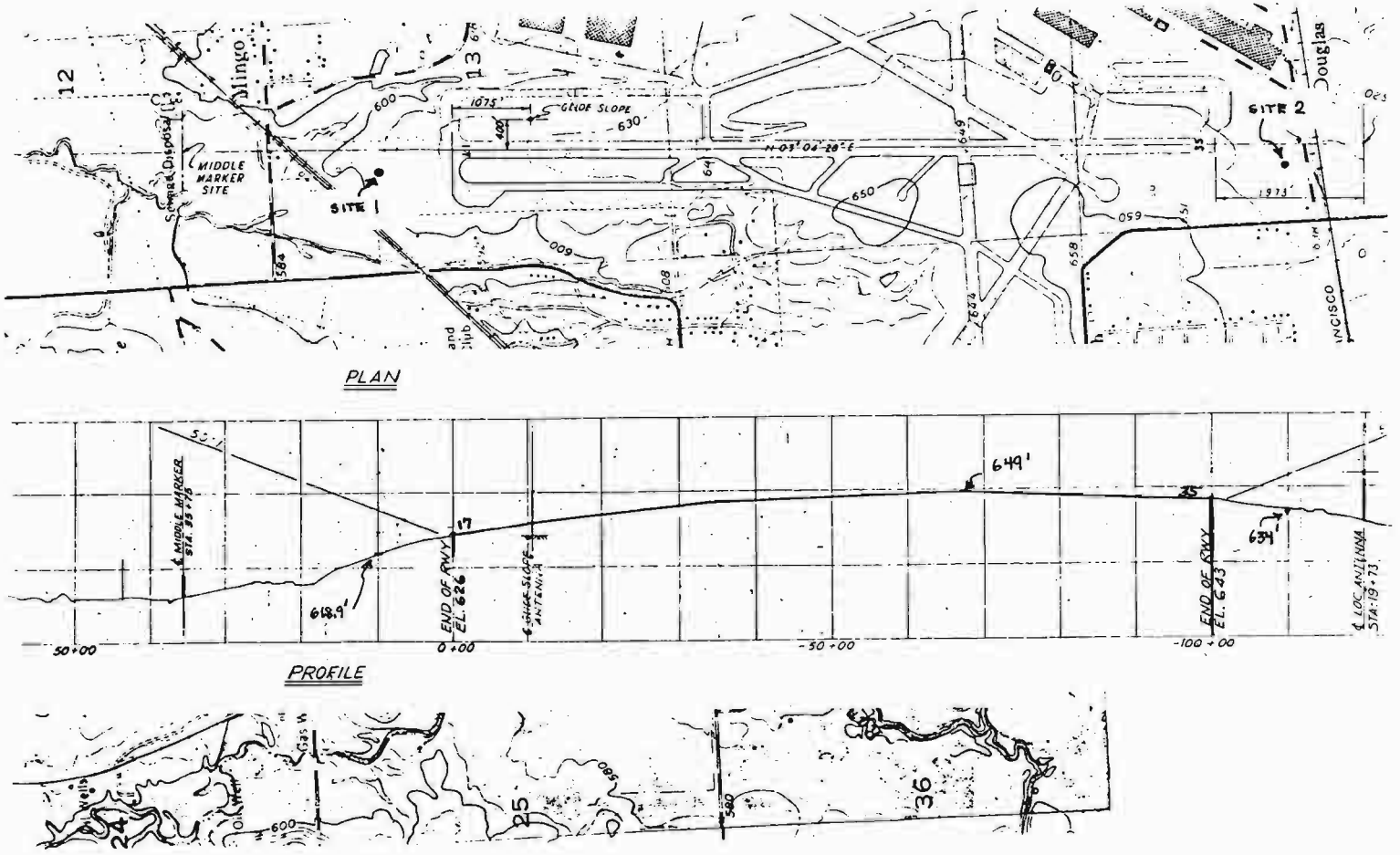

Fig. 5-5. Terrain contour along Tulsa runway 17-35.

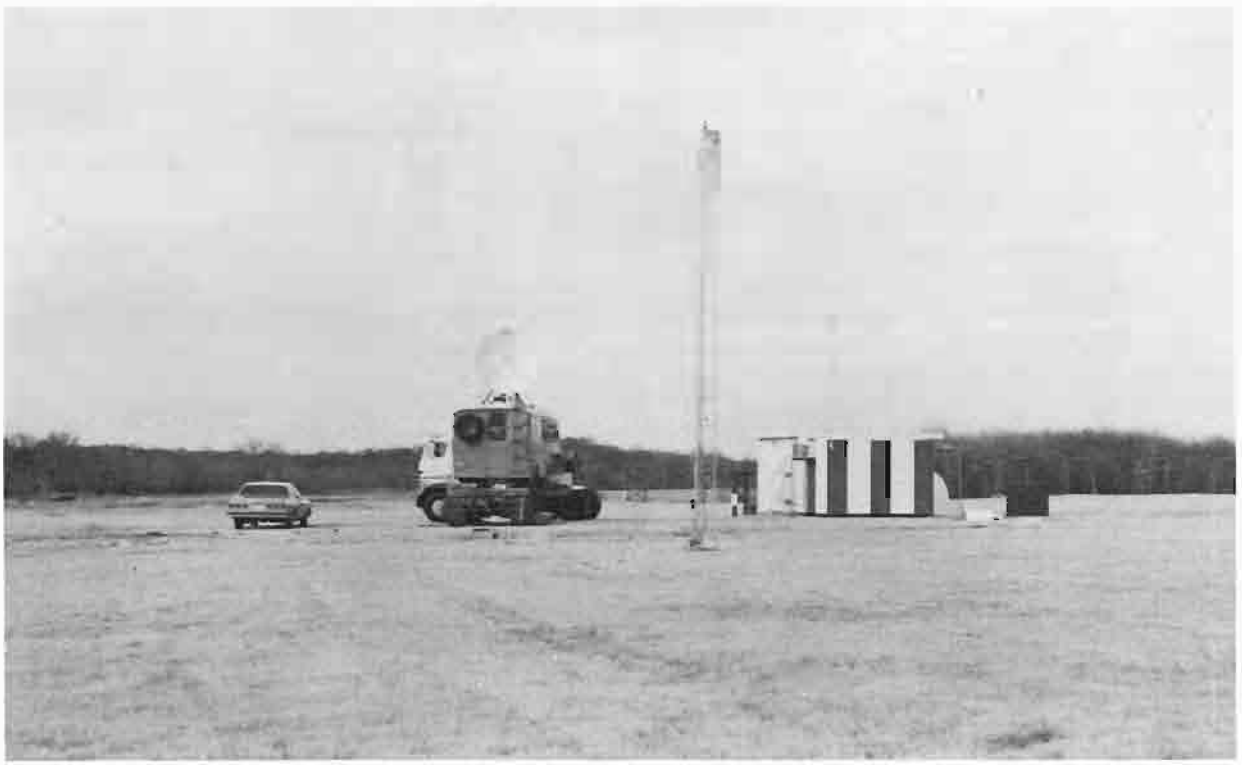

Fig. 5-6. Measurement equipment at site 1 next to runway 35R ILS localizer building.

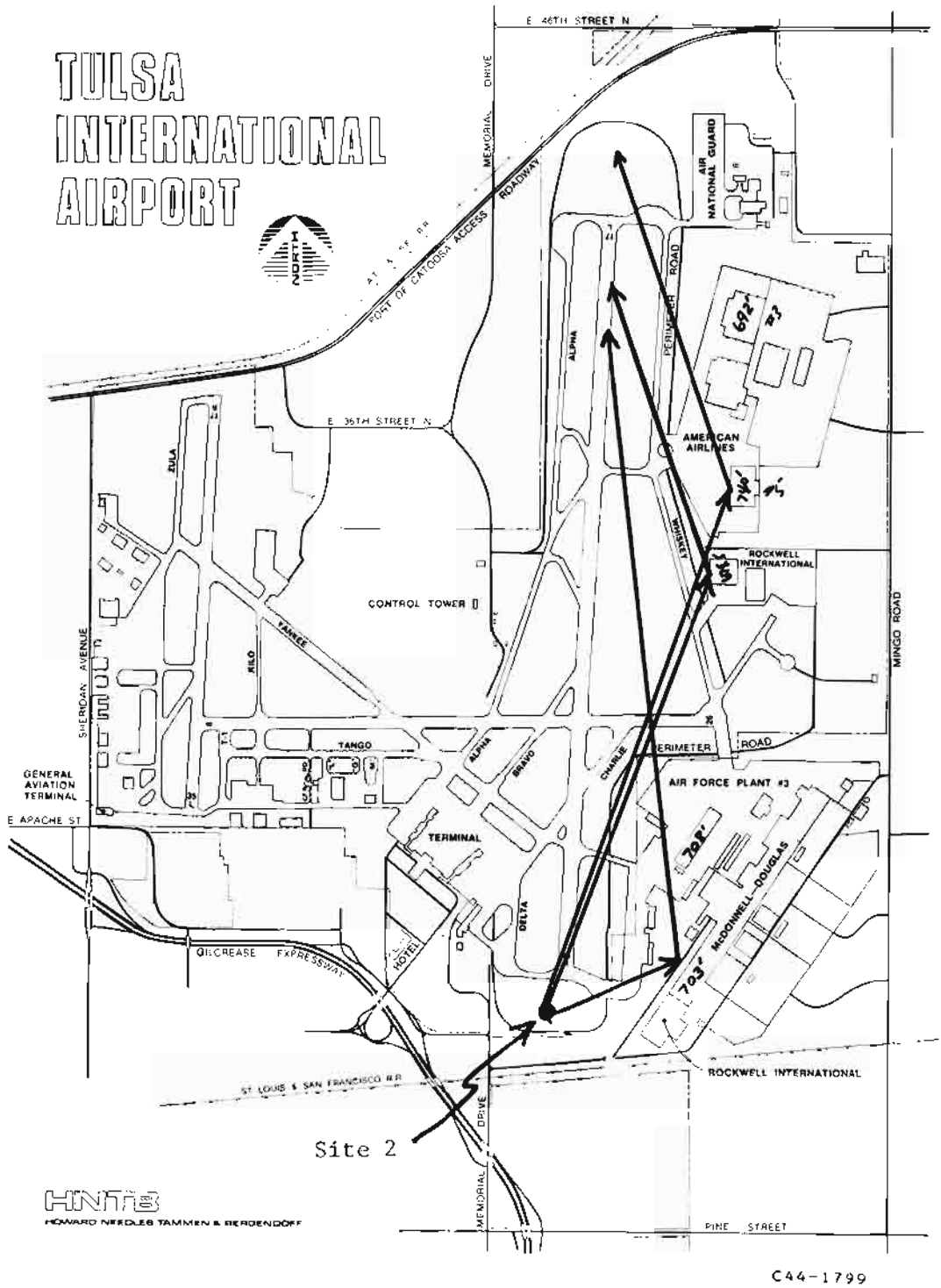

Fig. 5-7. Tulsa Site 2 measurement geometry and reflection rays.

The expected multipath relative time delays for a centerline approach to runway 17L are as follows:

Building	τ (nsec)
M-D hangar 1	1000
M-D hangar 2	1500
AA hangar	600

B. Measurements Made at Tulsa

Table 5-1 summarizes the measurements made at Tulsa. A total of 9 approaches were made to runway 35R between 4:00 p.m. and 7:00 p.m. on February 16 and 8 approaches to runway 17L between 3:00 p.m. and 6:00 p.m. on February 15. Additionally, five flights were flown at right angles to the extended runway centerline to emulate a turnon from the north at approximately 9 nmi from the threshold of 17 L as shown in Fig. 5-8. Taxi tests were made along the runway from both of the thresholds to the runway midpoint (i.e., throughout the flare region); however, the signal attenuation due to the runway hump was so high that no data was obtained in the regions of greatest interest.

C. Waveform Analysis Results

All of the approaches at Tulsa have been analyzed and representative results will be described in this section.

1. Site 1 (Approaches to Runway 35R)

The reflection rays shown in Fig. 5-1 suggest that specular multipath would be found only in the flare region for an approach to runway 35R, and this was found to be the case. Figures 5-9 and 5-10 show the summary results for two approaches to this runway. We see that virtually no multipath is encountered prior to threshold. A similar lack of multipath prior to threshold was found on the other 6 approaches to runway 35R.

TABLE 5-1

FLIGHT TESTS AT TULSA INTERNATIONAL AIRPORT

Runway Threshold	Run Numbers	Threshold Crossing Height (feet)	Height Above Runway (feet)
35R	215B through 215E	50	20
35R	215F through 215I	25	10
35R	215J	65	25
17L	216B through 216F	50	15
17L	216G through 216J	20	10
17L	216K through 2160	Partial orbit at right angles to extended runway CL from 5 nmi north of CL to CL. Intersection with CL at 9 nmi from 17L threshold. Height AGL of 1000 feet.	

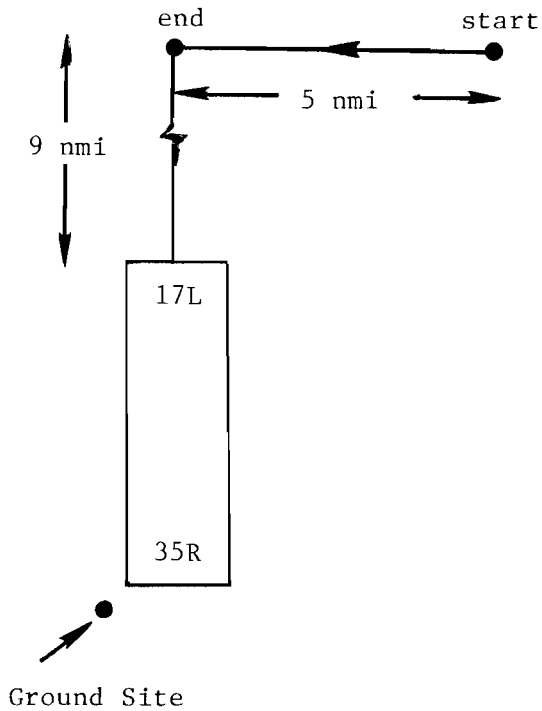

Fig. 5-8. Flight profile for partial orbit at Tulsa site 2.

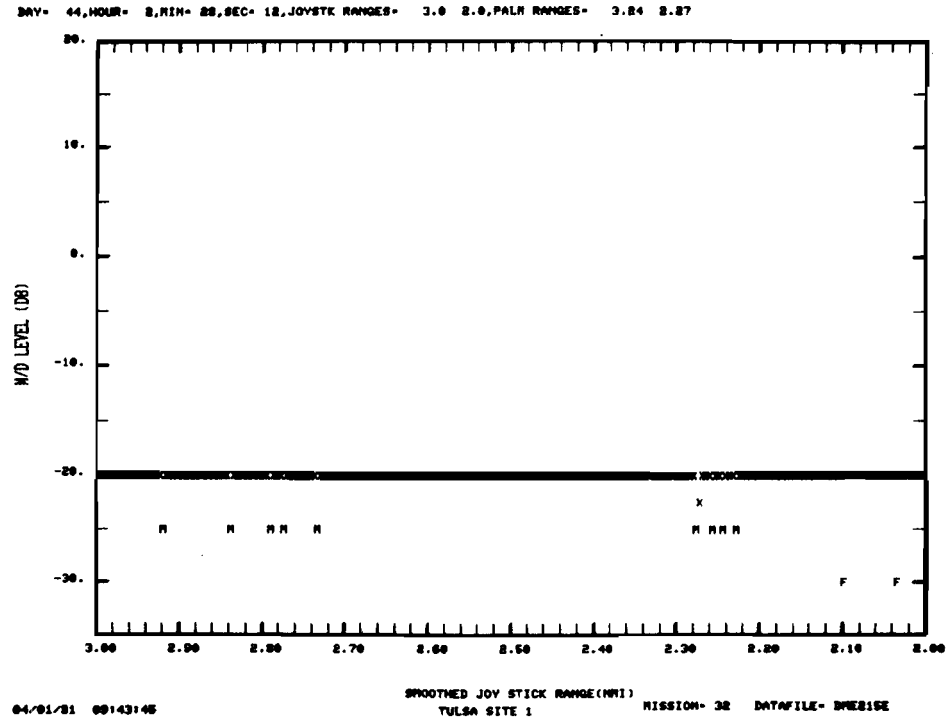

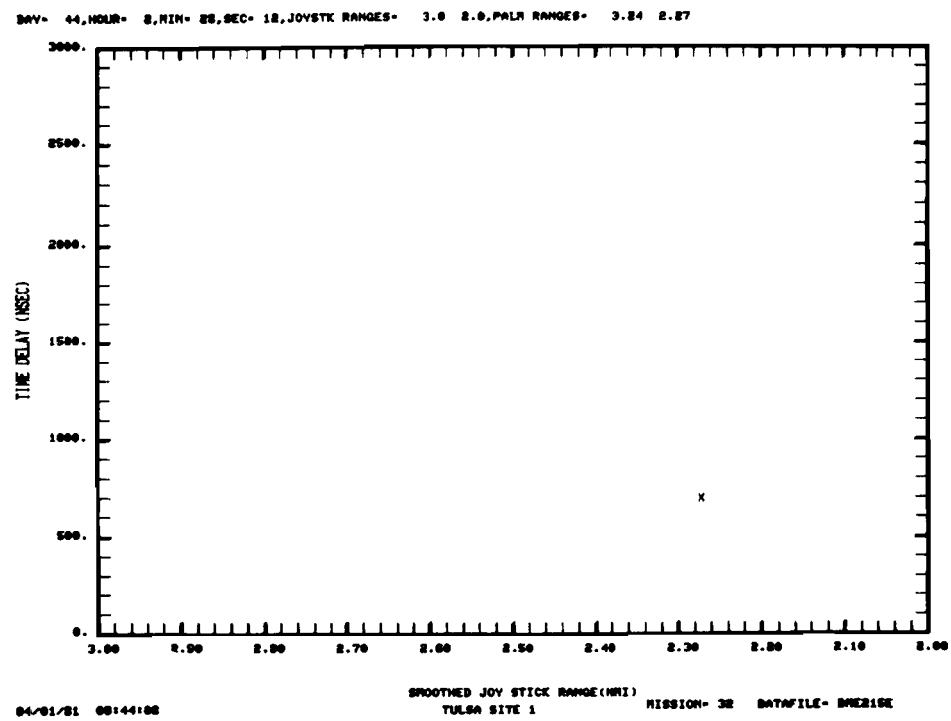

Fig. 5-9a. Tulsa site 1 data summary for 25 ft. threshold crossing height.

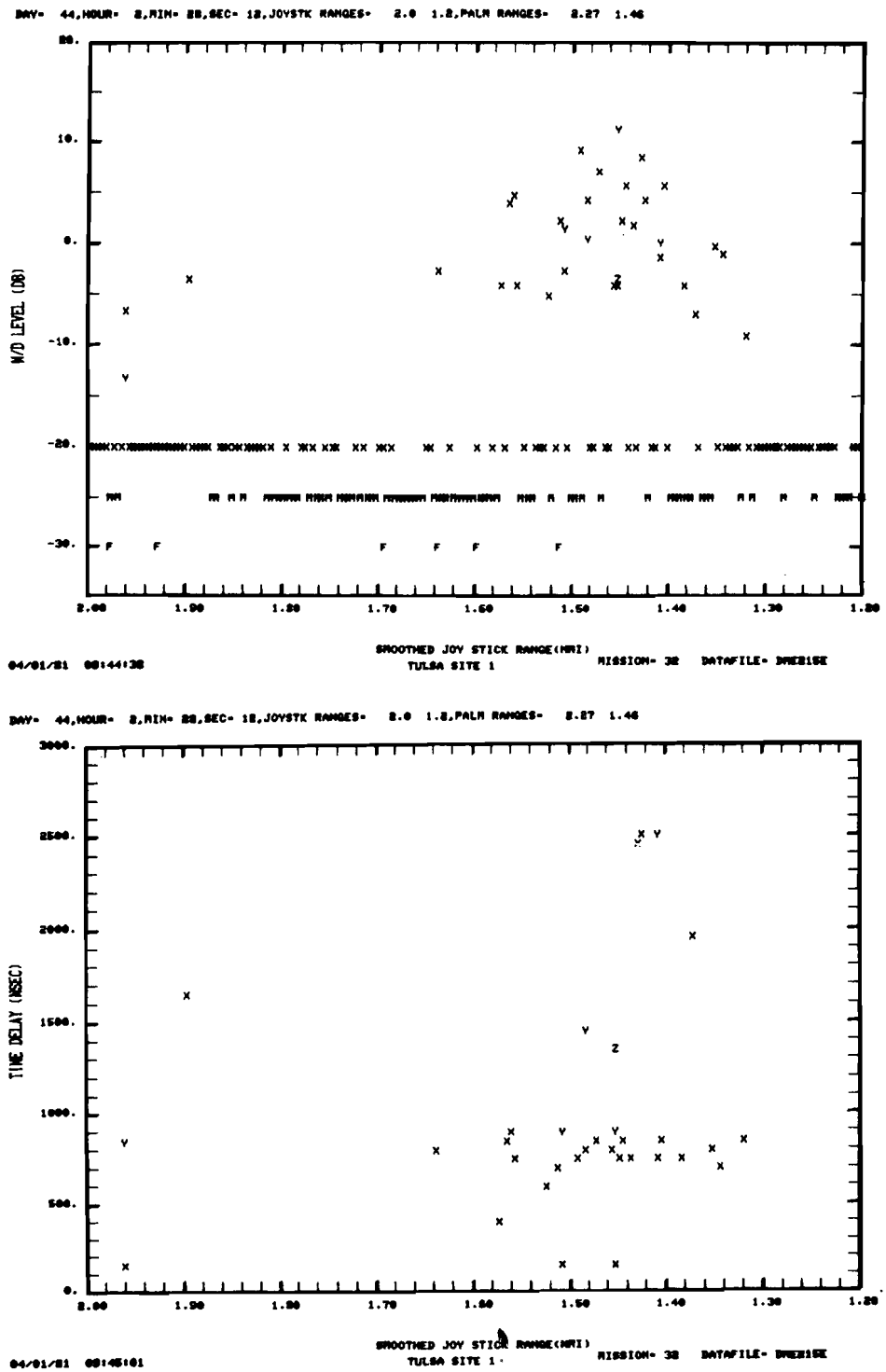

Fig. 5-9b. Tulsa site 1 data summary for 25 ft. threshold crossing height.

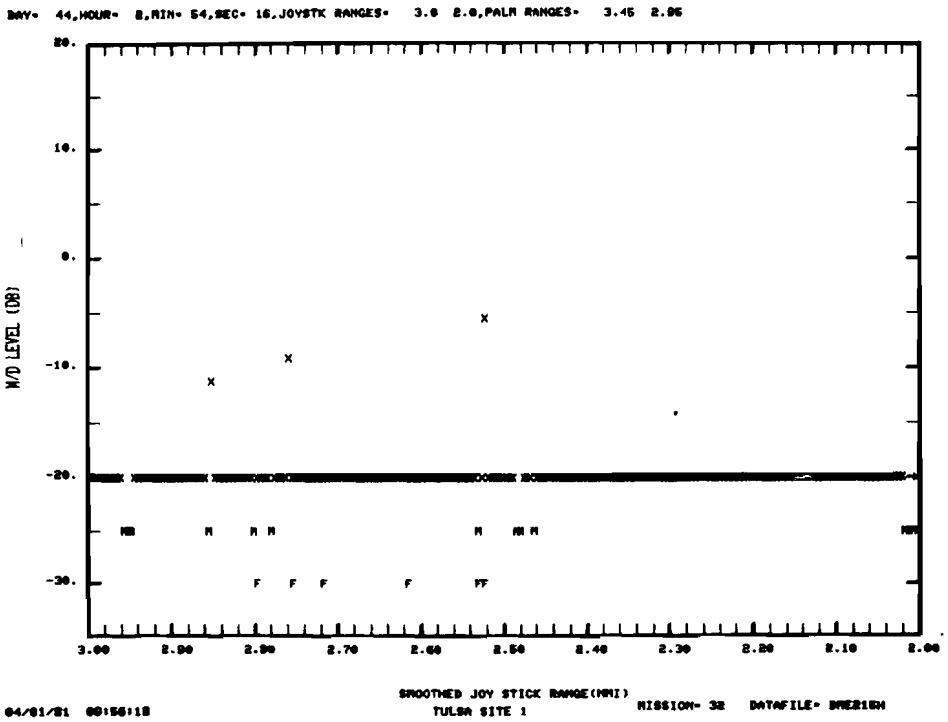

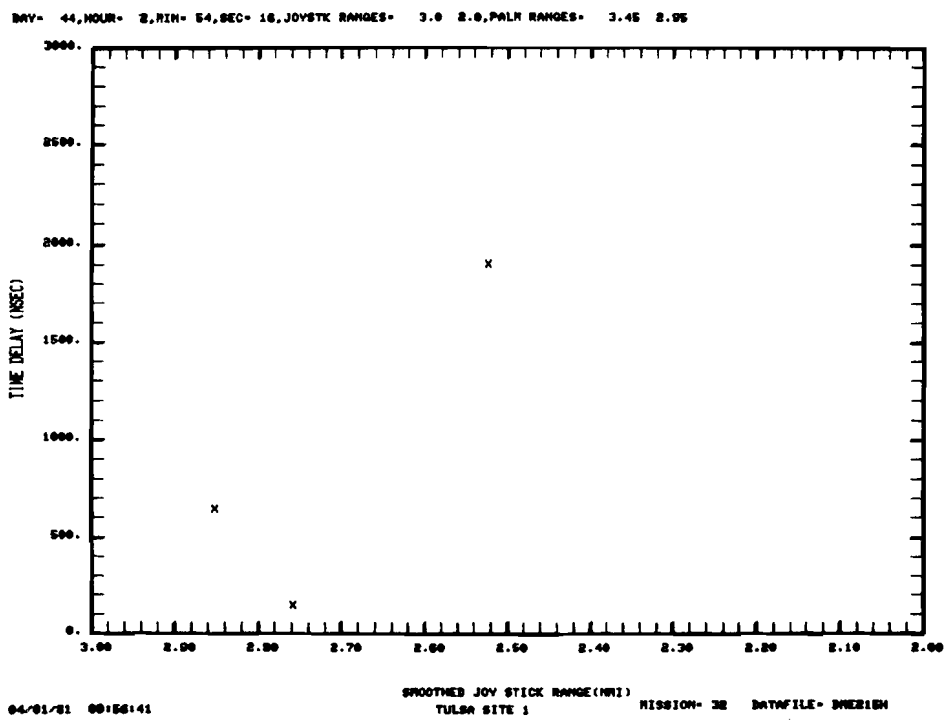

Fig. 5-10a. Tulsa site 1 data summary for 50 ft. threshold crossing height.

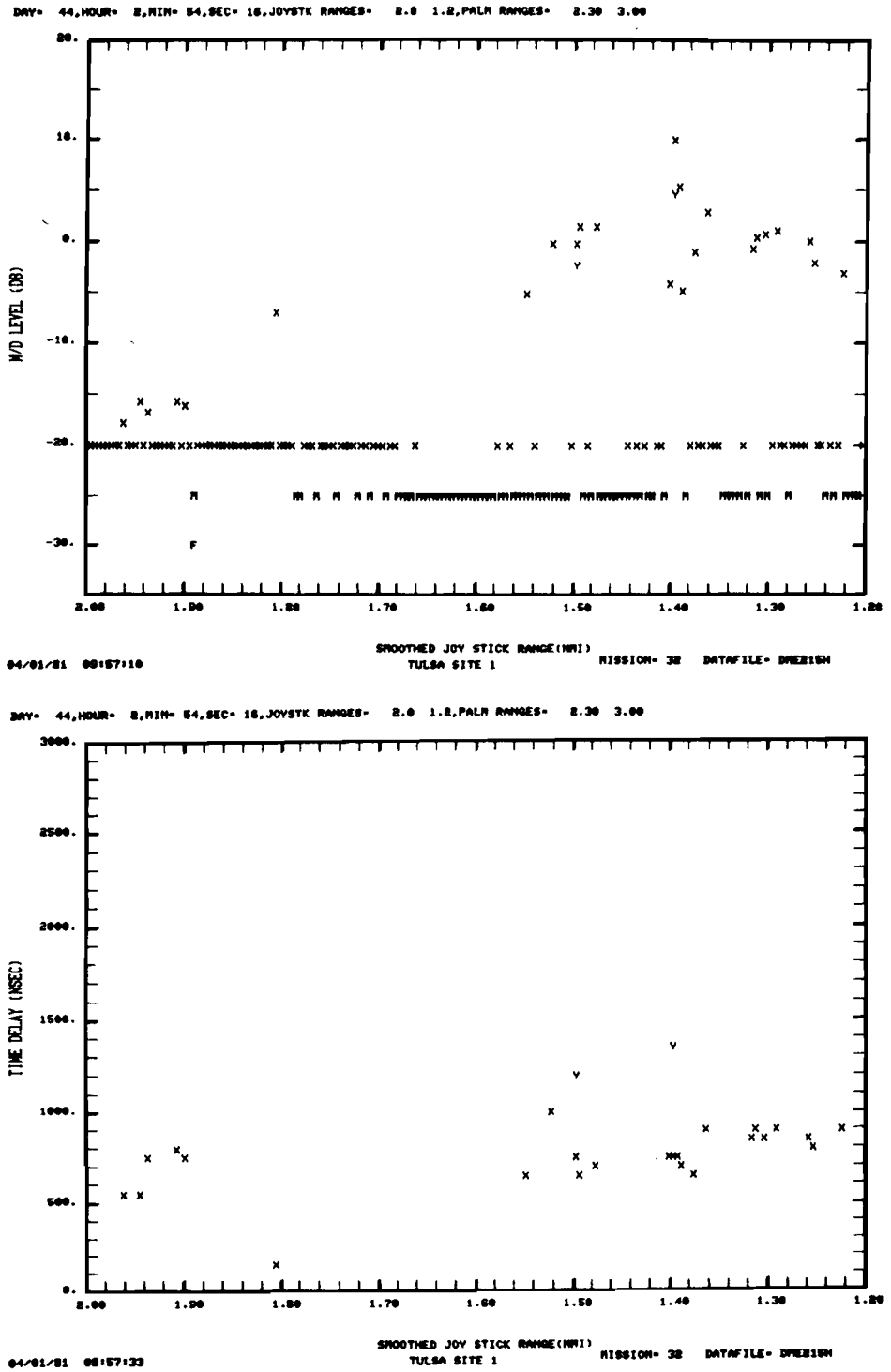

Fig. 5-10 b. Tulsa site 1 data summary for 50 ft. threshold crossing height.

However, just after threshold (joystick range = 1.81 nmi), much of the data was missed due to a combination of severe attentuation from the runway hump and/or suppression of the transponder by high level multipath from the McDonnell-Douglas factory building with delay times of approximately 2 μsec. The valid data points measured in the region indicate M/D levels between -5 dB and +10 dB with time delay of 700 nsec - 1000 nsec, presumably corresponding to the AA hangar. Figures 5-11 and 5-12 show the waveforms corresponding to the high M/D levels.

To summarize, the experimental data for approaches to runway 35R suggests that specular multipath with levels $\geq$ -20 dB was encountered only in the regions where expected from the specular ray considerations indicated in Fig. 5-1. Unfortunately, the expected specular region also coincided with a region of high direct path attentuation due to the runway hump, so only fragmentary data was obtained. However, this fragmentary data suggests high level multipath from the AA hangar.

2. Site 2 (Approaches to Runway 17L)

The reflection rays shown in Fig. 5-6 suggest that the specular multipath on this approach will be encountered throughout the approach region with reflections from two hangars in the threshold region. However, the long duration multipath from the McDonnell-Douglas factory buildings would be attenuated by the azimuth pattern of the receive antenna (Fig. 2-4).

Figures 5-13 to 5-15 show summary results for approaches with a 50-foot threshold crossing height. Figure 5-16 shows the summary results for a flight profile with a threshold crossing height of 20 feet and a height AGL of 15 feet along the runway. The results prior to threshold on the various runs are seen to be very similar. The M/D levels at threshold and further down the runway show a greater variation, with higher levels ocurring at the lowest aircraft heights.

Figures 5-17 and 5-18 show received waveforms corresponding to high M/D levels in regions just prior to and after the runway threshold. The waveforms

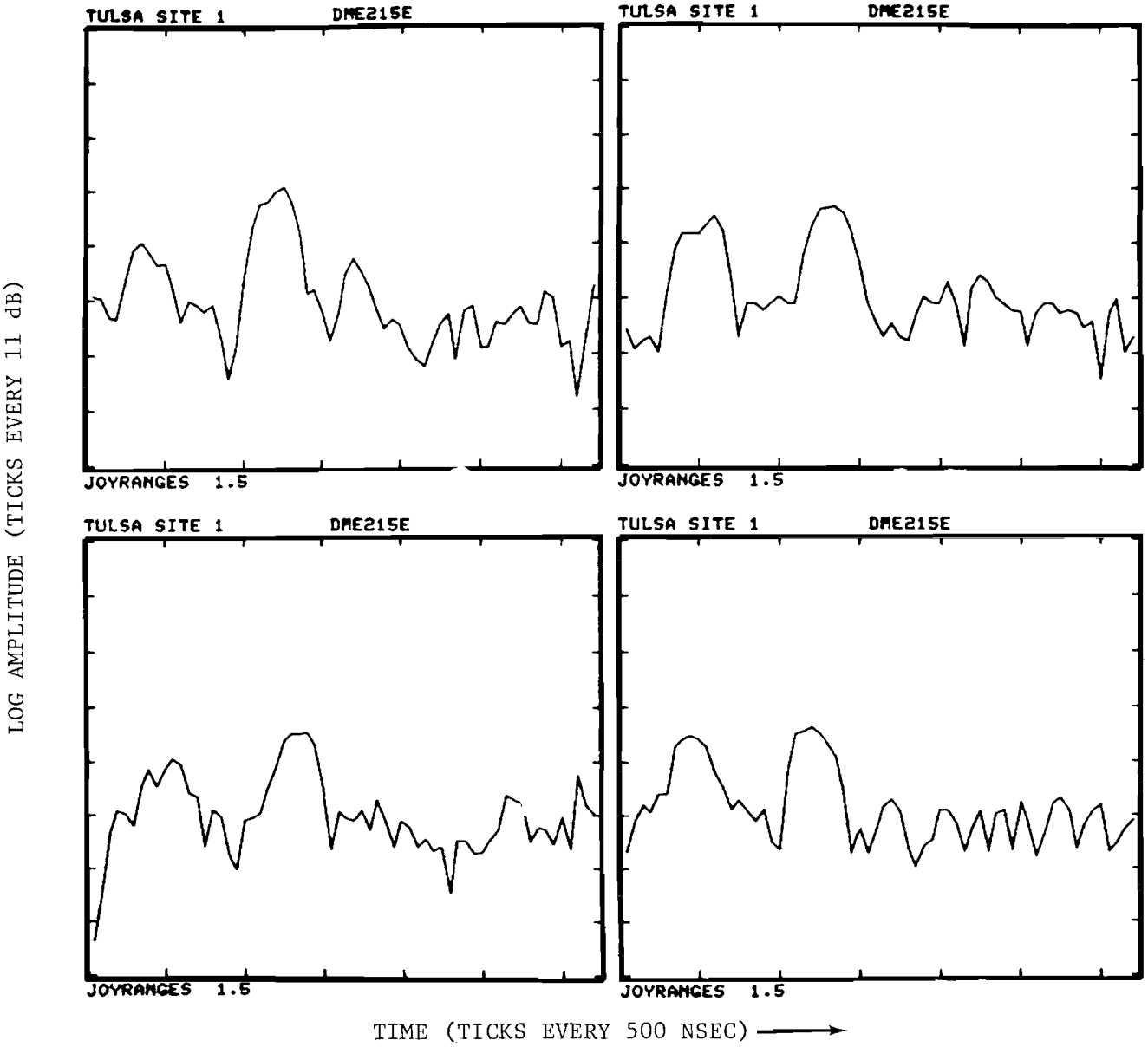

Fig. 5-11. Tulsa site 1 waveforms over runway on flight profile 1.

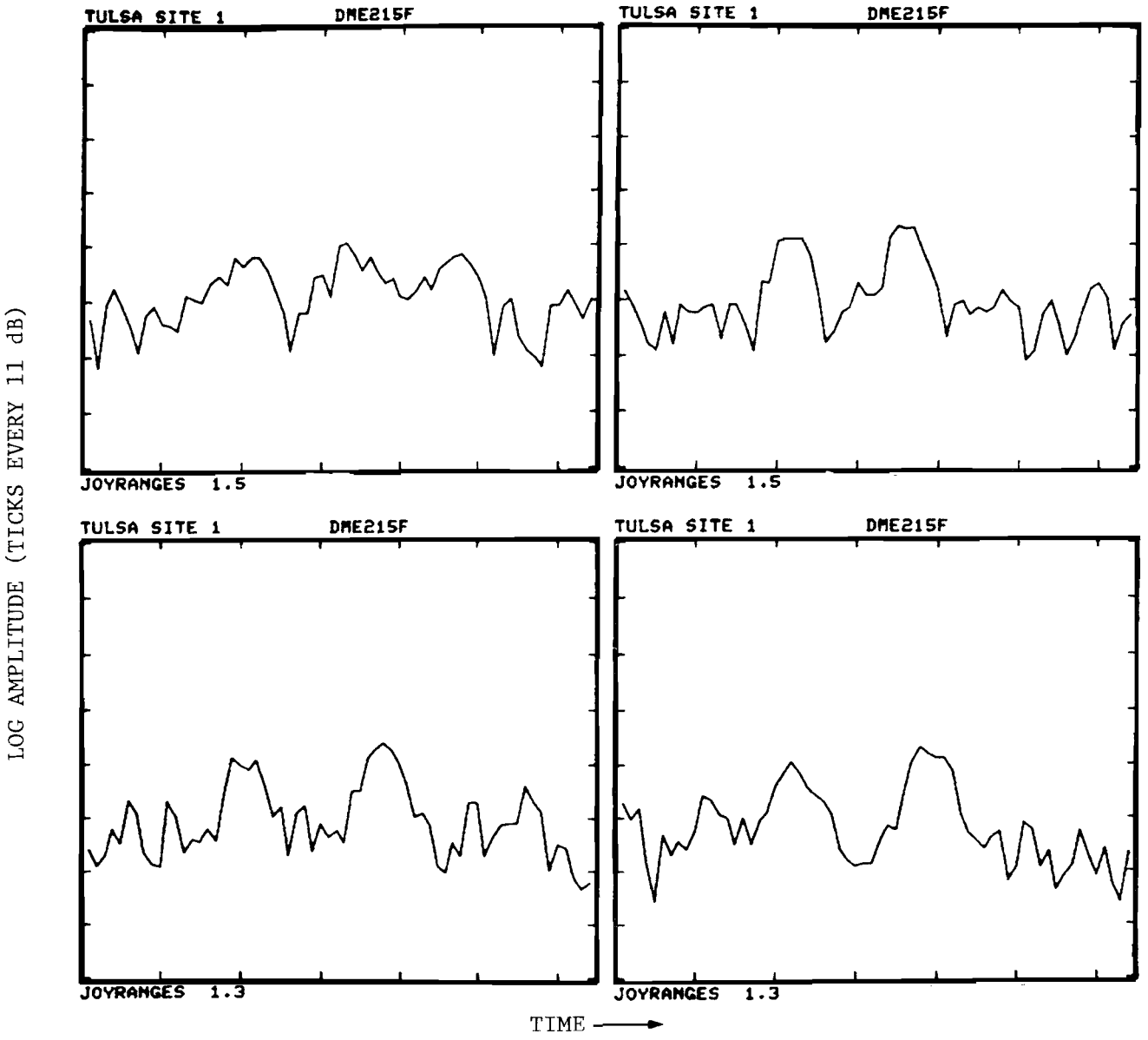

Fig. 5-12. Tulsa site 1 waveforms over runway on flight profile 1.

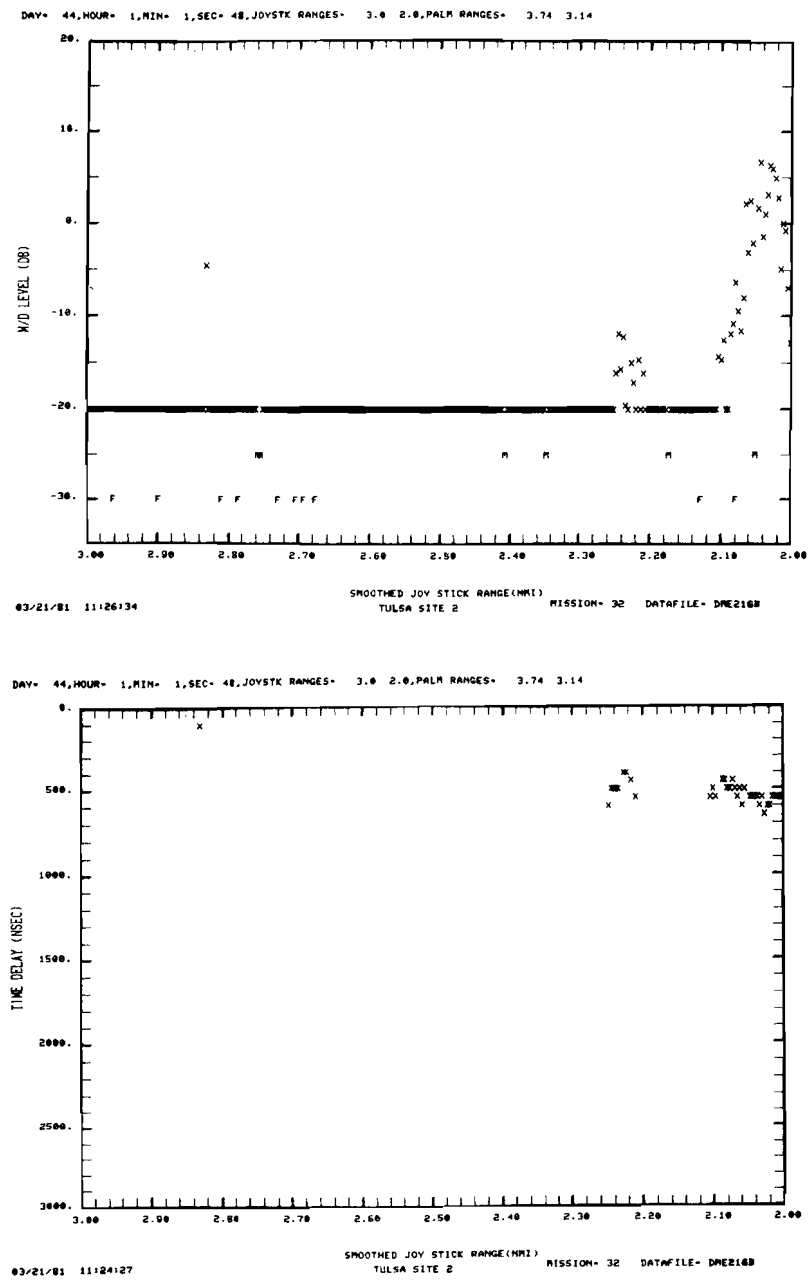

Fig. 5-13a. Tulsa site 2 data summary for 50 ft. threshold crossing height.

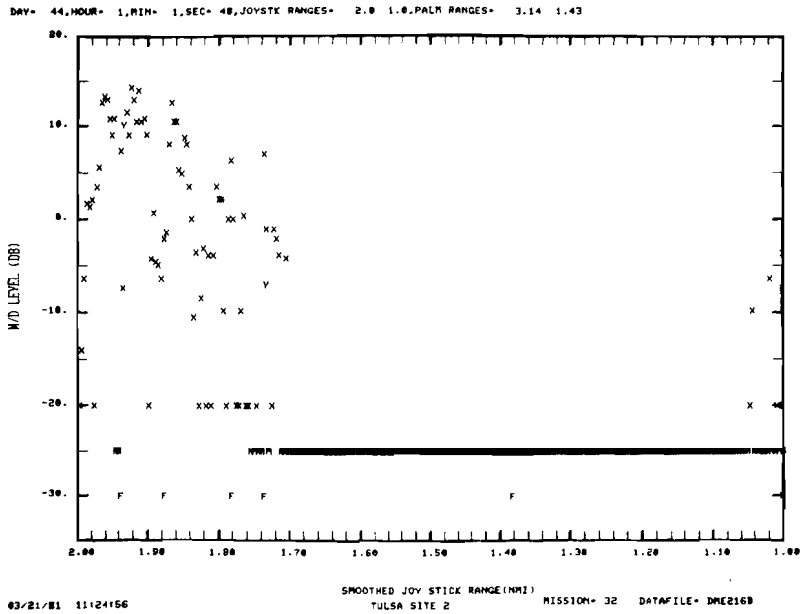

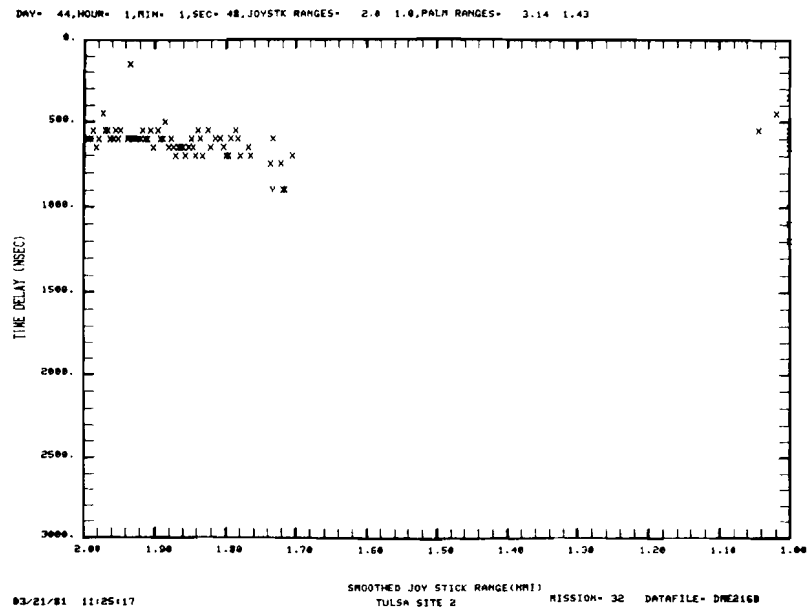

Fig. 5-13b. Tulsa site 2 data summary for 50 ft. threshold crossing height.

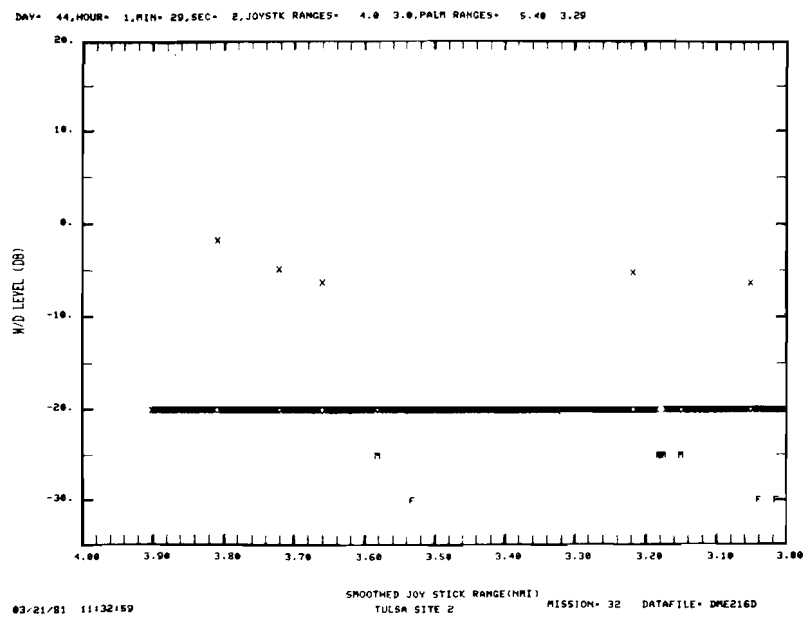

Fig. 5-14a. Tulsa site 2 data summary for 50 ft. threshold crossing height.

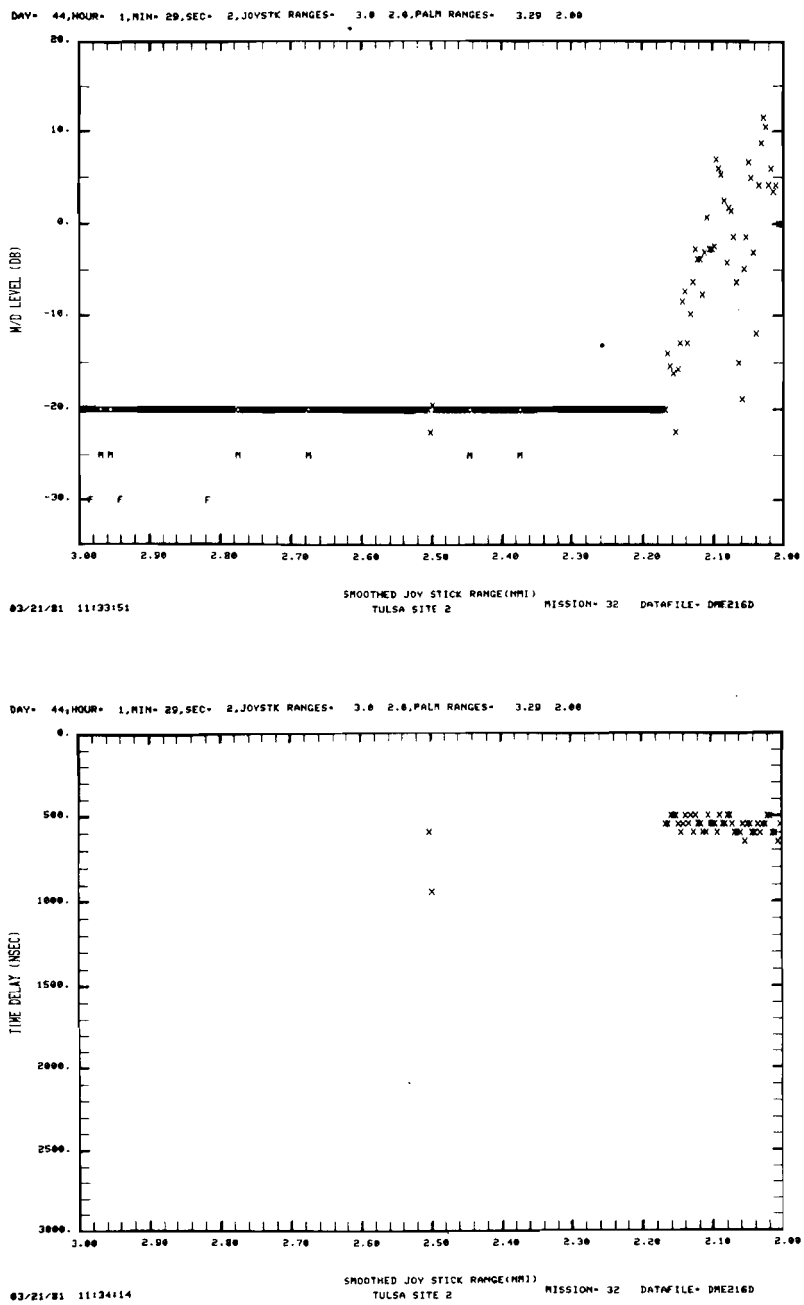

Fig. 5-14b. Tulsa site 2 data summary for 50 ft. threshold crossing height.

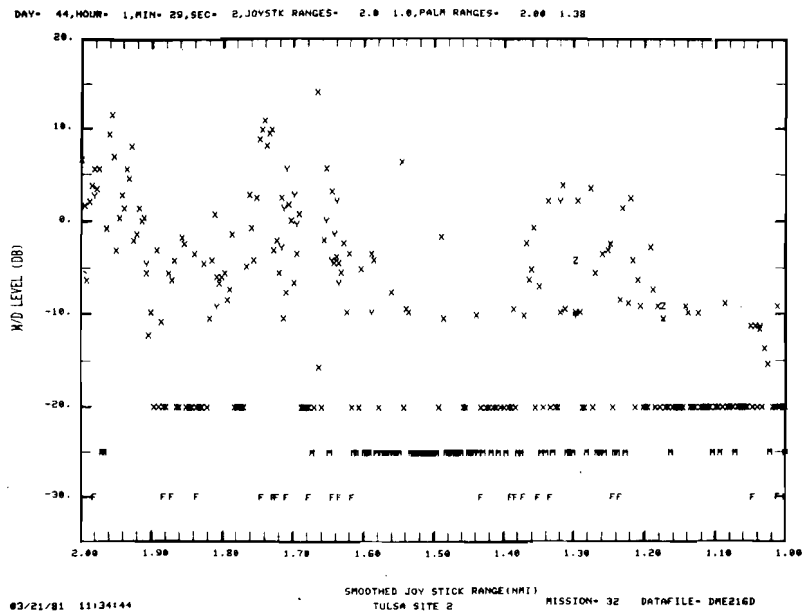

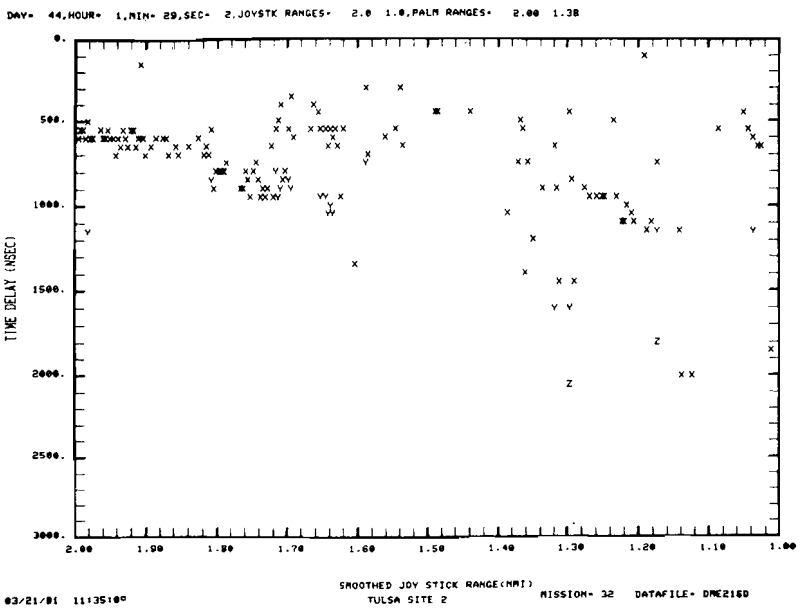

Fig. 5-14c. Tulsa site 2 data summary for 50 ft. threshold crossing height.

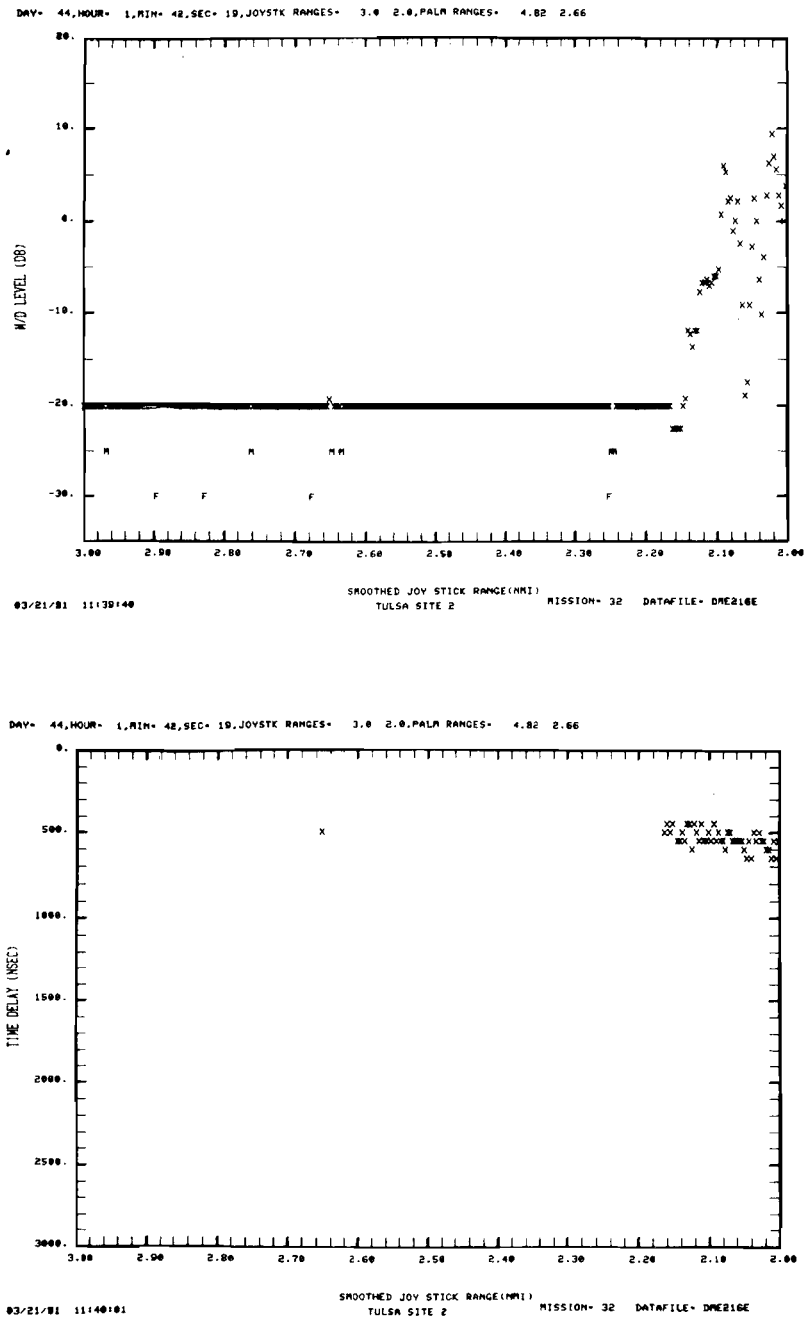

Fig. 5-15a. Tulsa site 2 data summary for 50 ft. threshold crossing height.

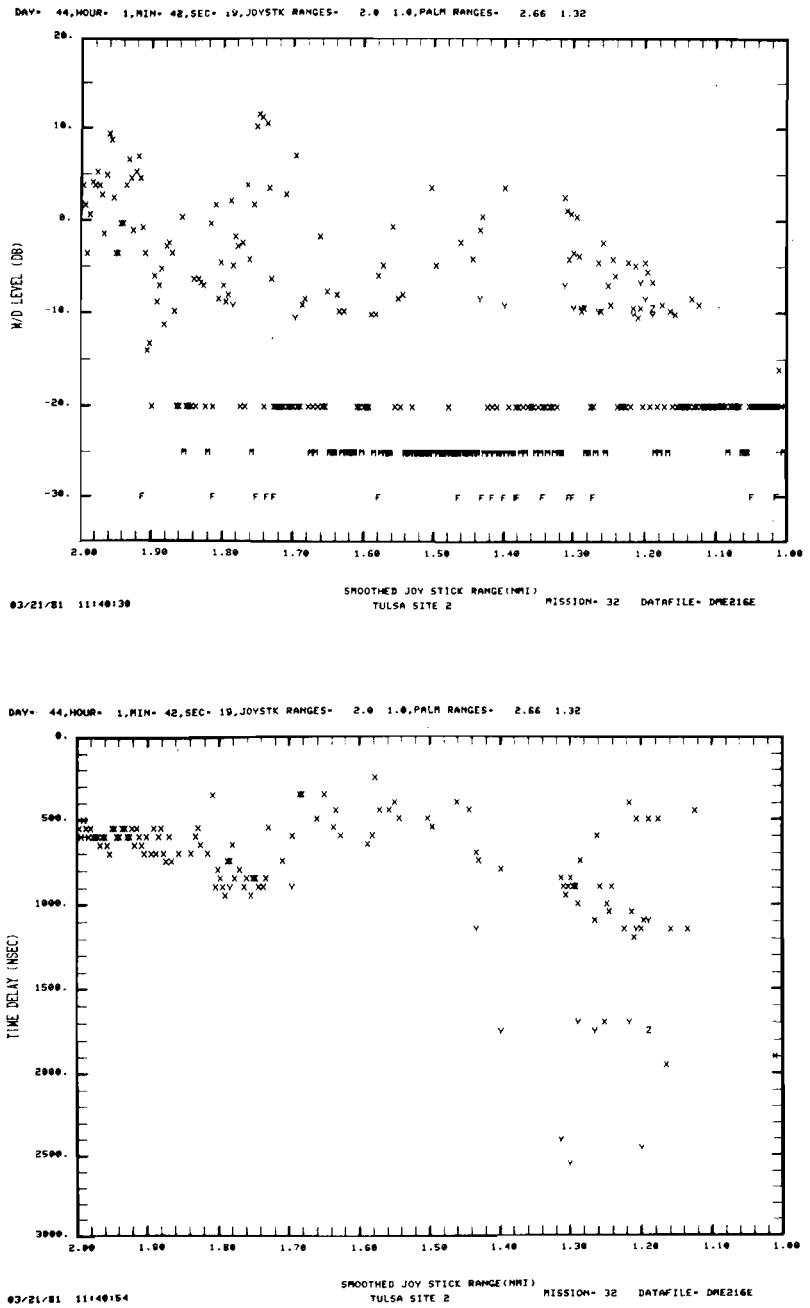

Fig. 5-15b. Tulsa site 2 data summary for 50 ft. threshold crossing height.

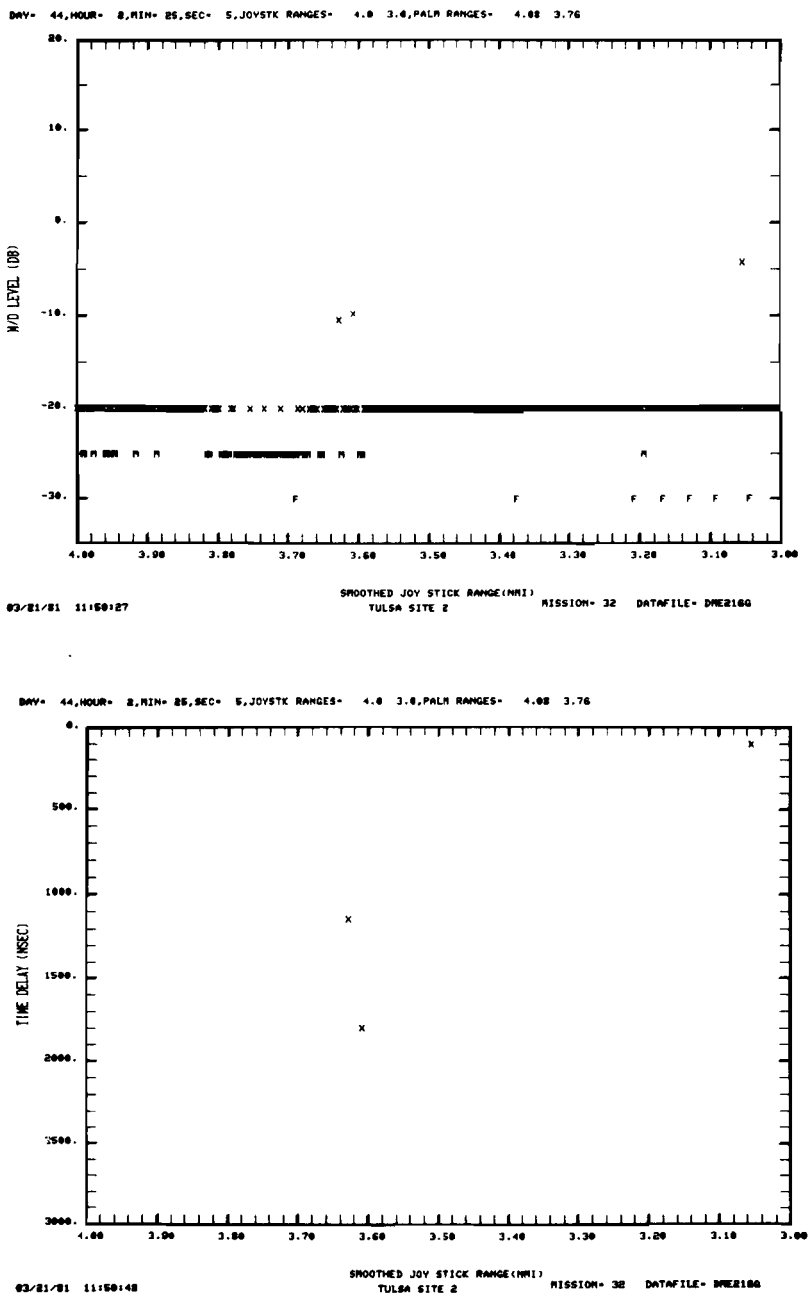

Fig. 5-16a. Tulsa site 2 data summary for 20 ft. threshold crossing height.

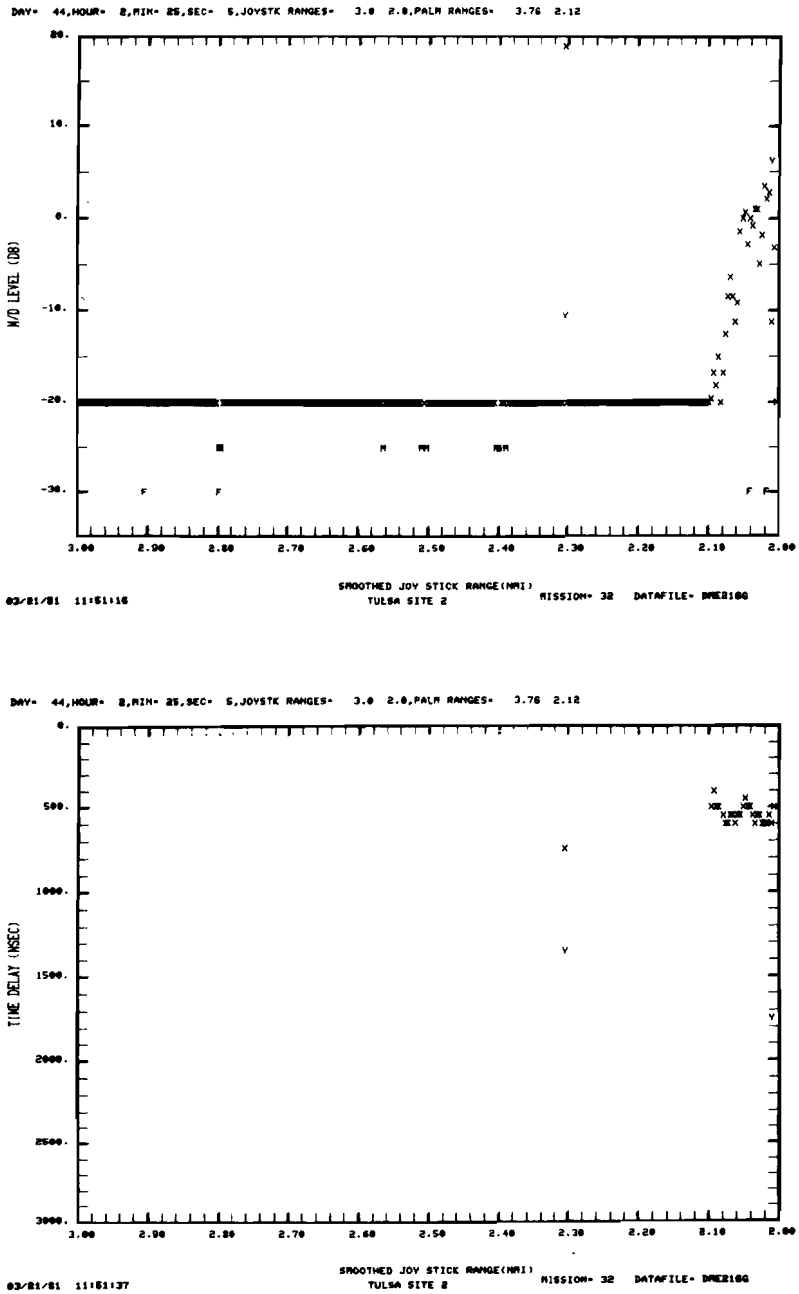

Fig. 5-16b. Tulsa site 2 data summary for 20 ft. threshold crossing height.

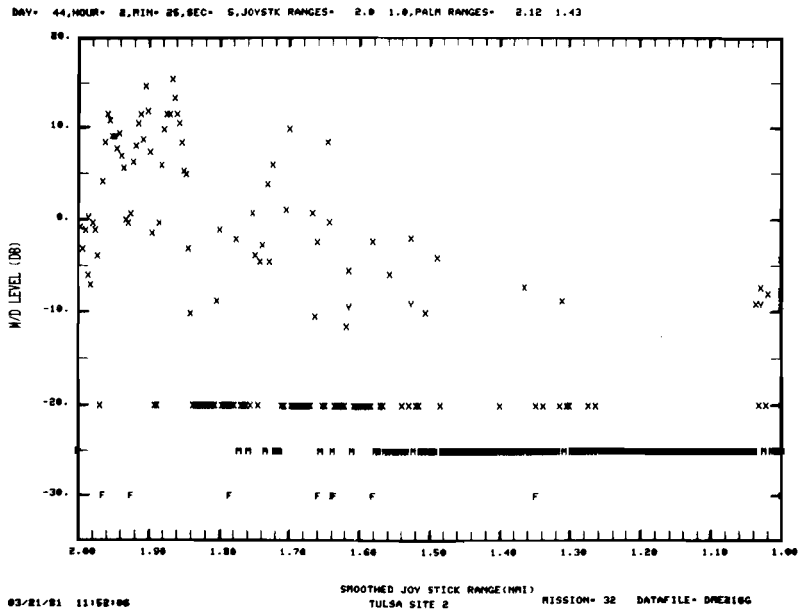

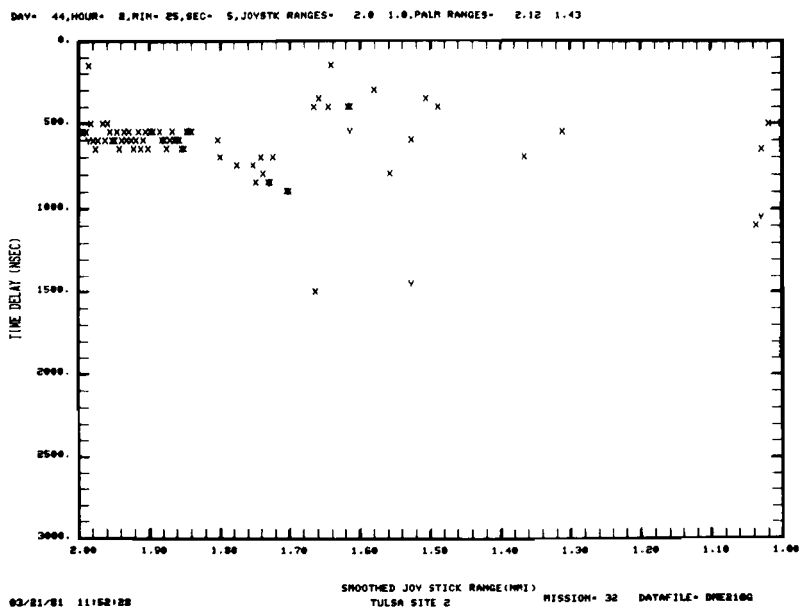

Fig. 5-16c. Tulsa site 2 data summary for 20 ft. threshold crossing height.

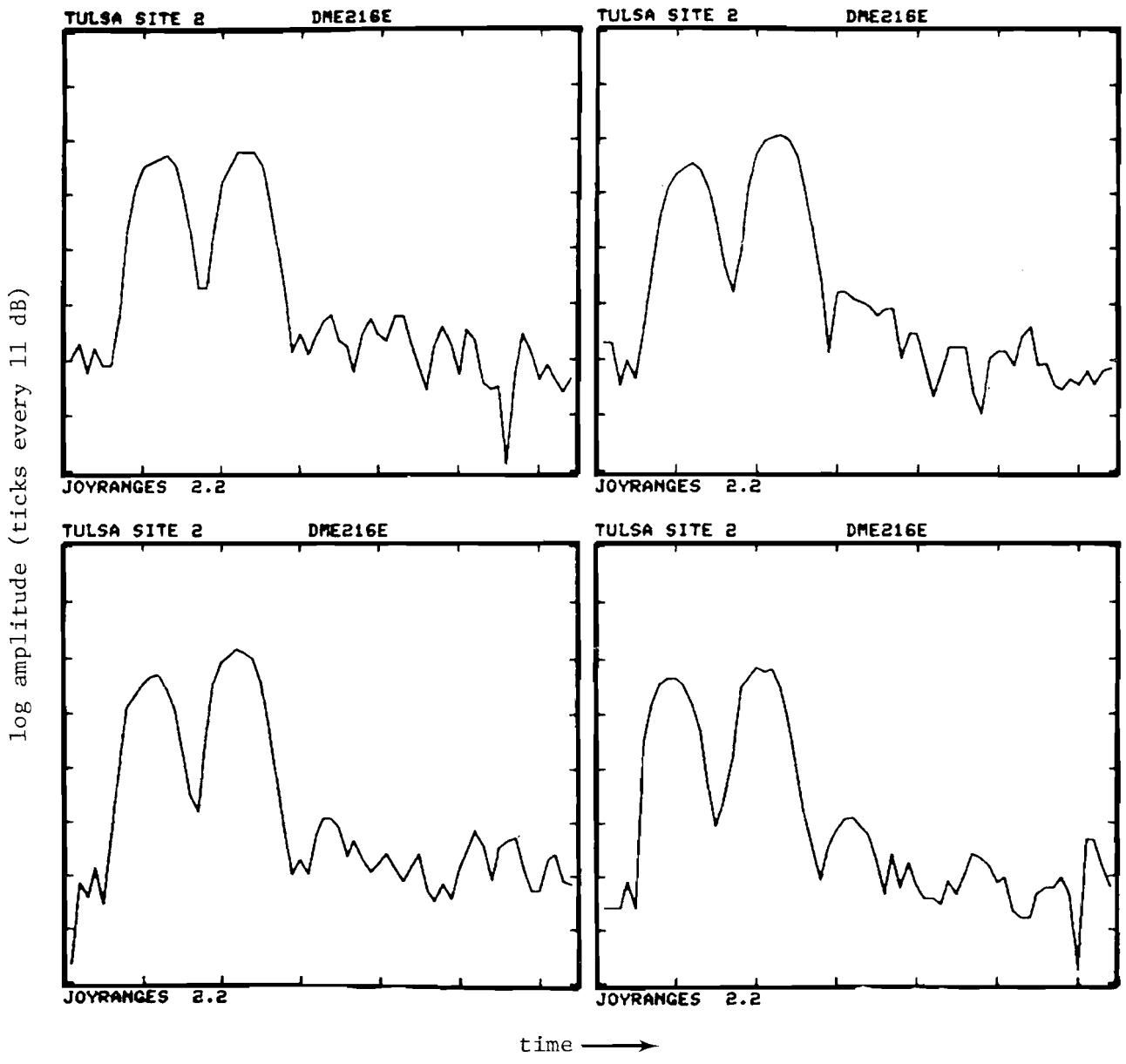

Fig. 5-17. Tulsa site 2 waveforms near threshold.

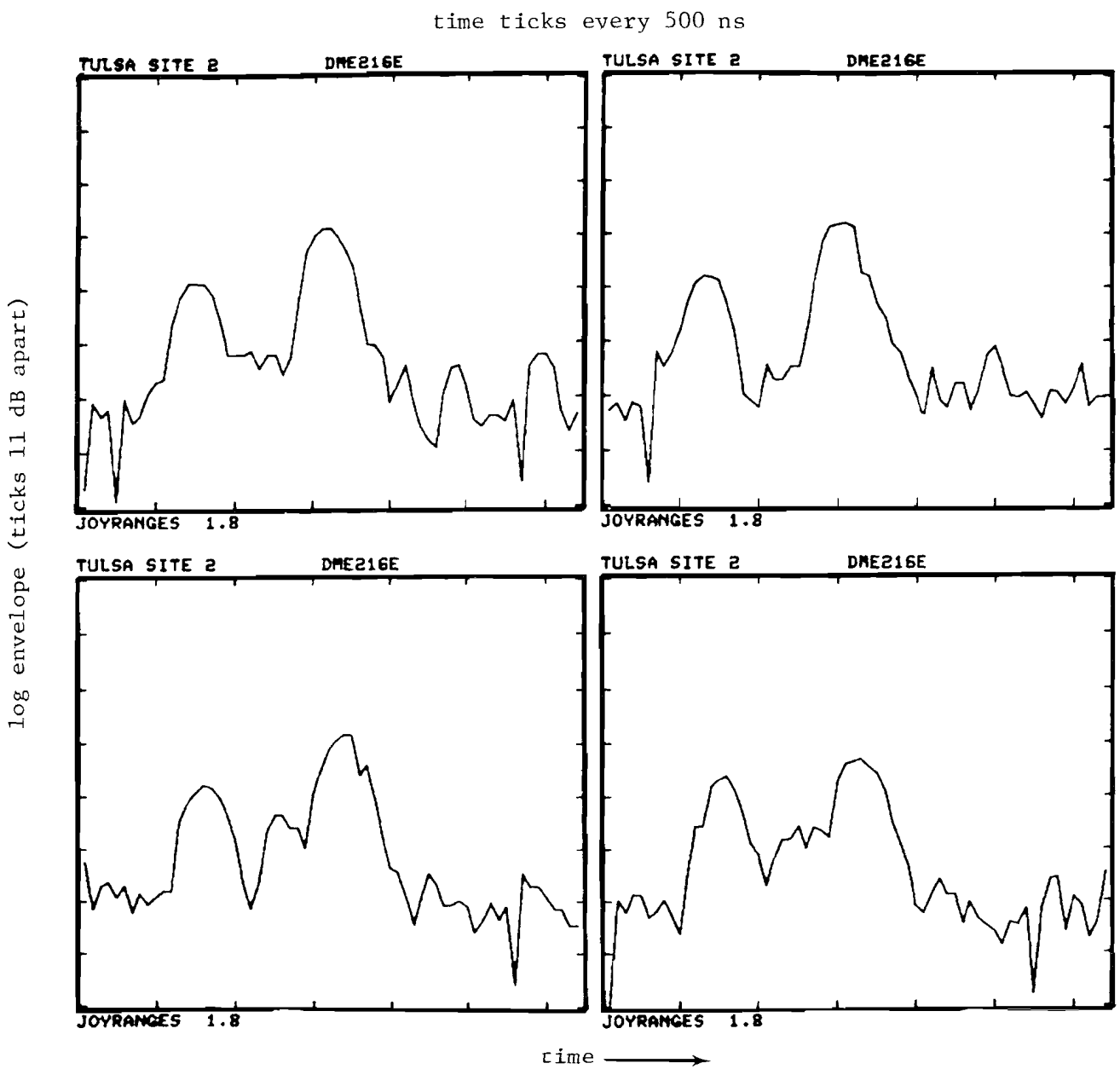

Fig. 5-18. Tulsa site 2 waveforms in flare/rollout region.

before threshold were fairly easy to analyze, whereas at and after threshold, the analysis was difficult due to the low SNR.

The very high level multipath (+5 dB to as high as +15 dB M/D ratios) at threshold with relative time delays in the 400 - 600 nsec range correlates quite well with the expected time delays and multipath region for the AA hangar. Further down the runway, high to very high level multipath is encountered with a variety of multipath delays corresponding to reflections from several of the buildings.

No multipath within 20 dB of the direct signal was encountered on any of the four off centerline partial orbit flights at a range of approximately 11 nmi. Figure 5-19 shows the summary results from one of the orbit flights. Although the McDonnell-Douglas factory buildings were oriented to produce specular reflections in this region at low elevation angles (e.g., $< 1°$), the levels were reduced by the 1) partial Fresnel zone spillage (approximately 6 dB), 2)blockage of reflections by intervening buildings, and 3) the pattern of the receiving antenna ($\sim$ -12 dB) such that no appreciable multipath was encountered.

D. Simulation Results

Both multipath measurement sites were simulated using a simple airport model in which

(1) building walls were represented by rectangular plates whose lateral dimension coincided with the locations on the airport map. The plate heights and base elevation were determined from the MLS multipath airport survey data [6]

(2) the runway hump was modeled as indicated in Capon [7]. The three points describing the hump were the runway 35R threshold, and points 3200 feet and 1500 feet down the runway from the 35R threshold. The runway heights of those points were obtained from Fig. 5-5

(3) the transmitter x,y coordinates were inferred from the location of nearby permanent structures (e.g., ILS local-

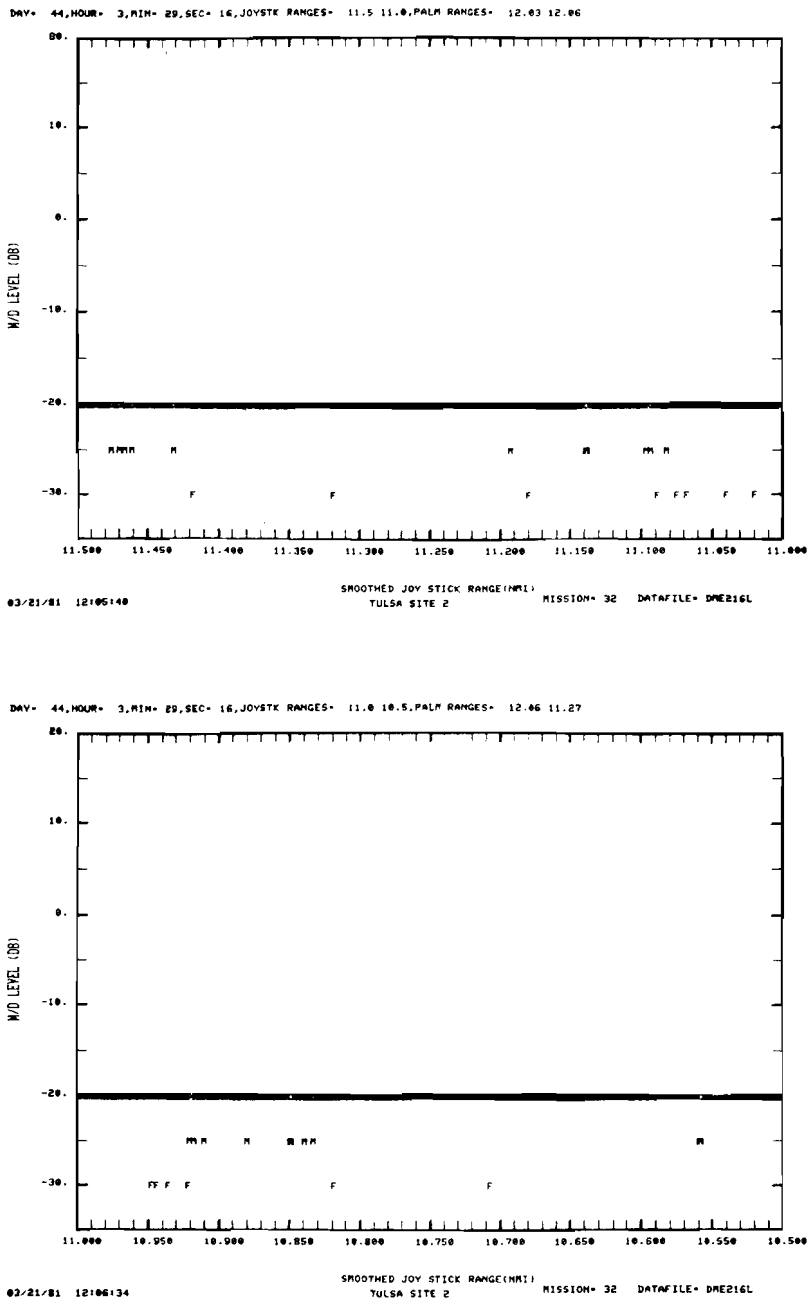

Fig. 5-19. Tulsa site 2 data summary for partial orbital flight.

izer, fences, etc) which appear on airport maps. The ground heights for the measurement site were estimated from Fig. 5-5

and

(4) no effort was made to model terrain features other than the runway hump. Thus, for example, it was assumed that the terrain along the building reflection paths was flat and at the same elevation as the DME measurement site. The runway hump, in fact, did not extend over to the buildings; however, the terrain was definitely not uniformly flat along these paths.

Figures 5-20 and 5-21 show the simulation results for an approach to runway 35R with a 50-foot threshold crossing height and a 25-foot height along the runway. We see that low level ($\geq$ -5 dB) multipath with a τ of 700 - 1100 nsec multipath is anticipated in a region approximately 2000 feet prior to the threshold from the McDonnell-Douglas factory building. This correlates resonably well with -15 dB multipath at 2.0 nmi joystick range in Fig. 5-10.

High level multipath is expected in the flare region (approximately 800 feet past threshold to 2000 feet past threshold) from both the AA hangar (800 nsec delay) and McDonnell-Douglas factory building (1000 to 3000 nsec delays). As noted earlier, these multipath levels and delay values do correlate with the few data points that were obtained in this region.

Figures 5-22 and 5-23 show the simulation results for an approach to runway 17L with a 50-foot threshold crossing height and a 25-foot height along the runway. High level ($>$ 0 dB) multipath with a τ of 550 - 650 nsec is predicted in a 600 foot region approximately 1000 feet prior to threshold (corresponding to a joystick range of approximately 2 nmi). This prediction of multipath region and delay correlates quite well with the measured results in Figs. 5-13 to 5-16; however, the peak measured M/D levels are considerably higher (6 dB to 12 dB) than the simulation results. This discrepancy probably reflects terrain contour features not considered in the simulation (see Chapters III and IV in [1] for a discussion of the effects of terrain height differences on the M/D levels).

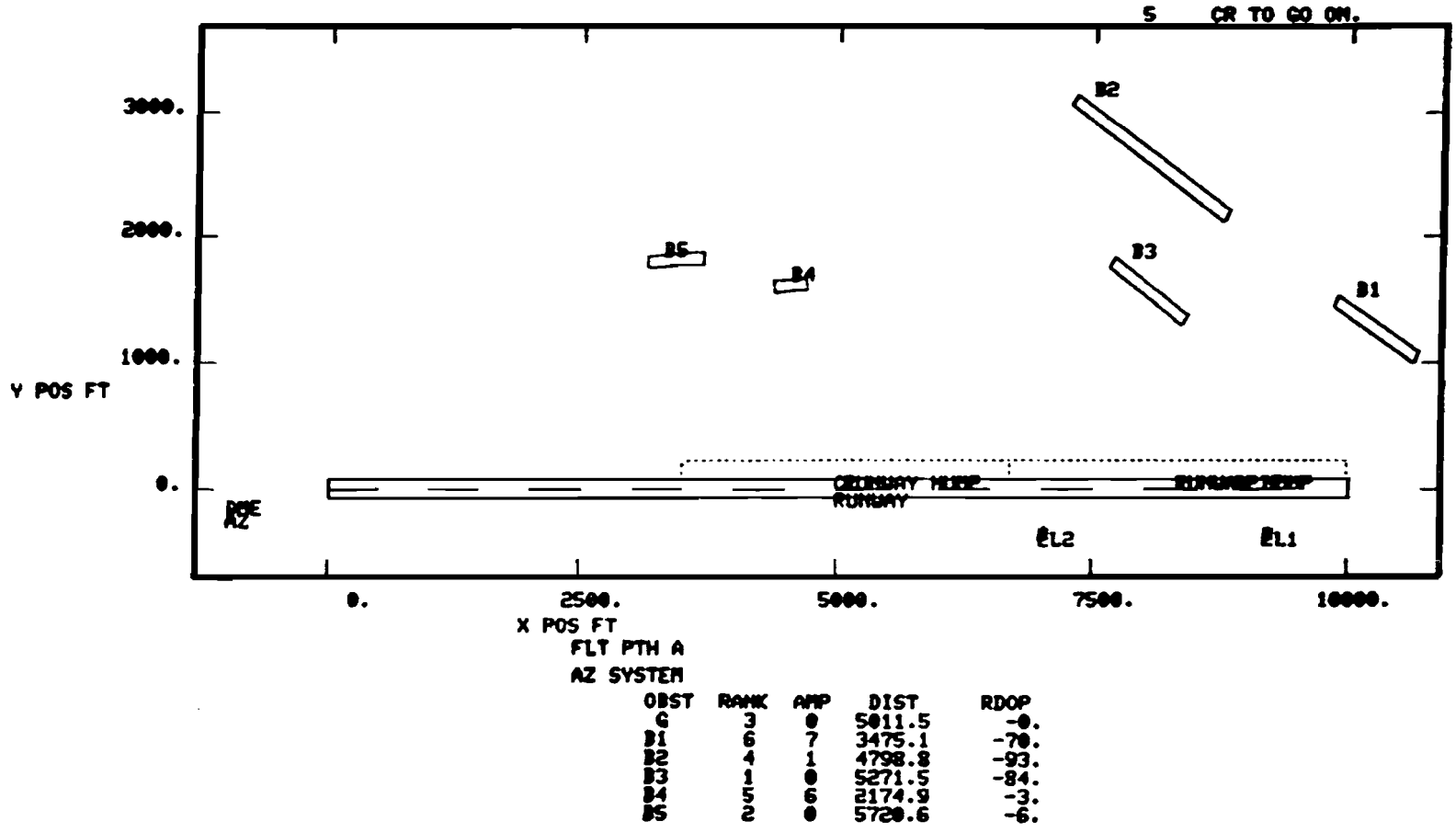

Fig. 5-20. Airport map for simulation of Tulsa DME measurement site 1.

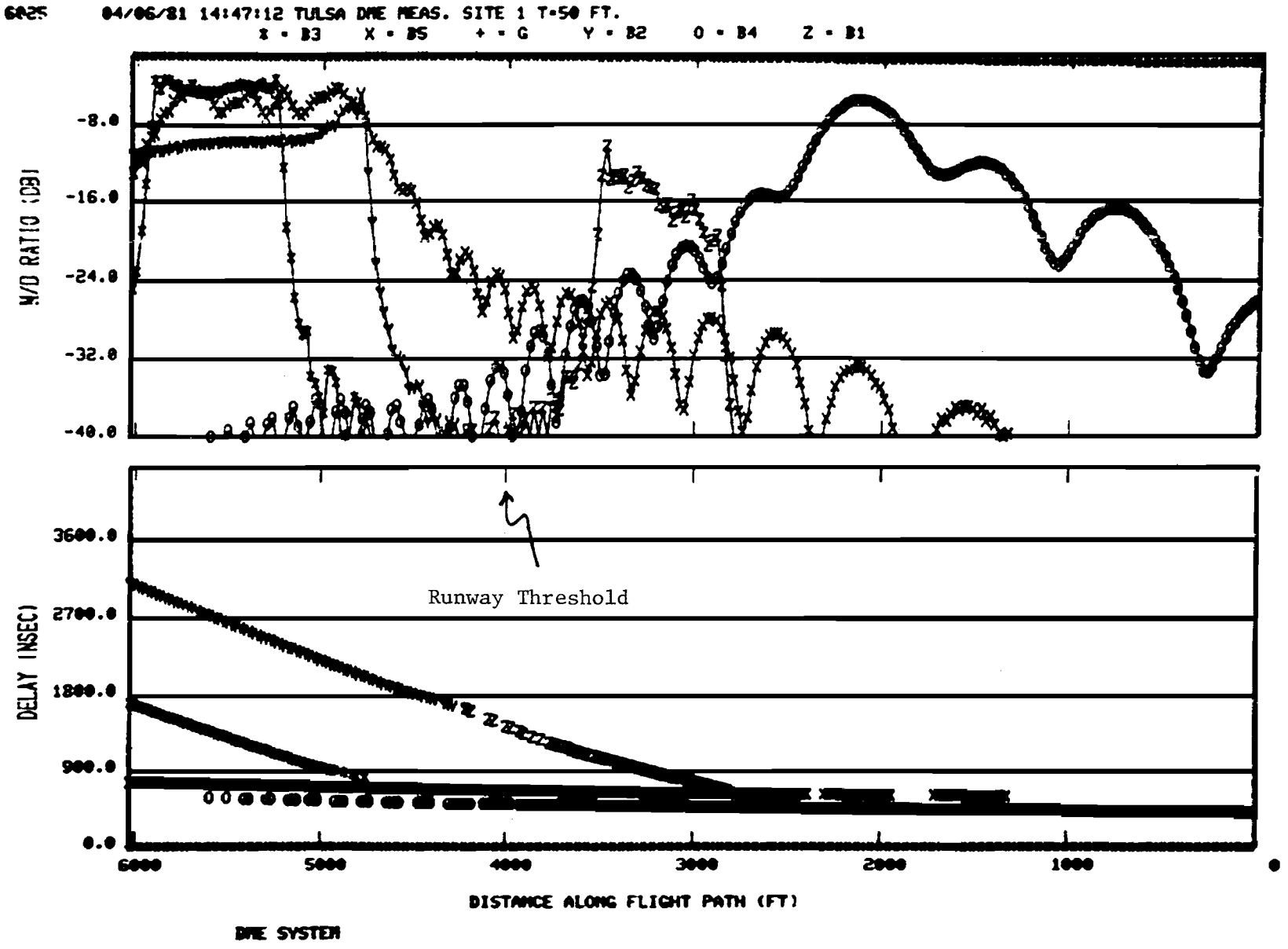

Fig. 5-21. Computed multipath characteristics for simulation of Tulsa site 1 measurements.

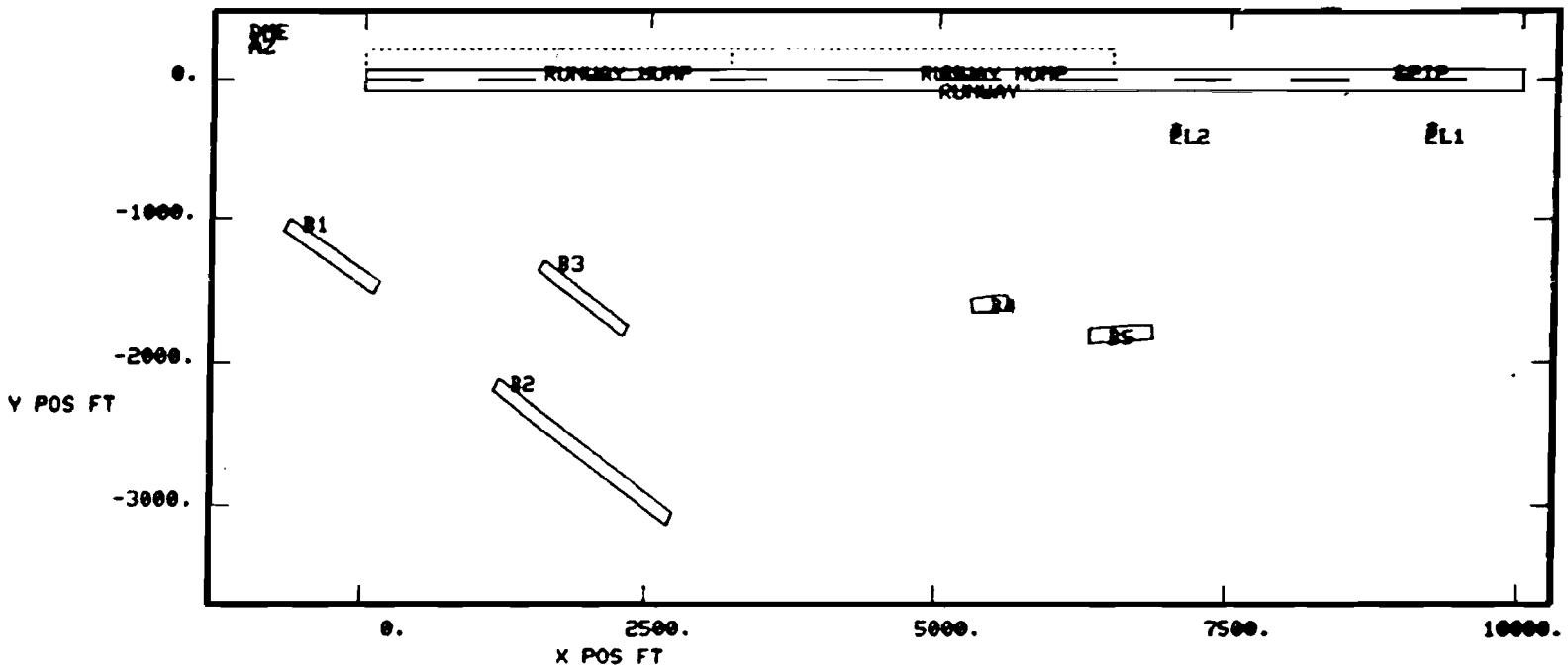

FLT PTH A
AZ SYSTEM

OBST	RANK	AMP	DIST	RDOP
G	2	0	5011.5	-0.
B1	3	0	3049.5	-1.
B2	5	42	1583.9	-2.
B3	6	80	0.0	0.
B4	4	4	4633.3	-8.
B5	1	-1	2624.0	-7.

Fig. 5-22. Airport map for simulation of Tulsa DME measurement site 2.

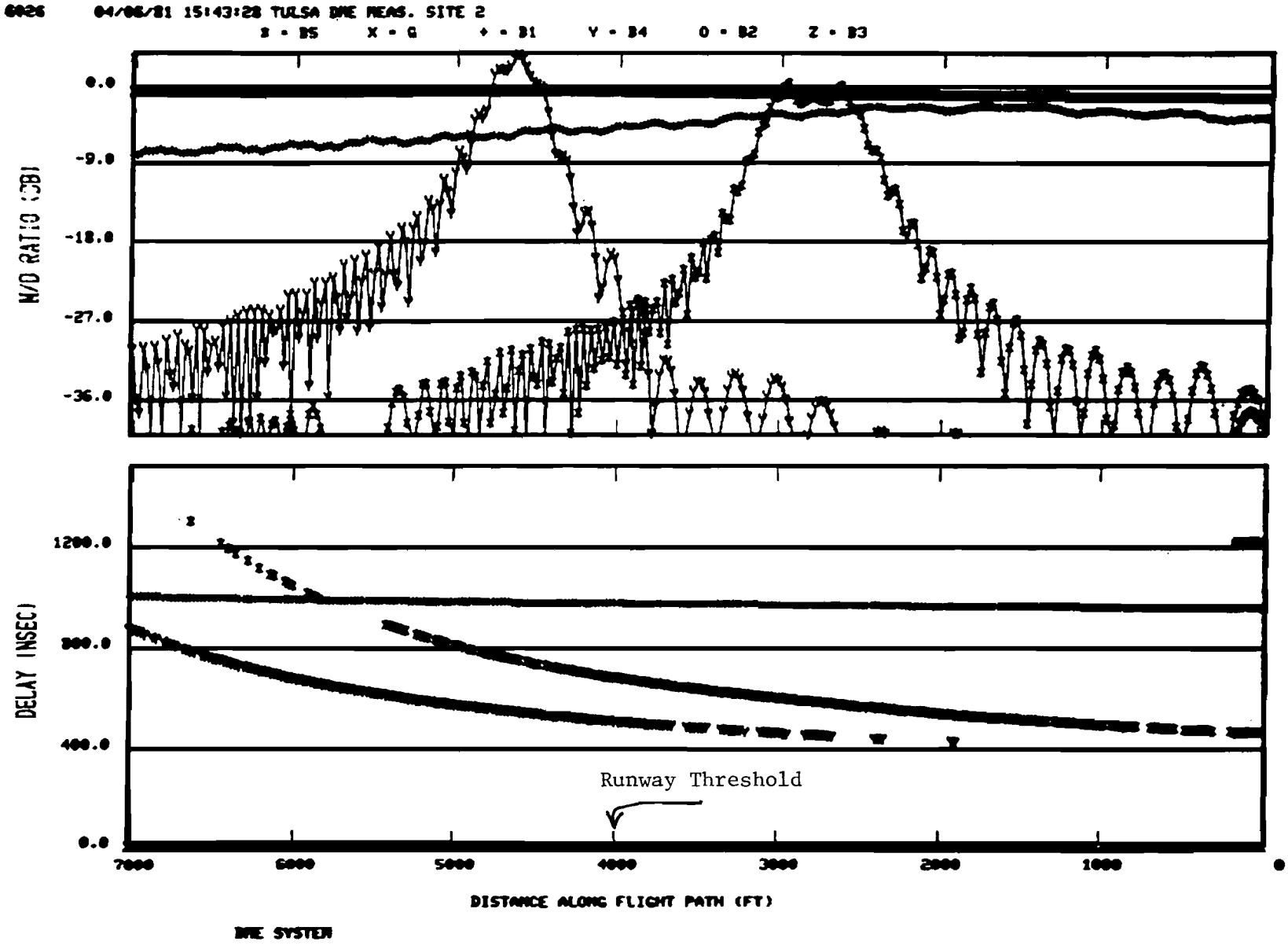

Fig. 5-23. Computed DME multipath characteristics for simulation of Tulsa DME measurement site 2.

E. Summary

The measured multipath regions and time delays at Tulsa International agreed quite well with the predicted characteristics using simple ray tracing. The measured M/D levels agreed reasonably well with the predicted levels at one site (although a detailed comparison in the flare region was not possible due to the many missed measurements), while at the other, the observed M/D levels were considerably larger (e.g., 6 to 12 dB) than those predicted. The large differences are felt to arise from the (sizable) differences in terrain contour features along runway centerline and along the paths to the buildings which were not considered in the simple airport model.

VI. WRIGHT PATTERSON AIR FORCE BASE

A. Multipath Environment

Figure 6-1 shows the airport geometry at runway 5-23 at Wright Patterson Air Force Base (WPAFB), Ohio. This airport had been used for tests of the Doppler MLS and had been shown to have substantial C band multipath over the runway [2]. Figure 6-2 shows an aerial view of the airport.

Figure 6-3 shows the various buildings on the runway south side as seen from the ground van site located approximately 200 feet northwest of the ILS localizer serving runway 23 as well as a closeup of hangar 206, which is a major multipath threat in the flare guidance region. The other buildings along the same apron as hangar 206 are much lower (typically 10 meters high) and typically made of wood or corrugated metal. The expected multipath time delays are as follows:

Building	τ(nsec)
152	1477
146	1654
206	1713
145	1832

The terrain along the path to the buildings is relatively flat; however, the runway slopes up noticeably as one proceeds from the threshold of runway 5 to the 23 end of the runway (see Fig. 6-4). Given the long measurement site to runway distance (5000 m), the receiving antenna was elevated to its full height (10 m).

A taxi test was conducted along taxiway 17 at approximately 5:00 p.m. on February 9 as indicated in Fig. 6-1, however, very high winds and rain prevented carrying out the flight tests until noon on February 11. Snow also fell during the period, but the ground was basically bare for both types of tests.

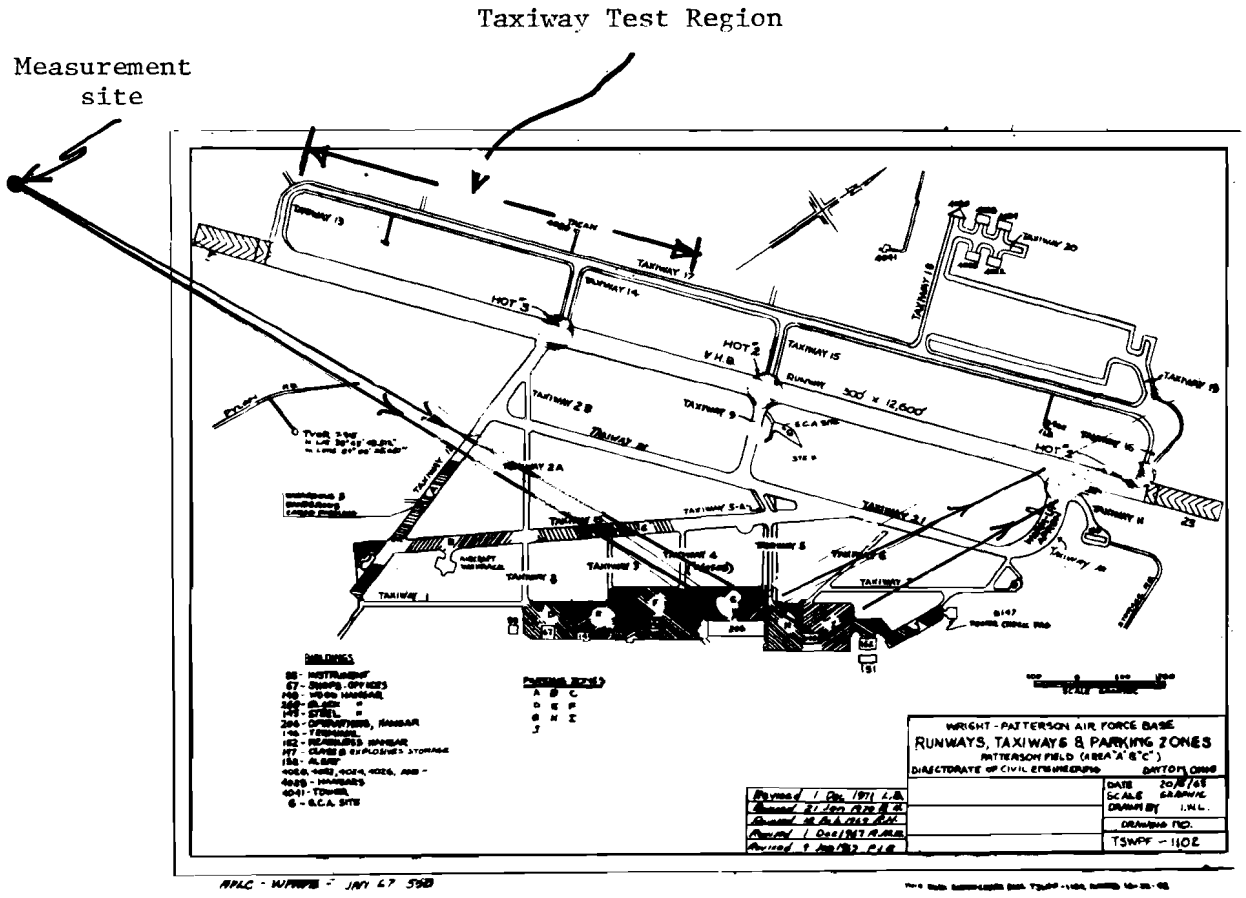

Fig. 6-1. Airport geometry at Wright Patterson AFB.

Fig. 6-2. Aerial View of Wright Patterson Air Force Base

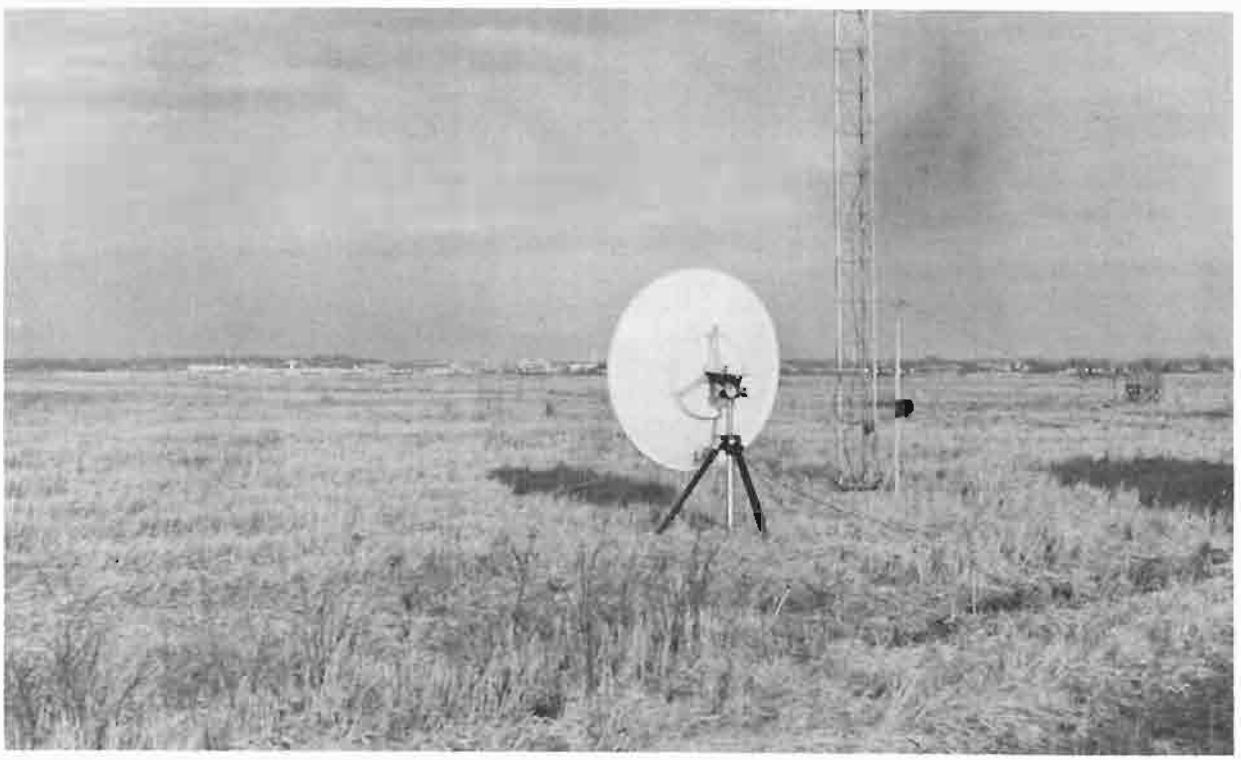

Fig. 6-3a. DME multipath measurement equipment at Wright Patterson AFB, Ohio.

Fig. 6-3b. Building 206 at WPAFB from near the transmitter site.

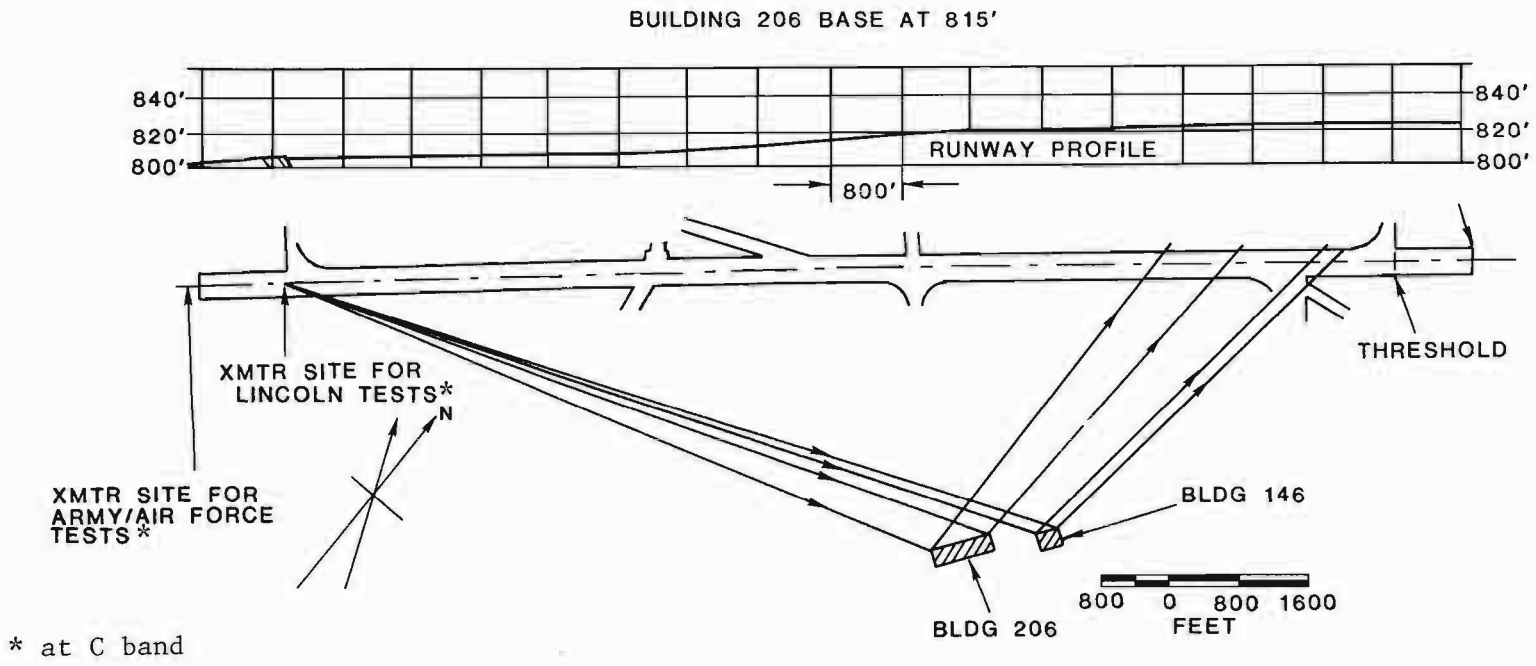

Fig. 6-4. Wright-Patterson Air Force Base.

B. Measurements Made

Table 6-1 summarizes the measurements made at WPAFB. The large number of approaches required was necessitated by difficulties in obtaining adequate SNR on the transponder reply. The low SNR represented a combination of low output power from the transponder and high attenuation due to the "focusing" runway contour. Successful data was finally achieved by keeping the engine rpm up during the approaches (so as to generate a higher power supply voltage). One of the runs with profile 2 was hopelessly corrupted with high level fruit interference, which appeared to be correlated with the transponder replies.

C. Waveform Analysis

All of the approaches with adequate SNR and the taxiway test have been analyzed and representative results will be described in this section. Figure 6-5 shows the results of the test along the airport taxiway. At the beginning of the test, strong multipath (M/D > -6 dB) is encountered with delays of approximately 300 nsec, while at the end of the run, a considerable amount of low level multipath (M/D < -10 dB) is encountered with progressively increasing delays. The beginning of the taxi test was at the midpoint of taxiway 17 and the test ended when abreast threshold of runway 05. The multipath delays here correlate with reflections from an elevated steam pipe and trees to the north of the runway which are shown on Fig. 6-2.

Figures 6-6 and 6-7 show the summary results for two approaches with flight profile 1. We see that a region of strong multipath with a τ of 1600 nsec is encountered just prior to threshold (joystick range 2.56 nmi), but that then much of the data is missed for the next nautical mile. There are a number of isolated measurement points just after threshold with extremely high M/D ratios and a τ of approximately 1600 nsec. Much further down the runway, low level multipath is encountered with delays in the 500 nsec - 1000 nsec range. These shorter τ multipath signals are believed to arise from the trees to the north of runway.

TABLE 6-1

PDME MULTIPATH MEASUREMENTS AT WPAFB

Taxiway Test (February 6)

1 run along taxiway 17 transmitting/receiving through top antenna on aircraft

Flight Tests (February 9)

Profile 1: 3° glideslope, 45-foot threshold crossing height, 10 feet AGL along runway
bottom a/c antenna: 9 unsuccessful runs, 4 successful runs
top a/c antenna: 5 unsucessful runs

Profile 2: 3° glideslope, 20 foot threshold crossing height, 5 feet AGL along runway
bottom a/c antenna: 2 unsuccessful, 4 successful*
top a/c antenna: 4 unsuccessful

*One of the runs contained synchronous fruit.

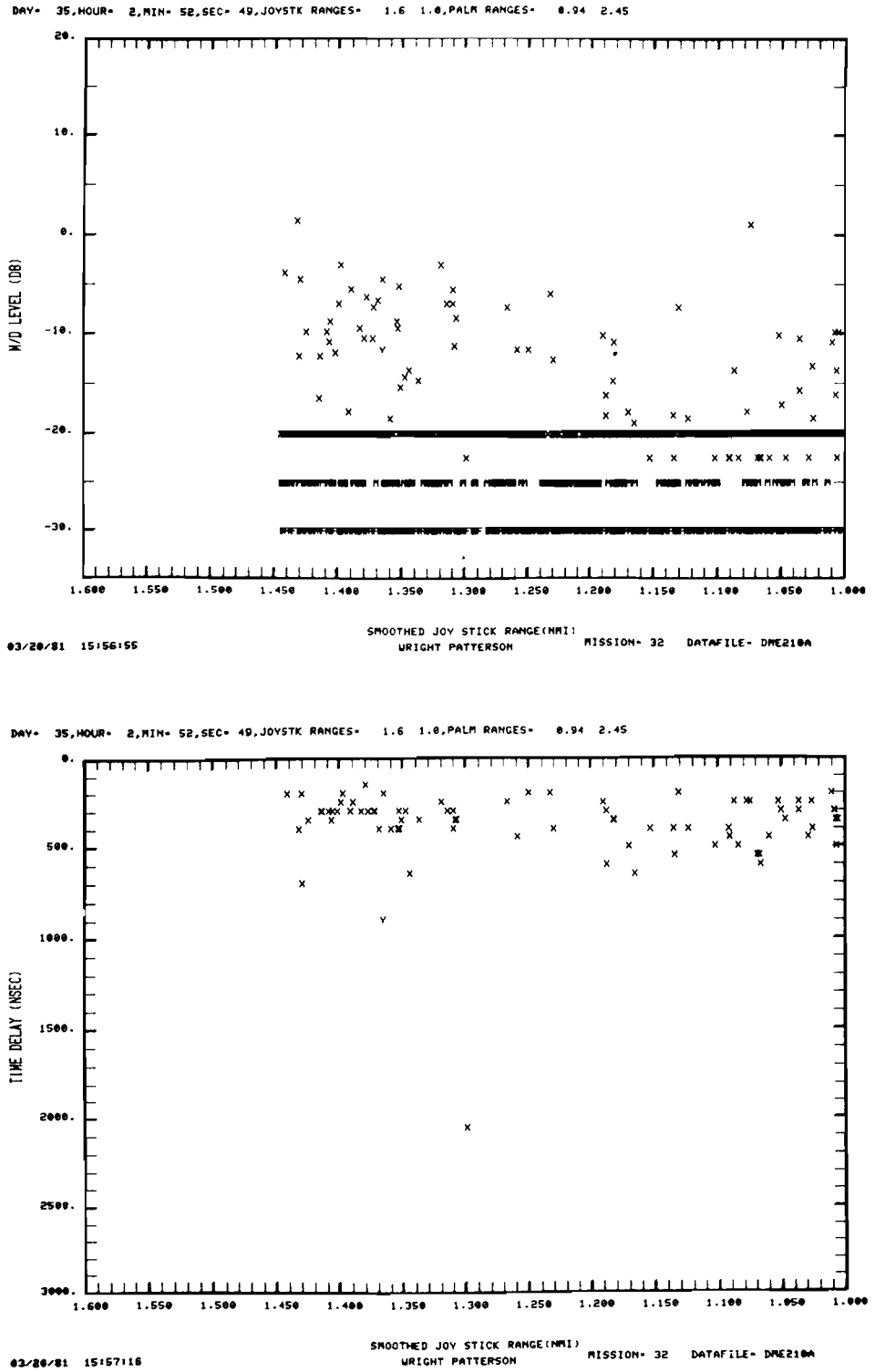

Fig. 6-5a. Summary results for taxiway test at WPAFB.

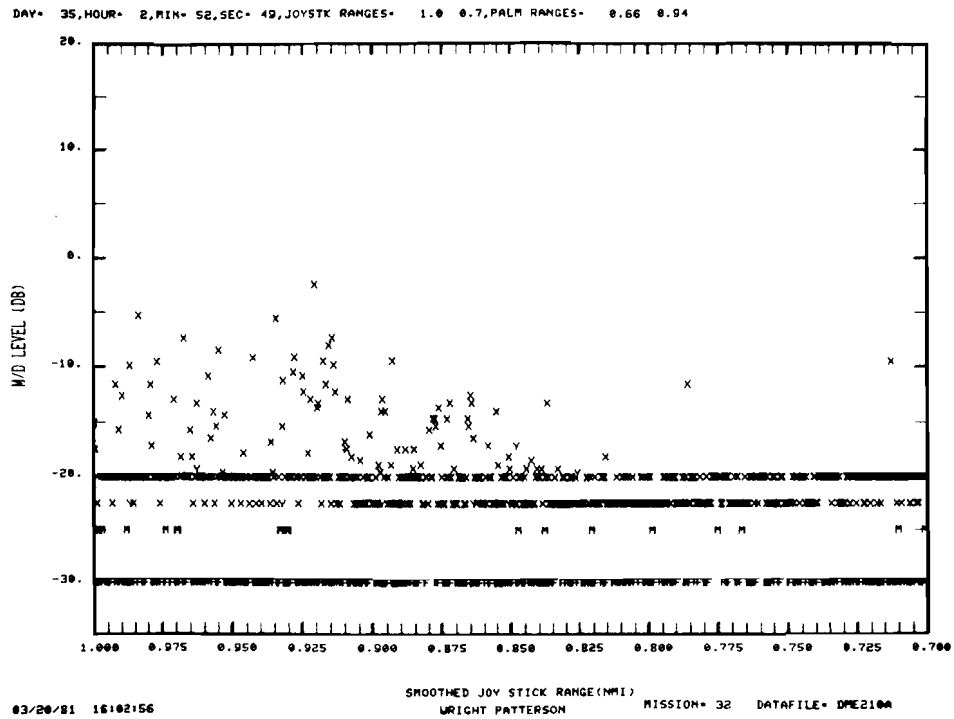

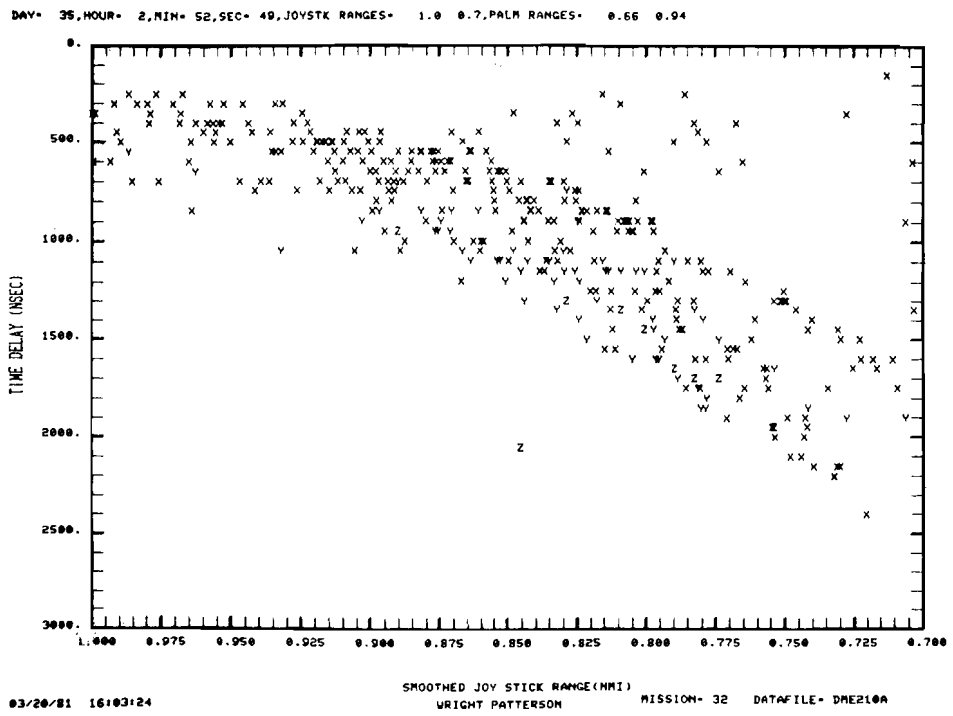

Fig. 6-5b. Summary results for taxiway test at WPAFB.

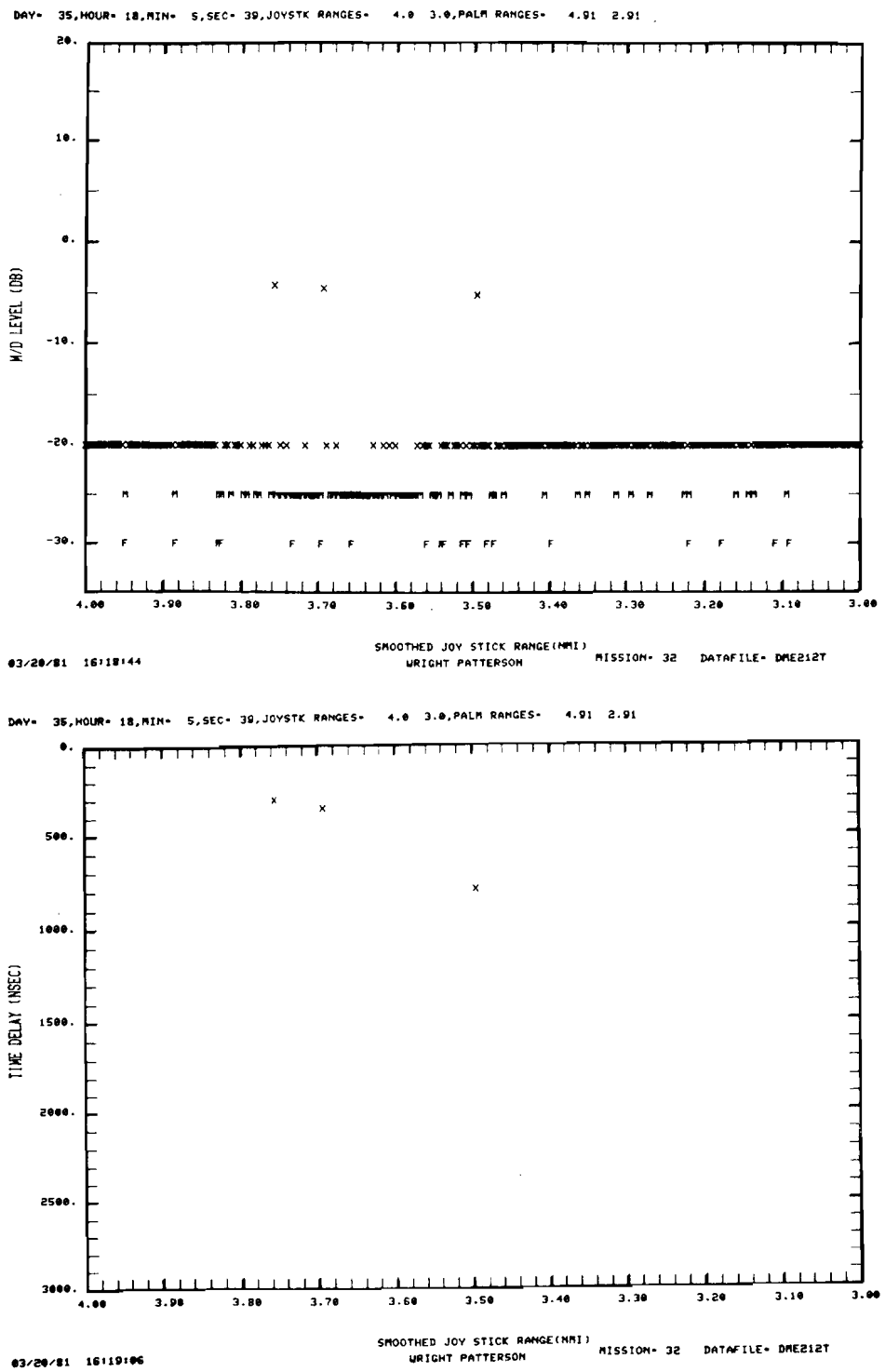

Fig. 6-6a. Summary results for Flight Profile 1 at WPAFB.

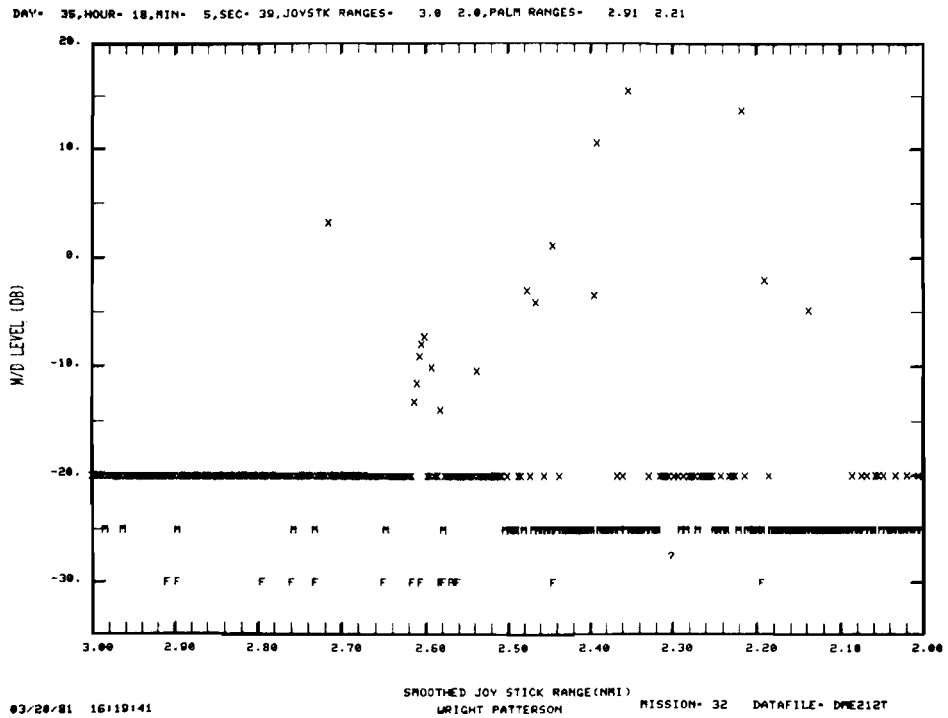

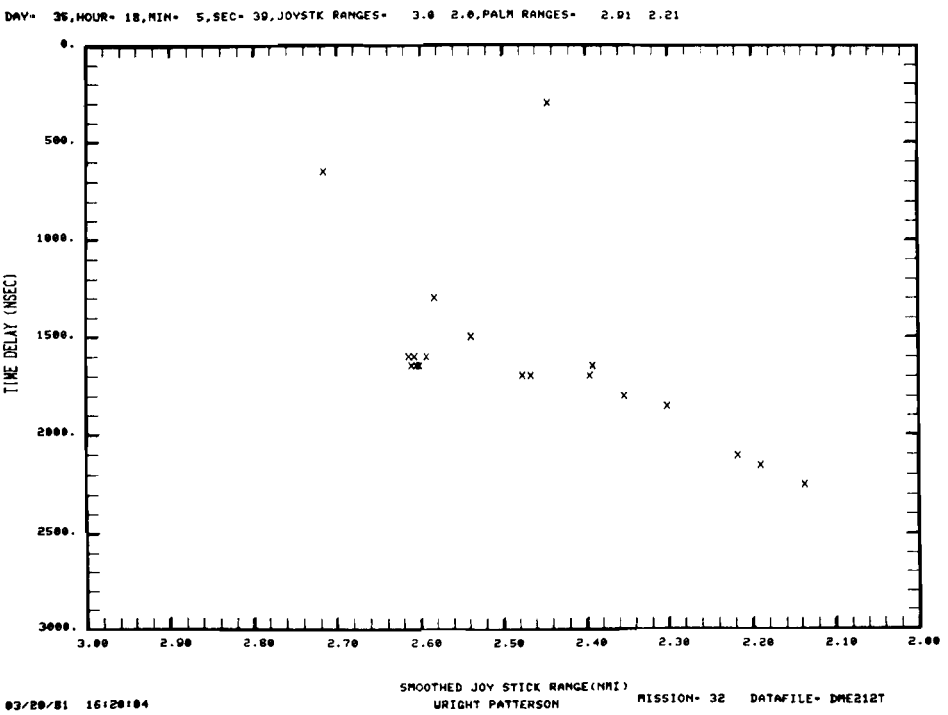

Fig. 6-6b. Summary results for Flight Profile 1 at WPAFB.

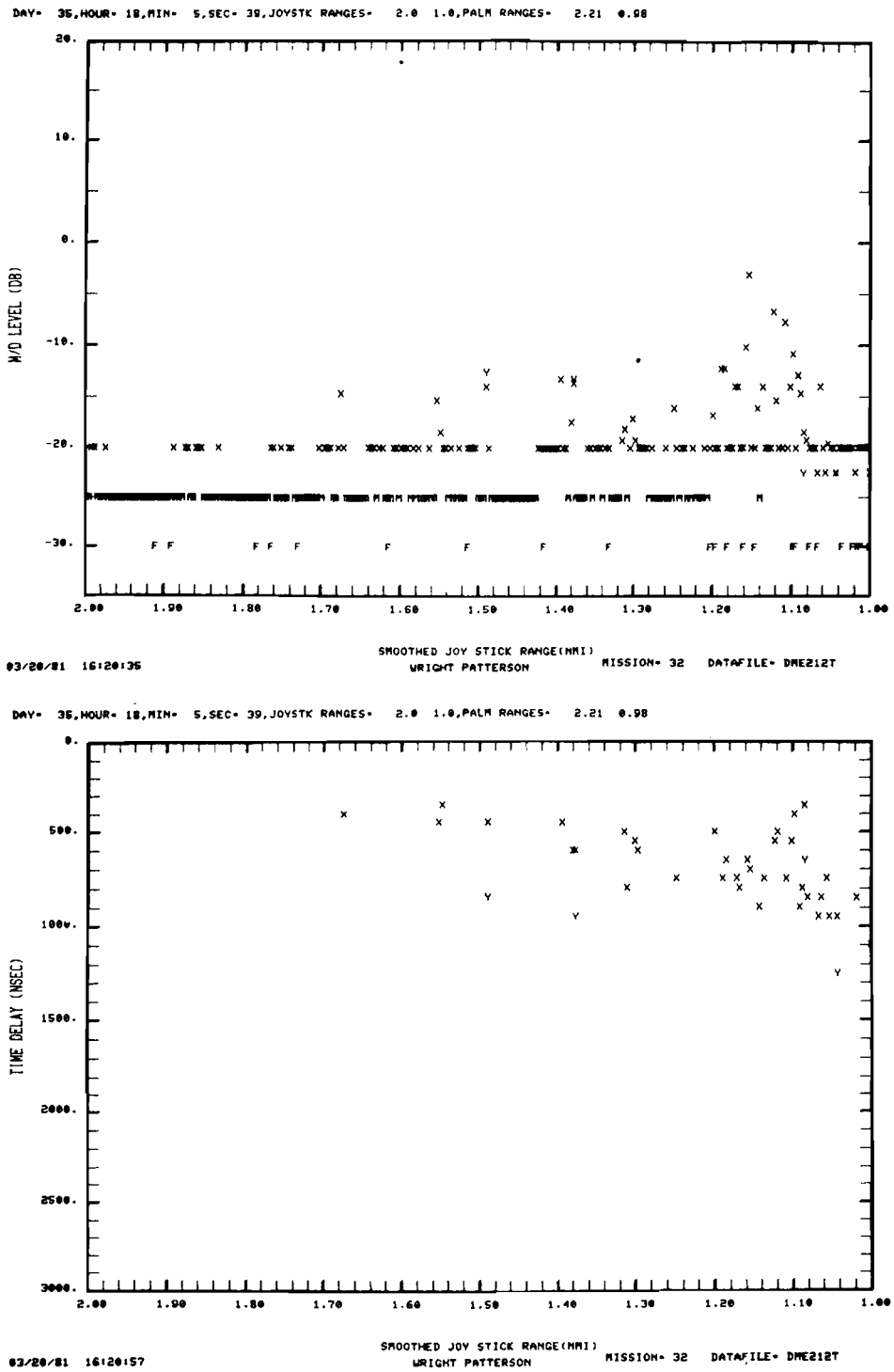

Fig. 6-6c. Summary results for Flight Profile 1 at WPAFB.

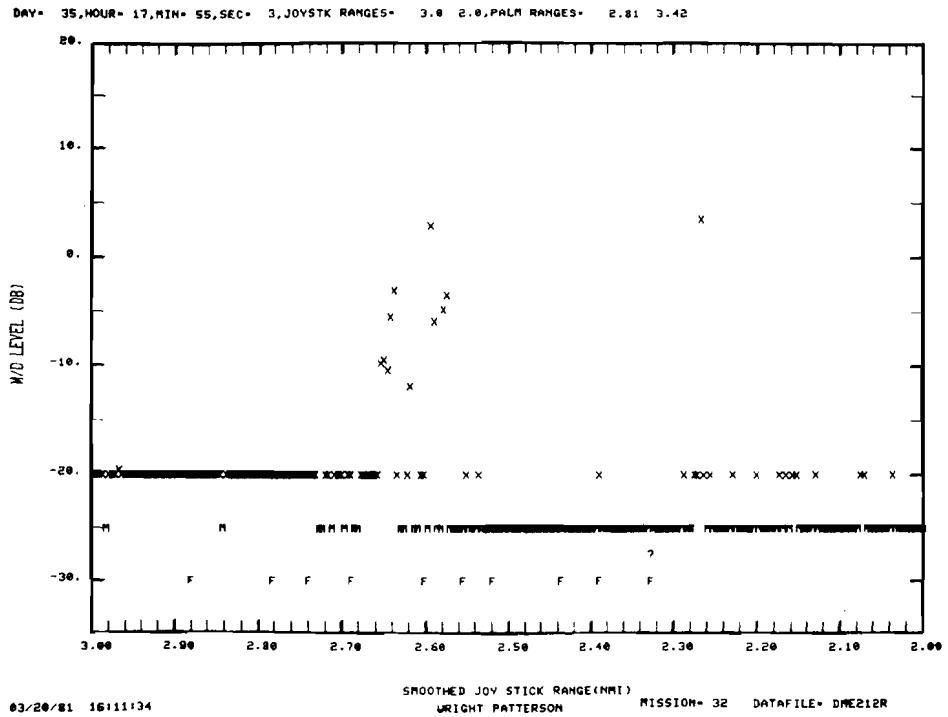

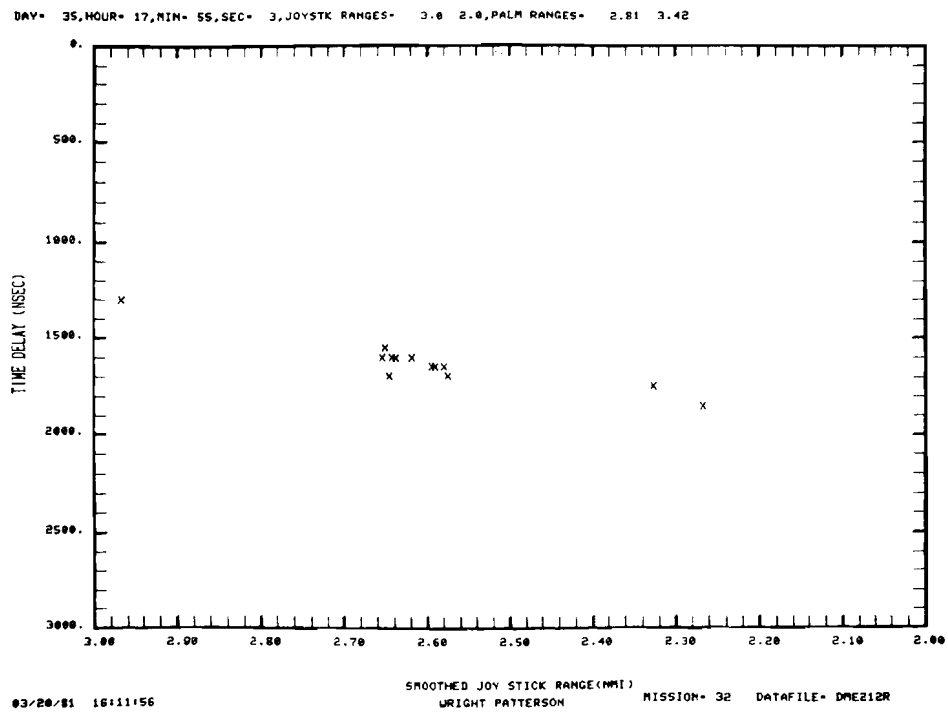

Fig. 6-7a. Summary results for Flight Profile 1 at WPAFB.

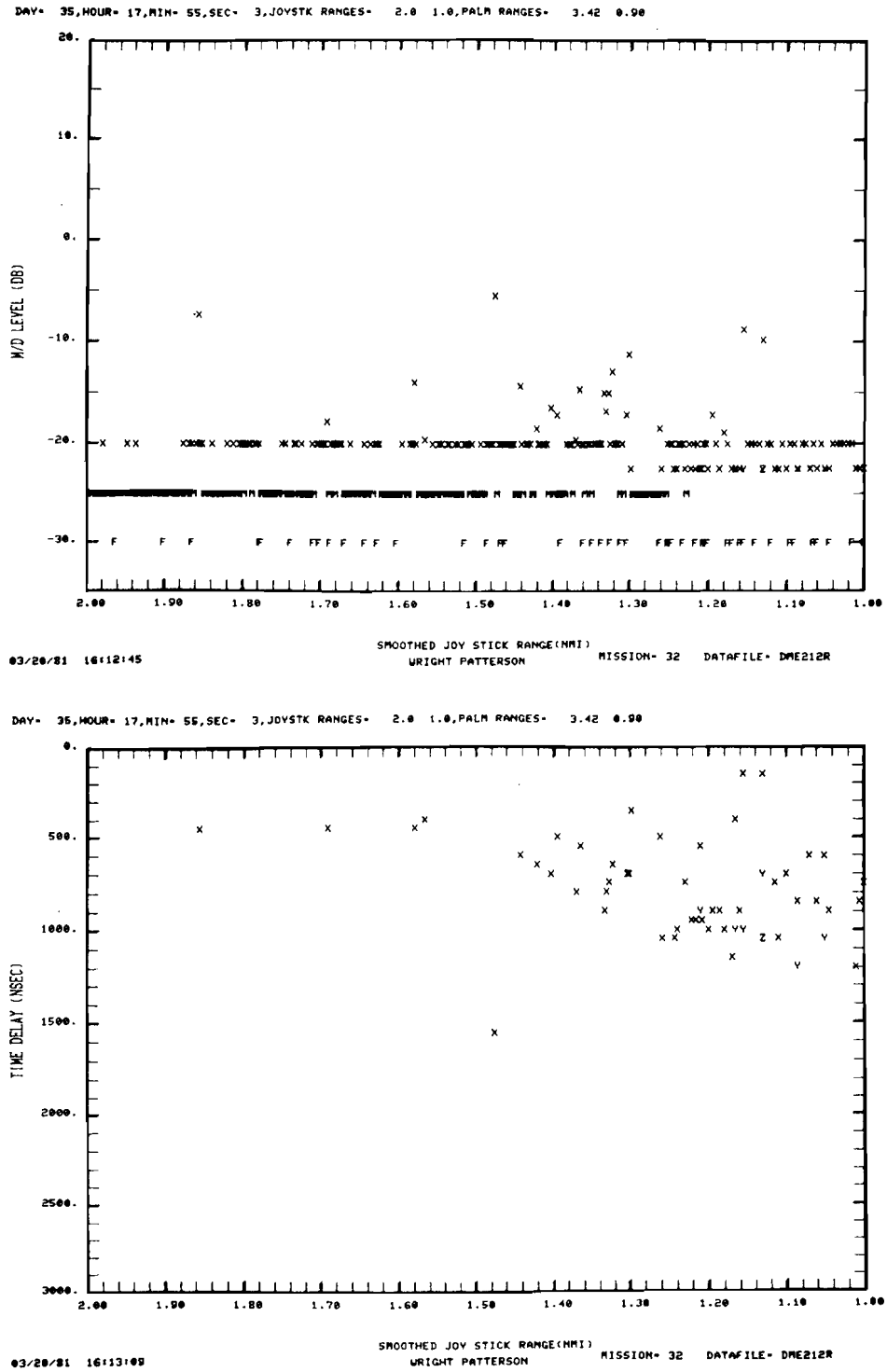

Fig. 6-7b. Summary results for Flight Profile 1 at WPAFB.

Figure 6-8 shows summary results for an approach with flight profile 2. The results here are quite similar to those of Figs. 6-6 and 6-7: no multipath until just at threshold, a region of very high level multipath with delays of approximately 1600 nsec and then a loss of valid data. Figures 6-9 and 6-10 show the received waveforms corresponding to the high M/D levels near threshold. The direct signal amplitude is seen to be roughly constant (as would be expected arise since ground lobing would change slowly), whereas large increases in multipath level occured at a few points.

These results near threshold correlate quite well with the expected multipath region and time delays expected for buildings 206, 146, and 152. The loss of data in this region may also reflect transponder suppression due to high level reflections of the P_1 pulse with a delay near 2 μsec. These buildings are approximately 1 - 1.5 beamwidths off the interrogation antenna boresight, so that they should not have caused transponder suppression if high level multipath (M/D $\leq$ 0 dB) had been encountered. However, the levels in this region were considerably in excess of even that and hence may have caused transponder suppression.

D. Simulation Results

Flight profile 1 wes simulated using a very simple airport model in which terrain contours were ignored and each building modeled as a single vertical rectangular plate. Figures 6-11 and 6-12 show the airport map and computed multipath characteristics for the simulation. The simulation predicts low level (-12 dB M/D) reflections from building 152 at threshold with a delay of approximately 1.6 μsec and high level (-3 dB M/D) reflections from hangar 206 with a time delay of 2 μs. The multipath regions and time delays correlate reasonably well with the field measurements, but the predicted M/D levels are, in some cases, considerably lower (e.g., 10 - 15 dB) than the measured values. This difference could arise from several factors:

1. the terrain contour along the runway and building reflection paths was assumed to be flat in the simulation. This may have understated the amount of differential direct

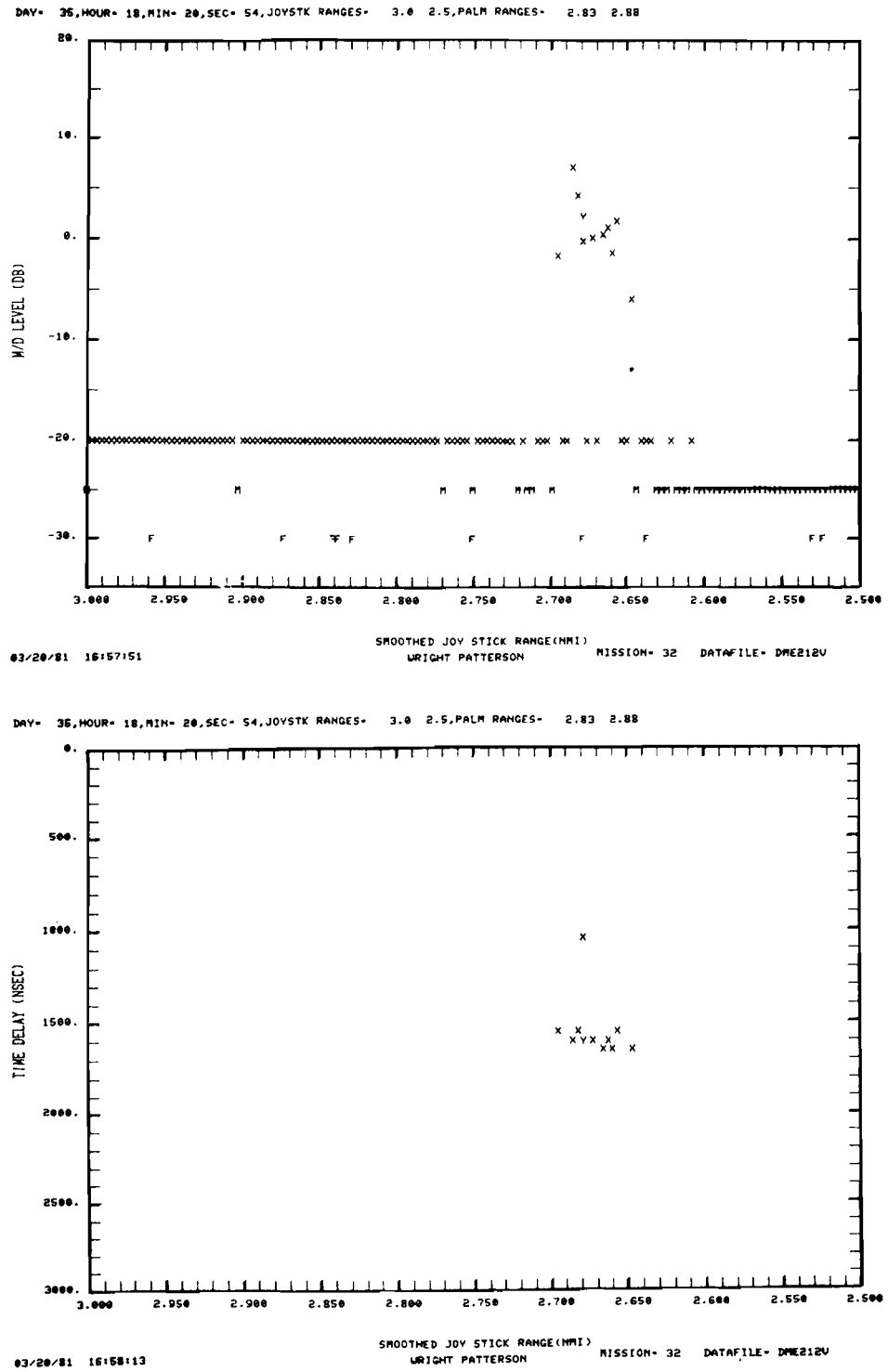

Fig. 6-8. Summary results for Flight Profile 2 at WPAFB.

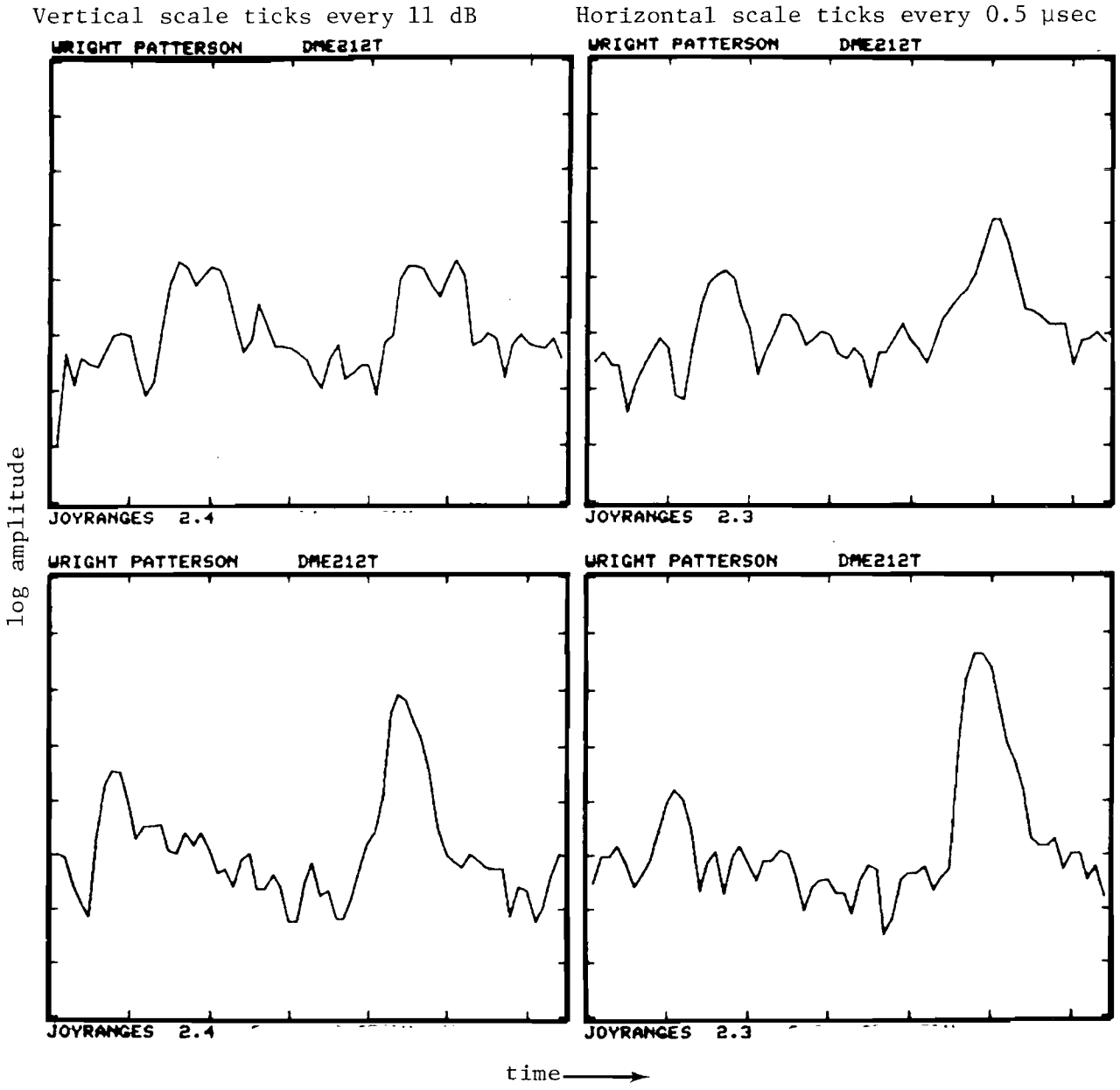

Fig. 6-9. WPAFB waveforms after threshold on flight profile 1.

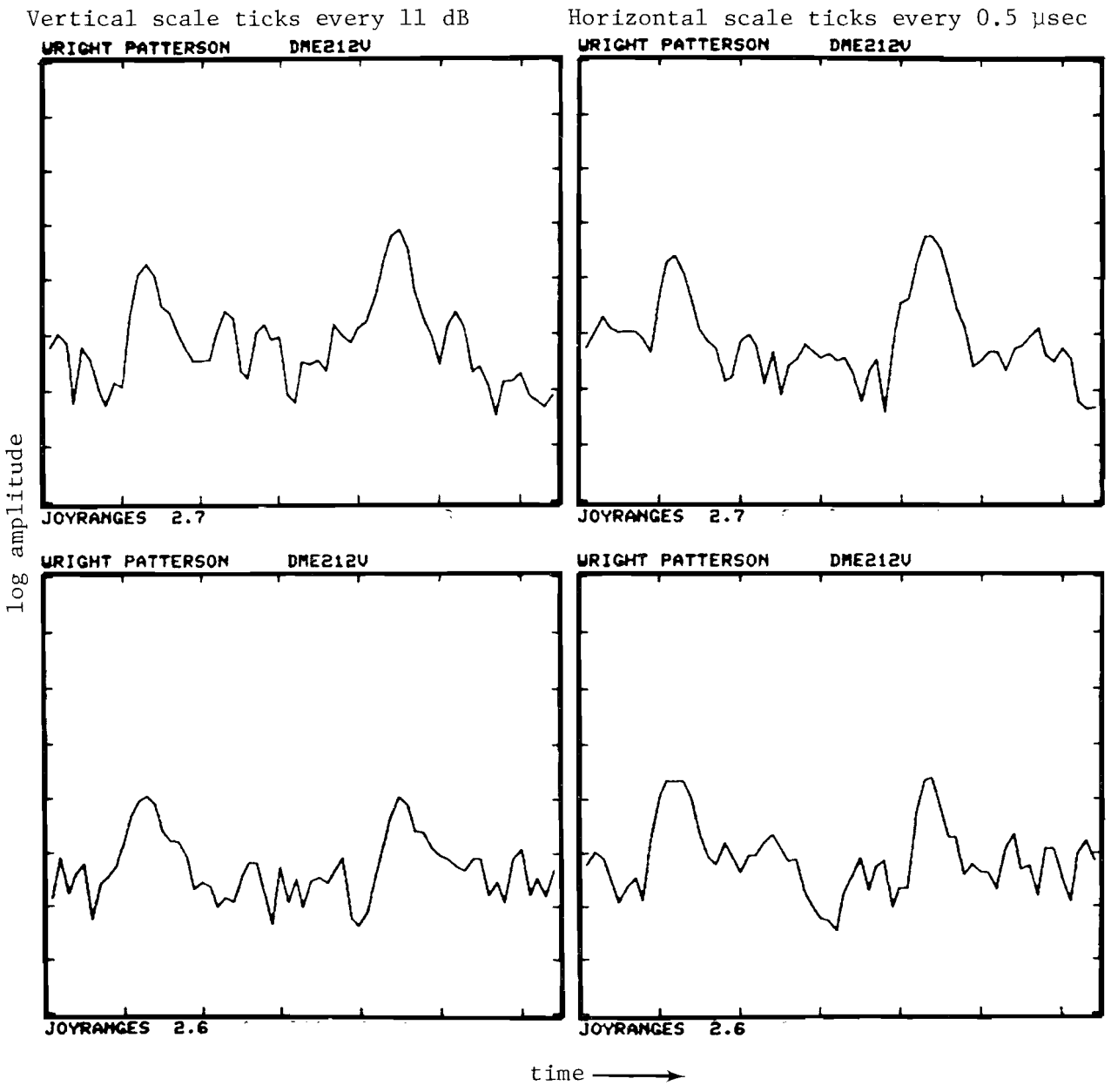

Fig. 6-10. WPAFB waveforms near threshold on flight profile 2.

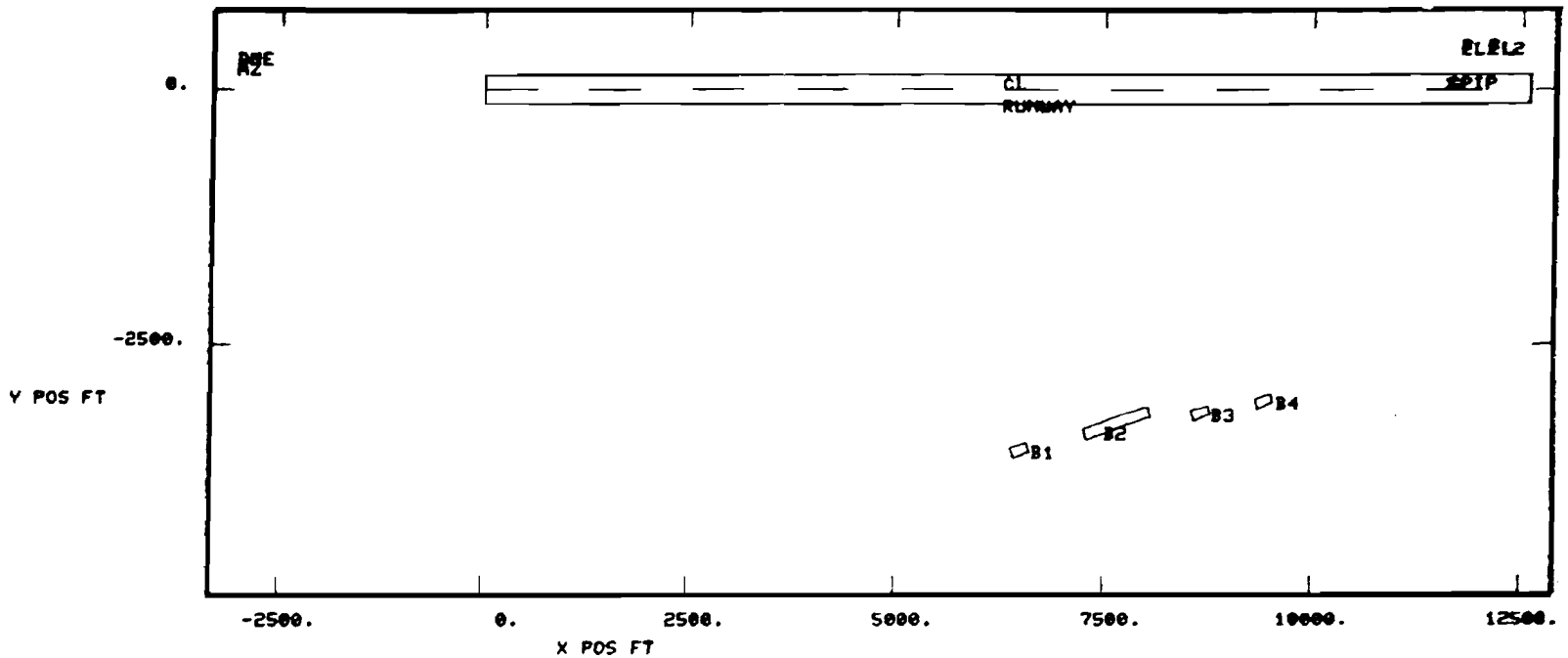

OBST	RANK	AMP	DIST	RDOP
G	2	0	6520.0	-0.
B1	5	9	9320.0	-75.
B2	1	0	8360.0	-68.
B3	4	8	6960.0	-61.
B4	3	8	6120.0	-57.
D	0	80	0.0	0.

Fig. 6-11. Airport map for WPAFB simulation

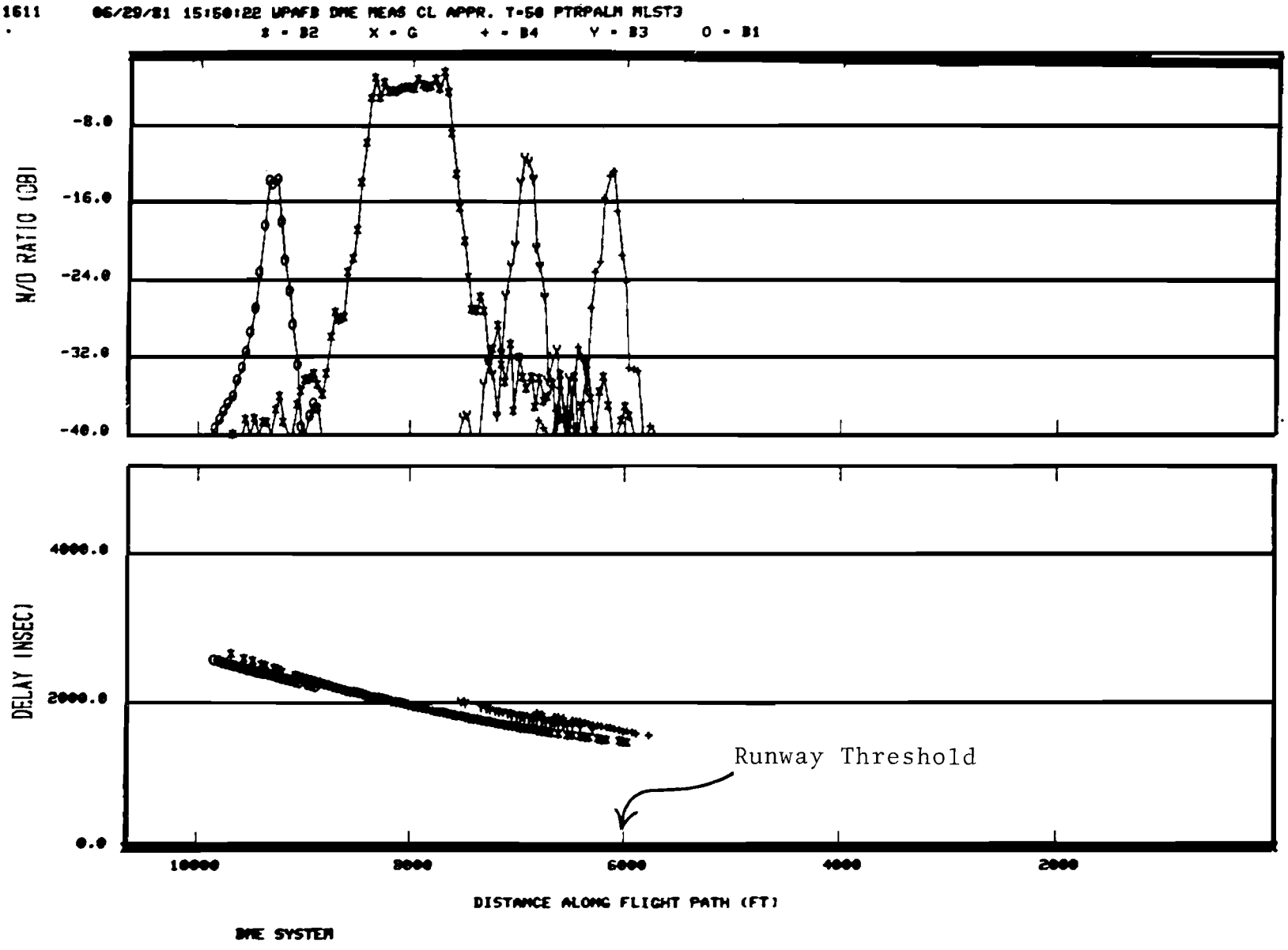

Fig. 6-12. Computed DME multipath characteristics for WPAFB scenario

signal lobing due to the ground since the off runway terrain is lower than the along runway terrain (see [1]).

2. the staggering of the doors on building 206 was ignored. In studies of C band reflection behavior along this runway, it was found that the reflected signal levels could oscillate very rapidly in the specular region due to reinforcement and cancellation of signals from adjacent doors [2].

E. Summary

The measured data at WPAFB correlated reasonably well with the multipath regions and time delays expected from ray tracing and computer simulations. Unfortunately, the severe reflection environment (terrain lobing and/or building reflections) was such that only fragmentary data was available in the flare region where the highest M/D levels were anticipated. The measured data available in that region suggests that the actual M/D levels were comparable to and, in many cases in excess of, the simulation results using a simple airport model. Several factors were identified which could account for much of these differences.

VII. PHILADELPHIA INTERNATIONAL AIRPORT

A. Multipath Environment

Figure 7-1 shows the airport layout at Philadelphia (PA) International Airport, while Figure 7-2 shows the reflection rays for the principal anticipated multipath threats. Philadelphia was chosen as a site exemplifying reflections from relatively low buildings in the flare/rollout region and because earlier C band van measurements [9] had shown high level multipath at low heights on the adjacent taxiway.

The main threats were the cargo buildings along the runway. A photograph of the United Airlines (UA) building is shown in Fig. 7-3. This building is approximately 10 meters high, as is the Cargo Unit number 1 building. The adjacent American Airlines/Eastern Airlines (AA/EA) building is 8 meters high, as is the Flight Kitchen buildings. The building surfaces are corrugated metal or concrete [6]. The expected multipath time delays for a centerline approach to runway 9R as as follows:

Building	τ (nsec)
Cargo Building 1	750
AA/EA Cargo	850
UA Cargo	950

The terrain contour along the runway and prior to the 9R threshold (see Fig. 7-4) presented some substantial siting difficulties. The original plan called for siting the van adjacent to the ILS localizer for runway 27L. However, the sharp drop in height meant that it would have been quite difficult to obtain a clear view of the aircraft for the interrogation antenna. This problem, together with the swamp-like terrain available in that location, forced us to utilize an alternate site at the edge of the holding apron for the 9R threshold. This site placed the measurement van in line with the path

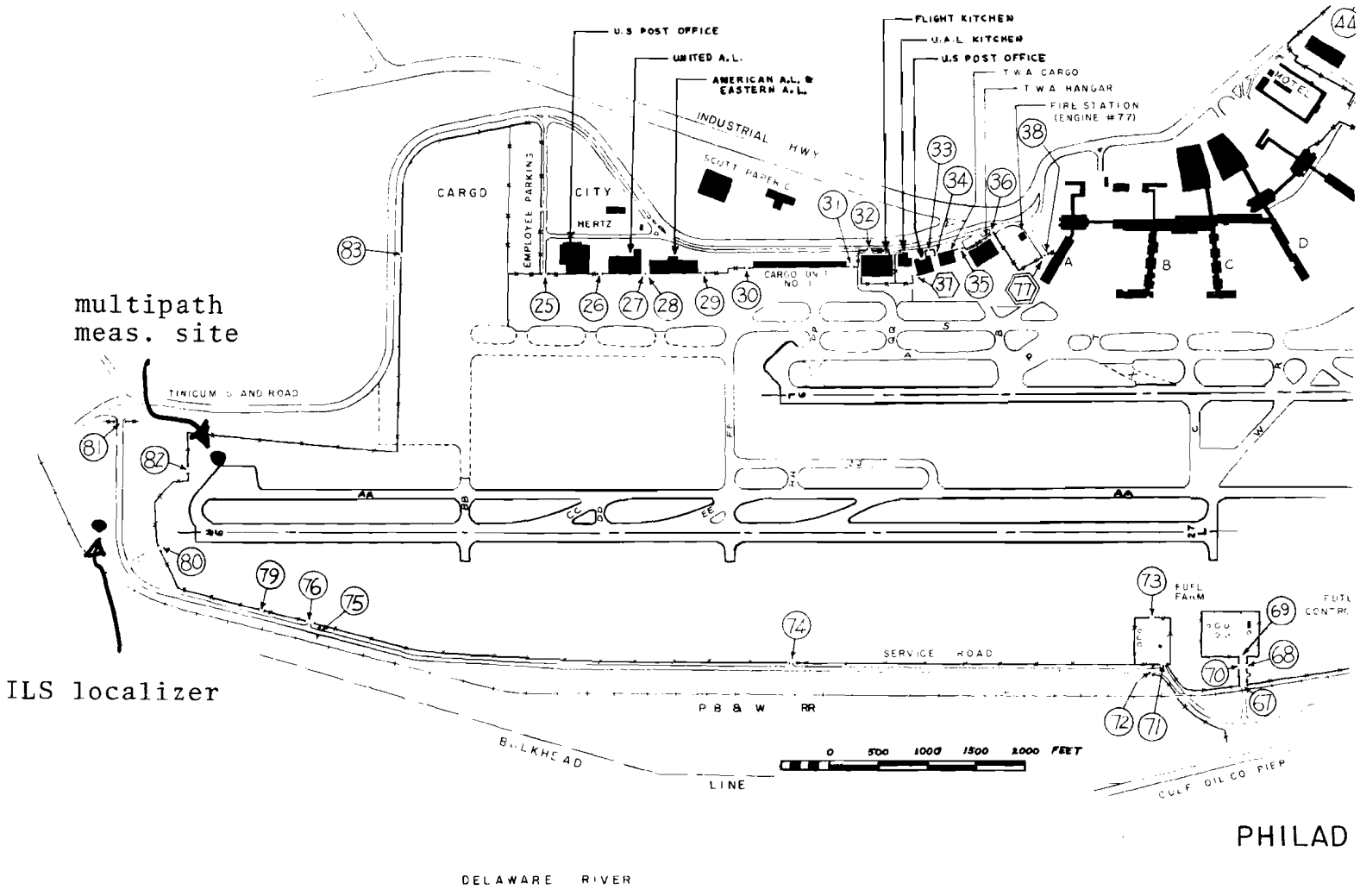

Fig. 7-1. Philadelphia International Airport in vicinity of Runway 9R-27L.

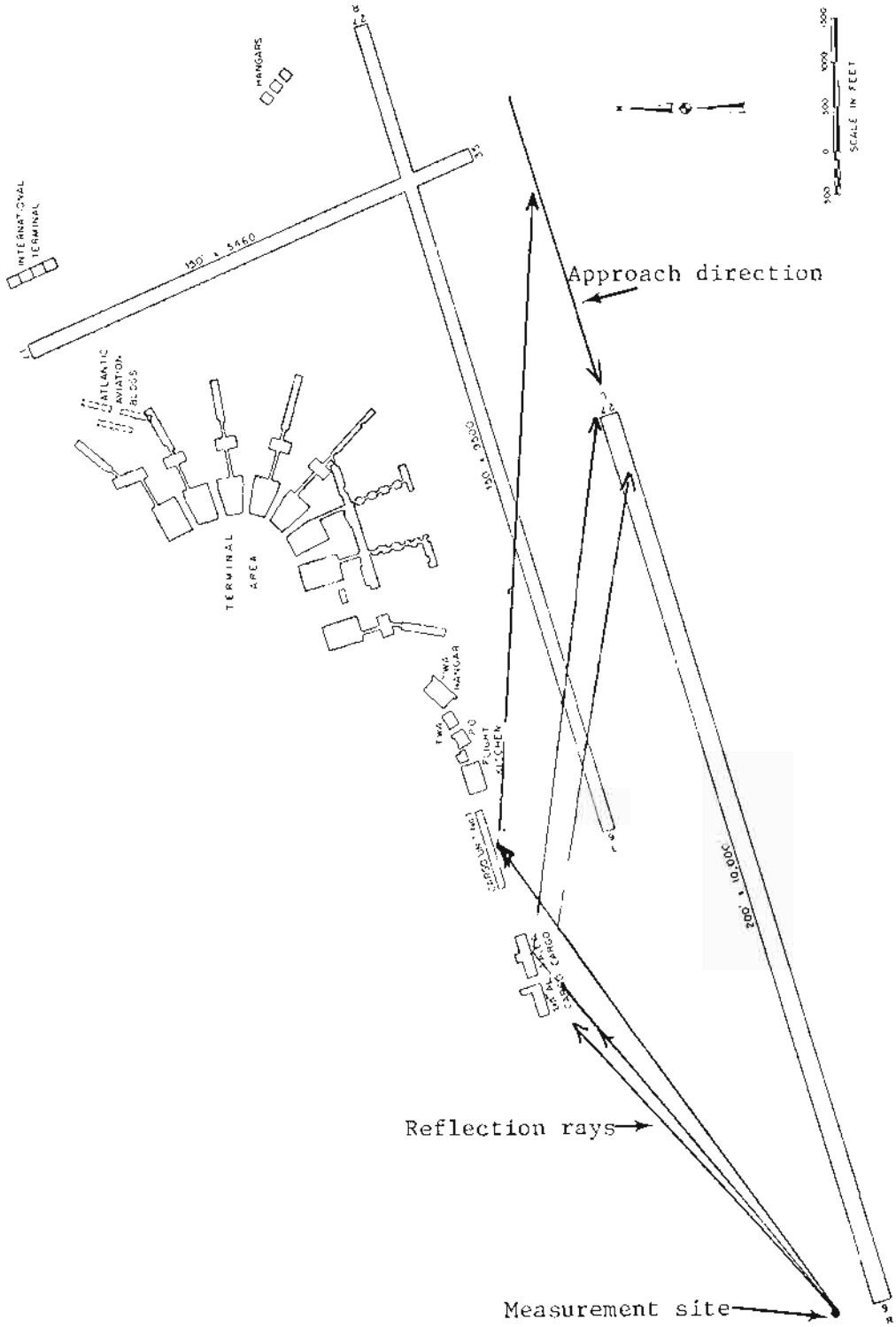

Fig. 7-2. Philadelphia International Airport

Measurement site and reflection rays.

Fig. 7-3. United Airlines cargo building at PHL.

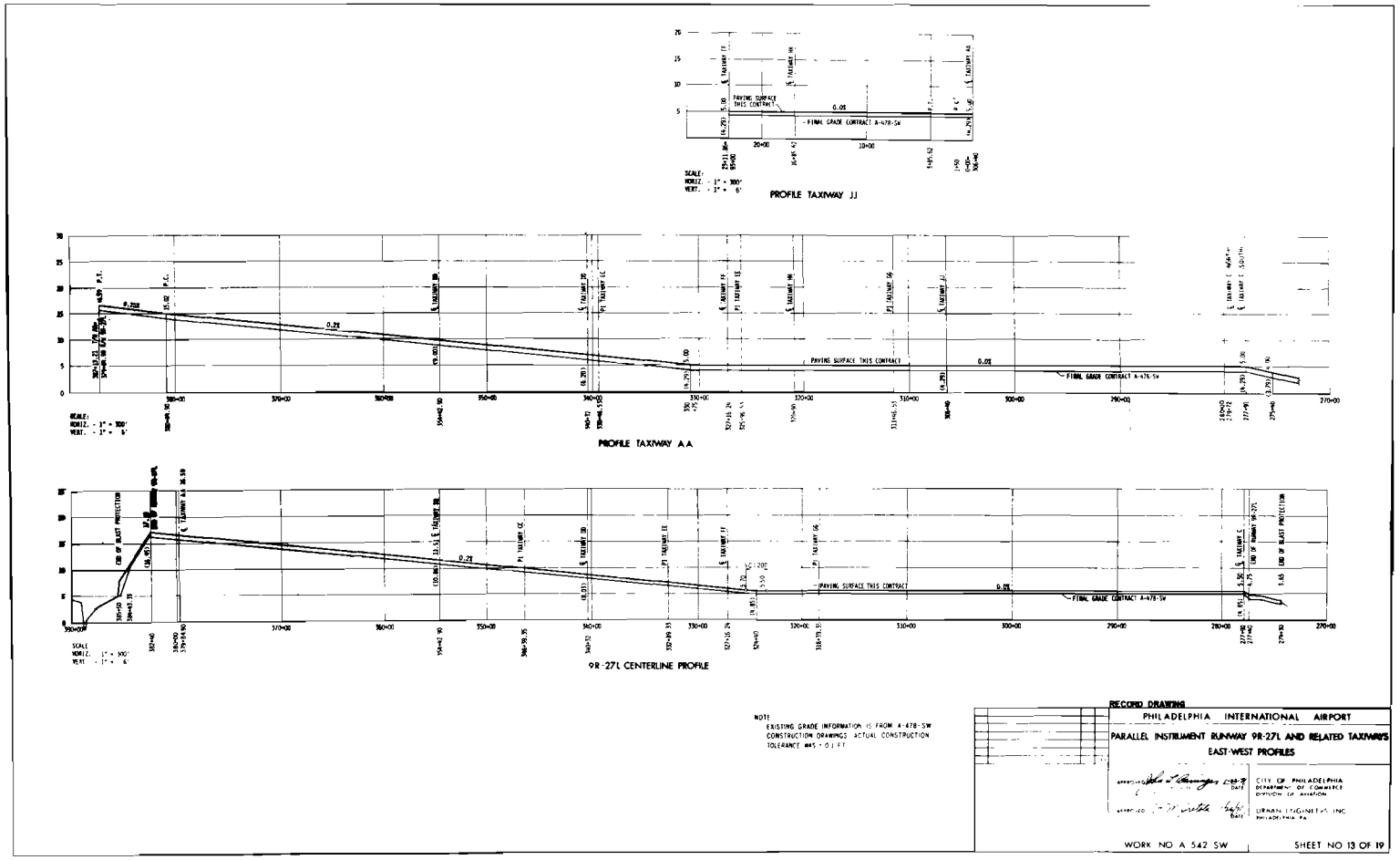

Fig. 7-4. Terrain profile along Philadelphia Runway 9R-7L.

from the localizer to the principal multipath threats and hence would yield essentially the same specular region. Since the ground at this location was 15 - 20 feet higher than the ground near the localizer, a 10-foot receiving antenna height was used to approximate the results with a 30-foot height at the localizer site.

B. Measurements Made

Table 7-1 summarizes the measurements made at Philadelphia. A taxi test was attempted along runway AA, but there was insufficient SNR to obtain useful data. A total of 13 runs were carried out between 4:30 p.m. and 7:00 p.m. on February 4, 1981.

C. Waveform Analysis Results

All of the approaches accomplished at Philadelphia have been analyzed and representative results will be described in this section. Figures 7-5 to 7-7 show summary results for three approaches with flight profile 1, while Fig. 7-8 shows results for an approach with flight profile 2. We see that no multipath is encountered until approximately 0.5 nmi before threshold (2.2 nmi joystick range). At this point, low level (e.g., -10 dB M/D ratio) multipath is encountered with a τ of 700 nsec. This correlates well with the expected multipath region and time delay for reflections from the Cargo Unit number 1 building.

In the vicinity and just after threshold (joystick range of 1.7 nmi), higher level multipath (e.g, -3 dB) is encountered. The numerous missed measurements (due to low SNR) and scatter in τ values make it difficult to correlate the multipath precisely with specific buildings. However, the bulk of the τ values are consistent with reflections from the UA and AA/EA cargo buildings.

Figures 7-9 to 7-11 show waveforms at various points where discernable multipath levels were detected. The direct signal levels are, in many cases, just at the minimum threshold we utilized (approximately +12 dB SNR) in data

TABLE 7-1

PDME MULTIPATH MEASUREMENTS AT PHILADELPHIA

Flight Tests (February 3)

Profile 1: 3° glideslope, 45-foot threshold crossing height 20 feet AGL along runway
bottom a/c antenna: 6 successful approaches

Profile 2: 3° glideslope, 20 foot threshold crossing height, 10 feet AGL along runway
bottom a/c antenna: 7 successful approaches

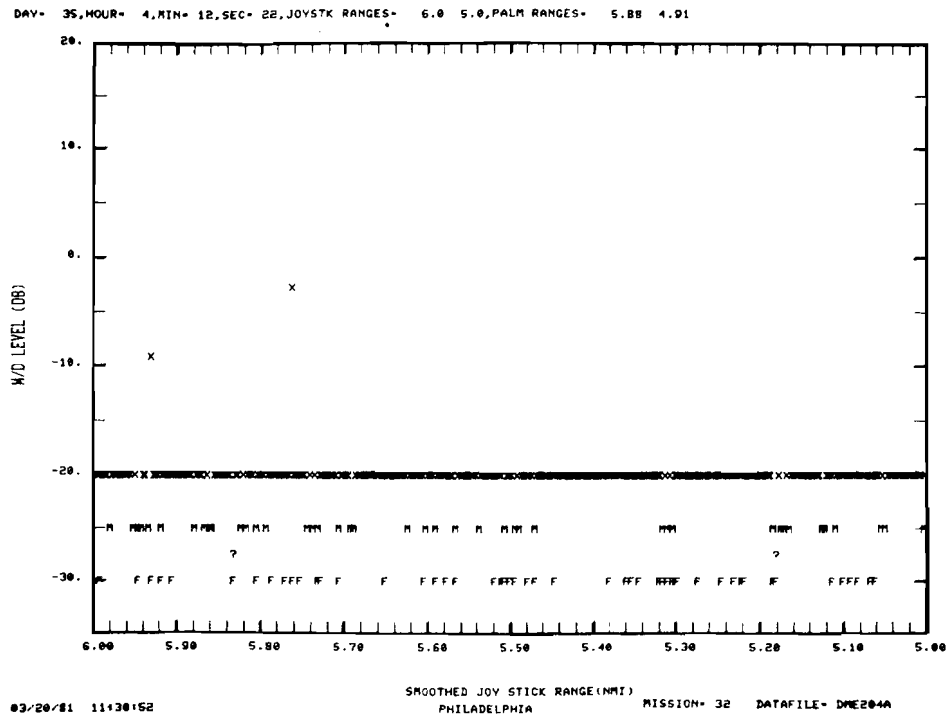

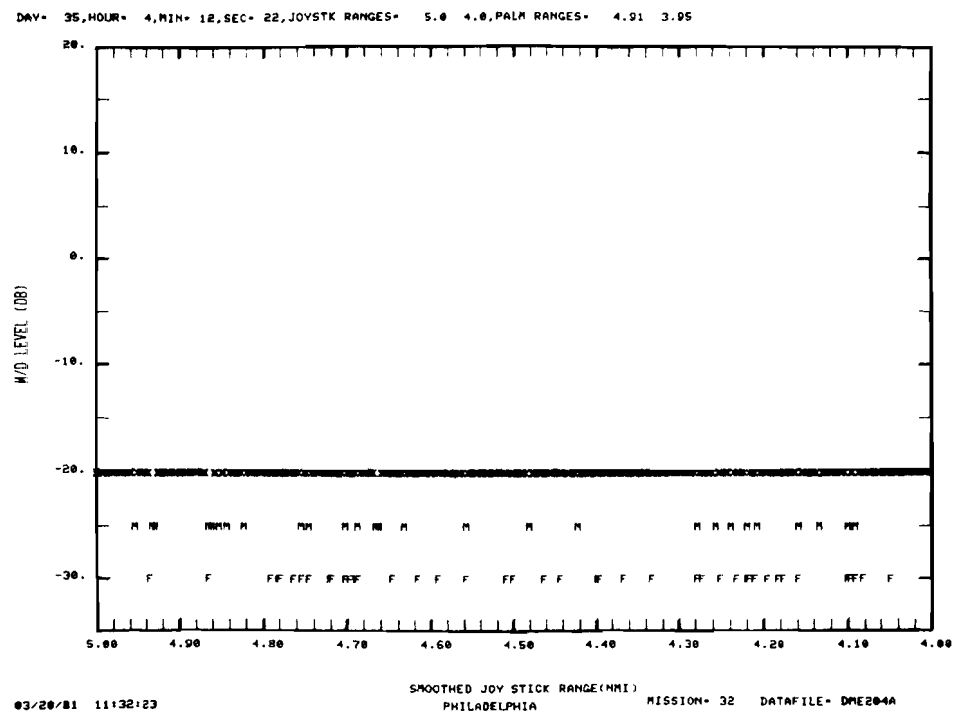

Fig. 7-5a. Summary results for flight profile 1 at Philadelphia.

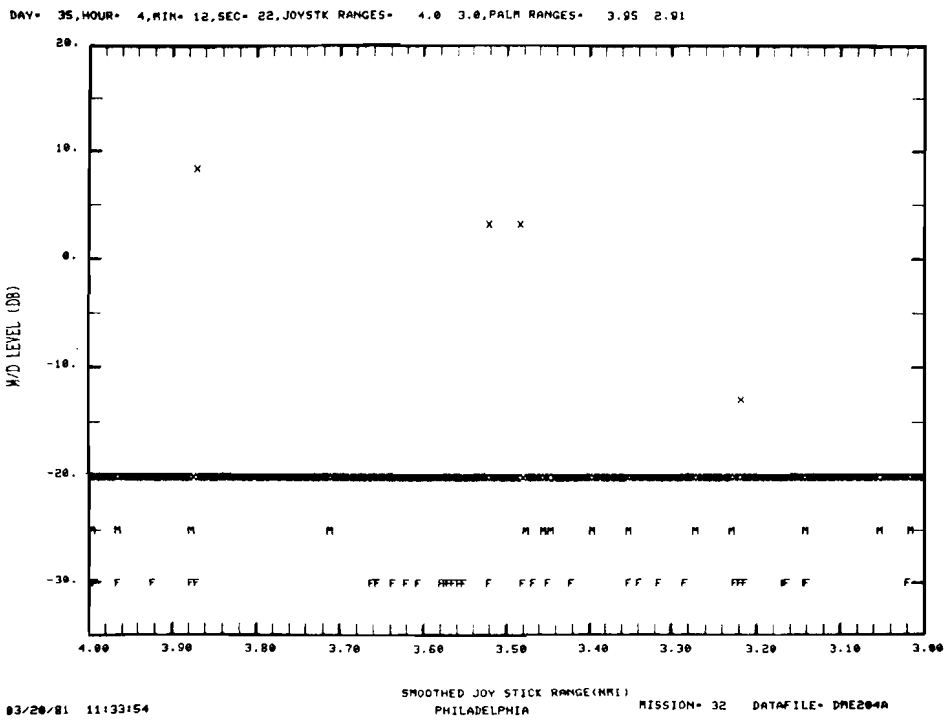

Fig. 7-5b. Summary results for flight profile 1 at Philadelphia.

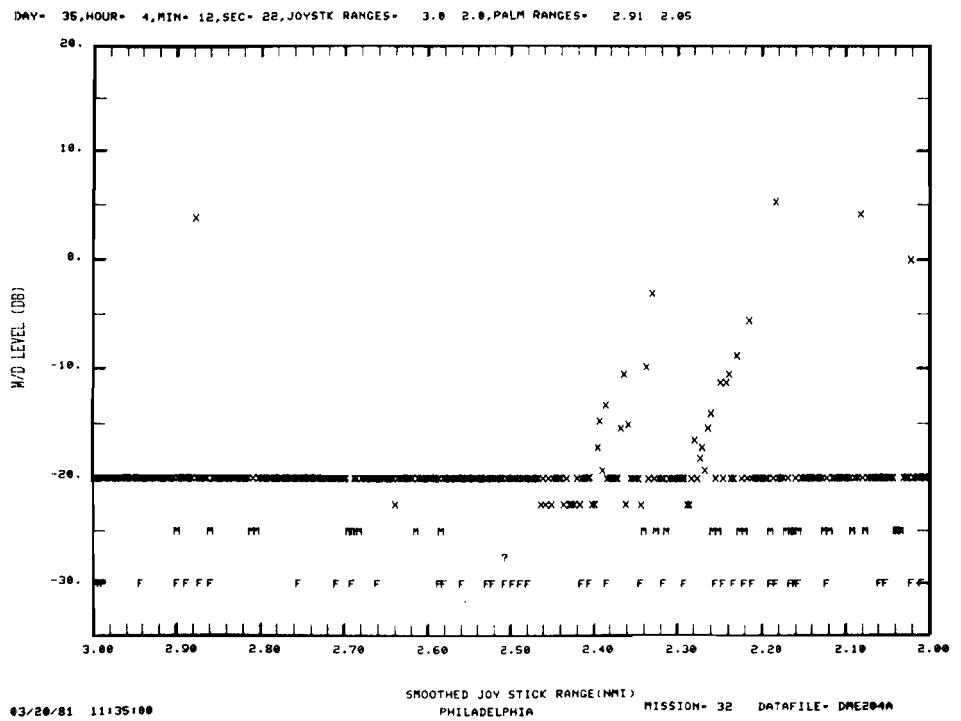

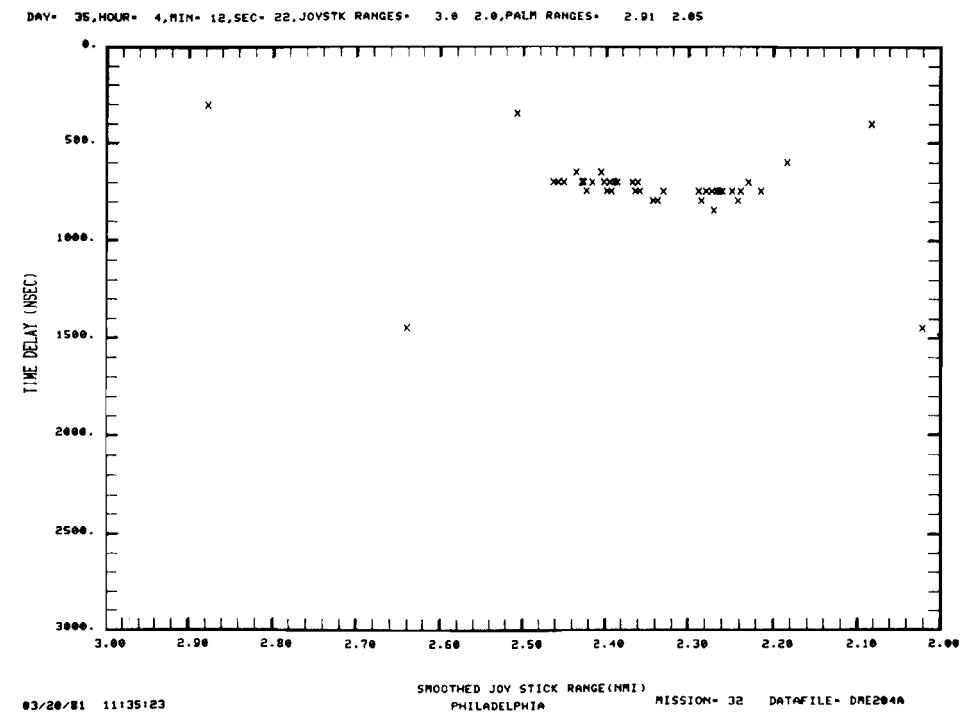

Fig. 7-5c. Summary results for flight profile 1 at Philadelphia.

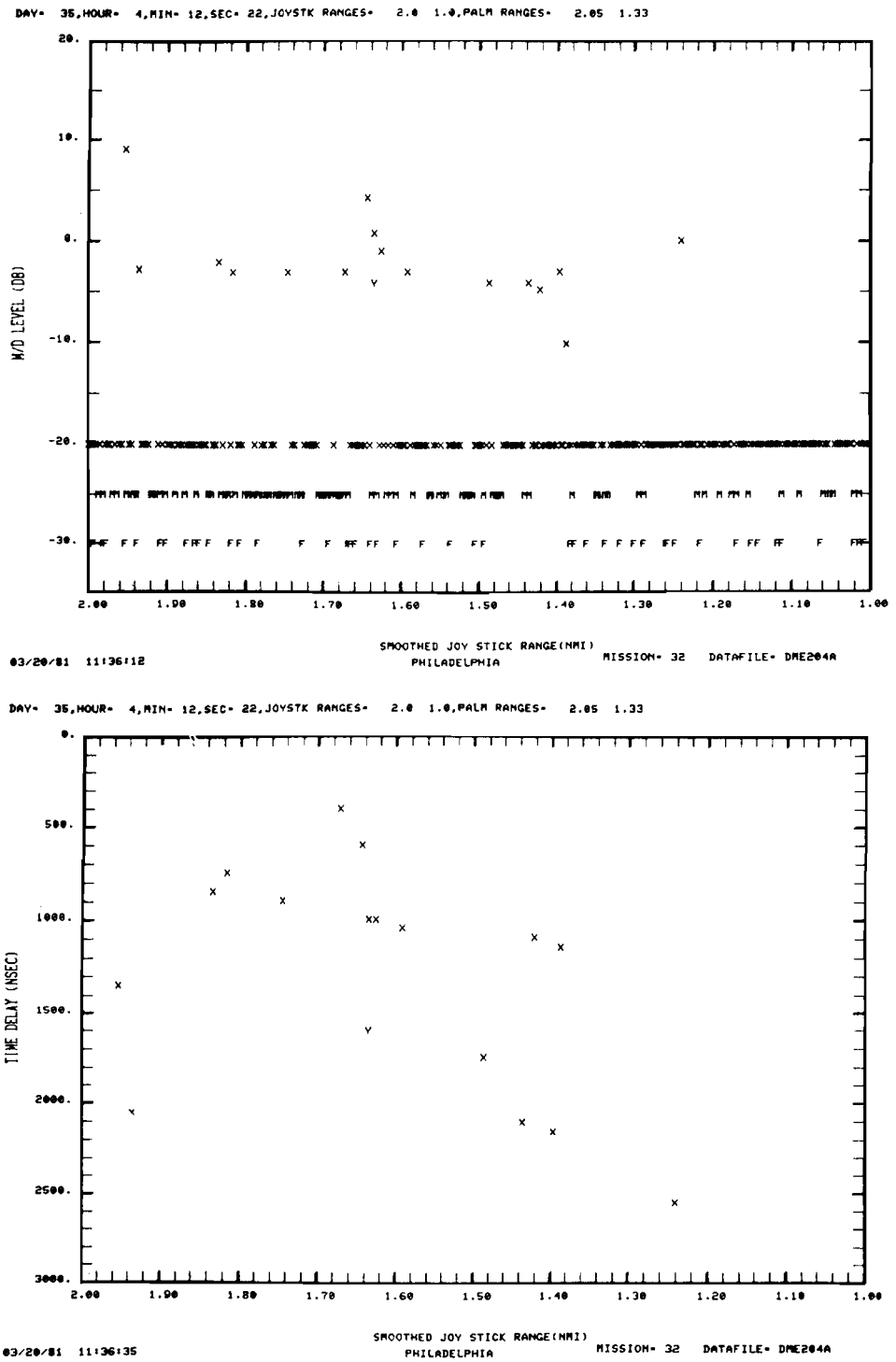

Fig. 7-5d. Summary results for flight profile 1 at Philadelphia.

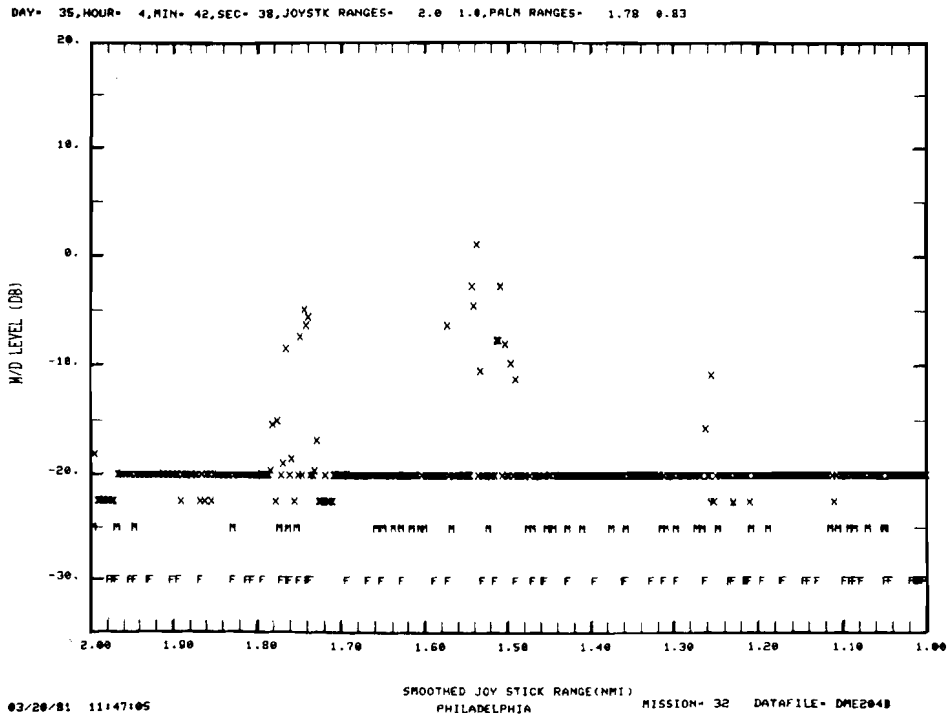

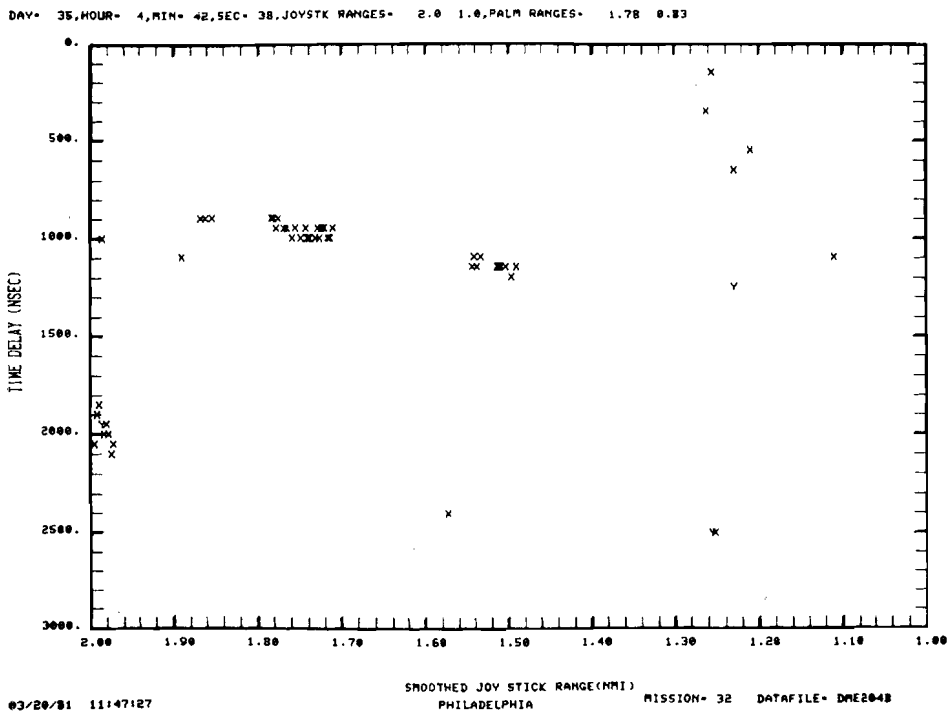

Fig. 7-6. Summary results for flight profile 1 at Philadelphia.

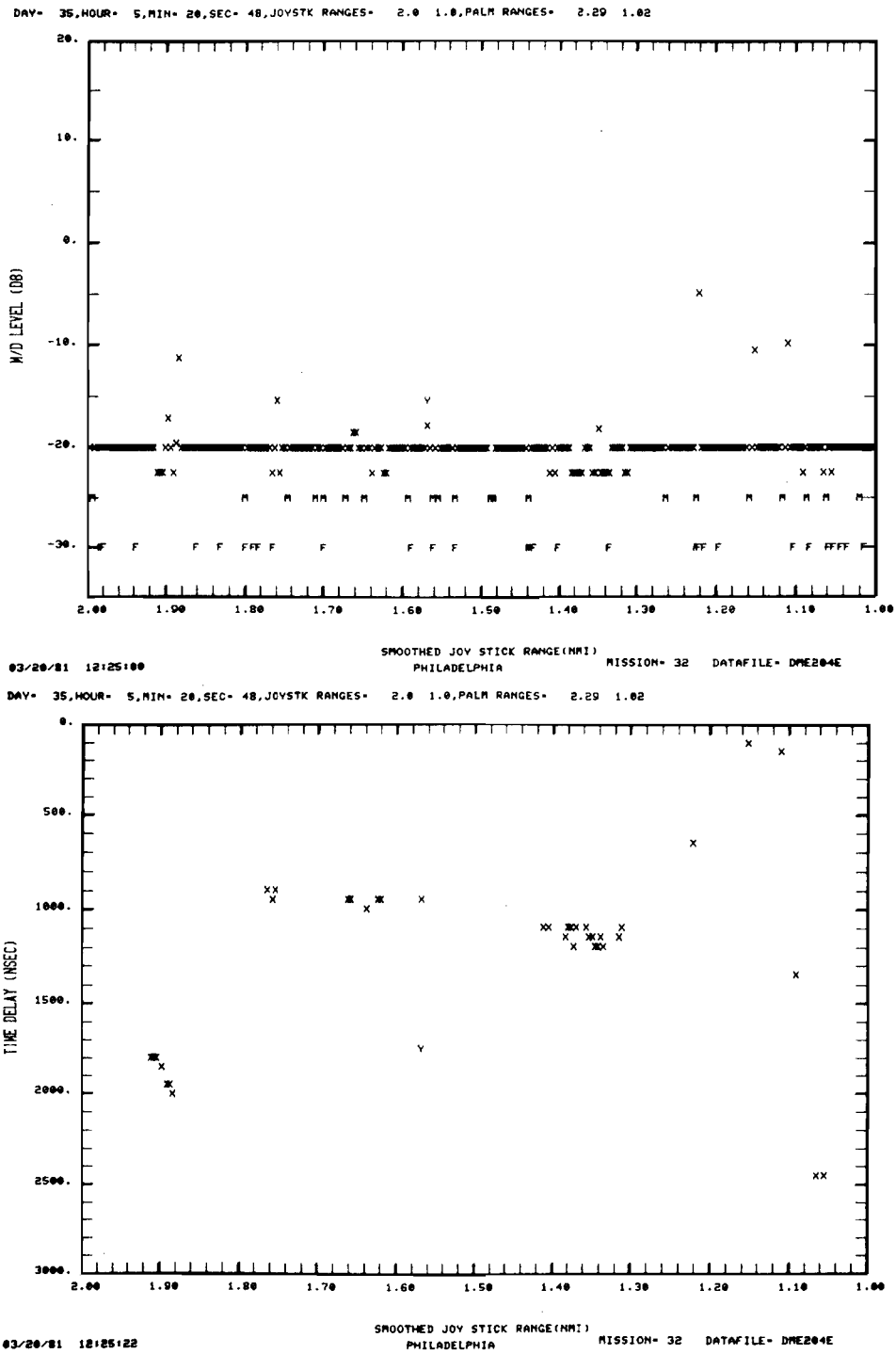

Fig. 7-7. Summary results for flight profile 1 at Philadelphia.

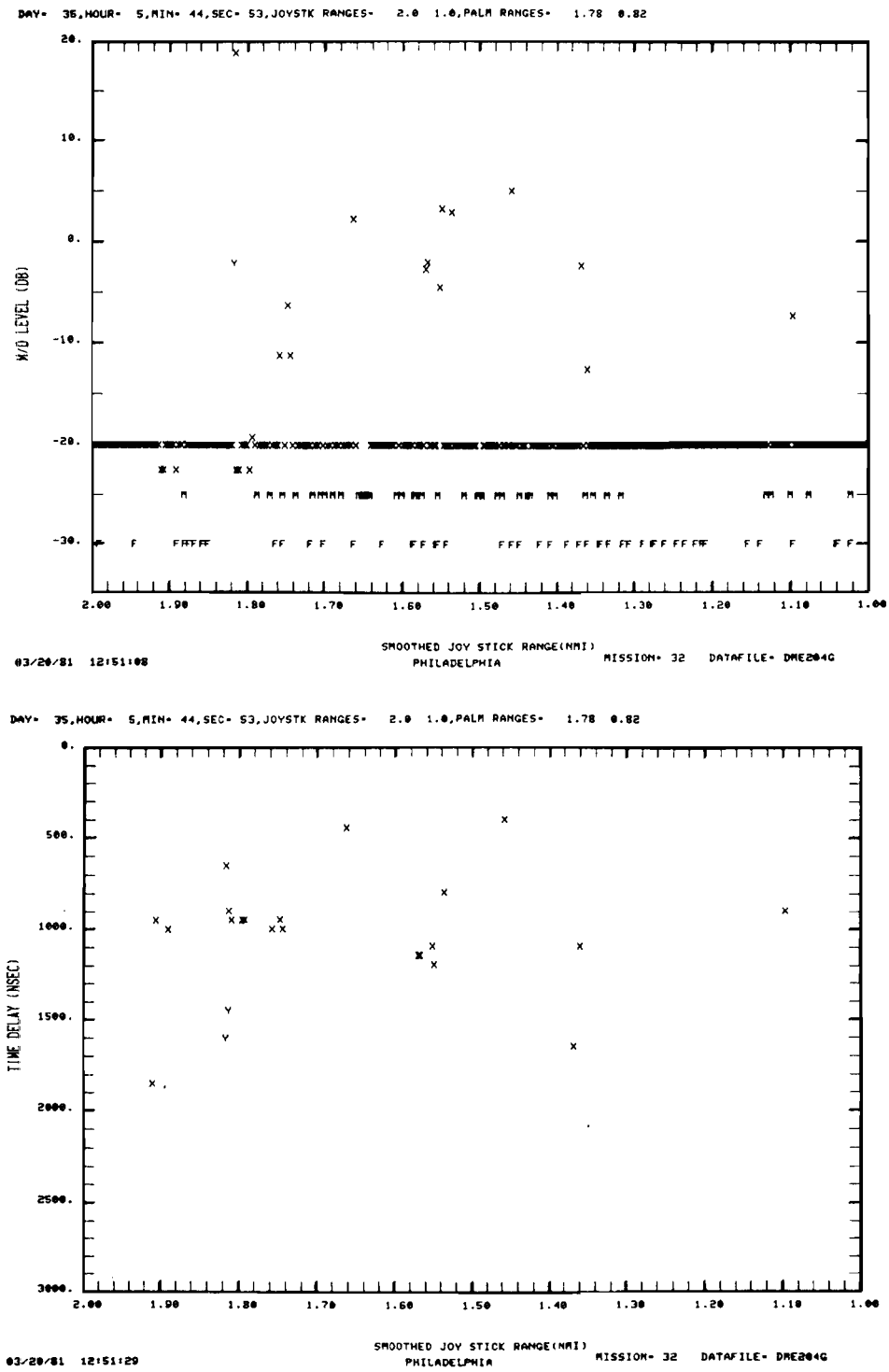

Fig. 7-8. Summary results for flight profile 2 at Philadelphia.

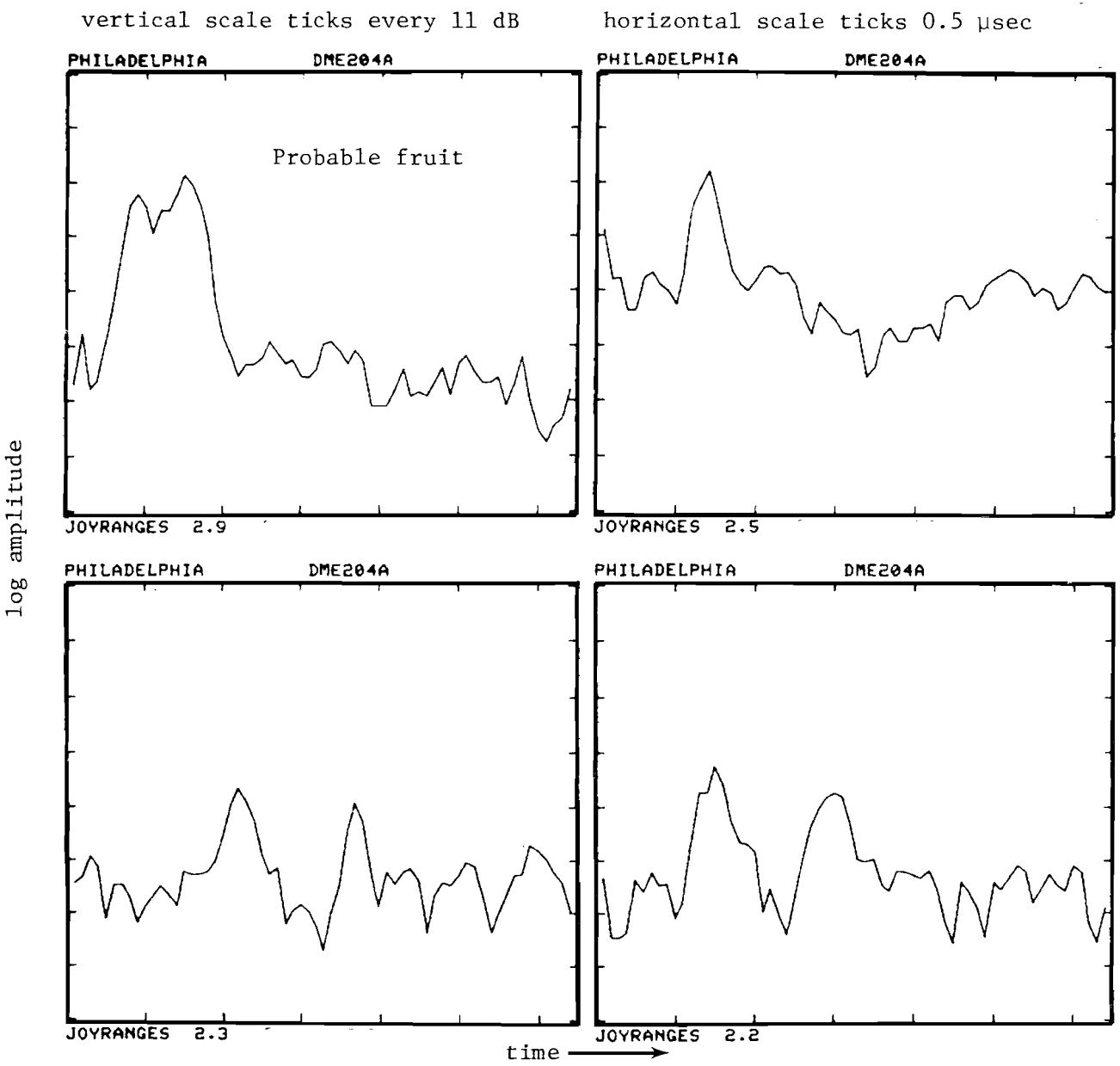

Fig. 7-9. Philadelphia waveforms prior to threshold.

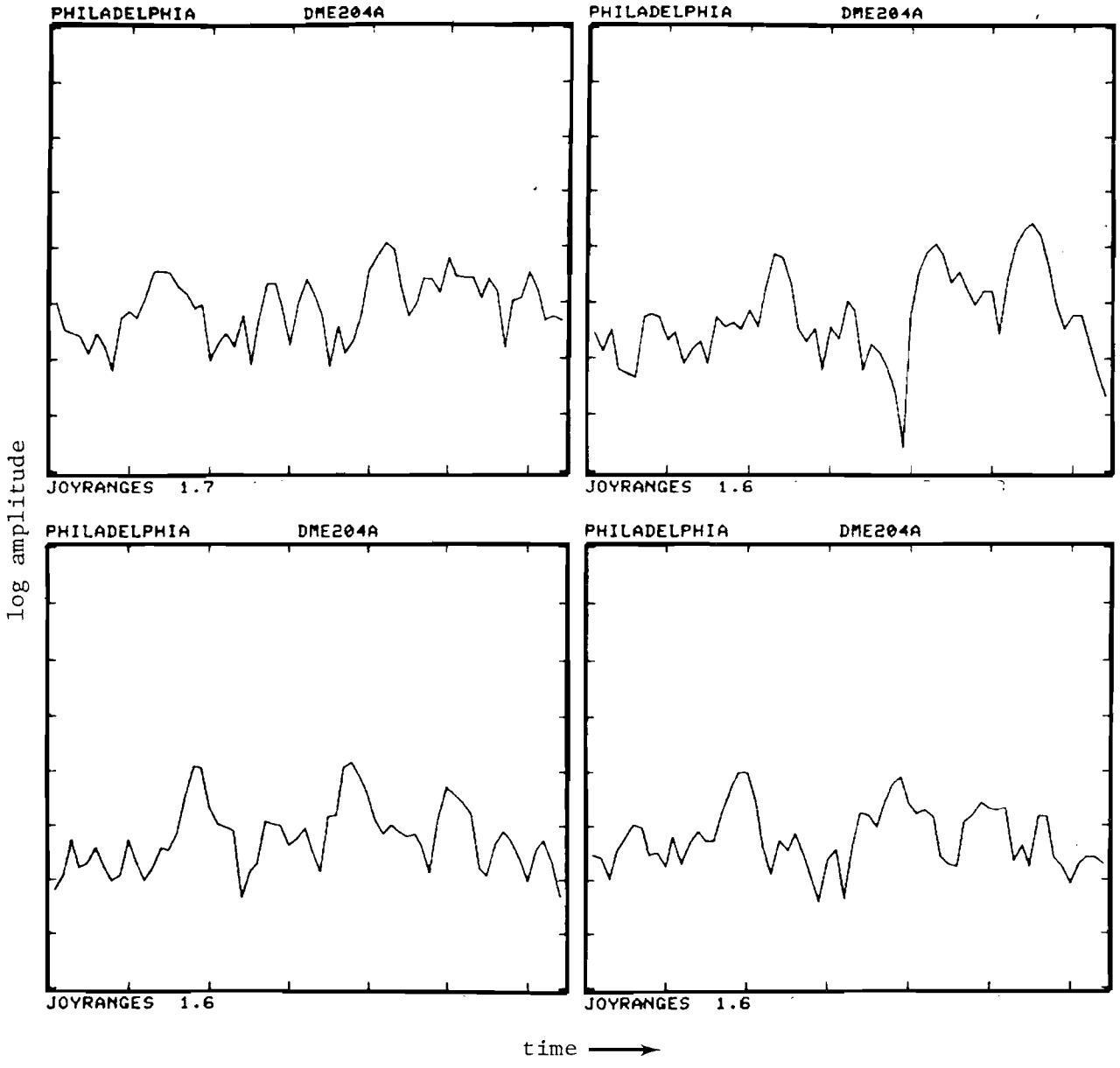

Fig. 7-10. Philadelphia waveforms near threshold.

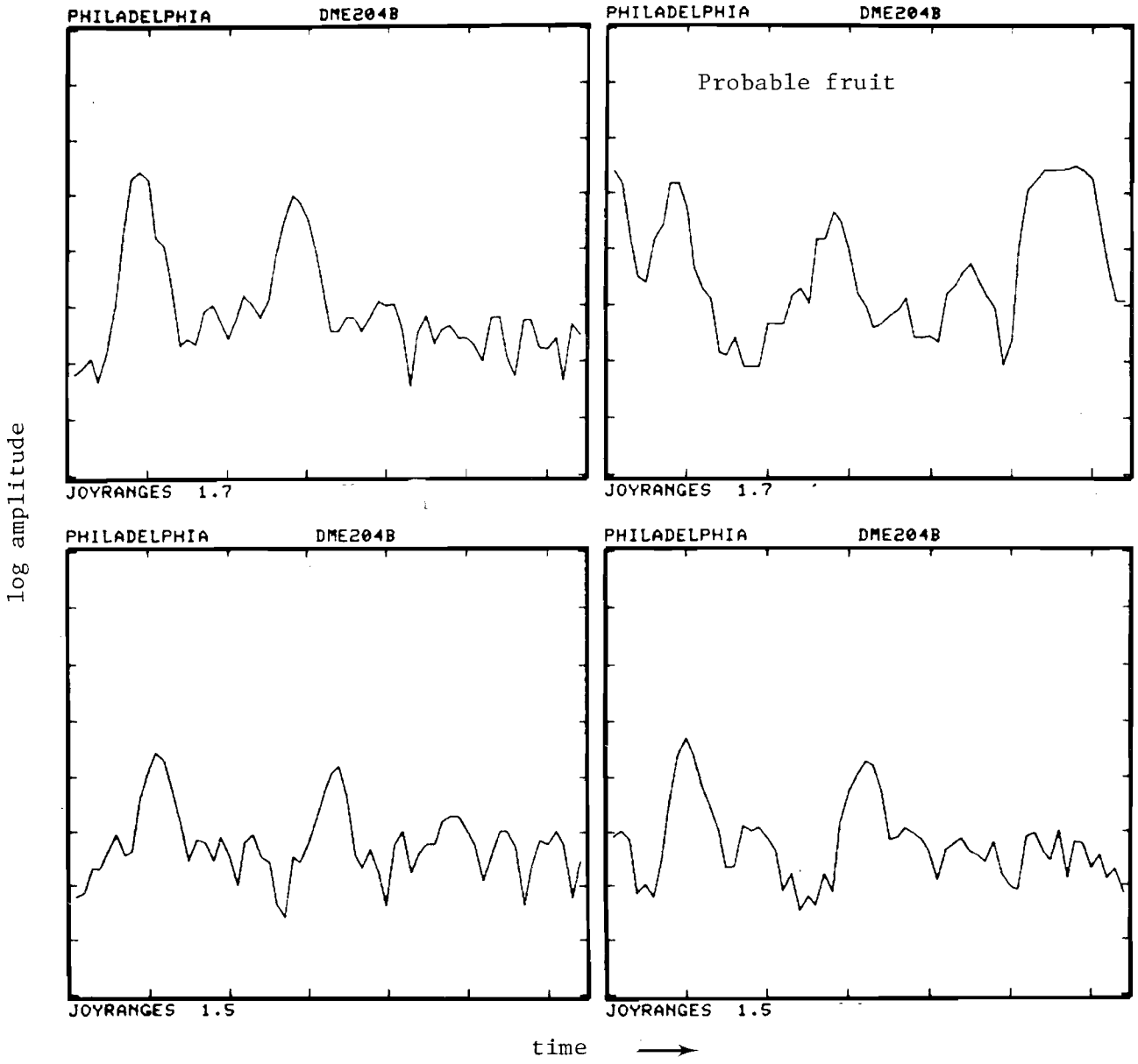

Fig. 7-11, Philadelphia waveform at and past threshold.

analysis. On the last group of approaches, pulses similar to those in Fig. 7-9 and 7-11 are visible, but below the threshold. In such cases, much of the multipath data was missed.

D. Simulation Results

A simple model of the Philadelphia airport was developed in which the relevant building walls were represented by flat rectangular plates and terrain contour features ignored. The building locations were taken from Fig. 7-1 with wall heights being obtained from the MLS airport survey data [6].

Figures 7-12 and 7-13 show the simulation airport map and computed multipath characteristics. The predicted M/D level of -8 dB for the UA cargo unit correlates reasonably well with Fig.7-5. It should be noted, however, that no multipath within -20 dB of the direct signal was detected on any of the other approaches. The predicted peak M/D levels of -18 dB and -28 dB for the AA/EA cargo building and cargo unit #1 are not inconsistent with Figs. 7-5 to 7-8, although here again the experimental data shows large variations which are not suggested by the computer simulation (e.g., in Fig. 7.5c, the measured M/D for cargo unit #1 is -10 to -15 dB, whereas on the other runs it was less than -20 dB).

E. Summary

The Philadelphia measured results correlated reasonably well with the predictions from ray tracing analysis and computer simulations using a simple airport model. The measured M/D ratios and τ values were quantitatively in reasonable agreement on the approaches with adequate SNR; however, in most cases, the SNR was so low as to cause significant problems in data interpretation.

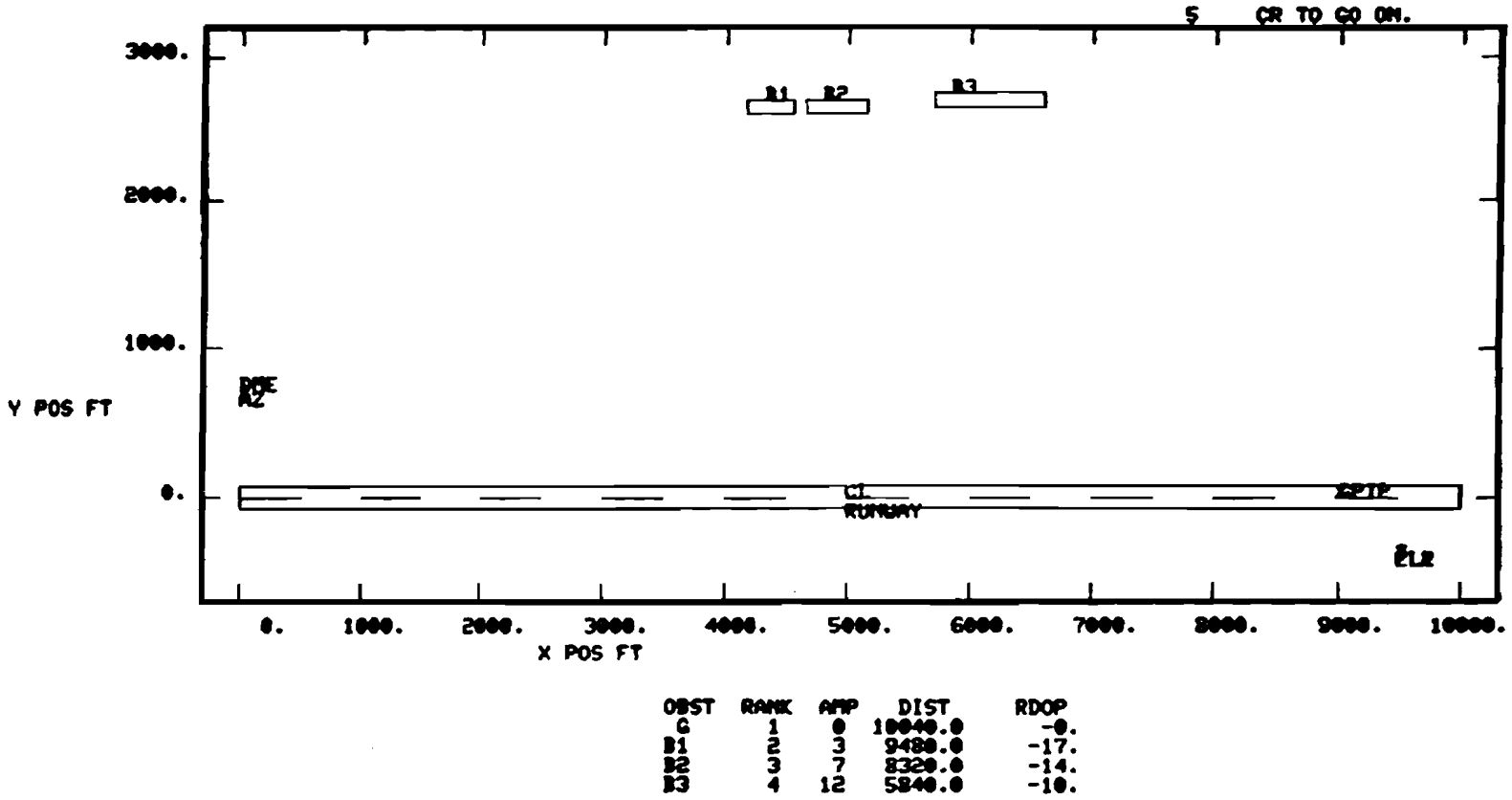

OBST	RANK	AMP	DIST	RDOP
G	1	0	10040.0	-0.
B1	2	3	9480.0	-17.
B2	3	7	8320.0	-14.
B3	4	12	5840.0	-10.

Fig. 7-12. Airport map for simulation of PHL multipath measurements.

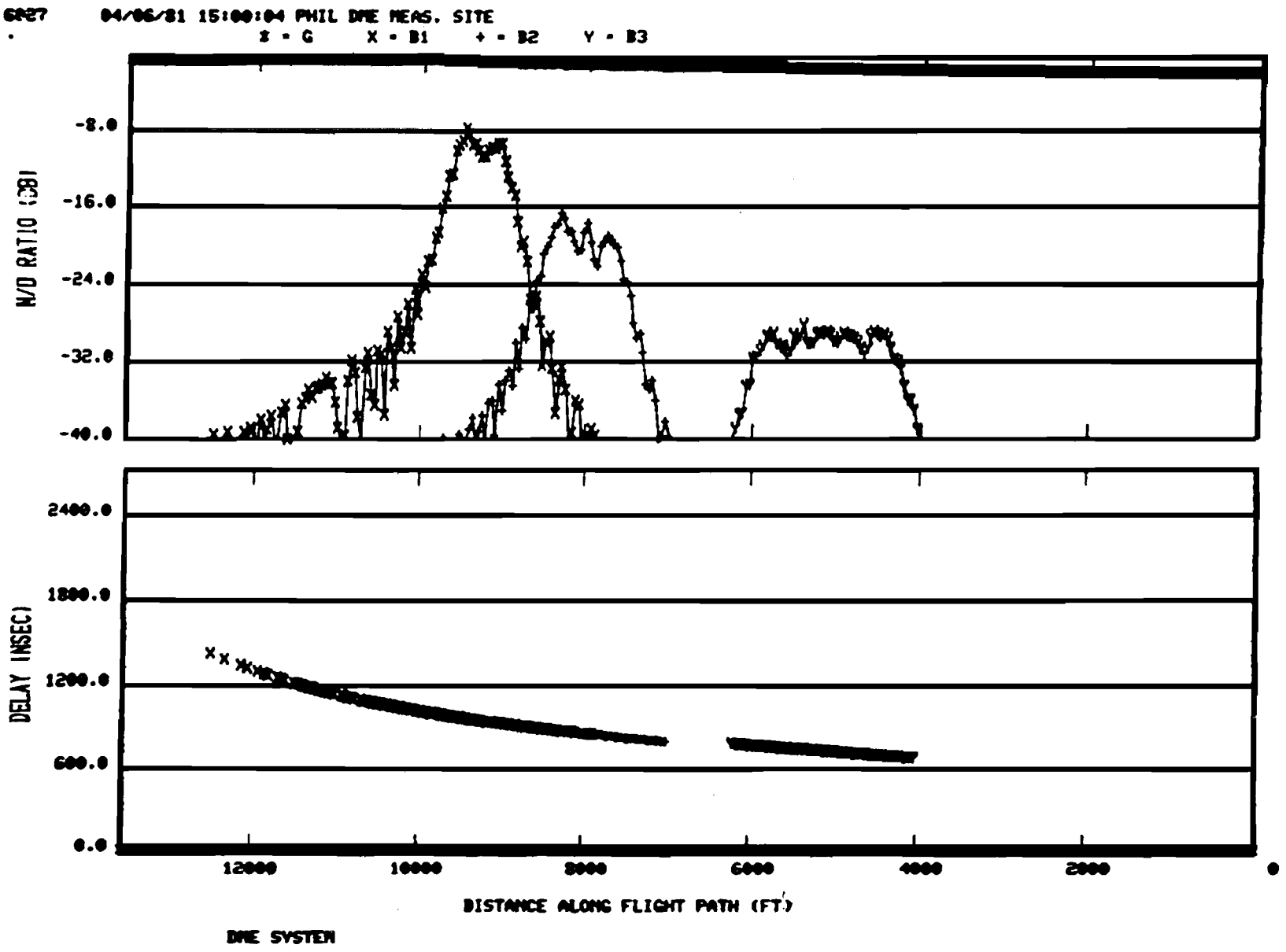

Fig. 7-13. Computed multipath characteristics for PHL measurement scenario.

VIII. WASHINGTON NATIONAL AIRPORT

Washington National was selected as a multipath test site because 1) the FAA has several MLS systems installed at the airport and 2) the particular runway chosen provided an opportunity to explore multipath for V/STOL approaches.

A. Multipath Environment

Figure 8-1 shows a map of Washington National Airport (DCA) in the vicinity of runway 15-33. An MLS small community with a conventional (Cardion) L band DME has been installed at this runway to support STOL operations by a commuter airline (Ransome). The principal multipath threats are the north hangar complex buildings which are typically 20m (60 ft) high with smooth metal doors facing the runway. Figure 8-2 shows the hangar complex from the multipath measurement site while Fig. 8-3 shows a closeup of the end hangar.

The hangar orientations are much that multipath was expected from approximately 3 nmi prior to threshold (reflections from the south edge of hangar 8) to midway down the runway (reflections from the north edge of hangar 12) if the aircraft were at a sufficiently low altitude. From the category I decision height (DH) downward, the aircraft elevation angles are such that specular reflections should be encountered more or less continuously. The expected multipath relative time delays were as follows:

Hangar	τ (nsec)
8	1100
9	950
10	850
11	750
12	700

The runway contour and terrain contours at Washington National are quite

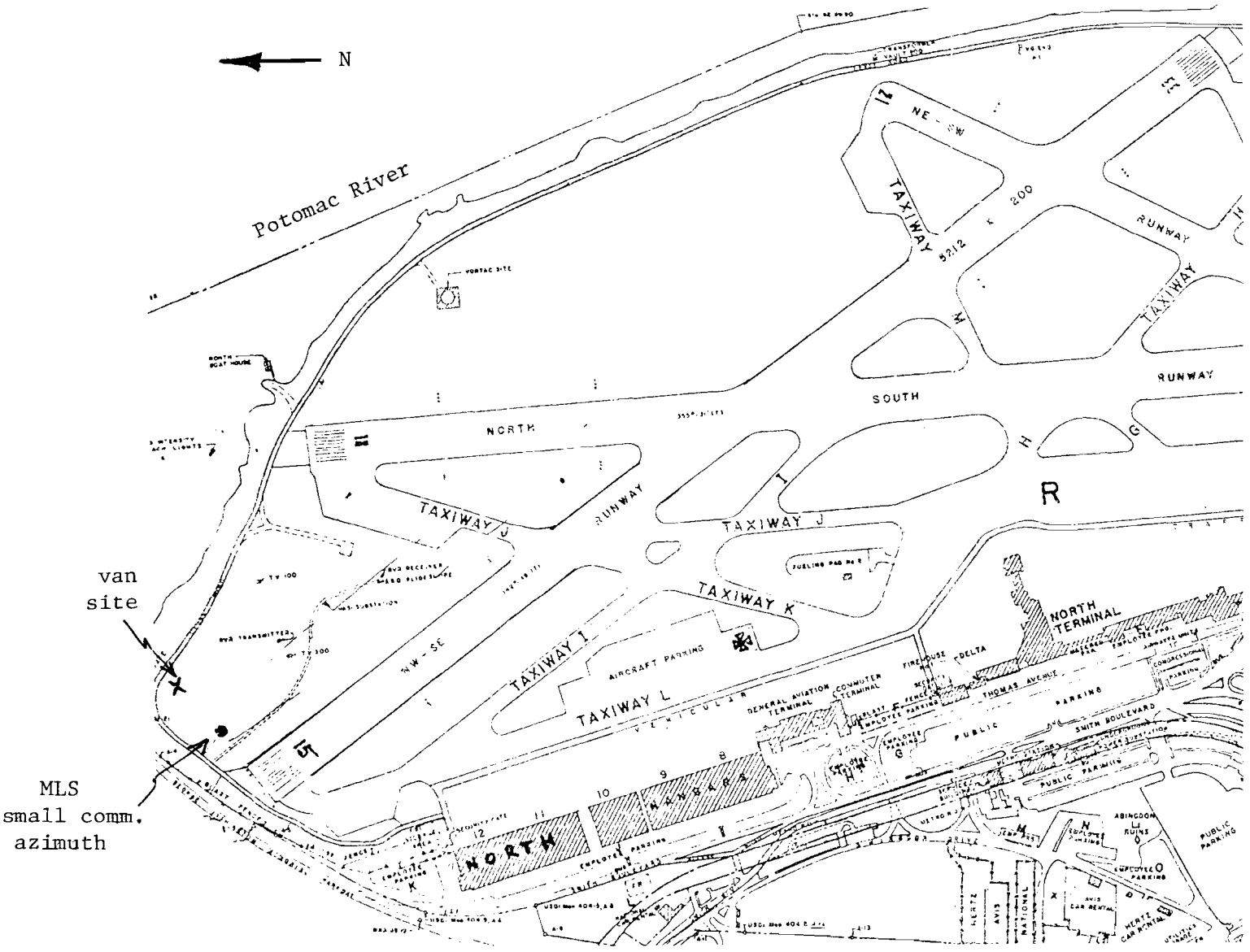

Fig. 8-1. Washington National Airport DME multipath measurement site.

Fig. 8-2. MLS small community azimuth and Washington National north hangar complex as seen from DME multipath measurement site.

Fig. 8-3. Closeup of hangar 12 at Washington National Airport.

flat (4 foot height variation over the entire runway length) and thus created no problems in achieving clear line of sight to the aircraft. The use of a site further off the runway than the small community azimuth was necessitated by obstruction clearance considerations. However, the specular region that resulted is fairly similar to that which would have occured if the van were sited immediately adjacent to the MLS small community azimuth.

B. Measurements Made at Washington National

Table 8-1 summarizes the measurements at DCA. A total of 8 centerline approaches were made to runway 33 between 6:30 a.m. and 8:00 a.m. on February 6, 1981. Due to unfavorable weather and wind direction as well as air traffic control constraints, we were not able to fly the off centerline portion of the curved approach to be utilized by the commuter airline.

C. Waveform Analysis Results

All of the approaches accomplished at DCA have been analyzed and representative results will be described in this section. Figures 8-4 and 8-5 show the summary results for approaches at 6° elevation angle, while Figs. 8-6 and 8-7 are the corresponding results for a 3° approach. Figures 8-8 and 8-9 show representative waveforms in the high level multipath regions 1.5 nmi before threshold and at threshold.

The multipath regions and time delays correlate fairly well with the expected regions using ray optics except in the case of the 800 nsec delay multipath between 5 nmi and 3.5 nmi. The aircraft x-y location here is at the edge of the specular region for the North Hangar complex, but the elevation angle of the aircraft is far in excess of the angle subtended by the lower level buildings (e.g., general aviation terminal and North Terminal complex) which are south of hangar 8. Thus, if the hangar walls and doors were vertical, large specular reflections should not have been encountered in this region. Actually, the facade above the doors is tilted approximately 3.9° toward the runway, so that some specular reflections may occur although the

TABLE 8-1

FLIGHT TESTS AT WASHINGTON NATIONAL AIRPORT

Flight Tests (February 6)

Profile 1:	6° glideslope, 45-foot threshold crossing height, 20 feet AGL along runway bottom a/c antenna: 4 successful approaches
Profile 2:	3° glideslope, 50 foot threshold crossing height, 20 feet AGL along runway bottom a/c antenna: 4 successful approaches

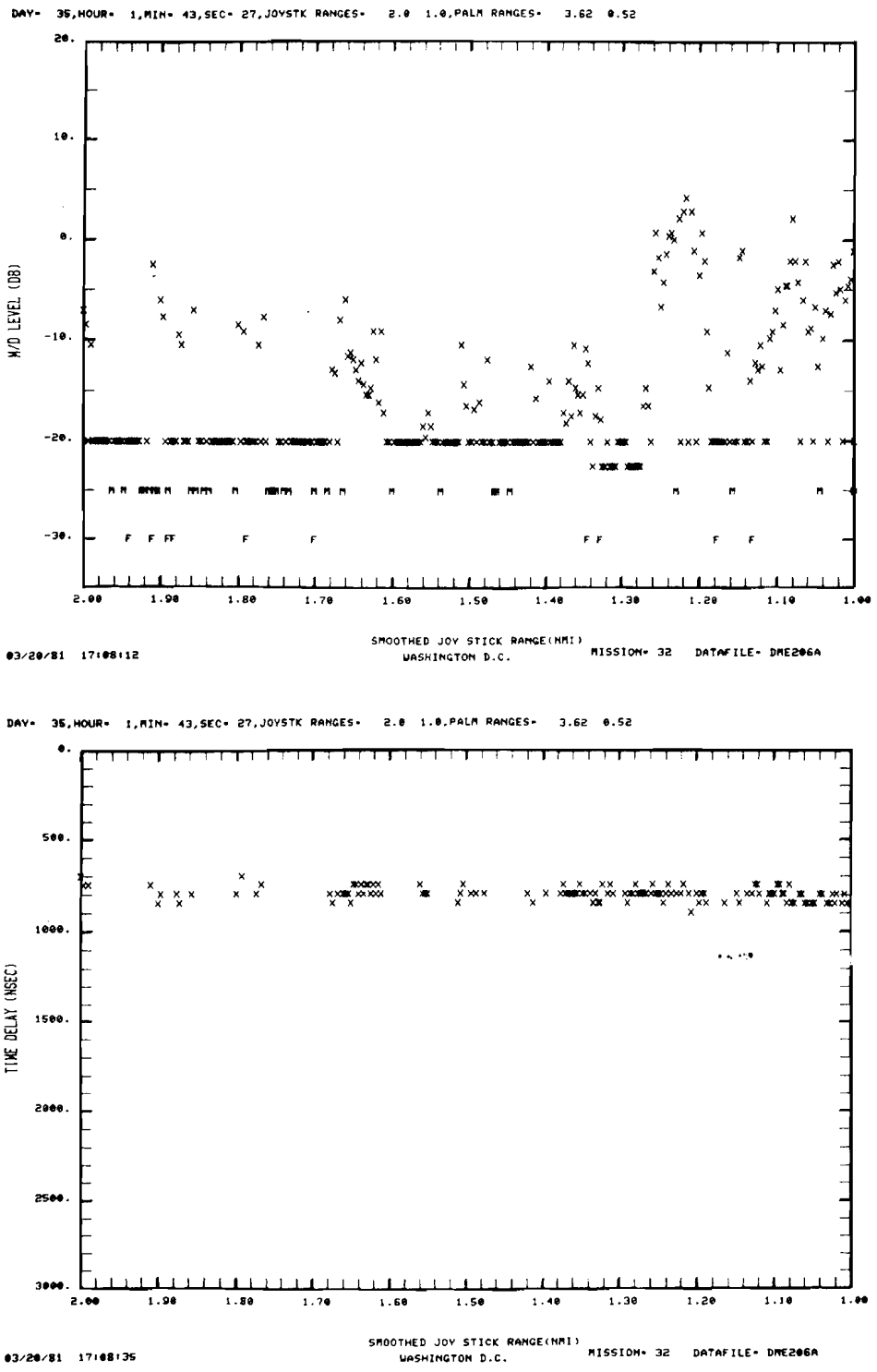

Fig. 8-4a. Summary results for 6° approach at DCA.

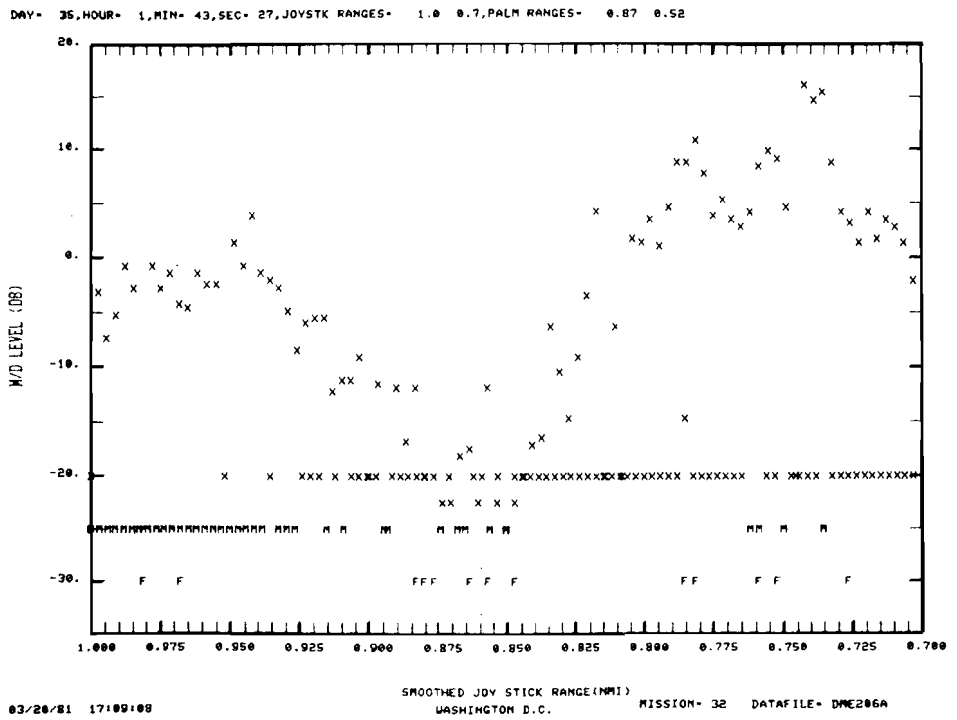

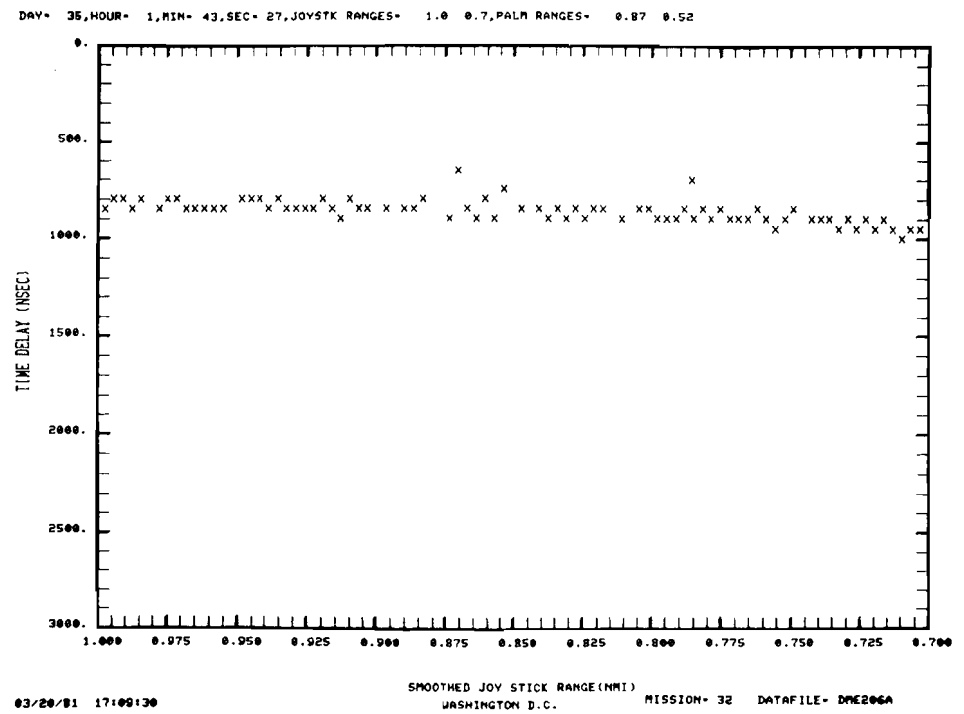

Fig. 8-4b. Summary results for 6° approach at DCA.

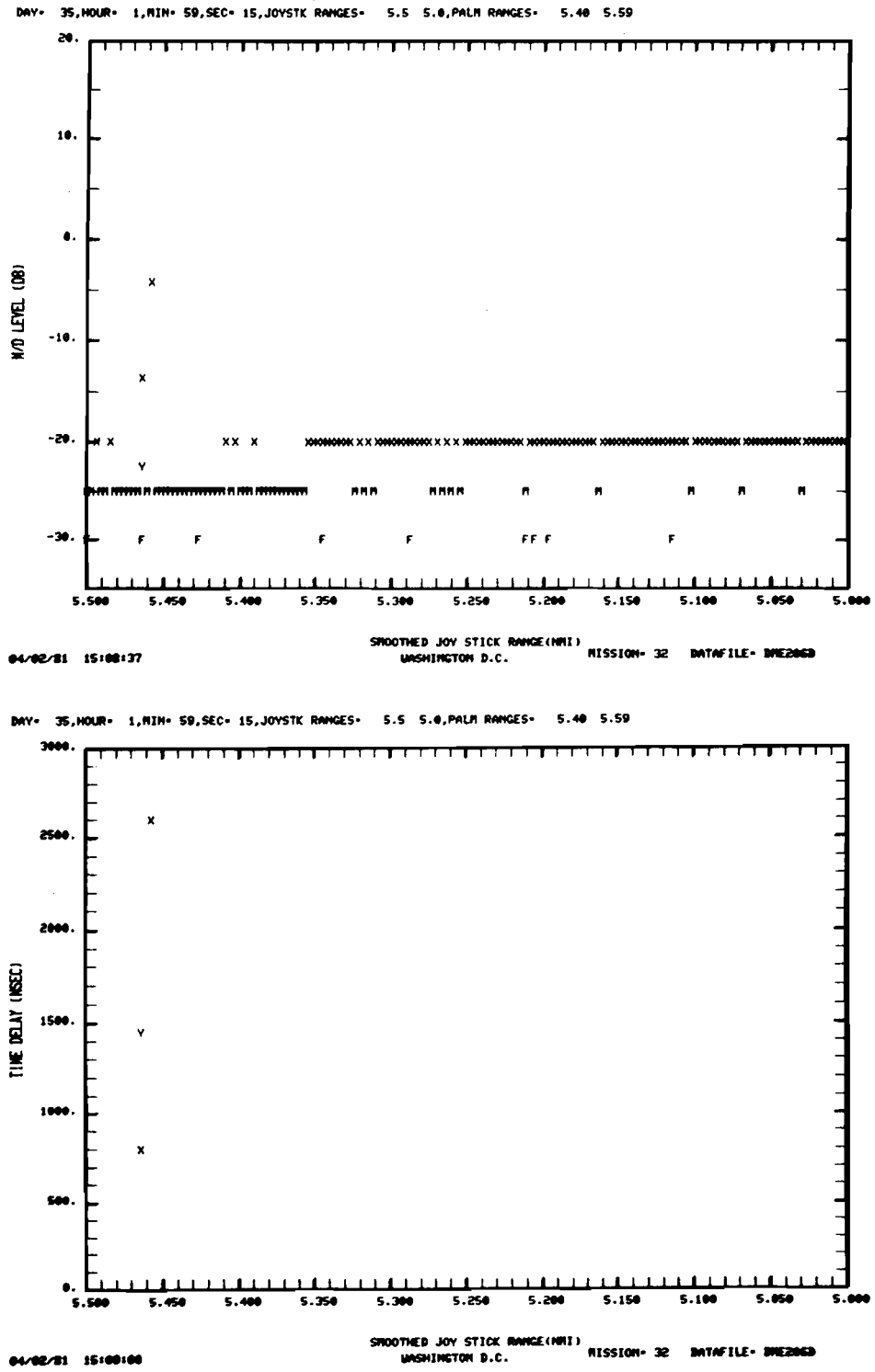

Fig. 8-5a. Summary results for 6° approach at DCA.

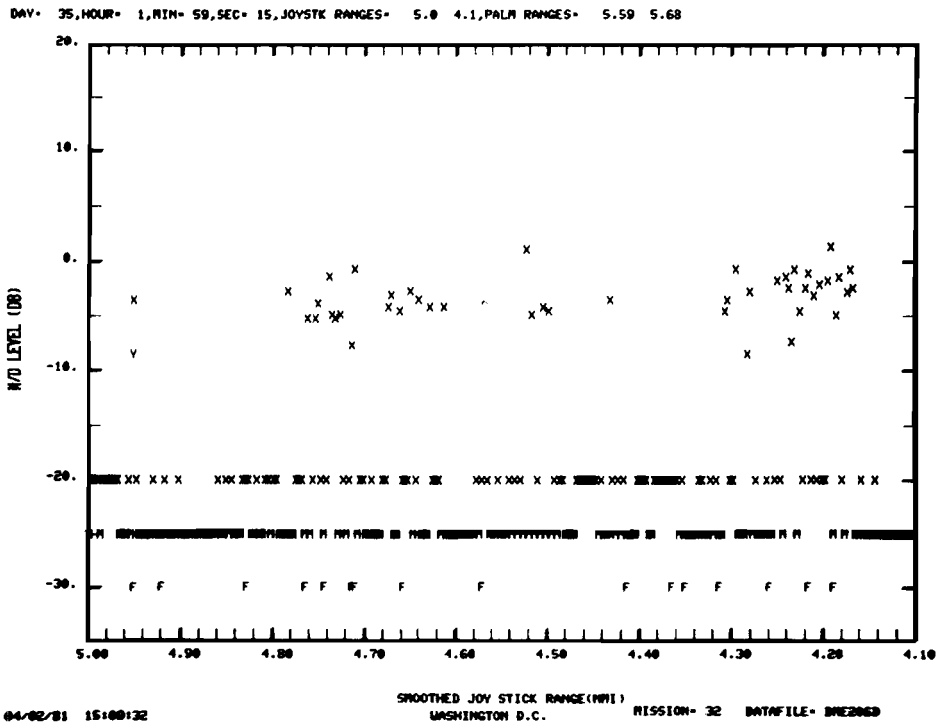

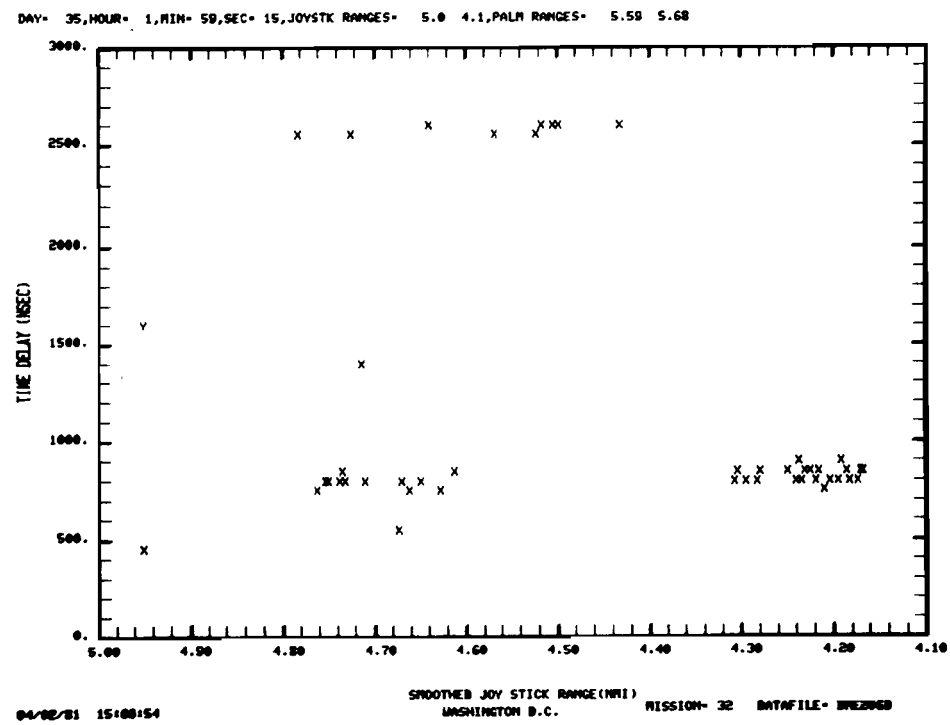

Fig. 8-5b. Summary results for 6° approach at DCA.

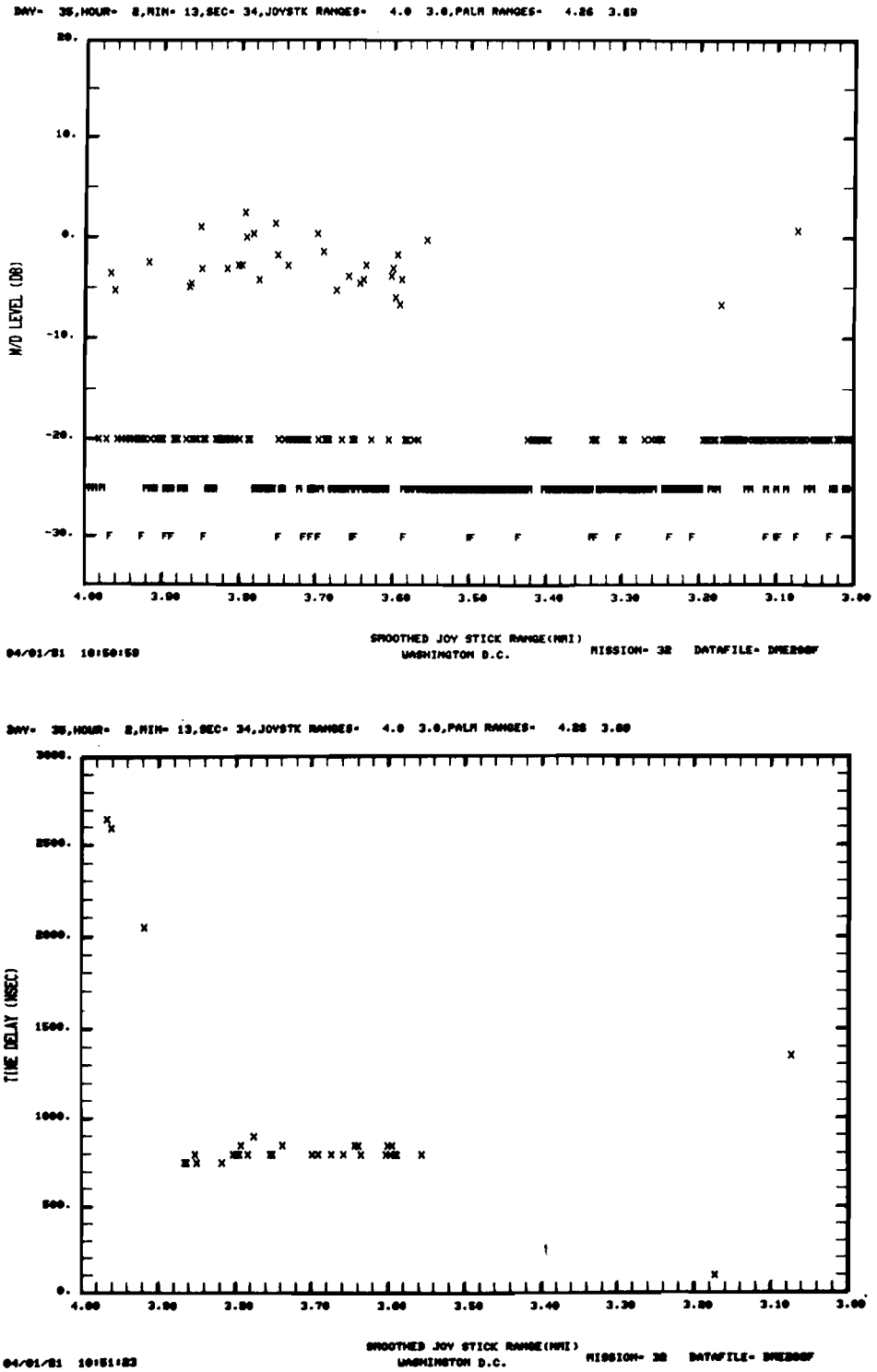

Fig 8-6a. Summary results for 3° approach to DCA .

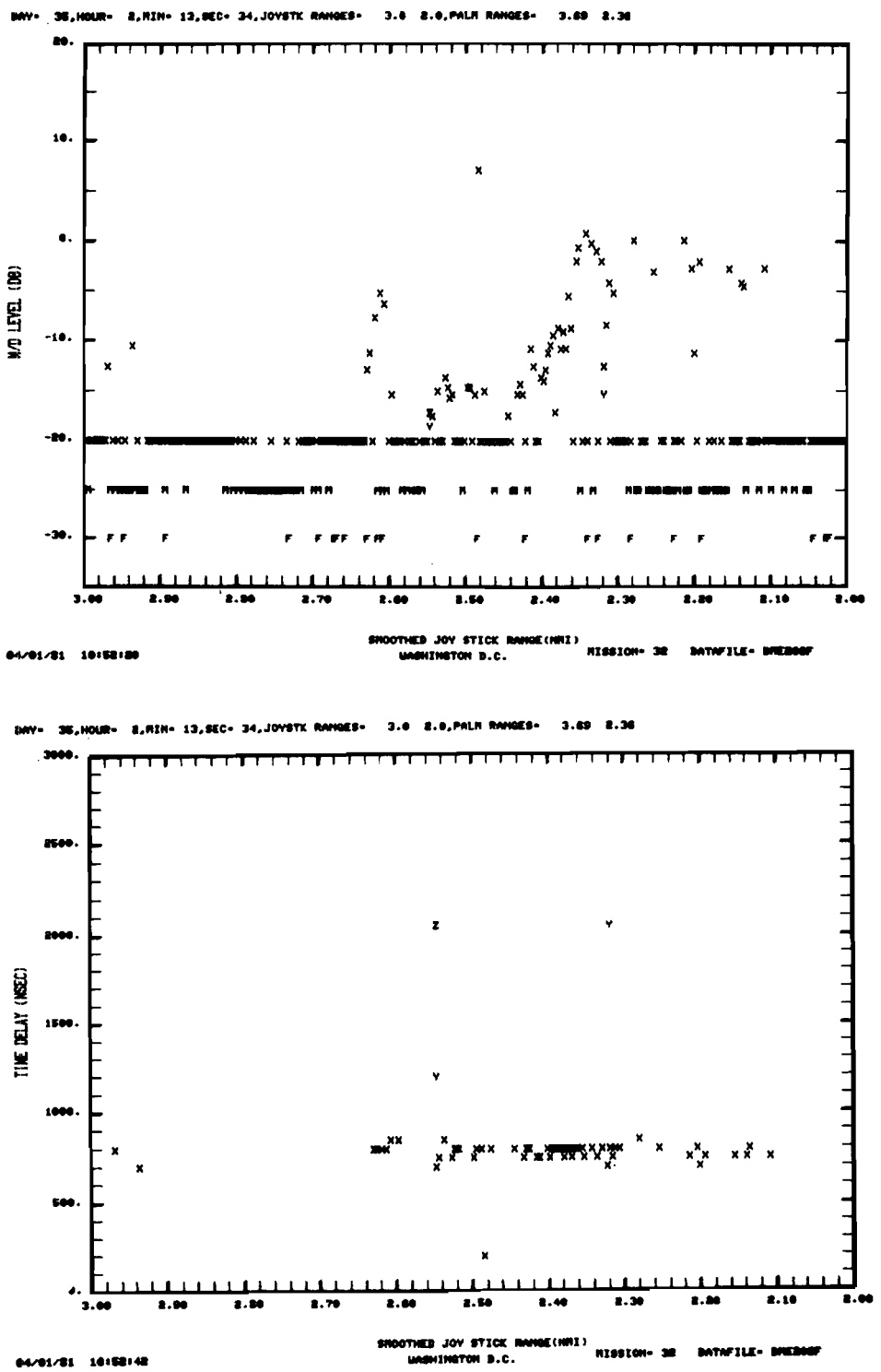

Fig. 8-6b. Summary results for 3° approach to DCA.

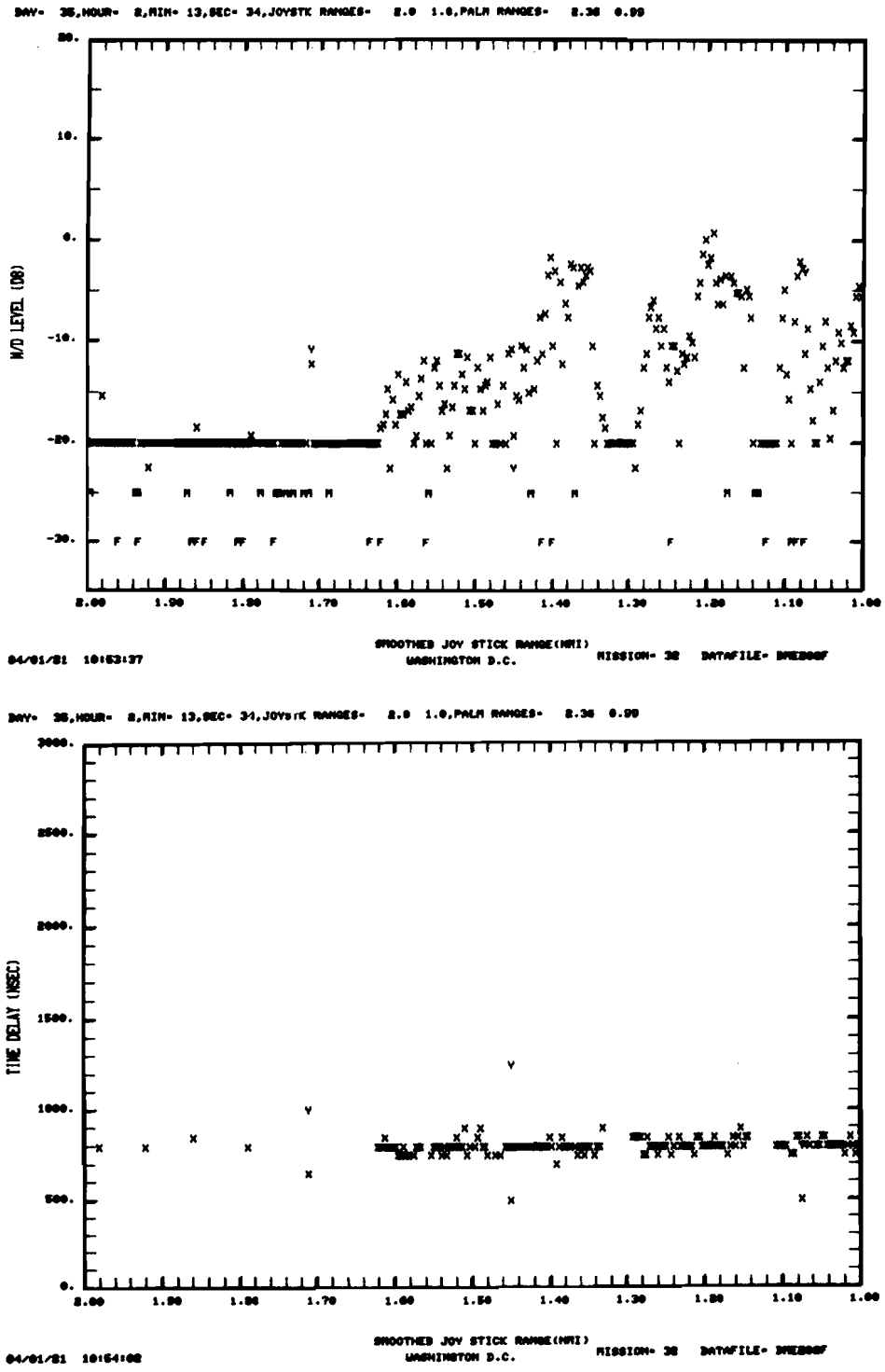

Fig. 8-6c. Summary results for 3° approach at DCA.

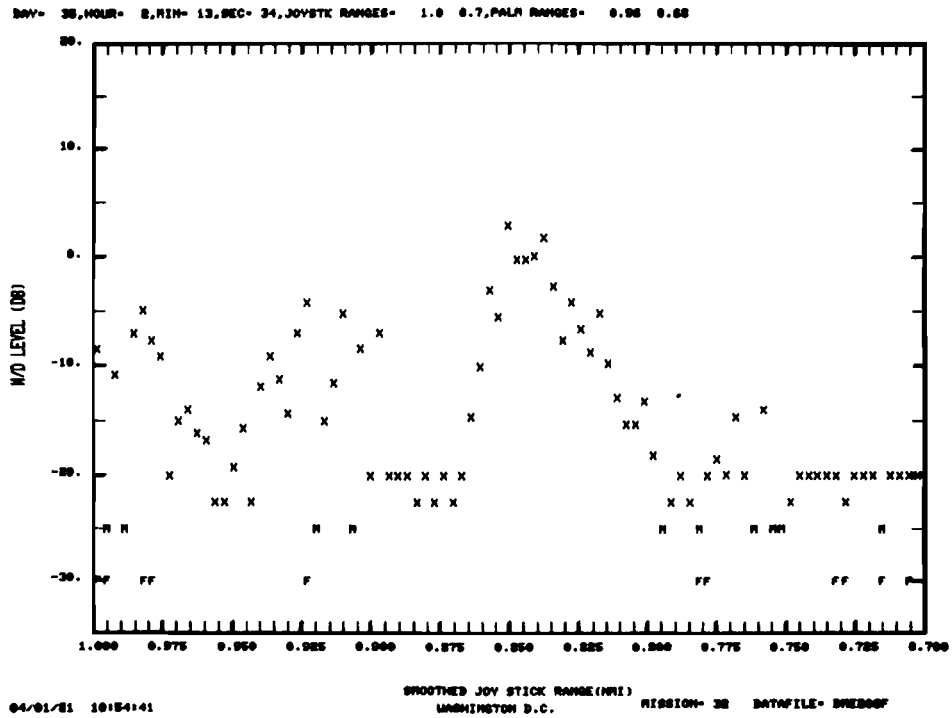

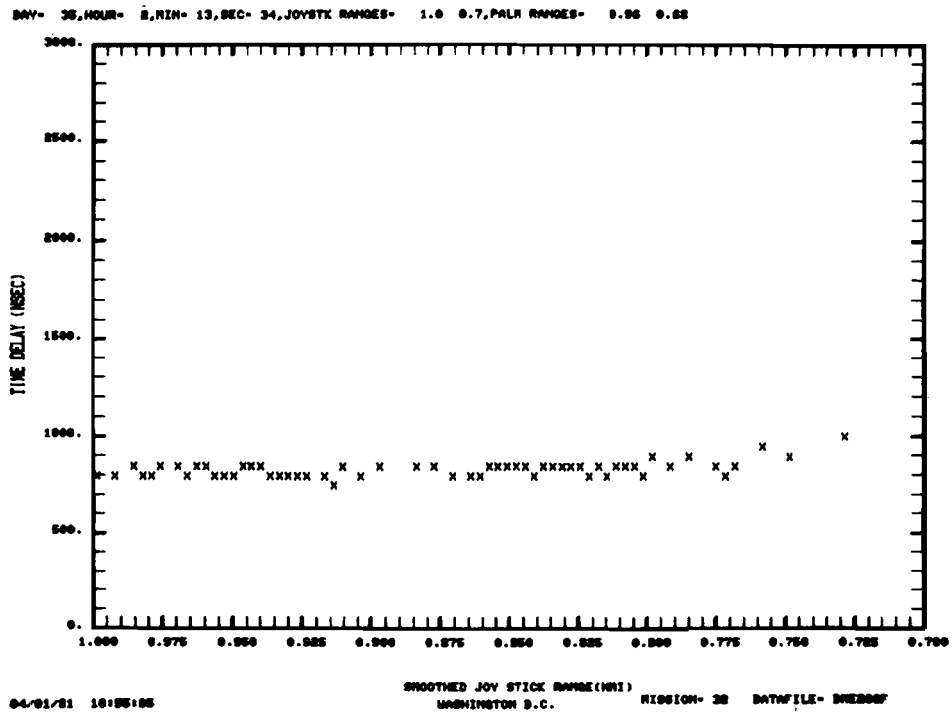

Fig. 8-6d, Summary results for 3° approach to DCA.

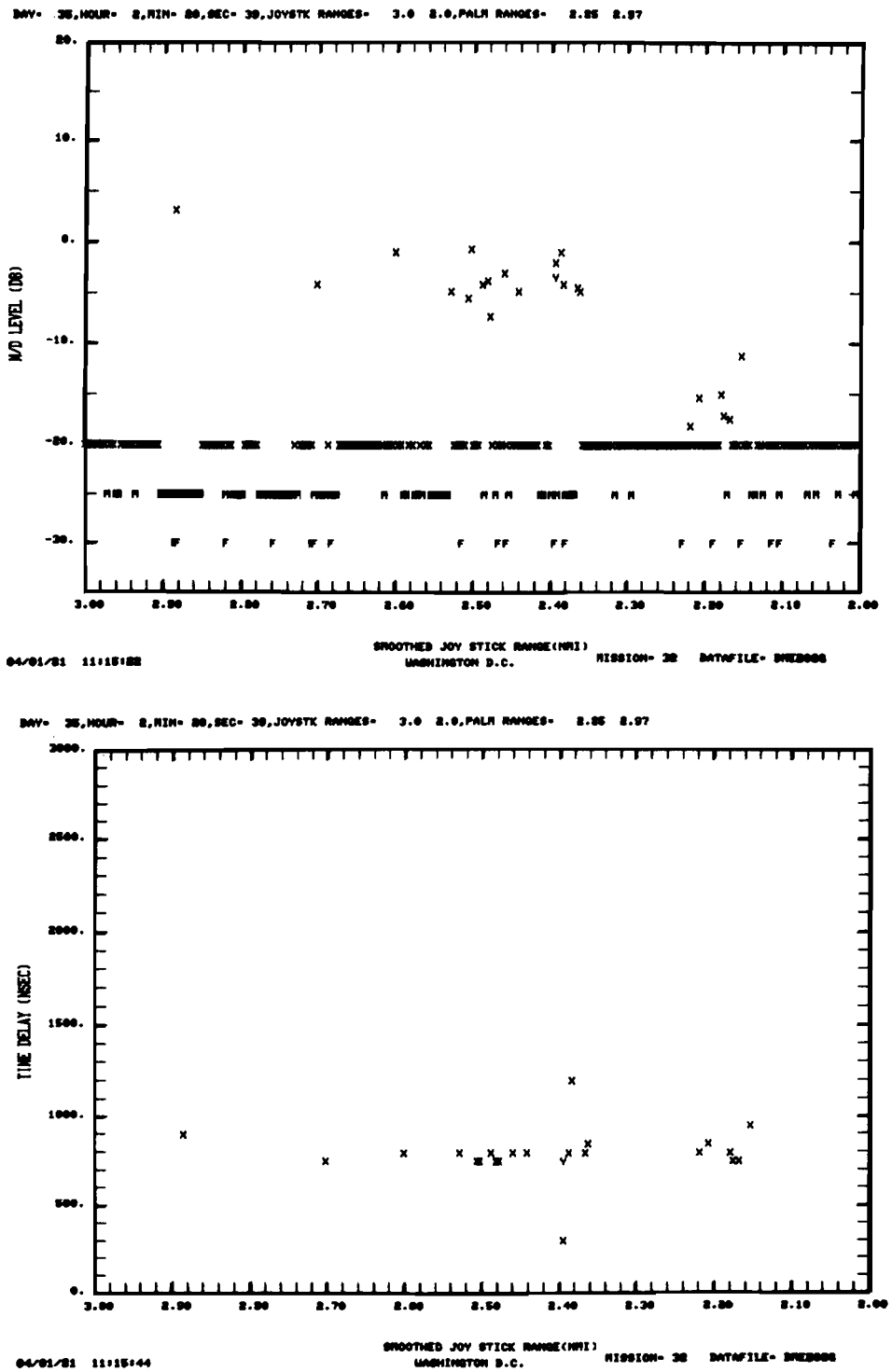

Fig. 8-7a. Summary results for 3° approach at DCA.

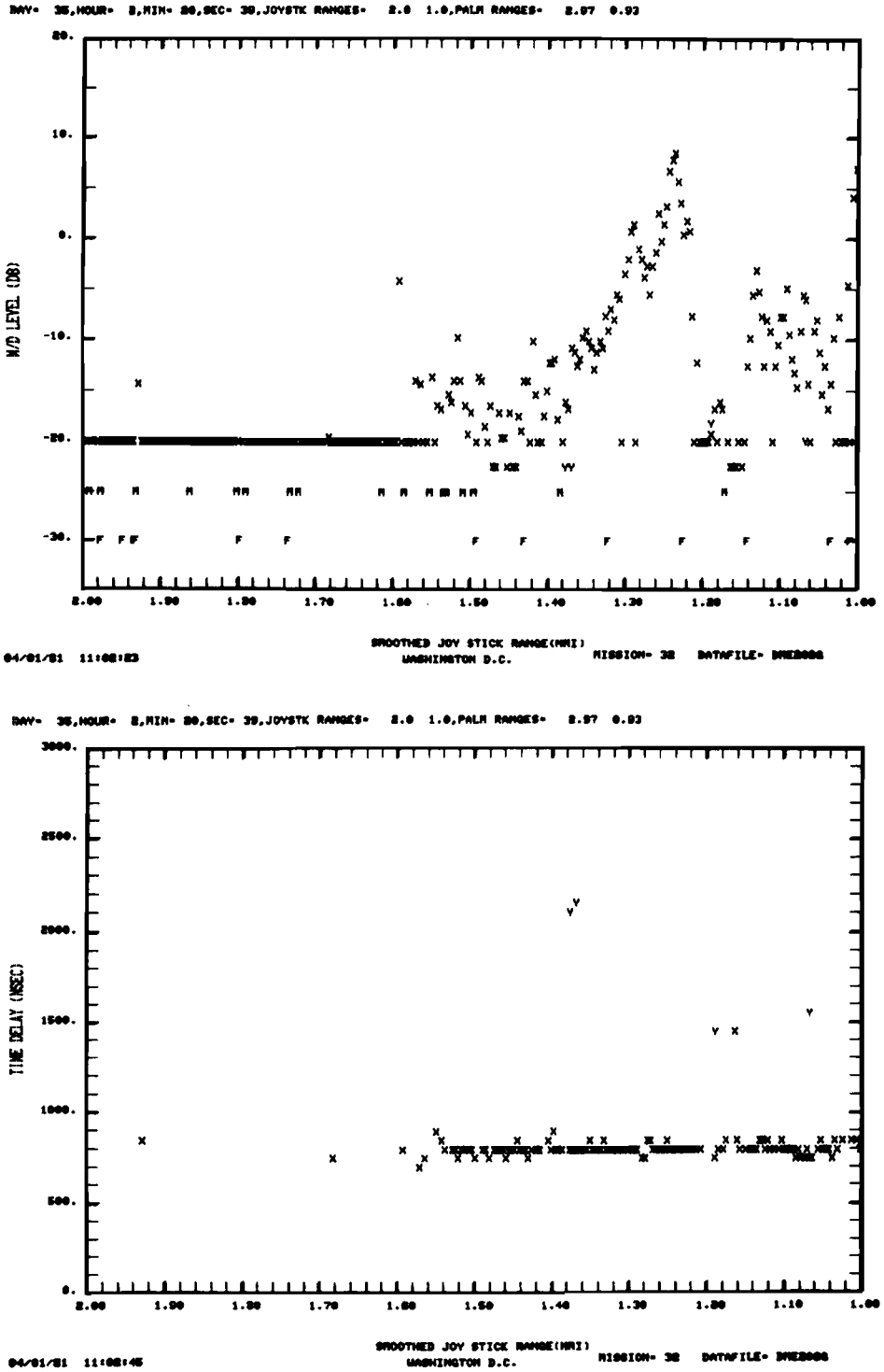

Fig. 8-7b, Summary results for 3° approach at DCA.

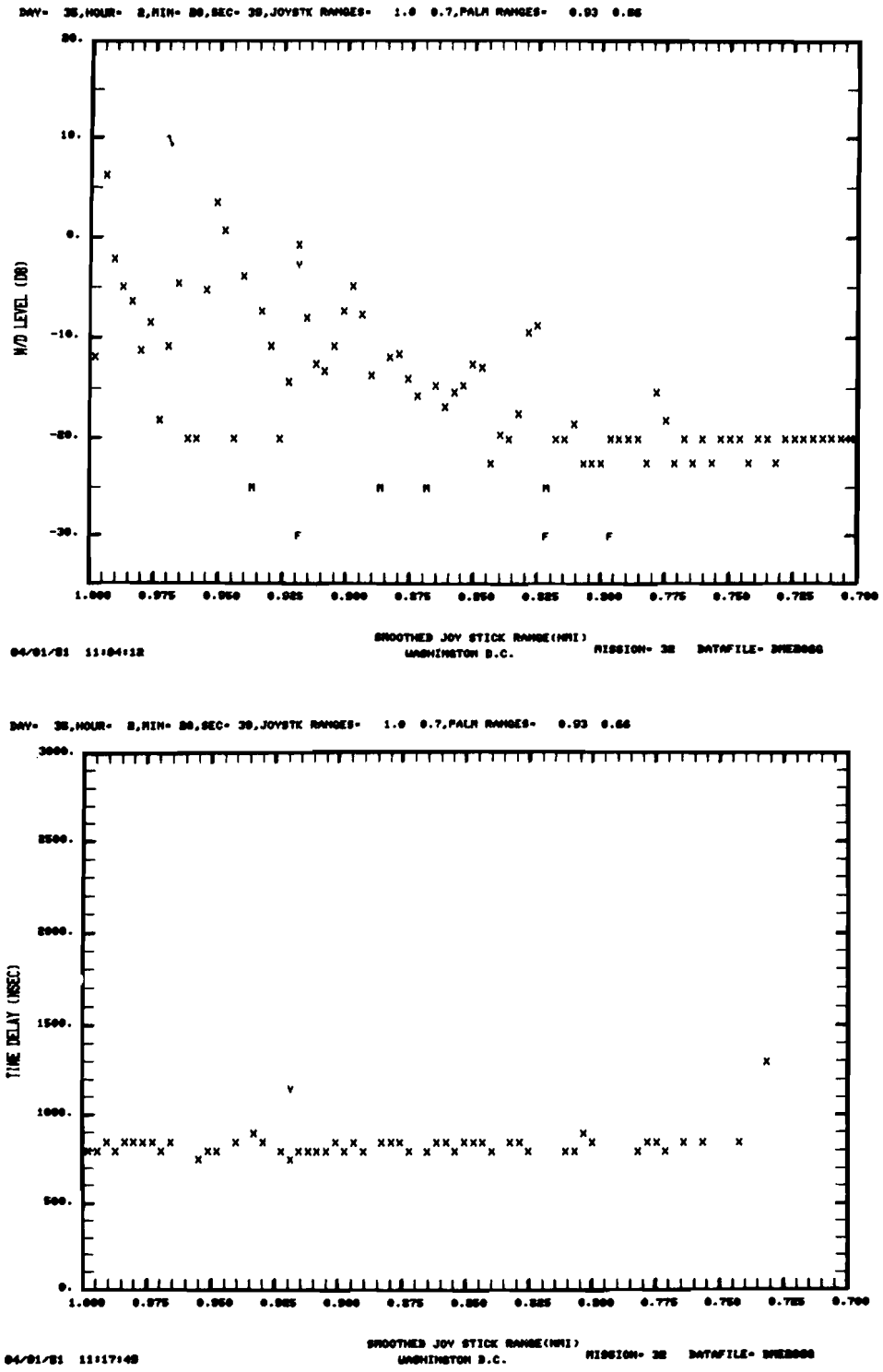

Fig. 8-7c. Summary results for 3° approach at DCA.

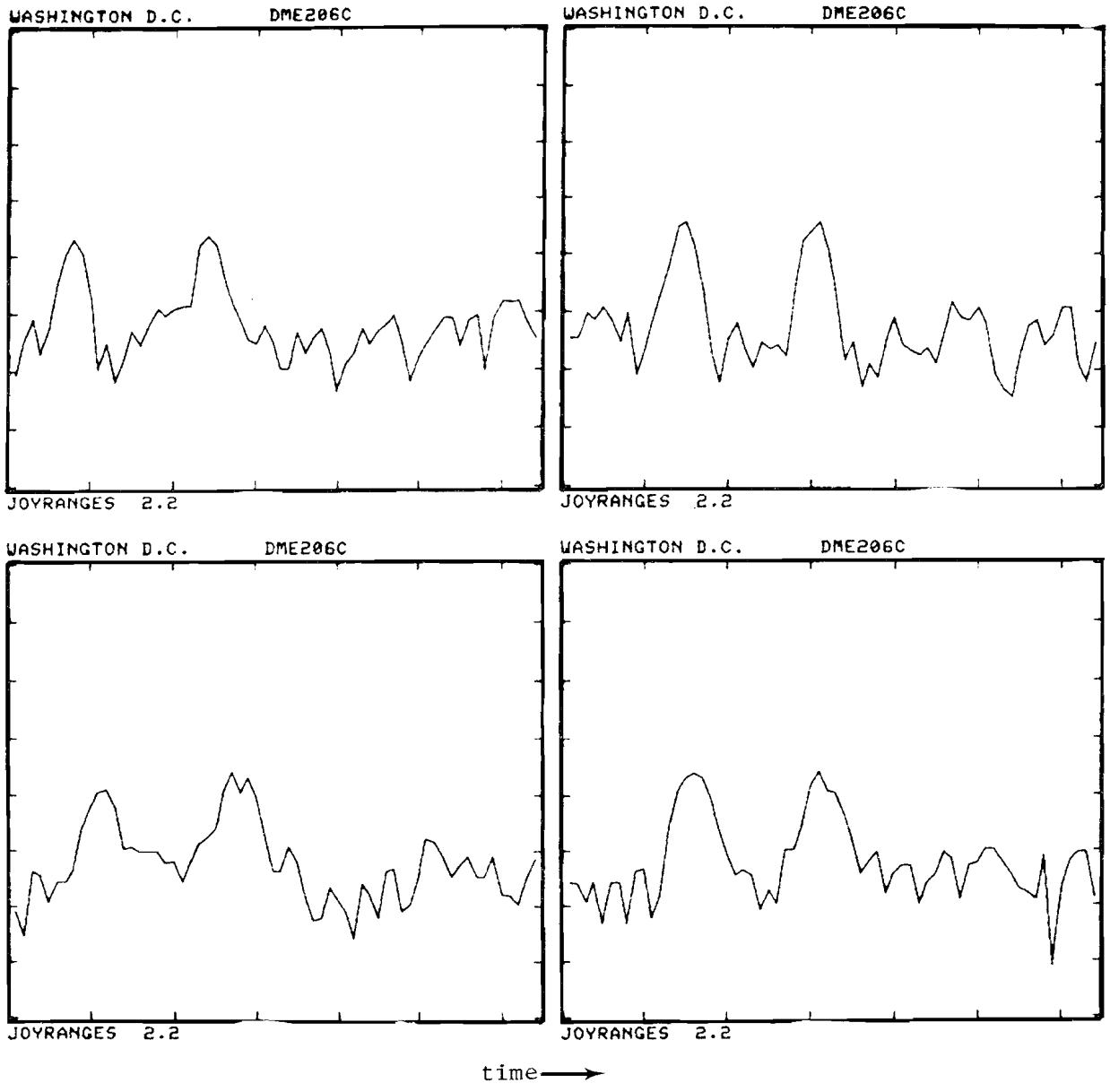

Fig. 8-8. DCA waveforms on 6° approach at 1.4 nmi from threshold.

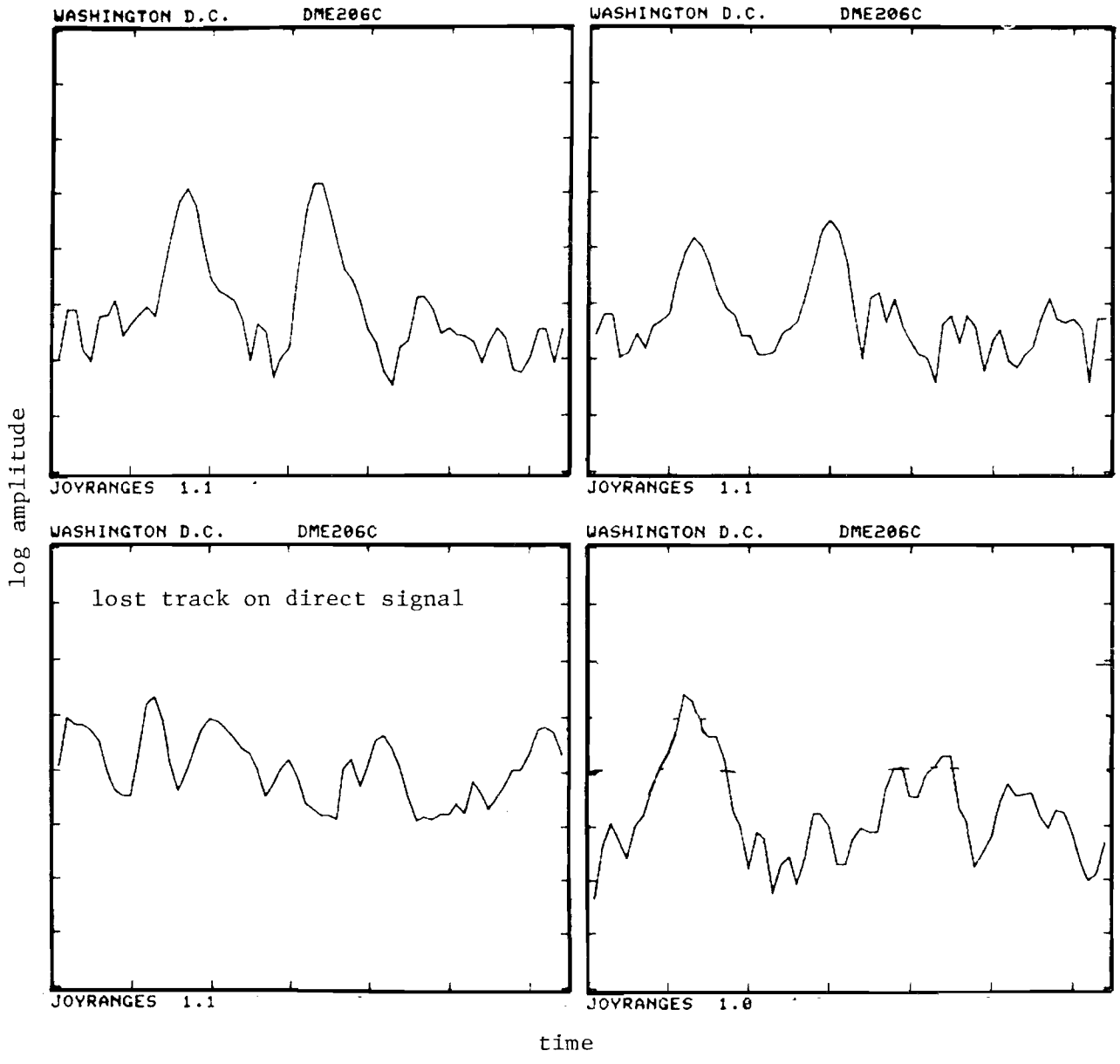

Fig. 8-9. DCA waveforms near threshold on 6° approach.

predicted levels are low (see section D.) Another possibility is that this multipath arose from the hillside between the public parking area and Thomas avenue and/or the Washington Metro Station which borders Smith Boulevard, since the 800 nsec delay is slightly greater than that associated with the hangar complex at this range.

Sizable oscillations in the M/D levels are evident on either side of threshold (joystick range = 0.83 nmi). This reflects the influence of multipath from different buildings as well as oscillations in the multipath level from individual scatterers as will be discussed in the section on simulation results. For the most part, the multipath delays in this region are tightly grouped in the 700 nsec - 1100 nsec region predicted by ray tracing considerations.

D. Simulation Results

A simple model of the DCA mesurement site was developed in which hangars 8 through 12 were represented by flat vertical rectangular metal plates and the terrain contour features ignored. Hangars 8 and 9 were represented by a single plate as were hangars 11 and 12. The runway facing wall of hangar 10 resembles a half circle and was represented by three rectangular plates. Figures 8-10 and 8-11 show the simulation airport map and computed multipath characteristics for a 6° approach to runway 33 and then flying along the runway to a 20 foot height. Figure 8-12 shows the computed multipath characteristics for a 3° approach to the same runway.

Since the front walls of hangars 8, 9, 11, and 12 consist of alternating strips of smooth metal and glass, the simulations were repeated using a model in which the metallic surfaces alone were represented. Figures 8-13 to 8-15 show the corresponding results for this alternative simple airport model. Unfortunately, the various metallic strips for a given building appear as separate entities in Figs. 8-9 to 8-15. When two strips have a comparable magnitude, the resultant could be 6 dB larger than the individual levels or very much less depending on the exact phasing of the signals. Since the top

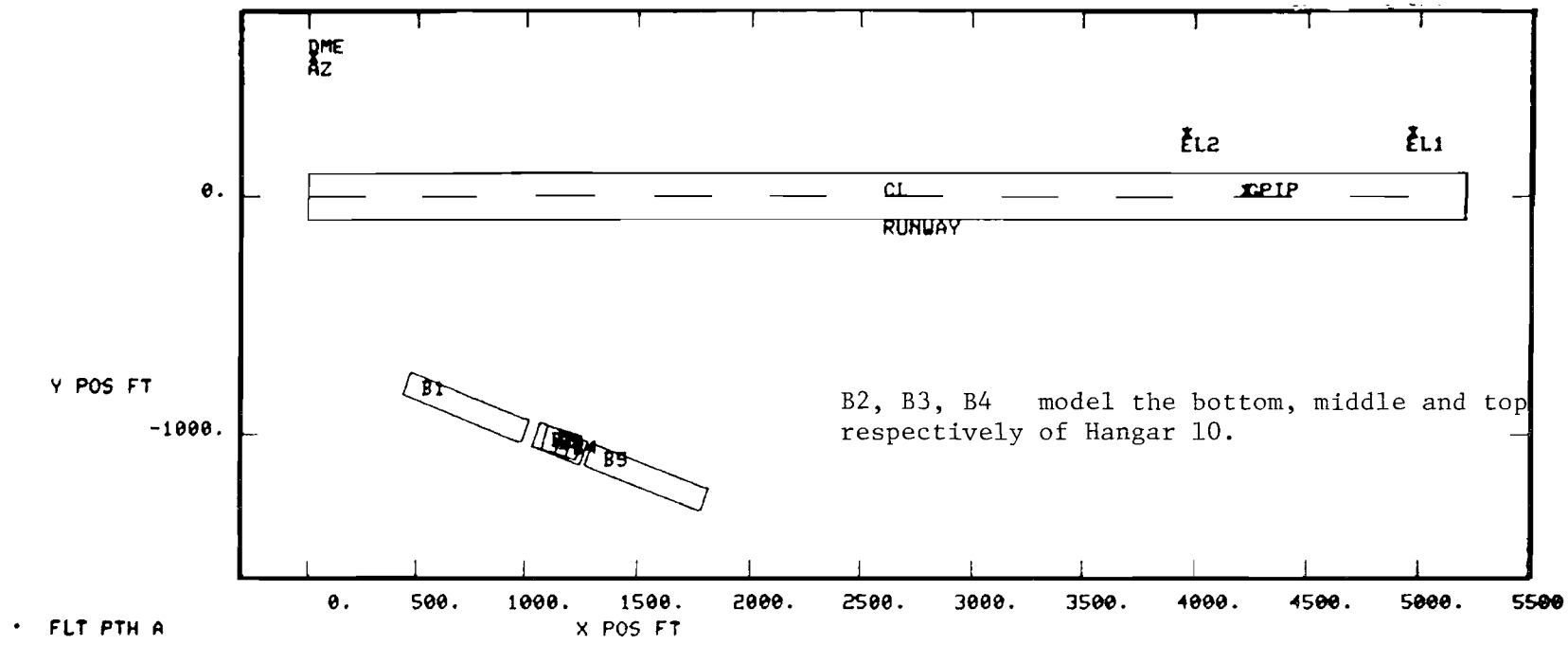

• FLT PTH A

AZ SYSTEM

OBST	RANK	AMP	DIST	RDOP
G	2	0	31440.0	0.
B1	1	-2	32640.0	-6.
B2	4	5	31600.0	-5.
B3	3	4	32640.0	-9.
B4	6	13	33240.0	-14.
B5	5	10	29680.0	-3.

EL SYSTEM

OBST	RANK	AMP	DIST	RDOP
G	1	2	33680.0	0.
B1	4	64	33680.0	1900.
B2	3	62	33640.0	1854.
B3	5	70	33600.0	1864.
B4	6	77	31080.0	43.
B5	2	61	33560.0	1710.

Fig. 8-10. Airport map for DCA 6° approach scenario.

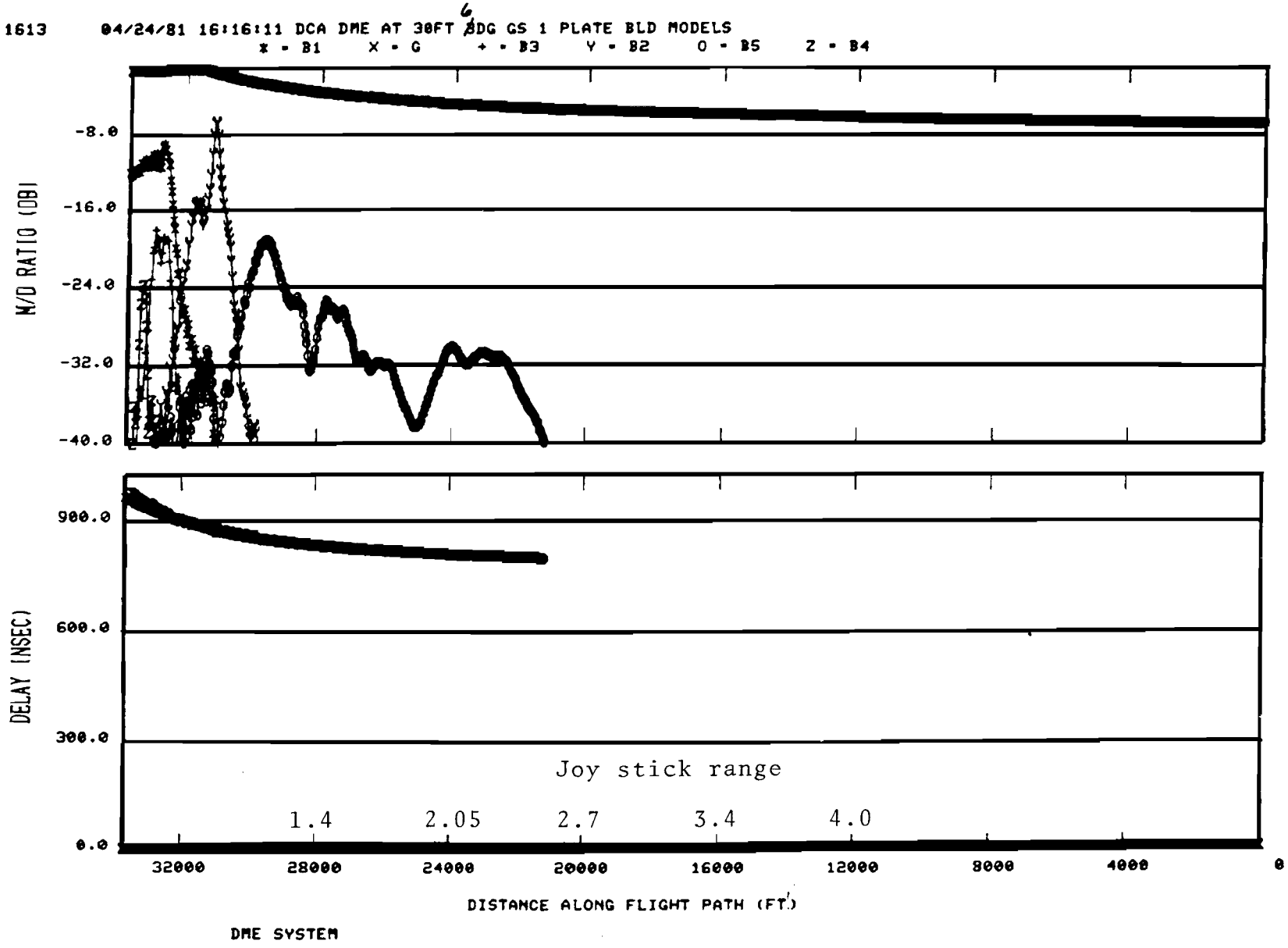

Fig. 8-11. Computed DME multipath characteristics on 6° glidestone for simplified building model.

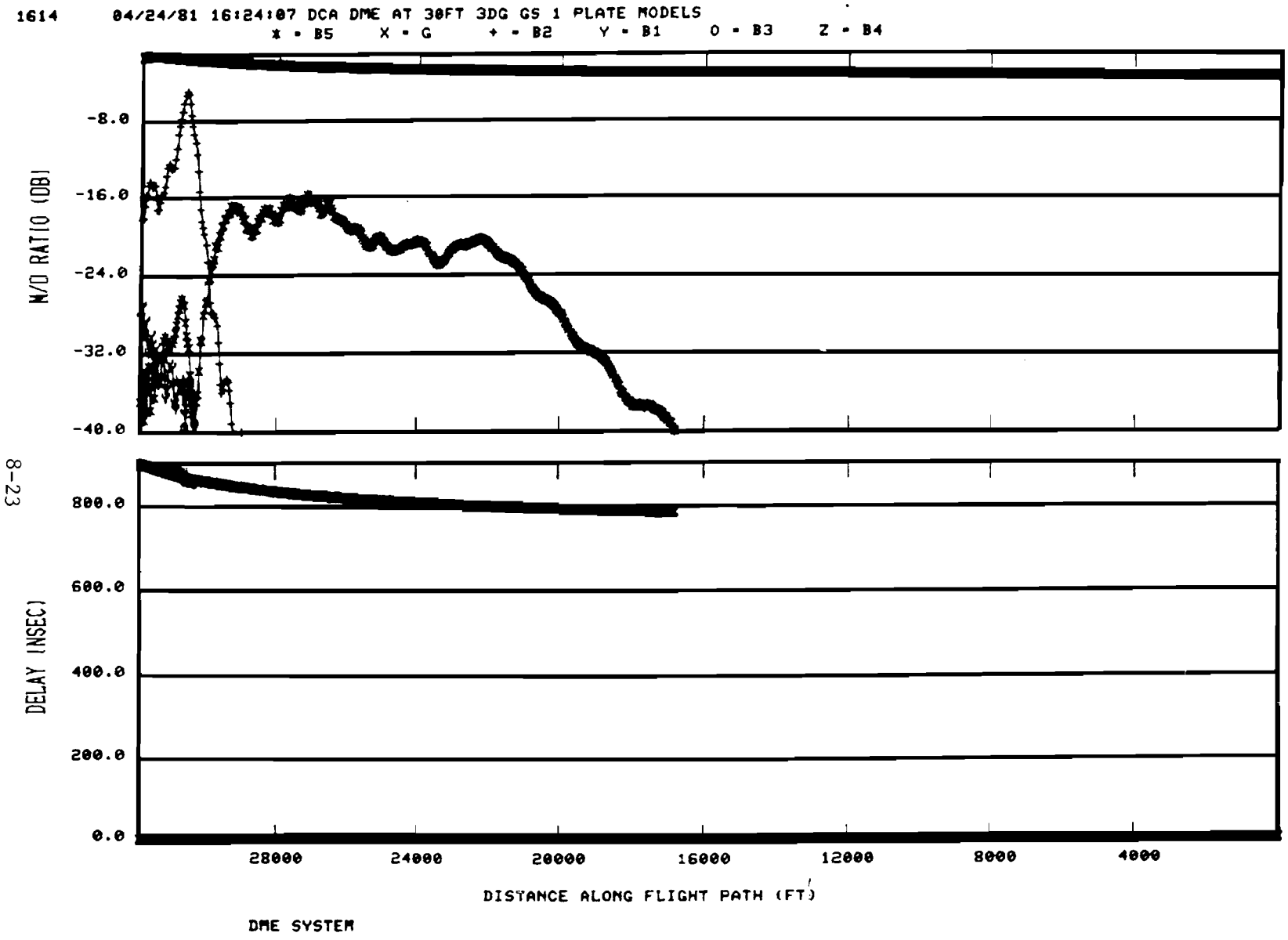

Fig. 8-12. Computed DME multipath characteristics on 3° glideslope for simplified building models.

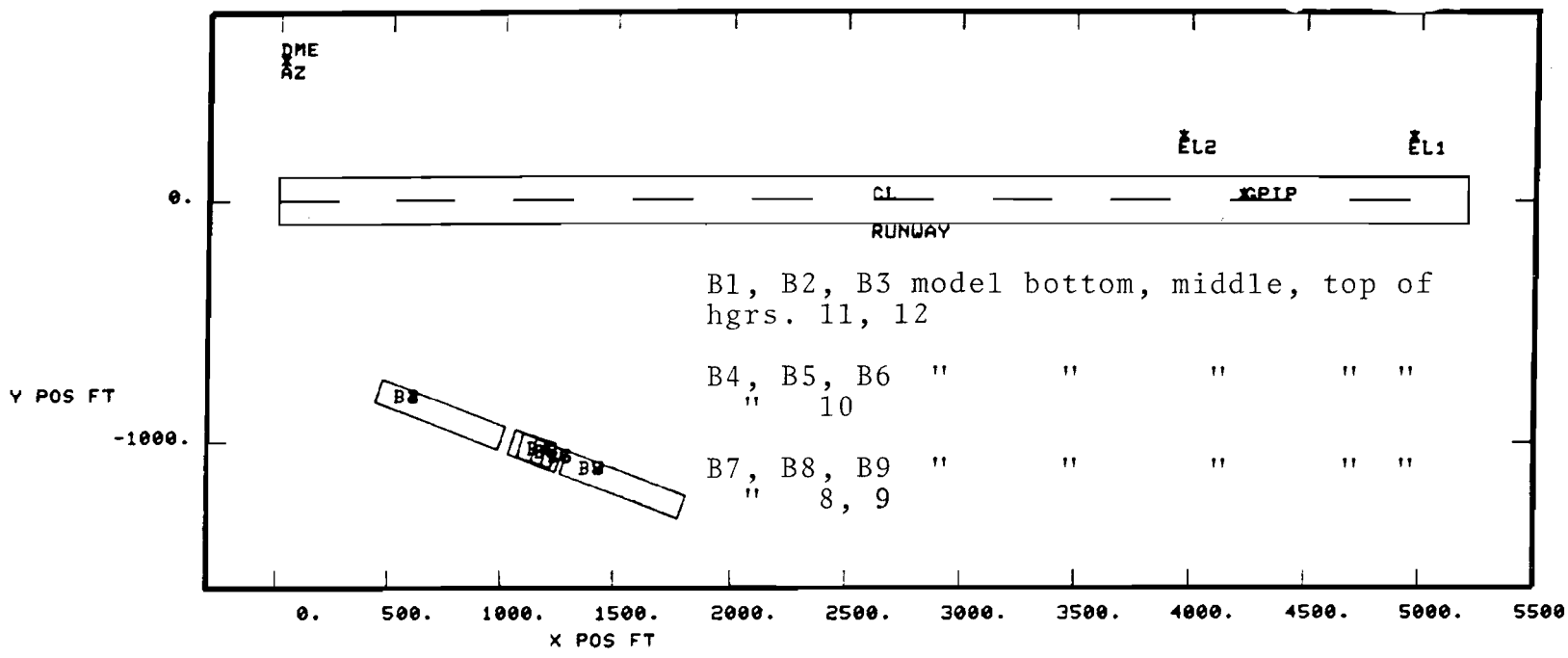

OBST	RANK	AMP	DIST	RDOP
G	1	0	31440.0	0.
B1	2	2	32640.0	-6.
B2	9	15	32640.0	-6.
B3	5	10	32640.0	-7.
B4	4	5	31600.0	-5.
B5	3	4	32640.0	-9.
B6	8	13	33240.0	-14.
B7	7	13	29600.0	-3.
B8	10	16	29320.0	-2.
B9	6	11	29320.0	-2.
D	0	80	0.0	0.

Fig. 8-13. Airport map for DCA 6° approach scenario with alternative building model.

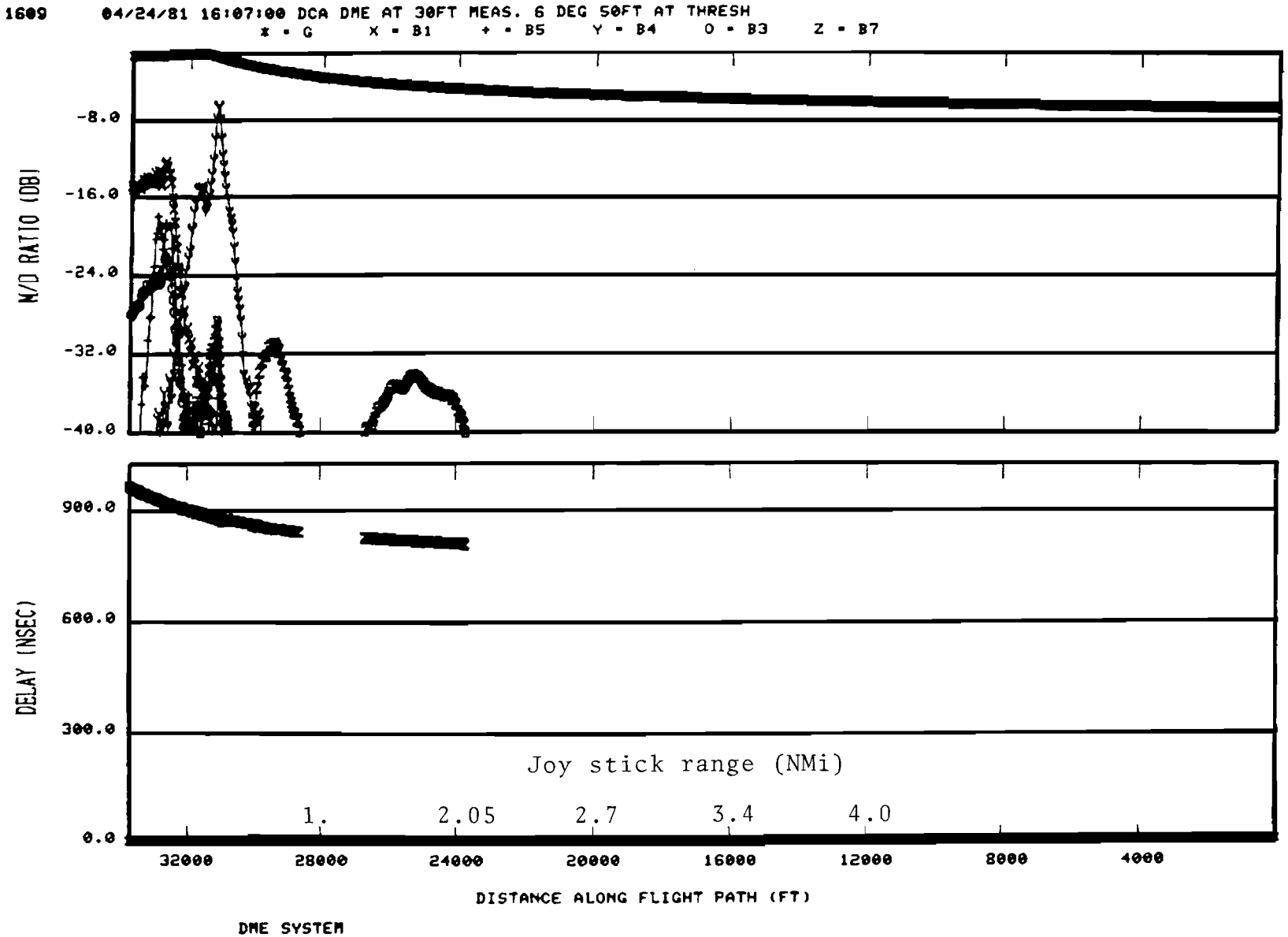

Fig. 8-14. Computed multipath characteristics for DCA 6° approach scenario with alternative building model.

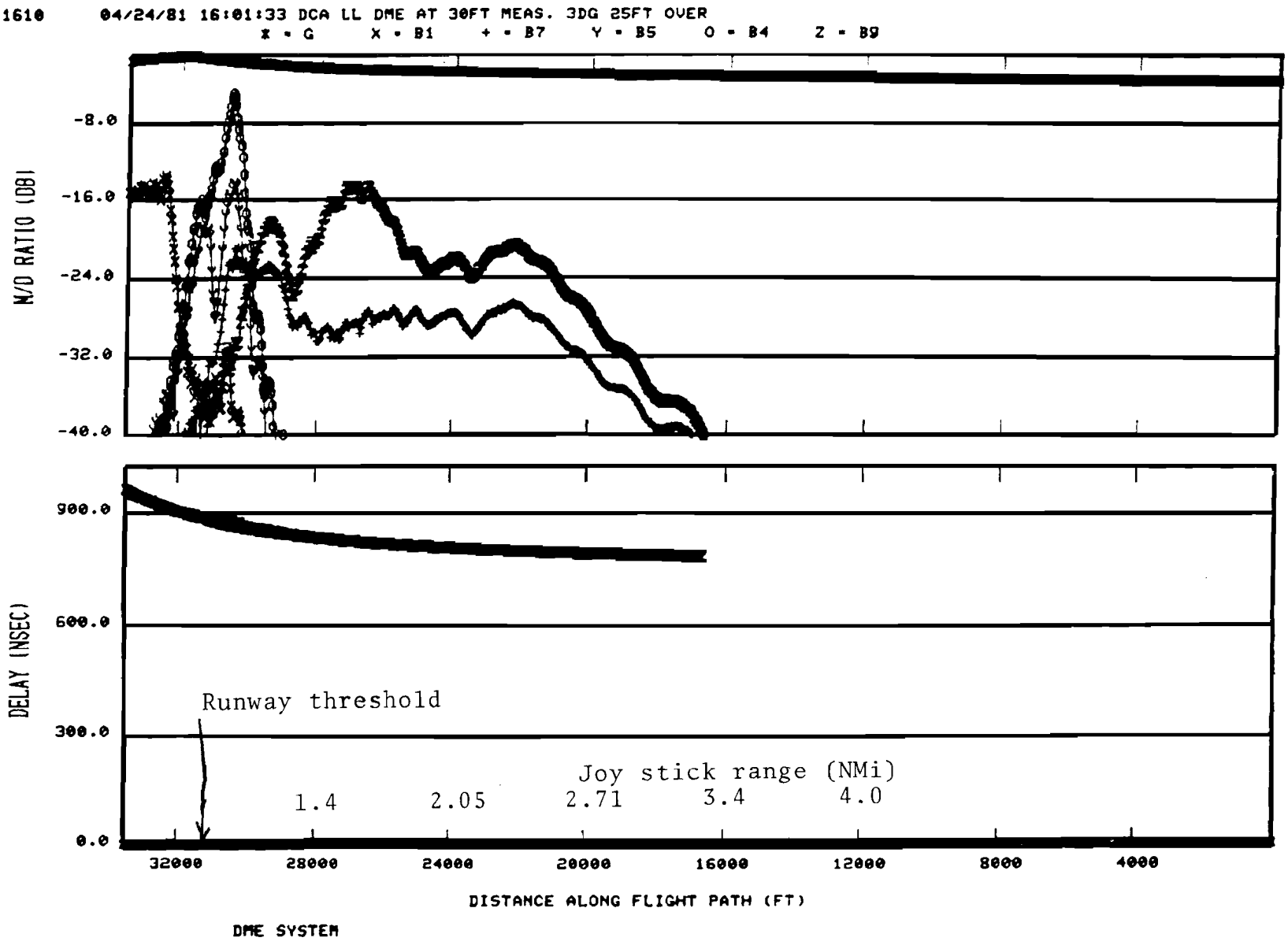

Fig. 8-15. Computed multipath characteristics for DCA 3° Approach scenario.

and middle metallic strips of the hangars 8/9 model have comparable contributions, it is felt that Figs. 8-10 to 8-12 should give a better approximation to the measured data.

The models suggest very low level (-36 dB M/D ratios) multipath commencing 2.15 nmi from threshold (3.0 nmi joystick range) and increasing almost linearly to -8 dB M/D ratios near threshold on a 6° approach. No multipath is predicted for these buildings at joystick ranges greater than 3.0 nmi. The peak observed levels in the 2.0 nmi to 1.3 nmi range from threshold are approximately 20 dB higher than the simulation results (-7 dB vs. -27 dB), but many of the experimental measurements have M/D values less than -20 dB. This variance probably is due to constructive and destructive reinforcement of the signals from the various staggered hangar doors.

Near the threshold (0.5 nmi from threshold = 1.32 nmi joystick range), the simulation results and experimental data show high level short duration multipath regions. Both experimental regions have high levels (-5 to +5 dB M/D ratio), whereas the simulation suggests only one high M/D region. Similarly, after threshold, the experimental results are significantly higher than the simulation results (0 dB to +8 dB vs. -9 dB M/D ratio).

The measured and simulation levels on a 3° approach increase rapidly near 1.5 nmi from threshold; however, the measured M/D ratio values range from -10 dB to 0 dB, whereas the simulation levels are closer to -27 dB. Both levels decrease sharply and then increase to near 0 dB near threshold. The fairly high level (-8 dB to 0 dB M/D ratio) multipath measured near 3.0 nmi from threshold cannot be explained by the simple airport model, as was noted in the discussion of experimental results.

Since terrain contour variations were small and reflection path shadowing by intervening obstacles not an issue here, a more detailed airport model was developed in an effort to better understand the origin of high level multipath

prior to threshold. This involved including a tilt from the vertical of 3.9°* toward the runway for the plate corresponding to the metal strip above the doors of hangars 8, 9, 11 and 12. The doors of these hangars were represetned by single vertical flat plates. Fig. 8-16 shows the airport layout while figs. 8-17 and 8-18 show the computed multipath characteristics for 6° and 3° glideslopes respectively. One of the interesting features of the tilted plate multipath is that the bulk of the multipath reaches the receiver by reflection from the ground after it has been reflected from the building as shown in fig. 8-19.

The simulation results using this model show no better agreement with the field data than do the the earlier results. The small vertical extent of this section (12 feet which is approximately 25% of the first Fresnel zone radius) makes it unlikely that alternative tilt values for it would yield better results.

The other possibility is that the effective direct signal may have been significantly reduced by ground lobing. Raw signal strength records such as shown in figures 8-20 and 8-21 show 1) a deep null (10 dB - 15 dB) for joystick ranges of 1.4 nmi to 1.5 nmi (i.e., 0.5 nmi before threshold) with a lesser null (~ 6 dB) at ranges of 1.1 nmi and 0.9 - 0.8 nmi, and 2) lesser nulls near 1.6, 1.3 and 1.0 nmi on the 3° approaches. These nulls are significantly sharper than were expected (<2 dB) given the receiving antenna elevation pattern (fig. 2-3). These may be due to differences in the aircraft antenna pattern in the elevation plane and/or a ground antenna which was not aligned properly in the vertical plane. Measurements on a scale model Piper Cherokee (fig. 8-22) suggest that the aircraft antenna gain in the direction of the ground reflection could be several dB higher than that in the direction of the direct signal.

---

*the 3.9° value was based on measurements by D. Huntington of the Bendix Corporation.

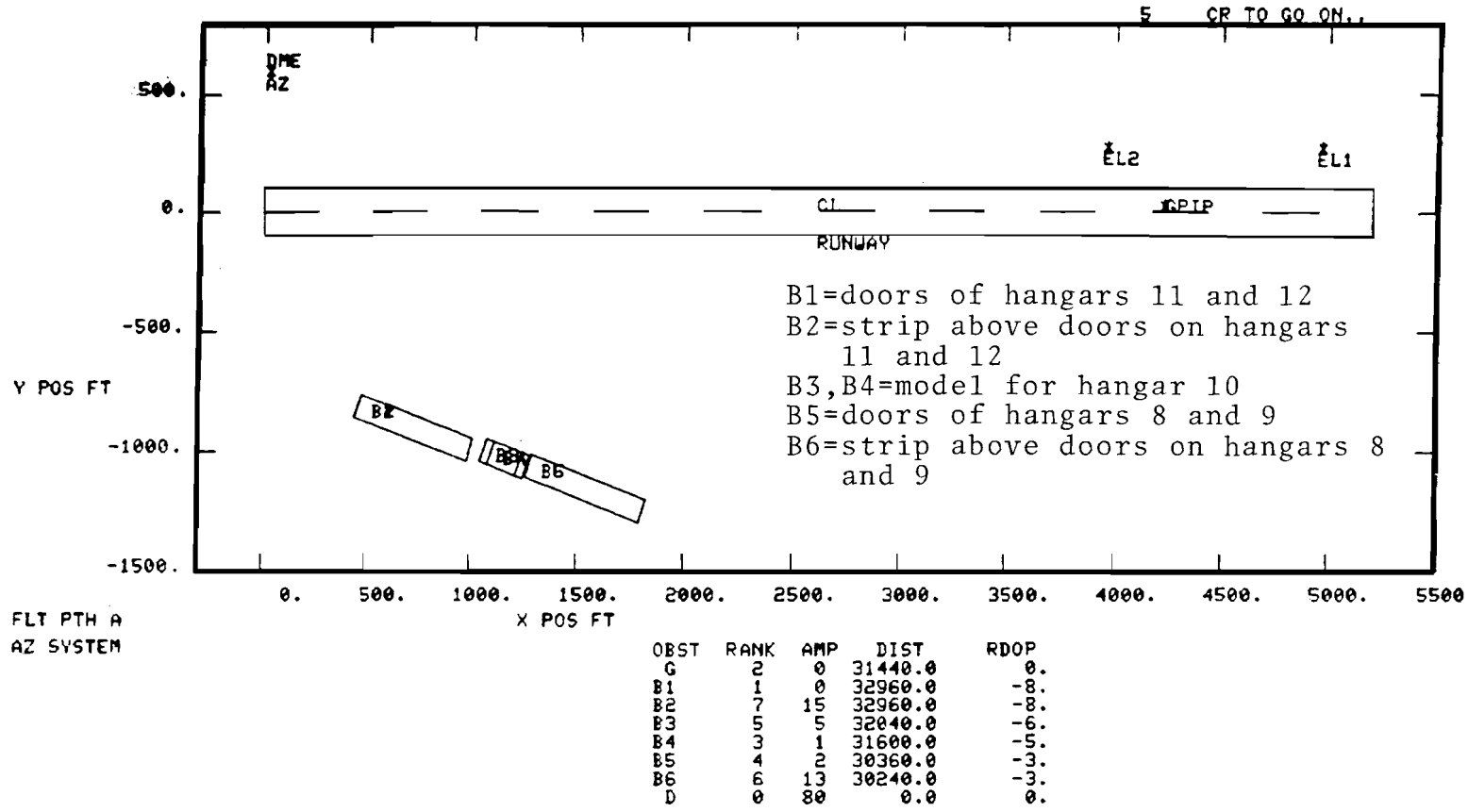

OBST	RANK	AMP	DIST	RDOP
G	2	0	31440.0	0.
B1	1	0	32960.0	-8.
B2	7	15	32960.0	-8.
B3	5	5	32040.0	-6.
B4	3	1	31600.0	-5.
B5	4	2	30360.0	-3.
B6	6	13	30240.0	-3.
D	0	80	0.0	0.

Fig. 8-16. Airport map for DCA DME measurement scenario with tilted building walls.

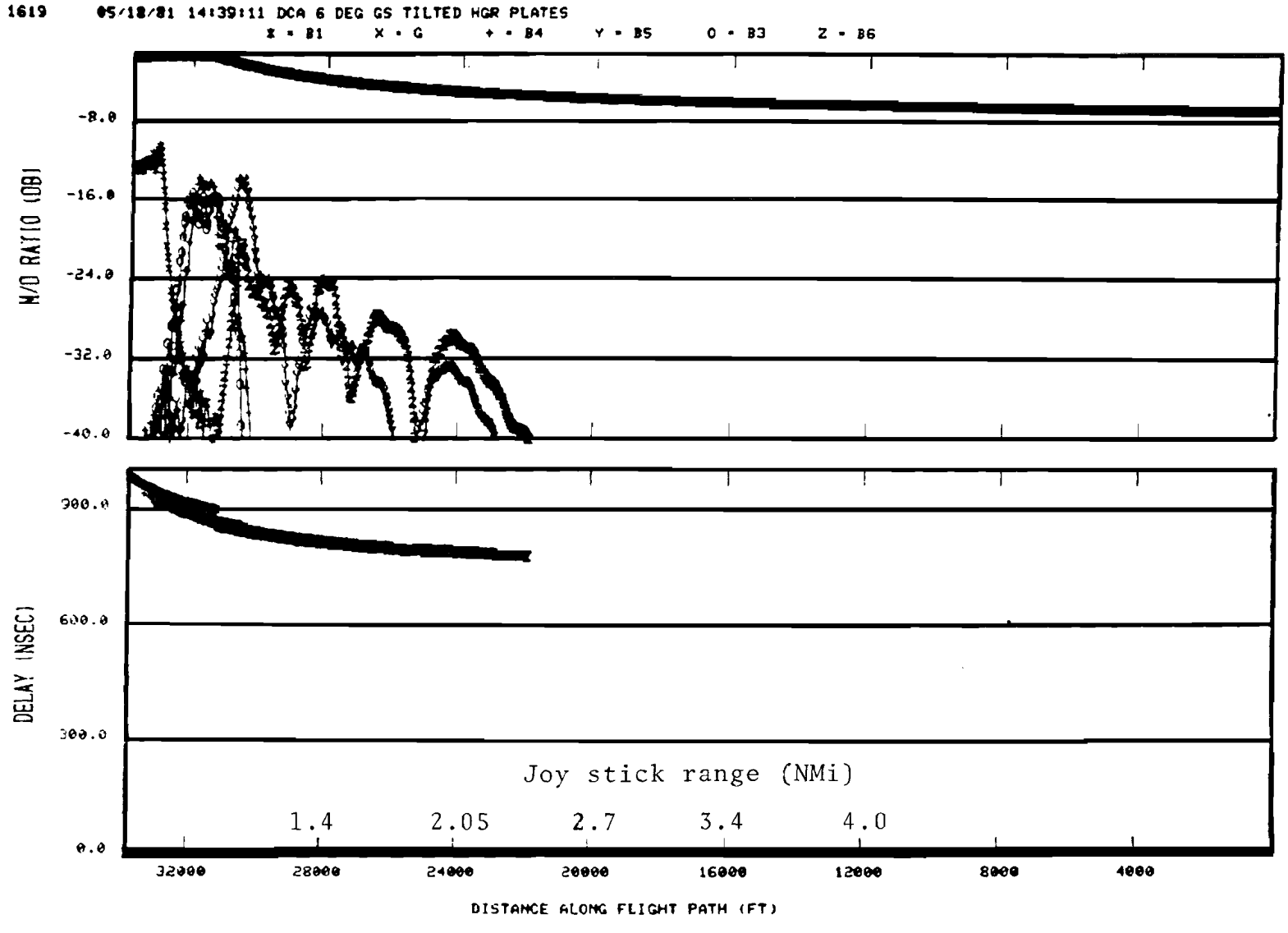

Fig. 8-17. Computed M/D level for 6° glideslope with tilted plate building model.

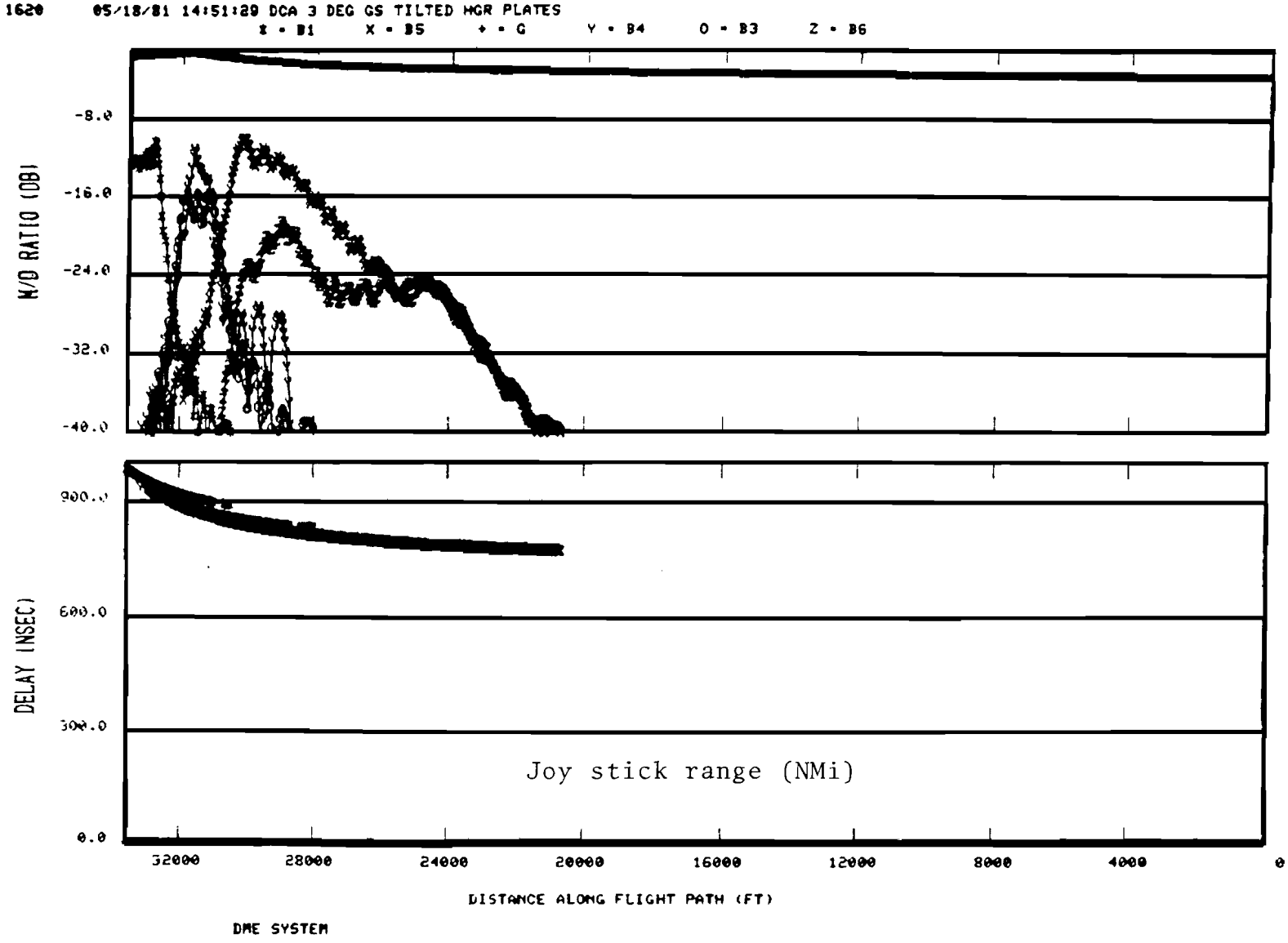

Fig. 8-18. Computed M/D level for 3° glideslope using tilted plate building model.

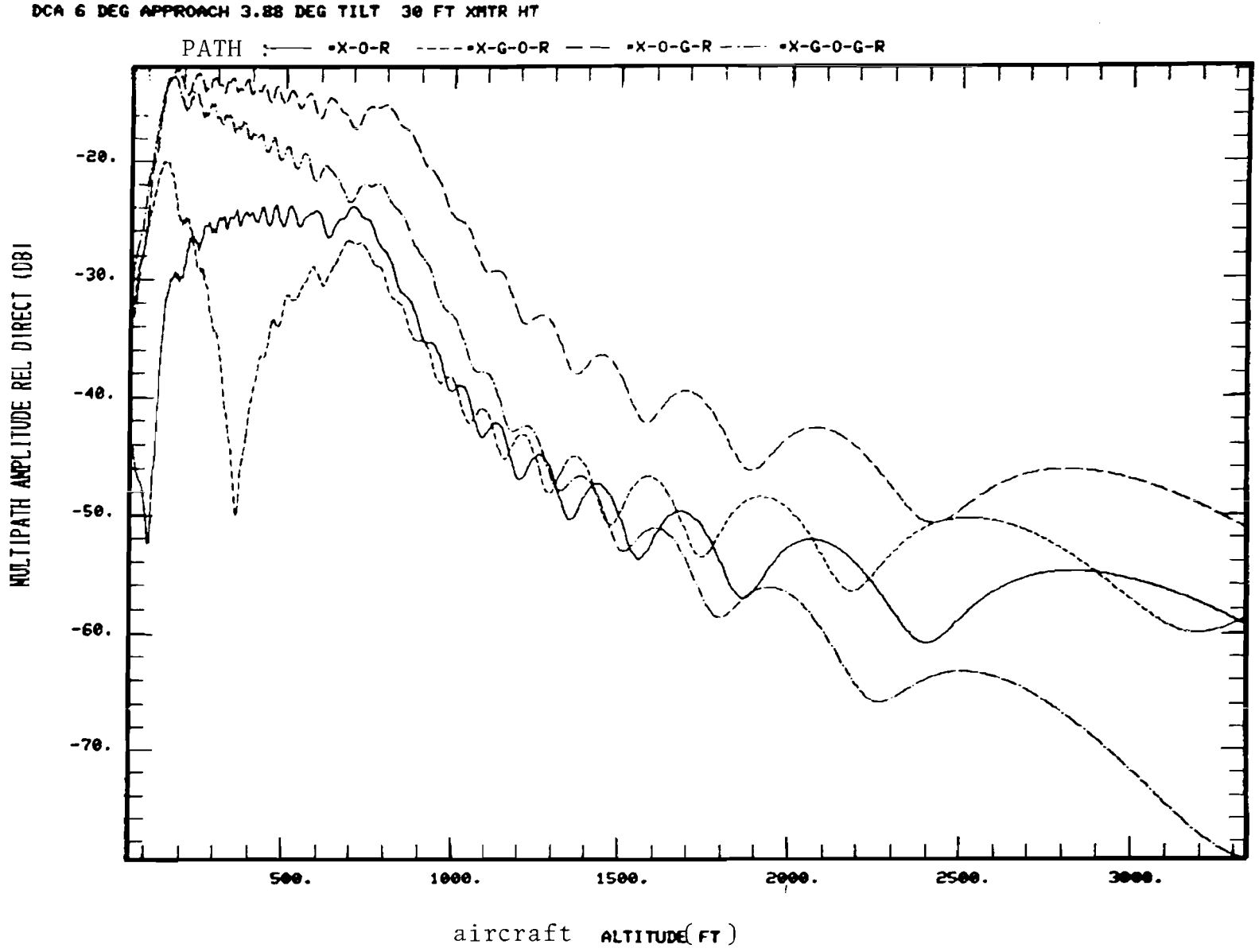

Fig. 8-19. Levels associated with various propogation paths for tilted strip above hangar 8 and 9 doors.

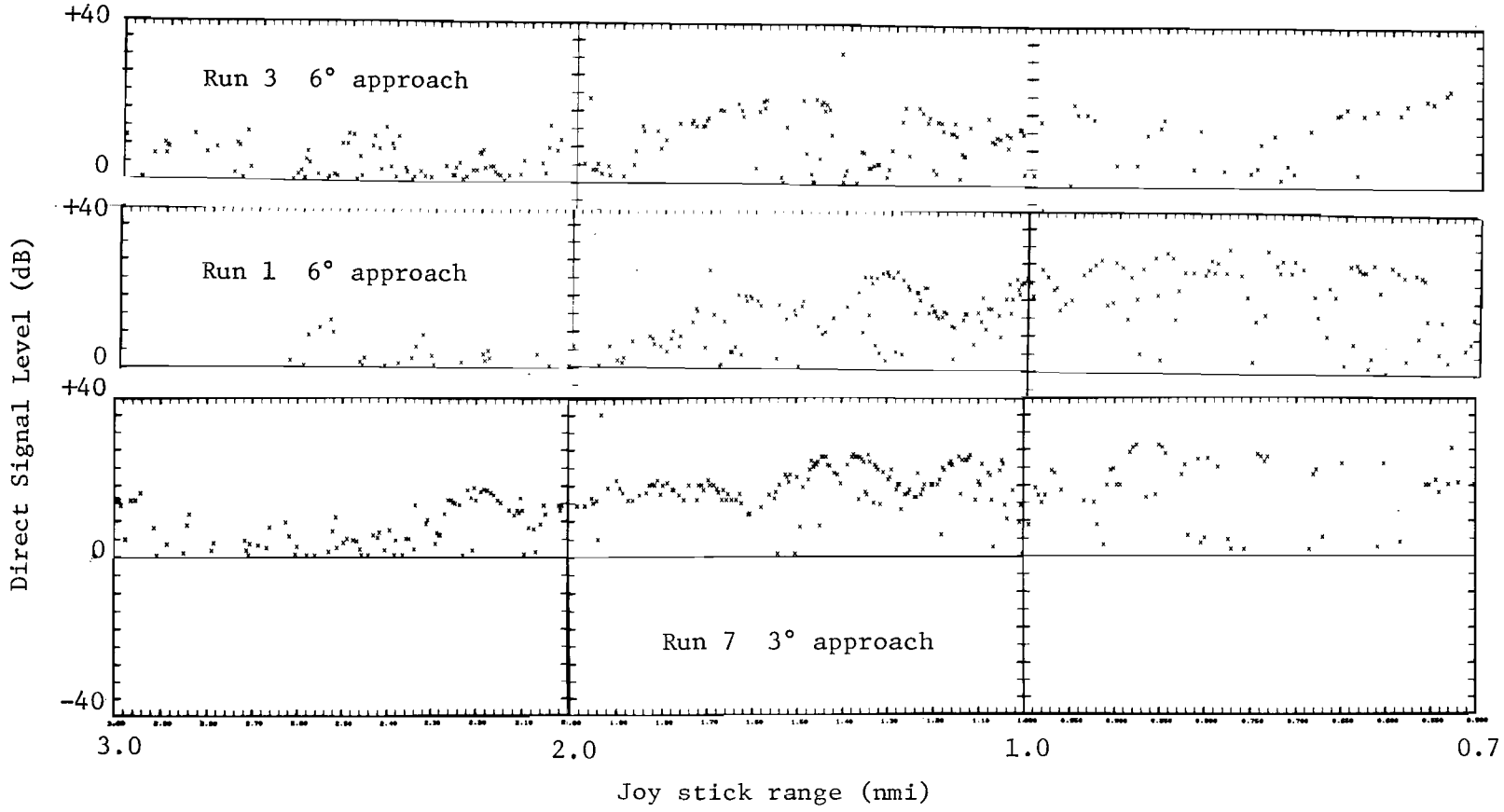

Fig. 8-20. Direct signal strength levels at Washington National Airport.

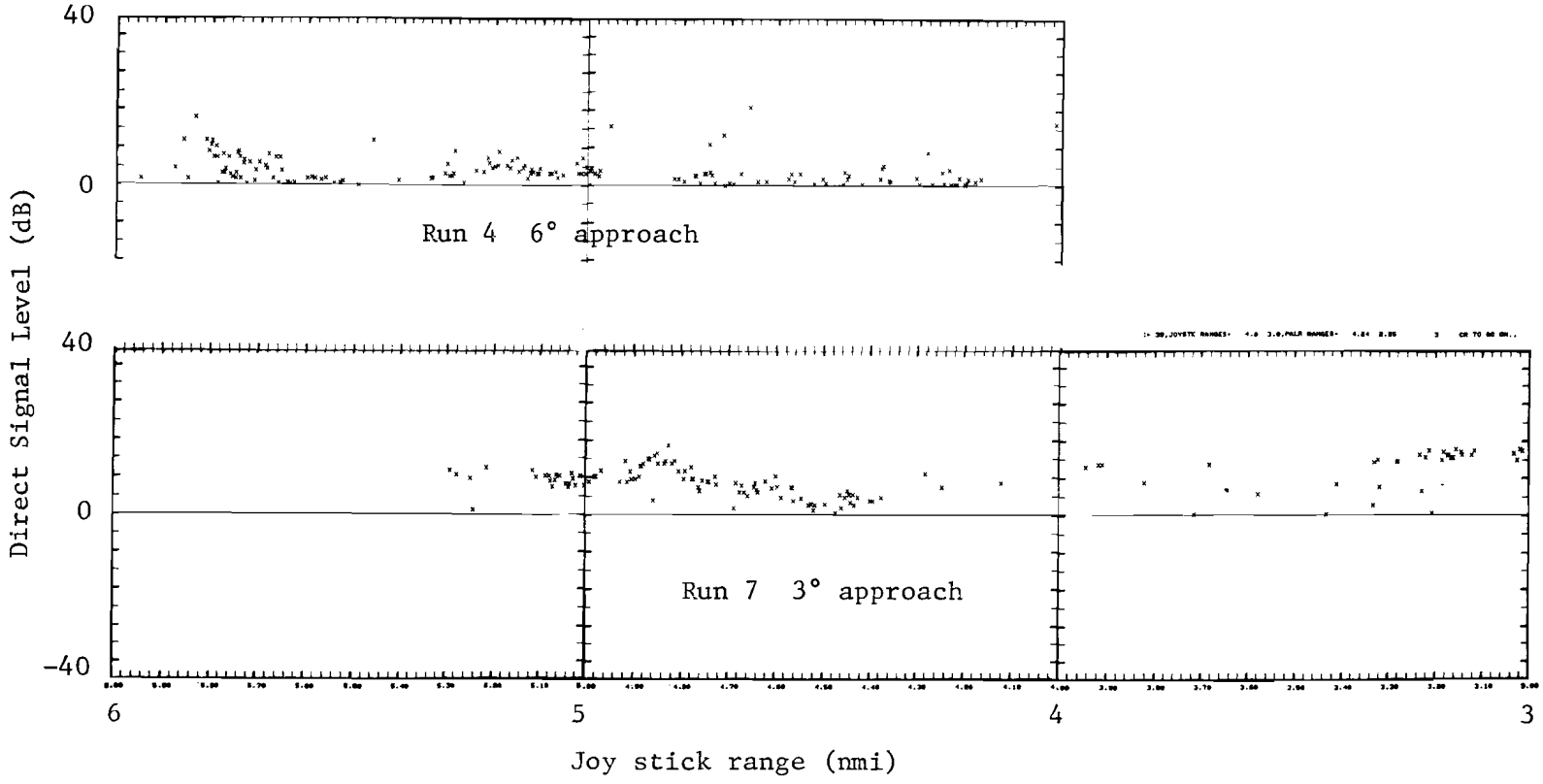

Fig. 8-21. Direct signal strength levels at Washington National Airport.

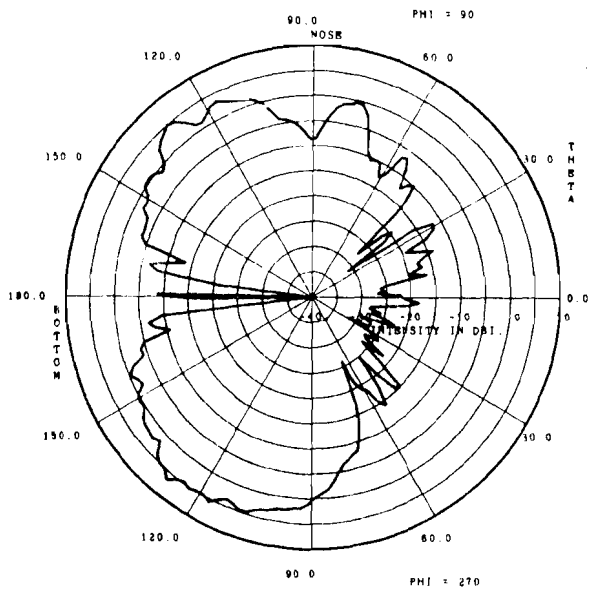

nose to tail

ATC-47(B.2-8)

Fig. 8-22. Elevation pattern measurements on Piper Cherokee model for bottom mounted antenna, flaps up, wheels down.

E. Summary

The multipath regions near the threshold of DCA runway 15-33 correlated fairly well with the specular regions associated with a row of hangars bordering the runway. The time delays of the multipath near threshold agreed quite well quantitatively with the predictions using a simple airport model, but the experimental M/D values were in several cases substantially larger than were predicted. Also, strong multipath was encountered at longer ranges on the approach (e.g., 3 - 5 nmi from threshold) which could not be explained by reflections from vertical walls of the hangars which border the runway. Several possible sources of this long range multipath were suggested, but none have been able to quantitatively explain the phenomena to date.

IX. SUMMARY AND CONCLUSIONS

In this section, we summarize the principal results of the measurement program and make some suggestions for additional measurements to clarify certain issues. Before summarizing, it is worthwhile repeating the program objectives:

1) measurements of the principal multipath parameters (amplitude and time delay) with realistic aircraft/ground site locations at runways which had the major DME/P multipath sources (large buildings) identified in previous analytical (simulation) studies.

2) determination of whether significant DME/P multipath sources exist which had not been considered to date in the DME/P studies to date.

and

3) comparison of the measured results with computer simulation results obtained with simplified airport models (such as have been used for DME/P system design to date).

The measurements placed particular emphasis on the final approach region including the flare and rollout regions since these areas correspond to the most stringent DME/P accuracy requirements and, have not been utilized operationally with the current L band DME.

All of the above objectives were achieved although in some cases (especially, WPAFB, PHL, Tulsa site #1) the experimental data in the flare/rollout region was of poor quality due to low signal to noise ratio. The spatial region and time delay of specular multipath generally correlated well with expectations based on simple ray tracing for these cases in which adequate airport maps were available. With the exception of Washington National (DCA) no significant (M/D ratio > -10 dB) specular multipath was encountered which was not predicted. In the case of DCA, there is some question as to whether the multipath encountered at 2-3 nmi from threshold arose from the identified buildings as opposed to other airport features.

The absence of significant specular multipath* other than from readily identified structures at aircraft altitudes above 100 feet is viewed as particularly important for the initial implementation of MLS since it currently is anticipated that the vast majority of MLS installations will provide category I/II service only.

When the aircraft antenna was at low altitudes (e.g., 10-20 feet) over runways and/or taxiways, a variety of multipath signals were encountered which generally correlated with the principal identified structures. On the other hand, the large number of potential multipath sources in this region precluded a detailed quantitative analysis for each of the various sites.

The airport models used for DME/P analyses to date have typically made a number of simplifying assumptions such as:

(1) buildings are represented by single flat vertical rectangular plates with a constant reflection coefficient.

(2) the terrain is assumed to be flat both along and off the runway centerline.

(3) blockage of reflection paths by intervening objects is ignored.

The physical features of actual airports differ considerably from each of these assumptions, but arguments can be advanced to support either higher or lower levels than predicted by the simplified models. Thus, we sought to determine to what extent simplified airport models could predict the measured data. The quantitative predictions of the simple airport models generally agreed with the experimental data, although in some cases, (especially near threshold at WPAFB, DCA, and Tulsa) the measured M/D values were considerably higher than predictions. We attribute the WPAFB and Tulsa higher levels to terrain contour features. In this context, it should be noted that 4 of the 6

*The possible existence of numerous low level (e.g., diffuse) specular reflections in this region is discussed below.

airports had runway contours which differed considerably from the nominally flat model used for DME/P power budget computations.

The cause of higher than expected multipath levels at DCA is unclear. Possible explanations include:

(1) non verticality of the hangar doors

(2) excess ground lobing due to the aircraft antenna vertical pattern and/or the runway slope

and

(3) greater aircraft antenna gain in the azimuth plane towards the hangars than towards the ground site (the approach was flown with the wheels down).

Two potential sources of significant DME/P multipath were not quantitatively assessed in the experiments presented here:

(1) diffuse reflections from an extended region of small scatterers. The current DME/P error budgets contain a significant allowance for diffuse multipath based on FAA experimental measurements at Wallops Island, Va.* Unfortunately, the range of diffuse multipath delays of greatest significance for DME/P (0-300 ns) is comparable to the pulse widths used in our multipath measurements. This overlap together with the low SNR on the bulk of our flights made it virtually impossible to estimate the diffuse multipath power vs. delay characteristic.

(2) reflections from rough and/or irregular terrain such as encountered in mountainous regions. Several of the U.S. interim MLS installations are located in mountainous regions (e.g., Aspen, Colorado) and it has been suggested [14] that three dimensional aircraft position information is particularly important in such regions. Limited L band measurements were conducted by the FRG at Salzburg, Austria [15], but the pulse widths used (2 μsec) were too large to resolve the multipath of greatest concern to DME/P. Long delay (2 μsec to 20 μsec) diffuse multipath was observed as well as some discrete specular multipath. It is unclear from the published results whether the high level (e.g., -6 dB) specular multipath

*R. Kelly, personal communication.

was due to mountains as opposed to the buildings and near the airport.

It is suggested that additional measurements be carried out to address both of these points. It should be noted that the instrumentation required to make analog measurements (e.g., scope photos) is fairly minimal.

The degree of ground reflection lobing of the direct signal is important both from the viewpoint of multipath sensitivity and power budgets. The measurements results suggest that ground lobing in cases of that predicted by the standard flat earth models can occur due to runway contours and/or nonisotropic aircraft antenna patterns. Calibrated measurements of signal strength at the thresholds of representative non flat runways should be relatively easy to carry out.

Aircraft antenna pattern measurements in the vertical plane on scale models are available for many aircraft [10 - 12] and could be analyzed to determine the implications of increased gain at negative elevation angles on the differential lobing. It should be noted that since the effective direct signal in a null is the difference of two signals:

$$D_{eff} = G(E_d) - R\ G(E_g)$$

where $G(E)$ = elevation pattern as a function of elevation angle
R = reflection coefficient
E_d = direct signal elevation angle for aircraft
E_g = ground reflection " " "

relatively small differences between $G(E_d)$ and $G(E_m)$ can produce large changes in D_{eff}.

REFERENCES

1. J. Evans and D. Easterday, "L-Band DME Multipath Environment in the MLS Approach and Landing Region," ATC Working Paper 44WP-5058, Lincoln Laboratory, M.I.T. (23 September 1980), presented as AWOP WG-M Paper M/4 - BIP/18, by J. Edwards (October 1980).

2. J. Evans, D. Sun, S. Dolinar, and D. Shnidman, "MLS Multipath Studies, Phase 3 Final Report, Volume I: Overview and Propagation Model Validation/Refinement Studies," Project Report ATC-88, Lincoln Laboratory, M.I.T. (25 April 1979).

3. R. Kelly and E. LaBerge, "Guidance Accuracy Considerations for the Microwave Landing System L-Band Precision DME," J. Navigation (May 1980).

4. J. E. Evans, "Synthesis of Equiripple Sector Antenna Patterns," IEEE Trans. Antennas Propag., Vol. 24, 347 (May 1976).

5. J. E. Evans, D. Karp, R. R. LaFrey, R. J. McAulay, and I. G. Stiglitz, "Experimental Validation of PALM - A System for Precise Aircraft Location," Technical Note 1975-29, Lincoln Laboratory, M.I.T. (3 March 1975), DDC AD-A010112/1.

6. D. A. Shnidman, "Airport Survey for MLS Multipath Issues," Project Report ATC-58, Lincoln Laboratory, M.I.T., FAA-RD-75-195 (15 Dec. 1975), DDC AD-A022937/7.

7. J. Capon, "Multipath Parameter Computations for the MLS Simulation Computer Program," Project Report ATC-68, Lincoln Laboratory, M.I.T. (8 April 1976), DDC AD-A024350/1.

8. P. Beckman and A. Spizzichino, The Scattering of Electromagnetic Waves from Rough Surfaces, (Pergamon Press, New York 1963).

9. D. Shnidman, "The Philadelphia MLS Experiments," ATC Working Paper 44WP-5045, Lincoln Laboratory, M.I.T. (28 Oct. 1976).

10. K. J. Keeping and J. C. Sureau, "Scale Model Measurements of Aircraft L-Band Beacon Antennas," Project Report ATC-47, Lincoln Laboratory, M.I.T., FAA-RD-75-23 (4 Mar. 1975), DDC AD-A010479/4.

11. G. J. Schlieckert, "An Analysis of L-Band Beacon Antenna Patterns," Project Report ATC-37, Lincoln Laboratory, M.I.T., FAA-RD-74-144 (15 Jan. 1975), DDC AD-A005569/9.

12. D. W. Mayweather, "Model Aircraft L-Band Beacon Antenna Pattern Gain Maps," Project Report ATC-44, Lincoln Laboratory, M.I.T., FAA-RD-75-75 (16 May 1975), DDC AD-A013184/7.

13. H. Postel, "Precision L-Band DME Tests", Federal Aviation Administration Technical Center Report, FAA-CT-80-25, FAA-RD-80-74, (August 1980).

14. Federal Republic of Germany, "The need for integrated navigation systems in the TMA", ICAO All Weather Operations Divisional Meeting Paper AWO/78 - WP/56 (March 1978).

15. Federal Republic of Germany, "Field tests for multipath propagation measurements in mountainous sites," ICAO All Weather Operations Divisional Meeting Paper AWO/78 - WP/101 (April 1978).

APPENDIX A

PILOT SCALE L-BAND MULTIPATH MEASUREMENTS AT QUONSET STATE AIRPORT, RHODE ISLAND

A pilot scale of L-band multipath measurements were conducted at the Quonset State Airport, operated by the Rhode Island Port Authority, on September 5, 1980. The objectives of this measurement effort were:

(1) to provide experience in operational procedures and evaluate equipment needs for conducting a full-scale measurement program,

(2) to obtain confidence in the validity of the Lincoln Laboratory multipath simulation model,

(3) demonstrate the existence of high level M/D ratios relevant to the DME/P operating environment.

A narrow width (≈ 100 nsec) pulse was used to allow resolution of the building multipath (M), and direct path (plus ground reflection), (D), returns. Building multipath reflections from four hangars were observed along the runway over a range of from 3500 to 6500 feet of separation between transmitter and receiver. Photographic data were recorded from an oscilloscope throughout this region showing M/D ratios of up to 6 dB. These (M/D) levels agreed well with the simulation model predictions over that region. The simulation results also reflected accurately the (M/D) variations with transmitter elevation.

1. Local Topography and Instrumentation Deployment

The Quonset State Airport was chosen from available sites proximate to Lincoln Laboratory due to its very light traffic levels and the fact that four large, uniform hangars dominated the surroundings so far as multipath reflections were concerned. An aerial view of the airfield is shown in Fig. A-1; note the relatively sparse amounts of equipment in the area surrounding the hangars. However, at surface level, it became apparent (Figs. A-1b, A-1c) that there were numerous parked aircraft which would partially block the

(a)

(d)

(b)

(c)

Fig. A-1. Aerial and ground views of Quonset Point State Airport L-band measurement site.

reflections. Also, the hangar walls themselves were a mixture of glass and concrete (Fig. A-1).

The tests were conducted using an interrogator/transponder pair with an additional complement of electronic test gear to produce a wide bandwidth (10 MHz) pulse following the transponder's reply at a delay of about 40 μsec. The 1090 MHz reply was hetrodyned to 74 MHz, filtered, and displayed on an oscilloscope. The wide receiver bandwidth and narrow pulse produced well-resolved returns of the (building) multipath and the direct (plus ground multipath) pulses. A diagram of the instrumentation is given in Fig. A-2.

With a fixed height receiving antenna, oscilloscope photographs were taken at twenty discrete stations as the transmitter travelled along a path stretching some 3000 feet parallel to the runway. These positions are indicated on the drawing of the airfield in Fig. A-3. Data were recorded at two different heights of the transmitting antenna. The reference line along which the transmitter travelled was surveyed to be parallel to the (co-linear) faces of the hangars. The reference point on this line was directly opposite the left hand corner of hangar #3. A precise reading of the distance of the transmitter along the reference line was made for each of the points where photographic data were recorded.

2. Measurement Results Summary

As indicated in Fig. A-3, one expects on the basis of geometric optics to find four distinct zones where high level multipath interference will exist. The zones are approximately 500 feet in length, with 500 feet between zones.

A representative set of the data are presented in Figs. A-4 to A-7 representing data stations #7, 8, 14, and 19 (refer to Fig. A-3).

3. Simulation Model Preliminary Predictions

Although the simulation model test program used for these preliminary results did not have the ability to model reflections from more than one

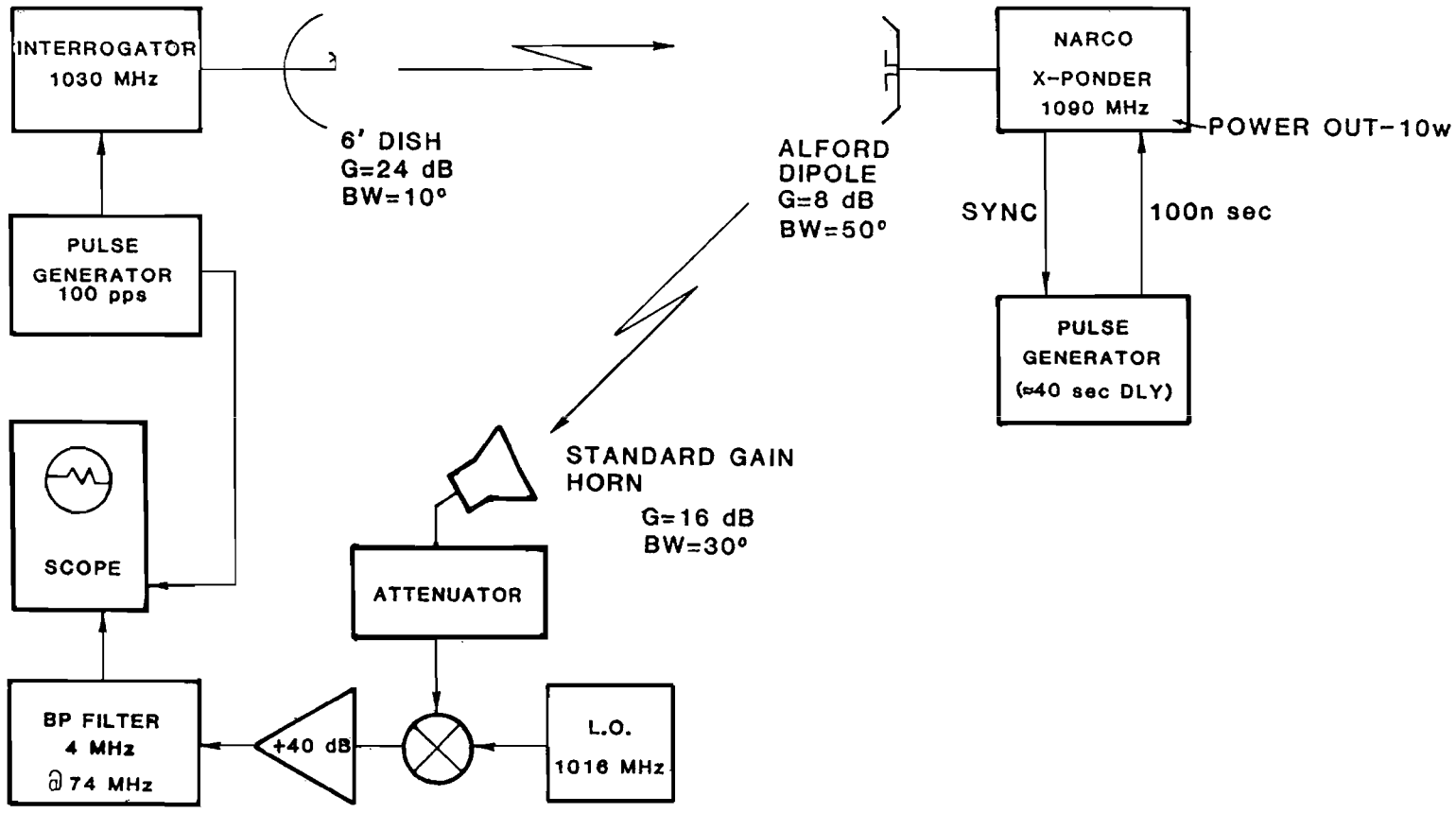

Fig. A-2. L-band multipath instrumentation.

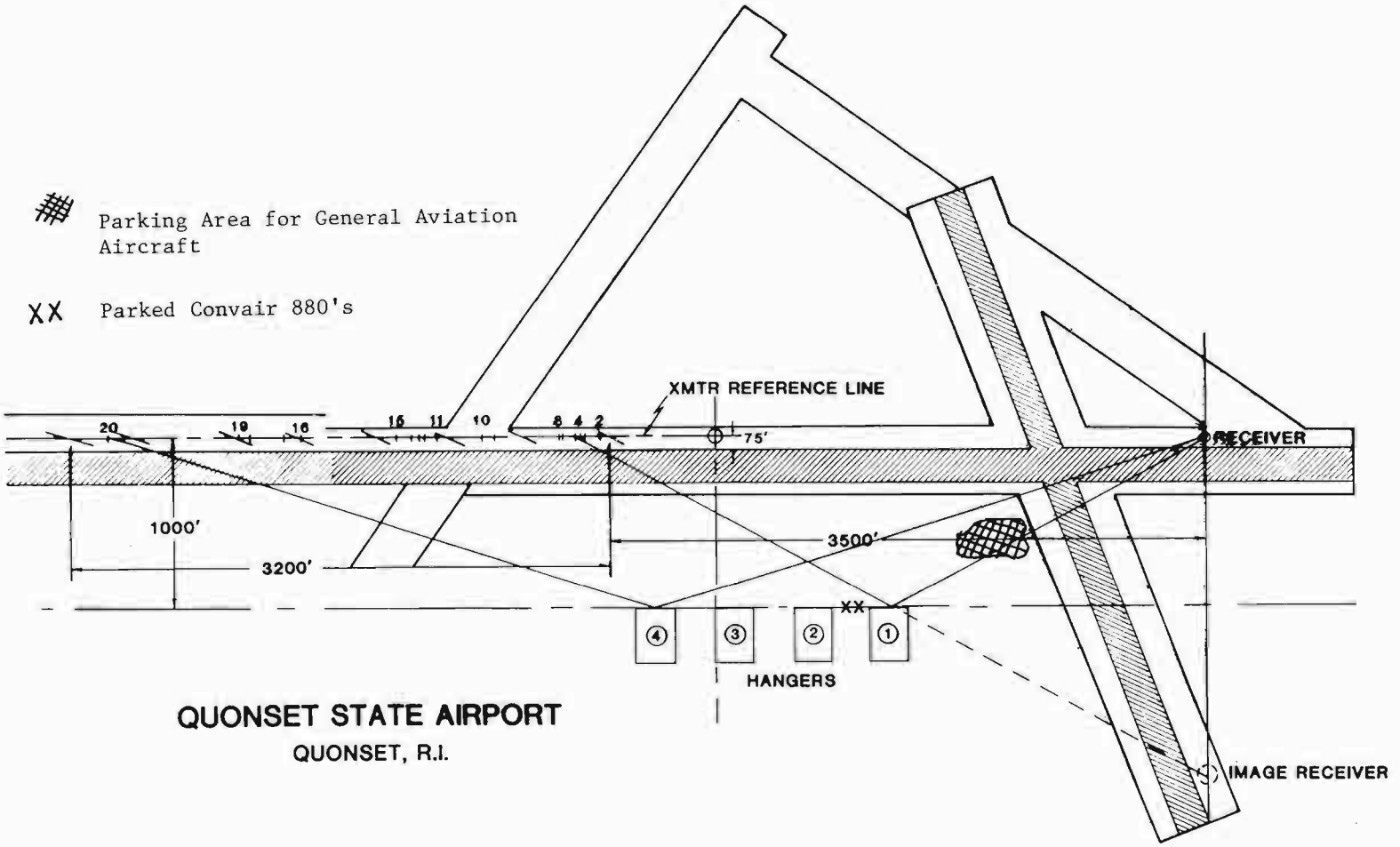

Fig. A-3. Measurement geometry.

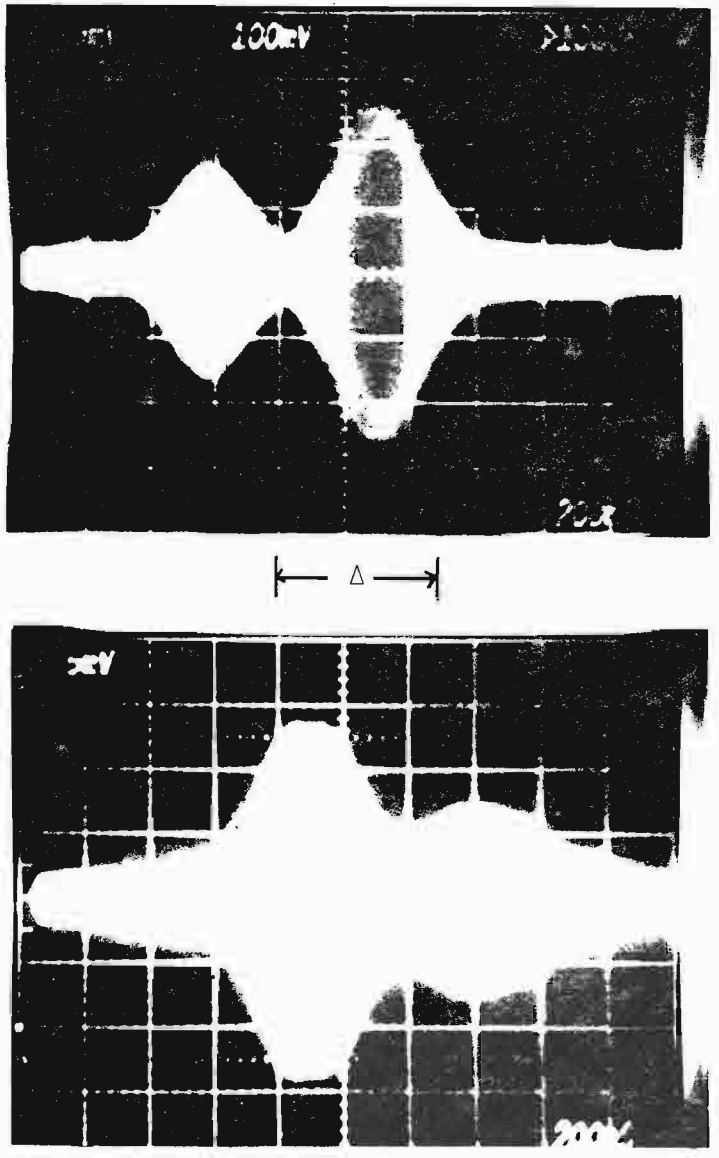

M/D = 4.1 dB

Δ = 520 μsec.

XMTR HT. = 11.5 ft.

M/D = -6 dB

XMTR HT. = 28 ft.

Fig. A-4. Measurement station #7 data.

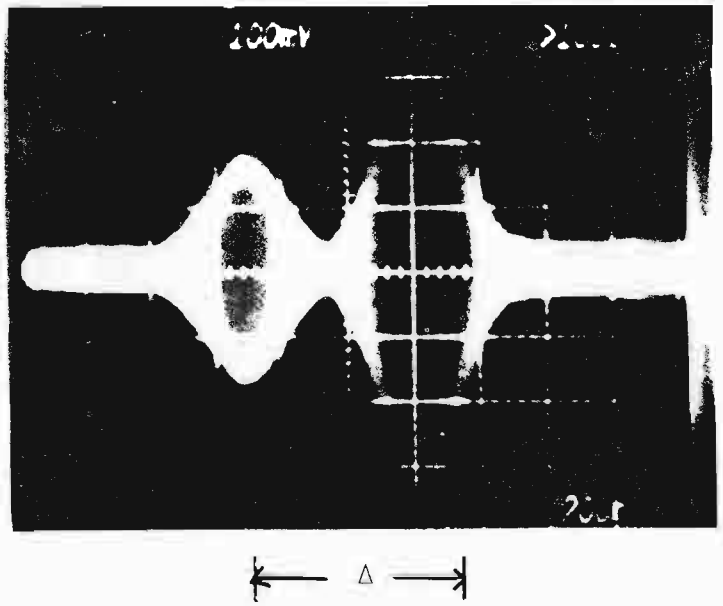

M/D = 5.8 dB

Δ = 520 μ sec.

XMTR HT. = 11.5 ft.

M/D = -9 dB

XMTR HT. = 28 ft.

Fig. A-5. Measurement station #8 data.

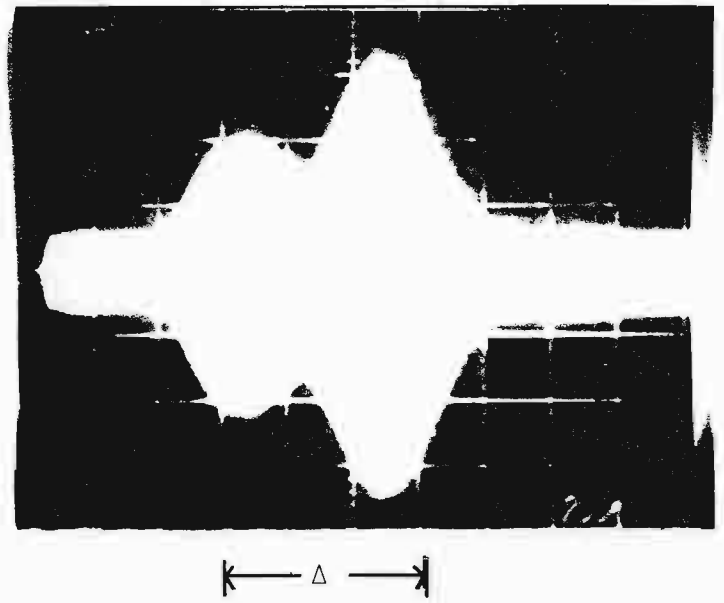

M/D = 4.3 dB

Δ = 420 μ sec.

XMTR HT = 11.5 ft.

M/D = 0.6 dB

XMTR HT = 28 ft.

Fig. A-6. Measurement station #14 data

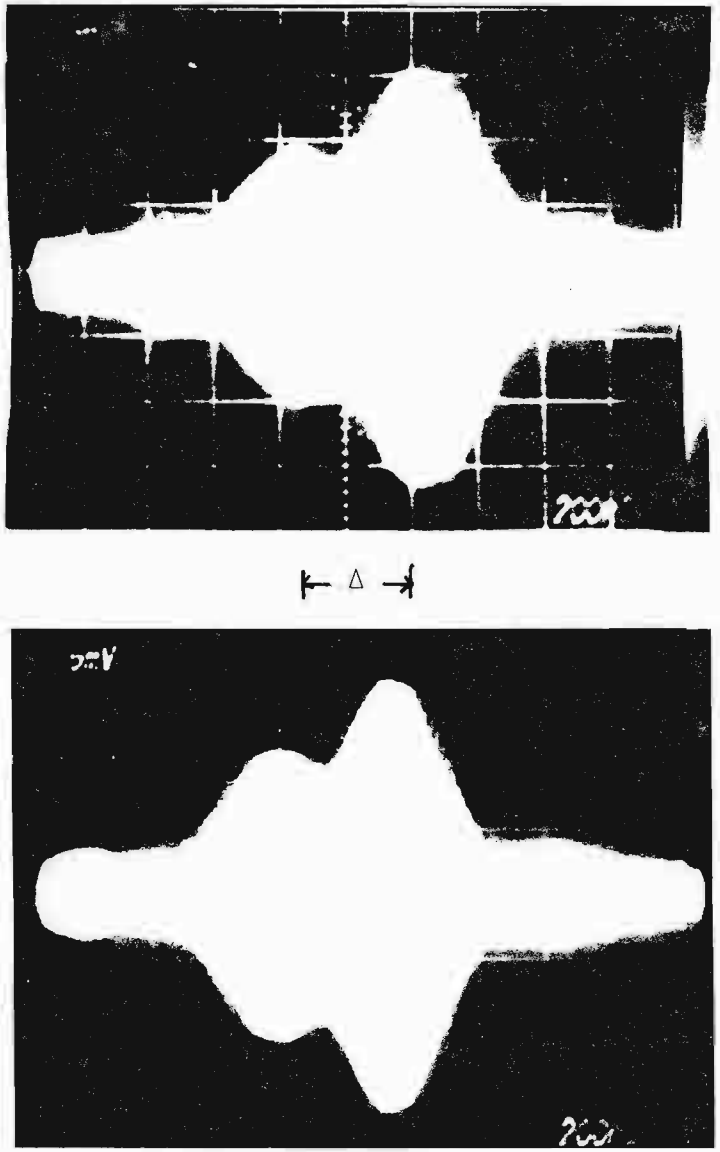

M/D = 4.1 dB

Δ = 360 μsec.

XMTR HT = 11.5 ft.

M/D = + 4 dB

XMTR HT = 28 ft.

Fig. A-7. Measurement station #19 data.

building at a time, because reflections from a single building will dominate in any given region, results of reasonable fidelity can be realized by considering just that pertinent building in each area. Similarly, although the building walls consist of several discrete scattering surfaces which could be modeled as discrete rectangular plates, only a single rectangular metallic plate was used for the model. Figs. A-8 to A-10 show the computed M/D ratios for each of the first three zones. In each figure, the boundary of the multipath reflection zone defined by geometric optics considerations has been indicated. The actual measured levels (from the photographs) are plotted.

The important conclusions to be noted are:

(1) The peak levels of M/D as measured generally agree with the model predictions, and

(2) The variation of peak M/D levels with transmitter height has also been predicted well (refer to Fig. A-9).

The agreement here is quite good considering the very crude building model used as well as the fact that blockage by intervening aircraft was ignored.

Reflection Zone for Hangar #1 - (Simulation)

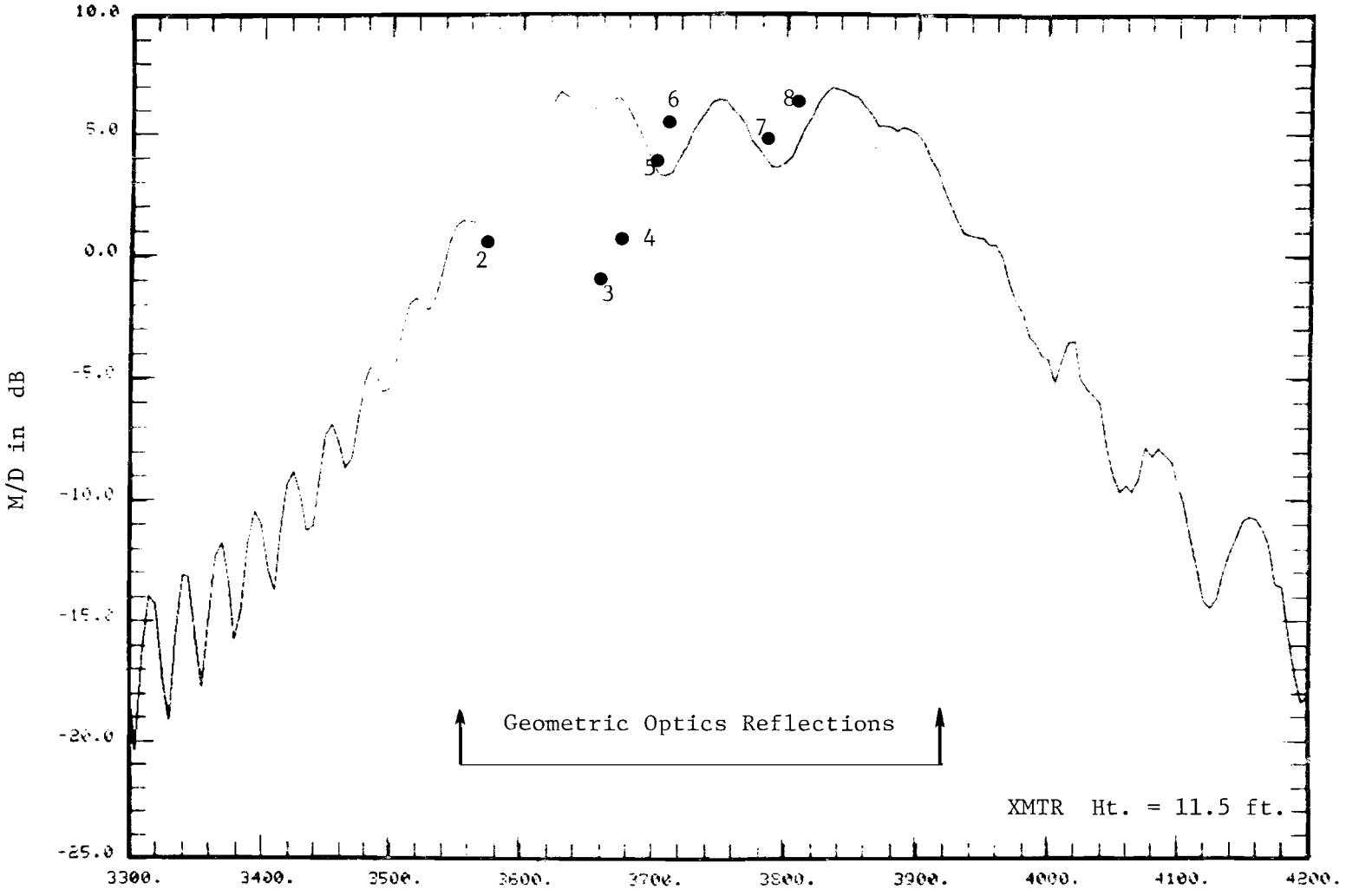

Fig. A-8. Separation of Transmitter and Receiver - ft.

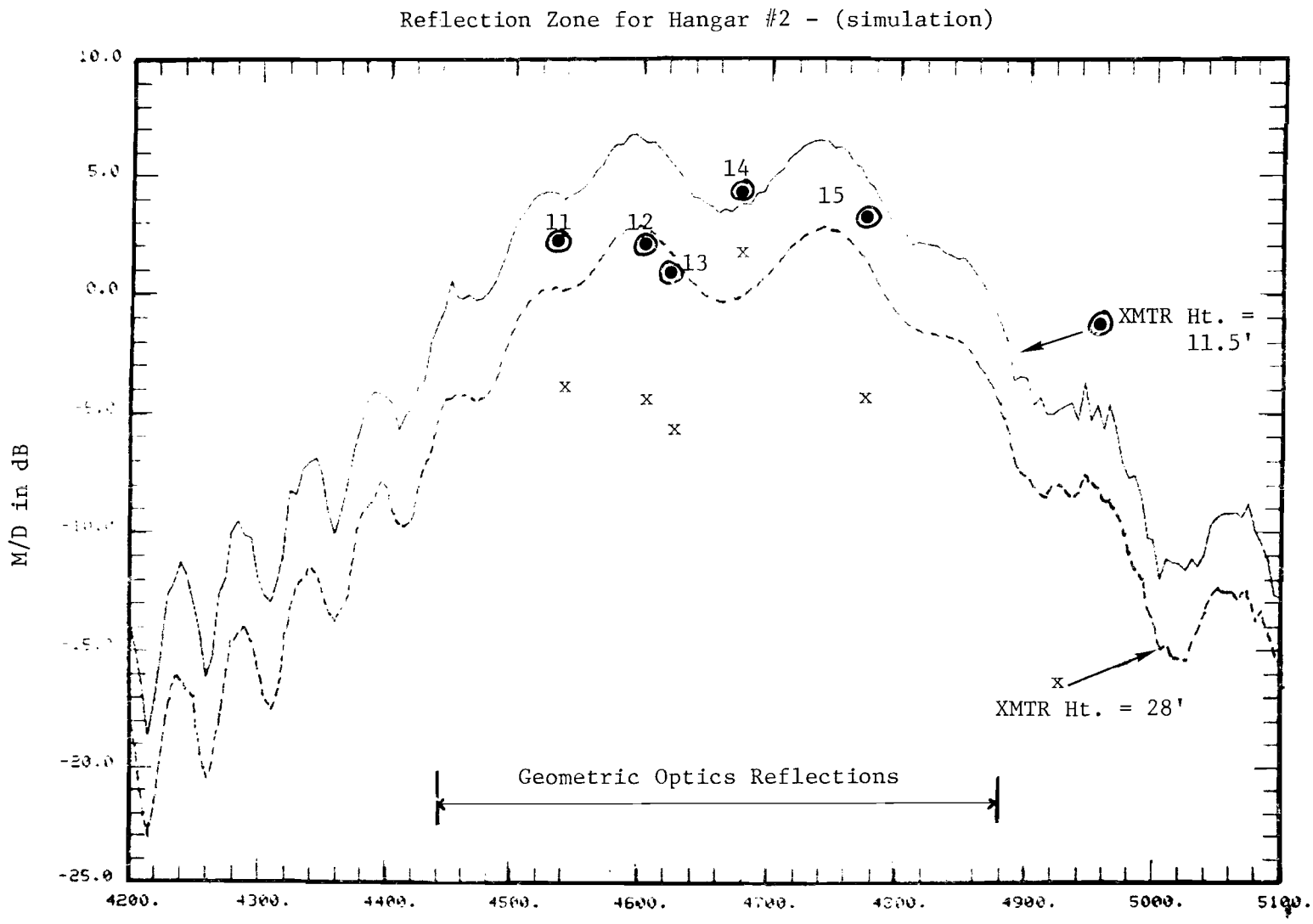

Fig. A-9. Separation of Transmitter and Receiver - ft.

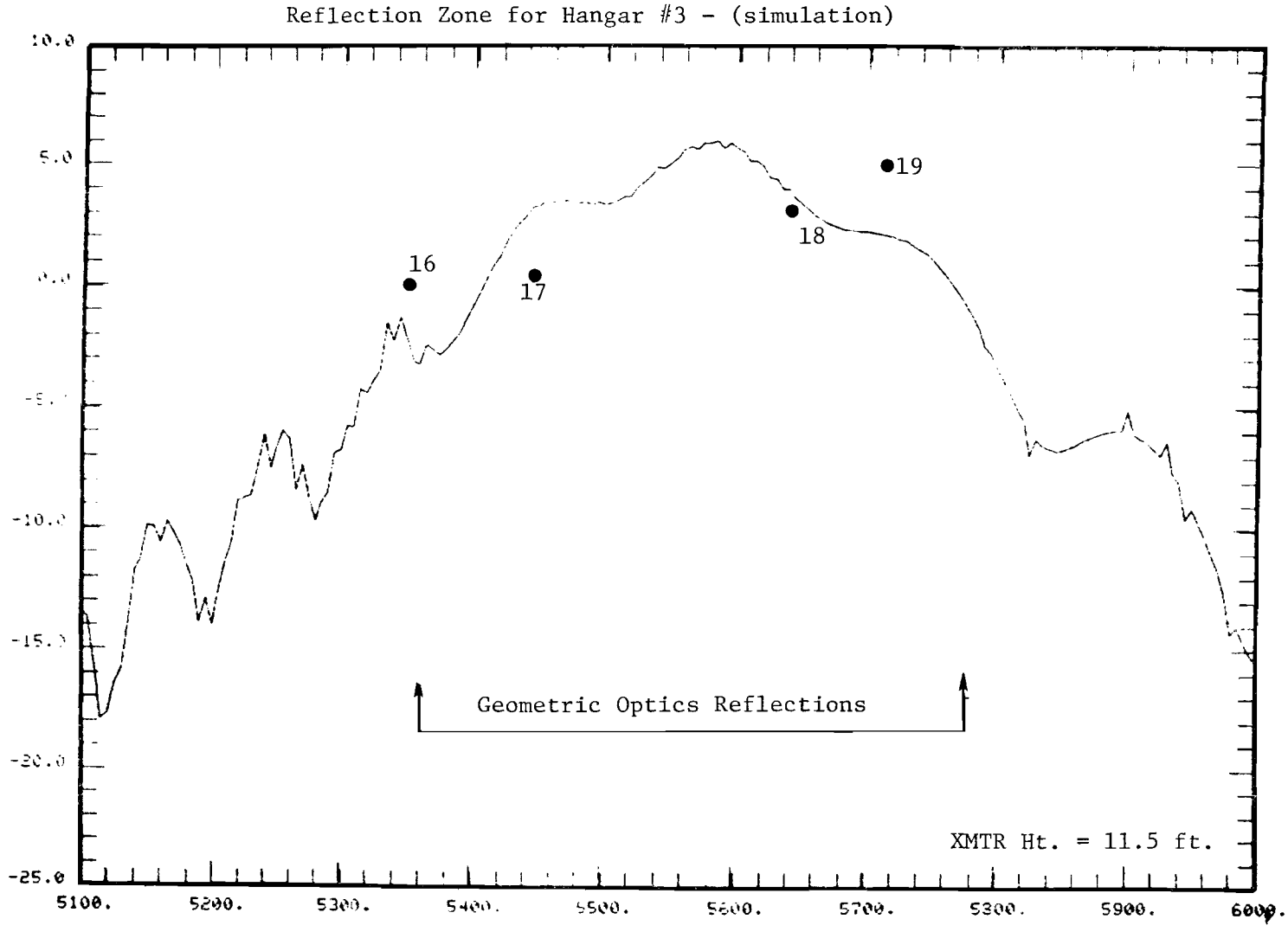

Fig. A-10. Separation of Transmitter and Receiver - ft.

☆ U.S. GOVERNMENT PRINTING OFFICE: 1981 700-002/32